TECHNISCHE UNIVERSITÄT MÜNCHEN

LEHRSTUHL FÜR EXPERIMENTELLE GENETIK

Identification and verification of novel disease-causing genes and therapy options for patients with mitochondrial disorders – Focus on *ACAD9*

Birgit Monika Repp

Vollständiger Abdruck der von der Fakultät Wissenschaftszentrum Weihenstephan für Ernährung, Landnutzung und Umwelt der Technischen Universität München zur Erlangung des akademischen Grades eines

Doktors der Naturwissenschaften (Dr. rer. nat.)

genehmigten Dissertation.

Vorsitzende:	Prof. Angelika Schnieke, Ph.D.
Prüfer der Dissertation:	1. apl. Prof. Dr. Jerzy Adamski
	2. Prof. Dr. Heiko Witt

Die Dissertation wurde am 24.01.2019 bei der Technischen Universität München eingereicht und durch die Fakultät Wissenschaftszentrum Weihenstephan für Ernährung, Landnutzung und Umwelt am 21.06.2019 angenommen.

„Das schönste Glück des denkenden Menschen ist,
das Erforschliche erforscht zu haben und das Unerforschliche ruhig zu verehren“
(Johann Wolfgang von Goethe)

TABLE OF CONTENTS

AAV	adeno-associated virus
ACAD	Acyl-CoA Dehydrogenase
ACAD9	Acyl-CoA dehydrogenase family member 9, mitochondrial
ACADM	Medium-chain specific acyl-CoA dehydrogenase
ACADVL	Very long-chain specific acyl-CoA dehydrogenase
ADP	Adenosindiphosphate
Anti A	Antimycin A
Asc	Ascorbate
ATP	Adenosintriphosphate
BN	Blue native
bp	Base pair
BSA	Bovine serum albumin
Chr	Chromosome
cDNA	complementary deoxyribonucleic acid
CI	Complex I
CII	Complex II
CIII	Complex III
CIV	Complex IV
CV	Complex V
cm	centimetre
CNV	Copy number variation
CoQ	Ubichinone
Cy2	cyanine 2
Cy3	cyanine 3
Cy5	cyanine 5
ddH_2O	Double distilled water
ddNTPs	Dideoxynucleotides
DIGE	Difference gel electrophoresis
DMEM	Dulbecco's modified eagle medium
DMSO	Dimethylsulfoxid
DNA	Deoxyribonucleic acid
dNTPs	Deoxynucleotides
ECL	Enhanced chemiluminescence
EDTA	Ethylene diamine tetra acetic acid
ESI	Electrospray ionisation
FBS	Fetal bovine serum
FCCP	Carbonyl cyanide 4-(trifluoromethoxy)phenylhydrazone

FIV	Feline Immunodeficiency virus
g	gram
Glu	Glutamate
h	hour
HBV	Hepatitis B Virus
HCV	Hepatitis C Virus
HEK	human embryonic kidney
HEPES	4-(2-hydroxyethyl)-1-piperazineethanesulfonic acid
HIV	Human immunodeficiency virus
HRP	Horse radish peroxidase
hrs	hours
IEF	Isoelectric focusing
IF	Immunofluorescence
l	litre
kb	kilo base
LOF	Loss of function
KCN	Potassium cyanide
M	molar
MAF	Minor allele frequency
Mal	Malate
min	minute
ml	millilitre
mM	millimolar
MMDS	multiple mitochondrial disorders
mmol	millimol
mRNA	Messenger ribonucleic acid
MS	Mass spectrometry
$NADH/NAD^+$	Nicotinamide adenine dinucleotide
NDUFB	NADH dehydrogenase (ubiquinone) 1 beta subcomplex
NDUFB3	NADH dehydrogenase (ubiquinone) 1 beta subcomplex subunit 3
NDUFB9	NADH dehydrogenase (ubiquinone) 1 beta subcomplex, 9, 22kDa
NDUFS	NADH ubiquinone oxidoreductase Fe-S protein
NDUFS1	NADH-ubiquinone oxidoreductase 75 kDa subunit
NDUFS8	NADH dehydrogenase [ubiquinone] iron-sulfur protein 8
Ng	nano gram
NGS	Next Generation Sequencing
NSV	nonsynonymous genetic variants

OXPHOS	Oxidative phosphorylation
OCR	Oxygen consumption rate
P	p-value
PAGE	Polyacrylamide gel electrophoresis
PBS	Phosphate buffered saline
PCR	Polymerase chain reaction
PDHA1	Pyruvate dehydrogenase E1 component subunit alpha
PI	Isoelectric point
PIGD	Preimplantation genetic diagnosis
PMP	Plasma membrane permeabilizer
PMSF	Phenylmethylsulfonylfluoride
PVDF	Polyvinylidene difluoride
RC	Respiratory chain
RCC	Respiratory chain complex
RCCI	Respiratory chain complex I
RCCII/III	Respiratory chain complex II/III
RCCIV	Respiratory chain complex IV
RIN	RNA integrity number
RNA	Ribonucleic acid
Rot	Rotenone
rpm	revolutions per minute
RT	Room temperature
s	second
SDS	Sodium dodecyl sulfate
SNP	Single nucleotide polymorphism
Succ	Succinate
TBS	Tris buffered saline
TEMED	Tetramethylethylenediamine
TMPD	N,N,N′,N′-Tetramethyl-p-phenylenediamine
Tris	Tris(hydroxymethyl)aminomethane
U	unit
UTR	Untranslated region
V	Volt
WES	Whole Exome Sequencing
WGS	Whole Genome Sequencing
Wb	Western blot
wt	Wildtype

Abstract

Mitochondrial diseases are a group of clinical, biochemical and genetically heterogeneous disorders that are based on a malfunction of the mitochondrial energy metabolism. In addition to the mitochondrial β-oxidation of fatty acids and the citrate cycle the re-oxidation by the aerobic hydrogen transmitting coenzymes, energy in form of ATP are formed. This reaction, also called oxidative phosphorylation (OXPHOS), takes place in the mitochondrial respiratory chain, one of five components (complex I-V) existing multi-enzyme complex. Defects in the first complex of the respiratory chain represent the most common enzymatic defect of oxidative phosphorylation.

Patients with complex I defect present a big clinical variability in symptoms ranging from mild muscle weakness in adulthood to neonatal death. The wide range of symptoms makes the finding of the right diagnosis challenging. During the last ten years Next-Generation-Sequencing (NGS) has been successfully used for the discovery of new causative genes. In this work, *ACAD9* was discovered as a new assembly factor for complex I via Whole-Exome Sequencing (WES). Functional analysis by the use of lenti-viral transduction, 2D-BN-SDS-Gels, Western Blots and oxygen consumption rate (OCR) measurements confirmed the pathogenicity of the mutation. WES in five other patients with complex I or combined deficiency discovered new variants in already described disease-causing genes (*BOLA3*, *NDUFS8*, and *MTFMT*) and for the first time in the complex I subunit *NDUFB3*. Realizing, that *ACAD9* mutations were found to be one of the most frequent causes of isolated complex I deficiency the genetic, clinical and biochemical data of 70 patients (of whom 29 previously unpublished) were collected and analyzed in detail. Causal variants were distributed throughout the entire gene but no obvious genotype-phenotype correlation was found. The main clinical findings were cardiomyopathy (85%), muscular weakness (75%), exercise intolerance (72%) and mild developmental delay (45%). The age of onset was in the majority of patients within the first year. These patients present the biggest subgroup (n = 52) and the group with the shortest survival (50% not surviving the first two years), suggesting the most severe course. Patients with an onset > 1 year have a better prognosis with 90% surviving ten years.

In spite of rapid progress in finding the molecular cause, in most instances no curative therapeutic options are available. In order to test potential substances (Bezafibrate, riboflavin, resveratrol and AICAR) 42 fibroblast cell lines from patients with isolated or combined complex I deficiency and three age-matched control cell lines were collected and established. A defined molecular diagnosis was present in 35 patient cell lines. After bezafibrate treatment no improvement of complex I activity in cell lines with mtDNA mutation (n = 4) was found, but in 60% of the cell lines with nuclear mutations (+15-140%). To obtain further insight about the mode of action, the effect of the bezafibrate treatment was additionally analyzed on genome-wide expression levels in a subgroup of 14 cell lines. A significant increase in expression levels of genes involved in lipid and fatty acid metabolism (*ACAA2*, *ACADVL*, *CPT1A, CPT1B, ECH1*), but no

increase in the transcription level of genes involved in the mitochondrial biogenesis (*NRF1*, *Tfam*, *PGC-1-α*), was found. The largest effect was observed in a group of patients with mutations in the same gene, *ACAD9* and was therefore studied more in detail. In 12 out of 17 cases the complex I activity increased significantly and five cell lines reached almost the lower level of the normal range. The increase in activity was accompanied by an increase in ACAD9 and ACADVL protein level in 6/7 patients and a larger amount of complex I assembled in supercomplexes visualized by 2D-BN/SDS-PAGE experiments (n = 4). Whole mitochondrial proteome analysis of four patients and one control (bezafibrate treated and untreated), in order to detect potential post-transcriptional effects, were performed by 2D-DIGE. Proteomics data confirmed increased expression of proteins involved in lipid and fatty acid metabolism (ACAA2, ACADVL, ACSL4) upon bezafibrate treatments. The treatment with the vitamin precursor of the flavin adenine dinucleotide (FAD) moiety, riboflavin significant increased respiratory chain complex activity in 9 out of 15 patient cell lines. In contrast to the bezafibrate treatment riboflavin did not change any protein levels. Riboflavin treatment may increase the activity and stability of the remaining ACAD9 protein and thereby leading to an increase of OCR in some patient cell lines. The positive effect in cell lines was also reported for most of the treated ACAD9 patients and is mirrored in the survival data. Patients with a disease-onset below 1year of age have a significantly better survival rate after oral riboflavin treatment (deceased n = 7/24) in contrast to untreated patients (deceased n = 16/17).

In summary, NGS coupled with functional validation of new disease alleles was successfully used to identify disease-causing variants in known and new complex I associated disease genes in six patients. Furthermore, the analysis of different treatment options support bezafibrate and riboflavin as promising treatment options for patients with complex I deficiency, especially for patients with mutations in *ACAD9*.

Zusammenfassung

Mitochondriopathien bilden eine Gruppe von klinischen, biochemischen und genetisch heterogenen Erkrankungen, die auf einer Störung des mitochondrialen Energiestoffwechsels beruhen. In den Mitochondrien werden neben der β-Oxidation der Fettsäuren und dem Zitratzyklus durch die aerobe Reoxidation wasserstoffübertragender Coenzyme, Energie in Form von ATP gebildet. Diese auch oxidative Phosporylierung (OXPHOS) genannte Reaktion erfolgt in der mitochondrialen Atmungskette, einem aus fünf Komponenten (Komplex I-V) bestehenden Multienzymkomplex. Defekte im ersten Komplex der Atmungskette stellen den häufigsten enzymatischen Defekt der oxidativen Phosphorylierung dar. Patienten mit Komplex I (KI) Mangel präsentieren eine große klinische Variabilität der Symptome von leichter Muskelschwäche im Erwachsenenalter bis hin zum neonatalen Tod. Die große Variabilität der Symptome erschwert die Erstellung der richtigen Diagnose. Durch den Einsatz von Next-Generation-Sequencing (NGS) konnten in den letzten zehn Jahren erfolgreich eine Vielzahl an neuen krankheitsverursachenden Genen identifiziert werden. Mit Hilfe von Whole Exome Sequenzierung (WES) wurde im Rahmen dieser Arbeit *ACAD9* als neuer Komplex I Assemblierungsfaktor entdeckt. Weiterführende funktionelle Analyse durch die Verwendung von Lentiviraler Transduktion, 2D-BN-SDS-Gelen, Western Blots und Atmungskettenenzymmessungen in den Zellen der Patienten bestätigten die Pathogenität der Mutation. Durch WES wurden in fünf weiteren Patienten mit Komplex I oder kombinierten Defekt neue Varianten in bereits beschriebenen krankheitsverursachenden Genen (*BOLA3*, *NDUFS8*, *MTFMT*) und zum ersten Mal in der Komplex I-Untereinheit *NDUFB3* entdeckt. Da sich zeigte, dass *ACAD9*-Mutationen eine der häufigsten Ursachen für einen isolierten Komplex I-Mangel darstellen, wurden die genetischen, klinischen und biochemischen Daten von 70 Patienten (von denen 29 zuvor unveröffentlicht waren) erhoben und detailliert analysiert. Krankheitsverursachende Varianten waren im gesamten Gen verteilt, es wurde jedoch keine offensichtliche Korrelation zwischen Genotyp und Phänotyp gefunden. Die wichtigsten klinischen Befunde waren Kardiomyopathie (85%), Muskelschwäche (75%), Belastungsintoleranz (72%) und leichte Entwicklungsverzögerung (45%). Der Krankheitsbeginn lag bei der Mehrzahl der Patienten innerhalb des ersten Jahres. Diese Patienten stellen die größte Untergruppe (n = 52) und die Gruppe mit dem kürzesten Überleben dar (50% überleben die ersten zwei Jahre nicht), was auf den schwersten Verlauf schließen lässt. Patienten mit einem Beginn > 1 Jahr haben eine bessere Prognose, da 90% zehn Jahre überleben.

Trotz des raschen Fortschritts bei der Suche nach der molekularen Ursache steht in den meisten Fällen keine kurative Therapie zur Verfügung. Um die Wirkung von potentiellen Substanzen (Bezafibrat, Riboflavin, Resveratrol und AICAR) zu testen, wurden 42 Fibroblastenzelllinien von Patienten mit isoliertem oder kombinierten Komplex I-Defekt und drei Kontrollzelllinien mit gleicher Altersverteilung gesammelt und etabliert. Eine gesicherte molekulare Diagnose lag bei 35 Patientenzelllinien vor. Nach der

Behandlung mit Bezafibrat wurde keine Verbesserung der Komplex I-Aktivität in Zelllinien mit mtDNA Mutation (n = 4), aber in 60% der Zelllinien mit nuklear kodierten Mutationen (+15-140%) gefunden. Um Aufschlüsse über den Wirkmechanismus zu bekommen wurde in einer Untergruppe von 14 Zelllinien die Wirkung der Bezafibratbehandlung durch genomweite Geneexpressionsanalysen untersucht. Es zeigte sich eine erhöhte Expression von Genen im Lipid-und Fettsäure-Metabolismus (*ACAA2*, *ACADVL*, *CPT1A*, *CPT1B*, *ECH1*) aber kein Anstieg der Expression der Gene die im Zusammenhang mit mitochondrialer Biogenese stehen (*NRF1*, *Tfam*, *PGC-1-α*). Der Anstieg an PDCK4 führt zu einer Runterregulierung der Glykolyse und somit auch zu einem verstärkten Fettsäuremetabolismus. Der größte Effekt der Bezafibratbehandlung wurde in Zelllinien von Patienten mit *ACAD9* Mutation beobachtet und daher intensiver untersucht. Die Komplex I-Aktivität erhöhte sich signifikant in 12 von 17 untersuchten Zelllinien, wobei zwei sogar den unteren Normbereich erreichten. Die Erhöhung der Aktivität wurde durch eine Zunahme von ACAD9 und ACADVL Protein in 6/7 Patienten und eine größere Menge von Komplex I assemblierten Superkomplexen, visualisiert durch 2D-BN/SDS-PAGE Experimente (n = 4), begleitet. Eine gesamte mitochondriale Proteomanalyse, zur Analyse von möglichen post-transkriptionellen Effekten, wurde mit Hilfe von 2D-DIGE-Gelen an vier verschiedenen ACAD9 Patienten und einer Kontrolle (Bezafibrat behandelt und unbehandelt) durchgeführt. Nach der Bezafibratbehandlung erhöht sich, im Einklang mit der Genexpressionsanalyse, die Expression von Proteinen die im Lipid-und Fettsäure-Stoffwechsel (ACAA2, ACADVL, ACSL4) beteiligt sind. Die Behandlung mit Riboflavin, als Vitamin-Vorstufe der Flavin-Adenin-Dinukleotid (FAD)-Gruppe, in der Gruppe von Patienten mit Mutationen in *ACAD9*, erhöht den Sauerstoffverbrauch in den Zellen in 9 von 15 Patienten. Im Gegensatz zur Bezafibratbehandlung bewirkte Riboflavin keine Veränderungen auf Proteinebene. Die Riboflavinbehandlung führt offensichtlich zu einer Steigerung der verbliebenen ACAD9-Restaktivität und Stabilität und damit zu einer Erhöhung der Atmungskettenaktivität bei einigen Patienten. Der positive Effekt in Zelllinien wurde auch für die meisten der behandelten ACAD9-Patienten berichtet und spiegelt sich in den Überlebensdaten wider. Patienten mit einem Erkrankungsbeginn unter einem Jahr haben eine signifikant bessere Überlebensrate nach oraler Riboflavin-Behandlung (verstorben n = 7/24) im Vergleich zu unbehandelten Patienten (verstorben n = 16/17).

Zusammenfassend konnte gezeigt werden, das NGS zusammen mit einer funktionellen Validierung neuer krankheitsverursachender Allele, zu einer erfolgreichen Identifizierung bekannter und neuer Komplex I assoziierter Gene in sechs Patienten geführt hat. Darüber hinaus wurde gezeigt, dass die Gabe von Bezafibrat und Riboflavin eine vielversprechende Behandlungsmöglichkeit für Patienten mit Komplex I-Defekt, besonders für Patienten mit Mutationen in *ACAD9*, darstellen.

1. Introduction

1.1 Mitochondria

The first records on intracellular structures that probably represent mitochondria go back to the middle of the 19th century. The term “mitochondria” was introduced by Benda in 1898 and comes from the Greek "mitos" (thread) and "chondros" (granule) [1]. Since the recognition that these small cellular organelles are responsible for energy production they have been intensively studied [2]. According to the endosymbiotic theory, over 1.5 billion years ago, mitochondria have evolved from an aerobically oxygen-breathing bacterium which was engulfed by an empty eukaryotic host cell. The interplay of the two organisms has developed into a mutual dependence over time [3]. The structure of mitochondria still reflects their bacterial origin, as these cellular organelles have a double membrane and β-barrel transmembrane proteins for example [4, 5]. Major steps in the loss of independence were the shift of many originally prokaryotic genes into the nucleus of the eukaryotic cell. The uptake of the bacteria into the cells led to the peculiarity that the organelles are surrounded by two highly specialized membranes, the inner and the outer membrane [6]. This resulted in the formation of four separate compartments within the mitochondria, the outer membrane, the intermembrane space, inner membrane and the matrix [7, 8]. The matrix contains a mixture of hundreds of enzymes for various functions of the mitochondrion the mitochondrial genome, specific mitochondrial ribosomes and tRNAs. The intermembrane space is delimited by the inner membrane, which has for the enlargement of its surface area numerous folds, called cristae [9]. The number of mitochondria per cell is highly variable. While erythrocytes have no mitochondria; in striated muscle cells can be several thousands. Additionally, they have their own small circular genome of a total of 16,569 base pairs [10, 11]. The double-stranded, circular mtDNA encodes for 37 genes, of which 24 are for RNAs: rRNAs (two genes) and tRNAs (22 genes), which are required for the translation of mtDNA and 13 are for polypeptides, which are all components of the respiratory chain [10, 12]. Mitochondria are highly dynamic cellular organelles that can regulate their morphology, distribution, and activity by fusion and fission [13, 14] and are therefore able to adopt to fluctuating energy demands of the individual cells. About 85% of mitochondrial proteins are nuclear-encoded, which are translated in the cytoplasm and transported into the mitochondria. Not only the sub-units of the respiratory chain complexes, but also the DNA and ribosomal RNA polymerases, different initiation, elongation and termination factors-, tRNA modification enzymes, aaRS`s (aminoacyl-tRNA synthetases) and many other enzymes for the tRNA maturation are needed. The transport machinery itself depends also on nuclear-encoded proteins. Three membrane complexes are involved in the transport of polypeptide chains in the mitochondria: the TOM (translocase of the outer membrane) complex in the

outer membrane as well as the TIM22 and TIM23 (translocase of the inner) membrane complexes in the inner membrane [15].

Overall mitochondria are involved in many metabolic processes in the cell; e.g. production of energy in the form of ATP by oxidative phosphorylation, TCA cycle, fatty acid degradation, biosynthesis of the iron / sulfur groups, apoptosis, and the synthesis of the heme molecules, nucleotides and of phospholipids [16, 17].

1.2 Respiratory chain

Oxidative phosphorylation is the main reaction sequence to produce energy in aerobic organisms. The complex metabolites of our daily food such as carbohydrates, lipids and proteins are first degraded into their monomeric units, mainly glucose, fatty acids, glycerol and amino acids, and then further degraded to acetyl-CoA. In the citric acid cycle, acetyl CoA is oxidized by O_2 to CO_2 and simultaneously the Coenzymes NAD + and FAD are reduced to their high-energy intermediates, NADH and $FADH_2$. In the last part of this pathway, electrons from NADH or $FADH_2$ are transferred to the oxygen O_2, which is then reduced to H_2O. The released energy drives the synthesis of the energy-rich ATP by phosphorylation of ADP with pyrophosphate (Figure 1.1 taken from [18]). The electron transfer from NADH or $FADH_2$ to O_2 is mediated by a number of enzymes connected in the inner mitochondrial membrane (respiratory chain). The electrons are transported by co-enzyme Q from the complexes I (CI) and complex II (CII) to Complex III (CIII) and are then transferred through the membrane protein complex of cytochrome C to complex IV (CIV) and finally to molecular oxygen. This metabolic process is the reason that mitochondria are referred as the powerhouse of the cell.

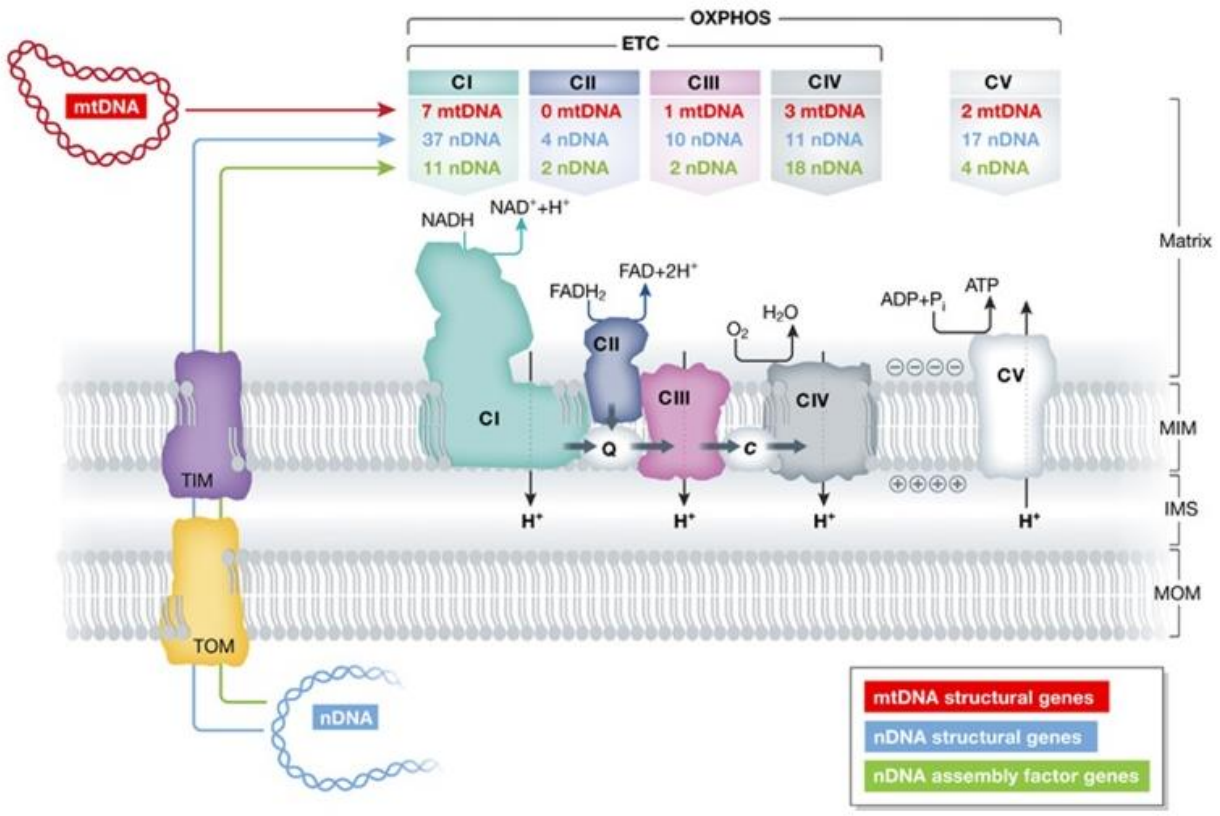

Figure 1.1: Genetic origin and functional interaction of the mitochondrial oxidative phosphorylation (OXPHOS) complexes (Picture taken from [18])

1.3 Complex I - NADH-ubiquinone oxidoreductase

The first enzyme complex, the NADH ubiquinone oxidoreductase (NADH dehydrogenase or complex I) was first isolated in 1962 and represents the first entry site for the electrons into the respiratory chain. Complex I is the largest, most complex and most well studied enzyme among the complexes of the respiratory chain. It consists of 44 different subunits with a molecular mass of 980kDa [19]. Seven subunits are encoded by the mitochondrial DNA (ND1-6 and ND4L) and the other 37 subunits are nuclear encoded [20, 21] (Figure 1.2 modified from [22]). The biosynthesis of complex I is highly complicated and involves at least 14 additional assembly factors (NDUFAF1, NDUFAF2, NDUFAF3, NDUFAF4, NDUFAF5, NDUFAF6, NDUFAF8, ACAD9, ECSIT, COA1, FOXRED1, NUBPL, TIMMDC1 and TMEM126B) and it is likely that more will be found [23-25].

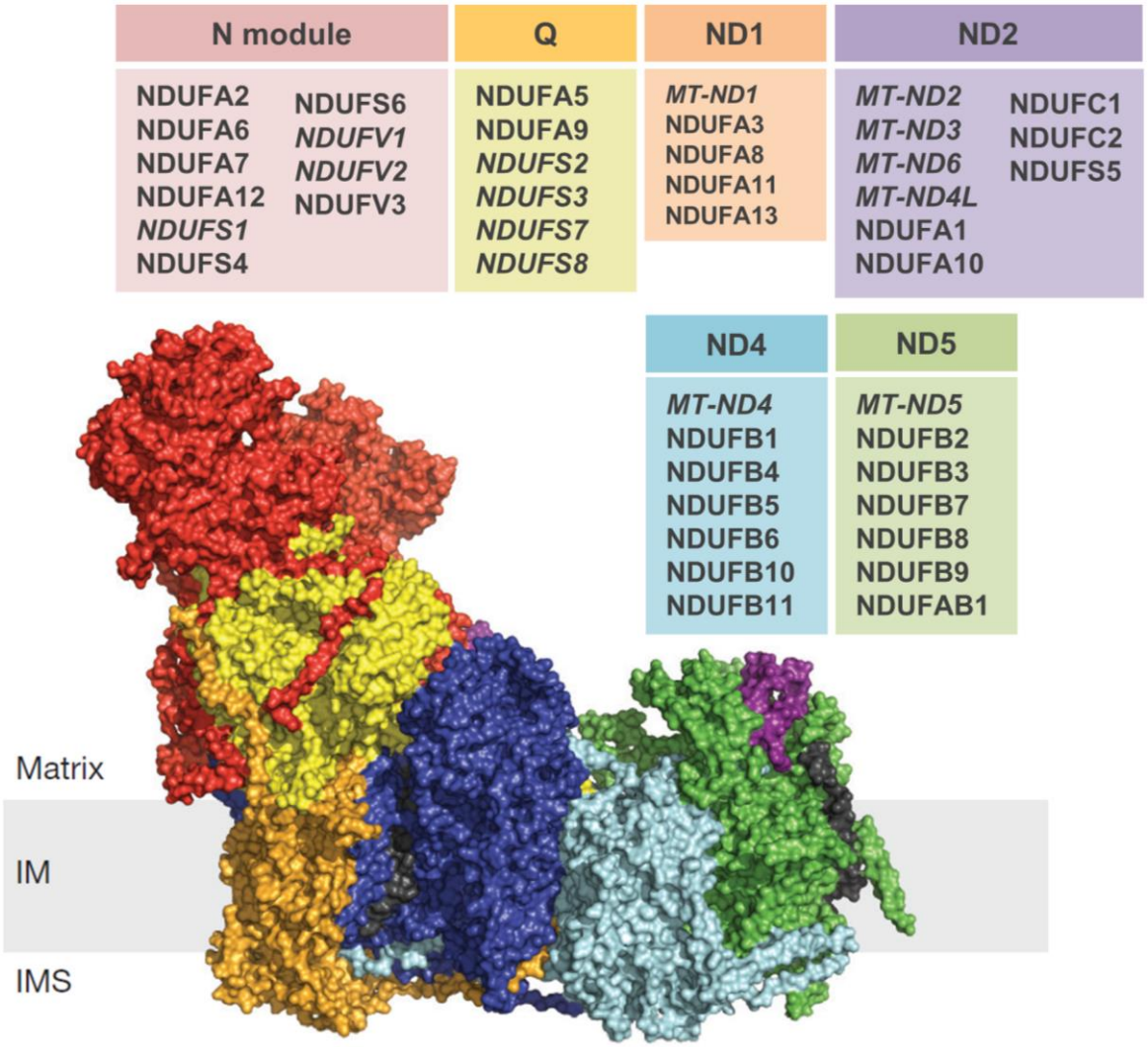

Figure 1.2: Structures of complex I. 44 subunits are divided into six modules. Italics represent core subunits (Picture modified from [22])

Complex I is an L-shaped enzyme with one arm integrated into the inner membrane and the other arm protruding into the matrix space. Fourteen core subunits, conserved from bacteria to humans, perform the catalytic activities. The remaining 30 proteins are called accessory or supernumerary subunits [26]. The hydrophilic arm contains seven core subunits: the primary electron acceptor flavin mononucleotide (FMN) and seven iron-sulfur (Fe-S) clusters. The electrons resulting from the oxidation of NADH in the citric acid cycle, the β-oxidation or pyruvate dehydrogenases are transferred to FMN and are subsequently passing eight Fe-S clusters on the way to the final electron acceptor ubiquinone (UQ) [27, 28]. The other seven core subunits (all complex I subunits encoded in the mtDNA) are located in the hydrophobic arm. Through the inclusion of the electrons, UQ is reduced to ubiquinol. The energy released during the reaction is used for the transport of four protons from the matrix into the intermembrane space [29]. This process produces a proton gradient and the proton-motive force that is used to synthesize ATP. The exact path of the electrons and the precise function of the intermembrane subunits is not yet known, however, it is suggested that they have a stabilized function and participate in the translocation of protons across the membrane

[30, 31]. The 44 subunits of complex I must be assembled correctly to form the properly functioning mature complex (Figure 1.3, taken from [31]). This assembly process is very difficult and complex because of its large size and dual control by nuclear and mitochondrial DNA [19]. During the last decade the crystal structure of the complex has been resolved and comprehensive complexome profiling approaches helped to get new insights into the complex I assembly [25, 31] .

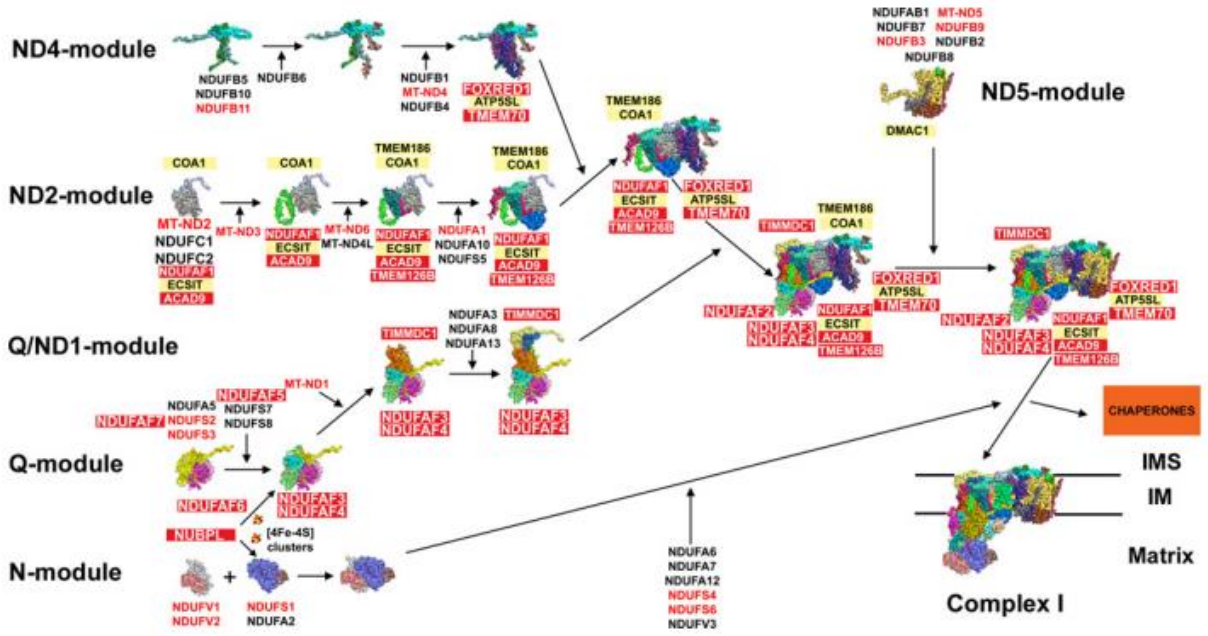

Figure 1.3: Assembly model of human complex I (Picture taken from [31])

The complex I subunits are organized in six modules (N, Q, ND1, ND2, ND4 and ND5) and with the help of specific assembly factors the mature form of complex I is formed. In brief, the Q-module is built by the formation of a small hydrophilic assembly complex of NDUFA5, NDUFS2 and NDUFS3, which expands by the addition of subunits NDUFS7, NDUFS8 and later NDUFA9 and is subsequently anchored to the membrane by the assembly factors NDUFAF3 C3orf60, NDUFAF4 C6orf66 and NDUFAF6 [32, 33]. At this stage the Fe-S clusters are then added by NUBPL resulting in the formation of the ~400kDa complex. NUBPL is important for the assembly of these clusters into various subunits of the holoenzyme [34]. With the help pf TIMMDC1 the ND1-module is built around the Q-module. MT-ND1, NDUFA4, NDUFA8 and NDUFA13 are added. The next step is the formation of the ND2-module by an initial intermediate containing MT-ND2, NDUFC1, NDUFC2 bound to NDUFAF1, ECSIT and ACAD9, followed by the addition of MT-ND3, together with TMEM126B, and binding of the subunits MT-ND6 and MT-ND4L. The final step of the assembly of the ND2-moldule is the incorporation of the subunits NDUFA1, NDUFA10 and NDUFS5 [20, 26]. The assembly factors NDUFAF1+ACAD9+ECSIT+TMEM126B build a stable formation known as the Mitochondrial Complex I assembly complex (MCIA) [35, 36]. Recent studies found two other chaperones interacting with this module: TMEM186 and COA1 [25]. The ND4-module, located in the inner membrane, is formed by the addition of NDUFB1, NDUFB4, NDUFB5, NDUFB6, NDUFB10, NDUFB11 and MT-ND4 assisted by the assembly factors FOXRED1, ATP5SL and TMEM70 (also described as complex V assembly factor [37]) [31]. The ND5-module, located in the

distal part of the membrane arm, is composed of the subunits MT-ND5, NDUFB2, NDUFB3, NDUFB7, NDUFB8, NDUFB9 and NDUFAB1 [20]. The N-module (NADH binding and oxidation), which forms the end of the hydrophilic arm, is assembled by the nDNA-encoded subunits (NDUFV1-3, NDUFS1, NDUFS4, NDUFS6, NDUFA6, NDUFA7, NDUFA12 and NDUFV3). The six modules are finally joined together. ND2 and ND4-module get together first, followed by the addition of the Q/ND1 and ND5 module. This intermediate is stabilized by NDUFAF2 [38]. In the last step the N-module becomes attached, the assembly factors are released and the mature complex I is built [25, 31].
This work focuses on patients with complex I deficiency, therefore the function and assembly of the other complexes II, III, IV and V of the respiratory chain will not be further described.

1.4 Mitochondrial disorders

1.4.1 General information

About 65 years ago, in 1962, Luft et al. reported for the first time that mitochondria play a role in the pathogenesis of diseases [39]. The number of diseases due to impaired function of this organelle steadily increased since then. Mitochondrial dysfunction can be found, for example, in frequently occurring diseases such as diabetes mellitus [40] and many cancers [41, 42]. Mitochondria are the most important energy sources of the cells. Therefore, all diseases leading to an impairment of oxidative phosphorylation are combined together under the term mitochondrial disorders. This can be both indirectly by a failure of cardiolipin metabolisms as in Barth syndrome [43] as well as directly, for example by respiratory chain defects (see chapter 1.3) or pyruvate dehydrogenase deficiency [12, 44]. Since mitochondria are present in almost all cells and run numerous metabolic processes within them that cannot be adopted or compensated for any other organelle, the clinical presentations of mitochondrial diseases are very varied. The prevalence of mitochondrial disease, including pathogenic mutations of both the mitochondrial and nuclear genomes is minimum 1/1100 in children and 1/4300 in adults [45, 46] and they cause a wide spectrum of clinical phenotypes. Due to their central role in energy metabolism in the cells of tissues with high energy demand, such as the nervous system, skeletal muscle, heart, eye, liver, gastrointestinal system, hematopoietic systems and endocrine apparatus are mainly affected [47-49] (Figure 1.4).

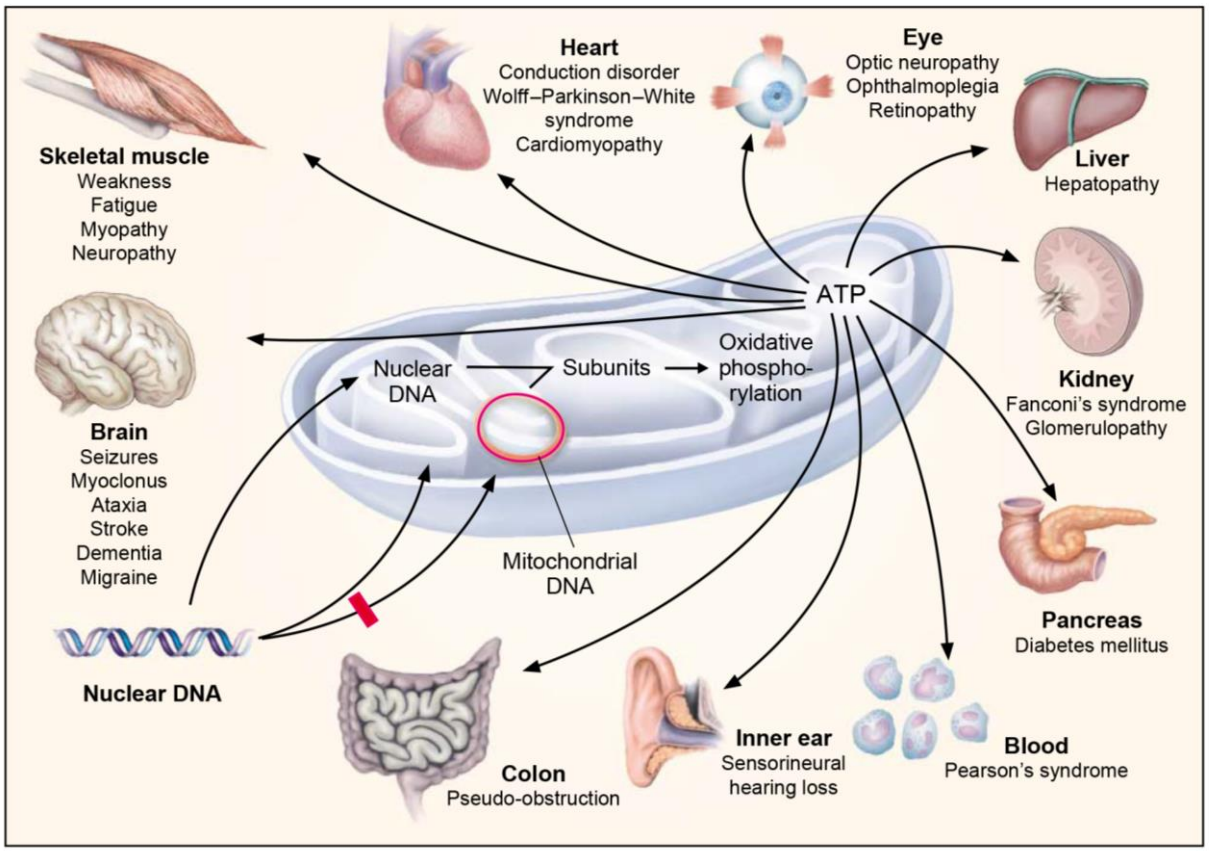

Figure 1.4: Main affected organs and tissues in patients with mitochondrial disorders (Picture taken from [47])

The manifestation of the disease is often neurological in form of symptomatic dystonia [50, 51], ataxia or epilepsy [52, 53]. The severity of the disease depends on the extent of the impairment of energy metabolism; leading to only a slight reduction of cell function barely noticeable and only under stress occurring symptoms up to a massive dysfunction with complete cell death in an organ [54]. Especially in tissues with limited regenerative capacity, such as the nerve tissue, cell death can lead to early onset of symptoms. Some defects can cause already an intrauterine death of the organism, whereas others are manifested postnatal, in youth or in adulthood.

1.4.2 Inheritance

Mitochondrial diseases are not only caused by mutations in the 13 mitochondrial encoded proteins, but can also be caused by some of the approximately 1500 nuclear encoded proteins which are imported into the mitochondria [55-57]. To classify primary mitochondrial disorders the genetic origin of the defect can be used. We can distinguish between mutations in the mitochondrial and nuclear DNA. While the nuclear genes are inherited autosomal recessive, autosomal dominant or X-linked, the inheritance of mitochondrial DNA defects show some peculiarities. Almost all mitochondria of a zygote descended from the egg. That's the reason why the mtDNA is primarily inherited from the mother and follows a maternal inheritance.

Another peculiarity is that each cell contains thousands of mtDNA molecules. If the genotype of an individual is made only of one mtDNA species, it is designated as homoplasmic. Due to the high mutation rate of the mtDNA and at the same time a less efficient repair mechanism there may be common occurrence of mutant and wild-type mtDNA within a cell. Therefore the impact of a mitochondrial mutation on the phenotype depends very much on the degree of heteroplasmy (ratio between normal and mutant mtDNA) [58]. The ratio between mutated and normal mtDNA can also change during several cell divisions. The mitochondrial genome is duplicated and distributed randomly to the daughter cells. The shift of the mutation load is responsible for the late appearance of some symptoms or even the change in phenotype [59, 60].

1.4.3 Respiratory Chain Complex I – Deficiency

Besides the genetic classification of the defects, they can be also divided according to their measurable biochemical phenotype. Isolated defects, in which only one complex is affected and combined defects, in which at least two complexes show a limitation in activity. Among the big group of mitochondrial disorders isolated complex I deficiency is the most commonly identified biochemical defect in childhood-onset mitochondrial disease [61], and accounts for ~1/3 of all cases of OXPHOS disorders [46, 62-64].

1.4.3.1 Clinical spectrum of complex-I defect patients

As with all mitochondrial disorders the clinical spectrum of patients with a complex I-defect is very broad. The disease may be displayed by basal ganglia and/or brainstem lesions, in the form of muscle weakness, hypotonia, failure to thrive, seizures, subacute necrotizing encephalopathy, growth retardation, lactic acidosis, respiratory disorders, cardiomyopathy, neurosensoric hearing loss, retinopathy hepatic, gastrointestinal or endocrine disorder [63, 65, 66]. MtDNA mutations become often symptomatic in youth or in adulthood. In contrast to that, patients with nuclear mutations have mostly a normal prenatal development and are born at term with no obvious organ anomalies or dysmorphic features. Nevertheless, the majority of children demonstrate the first symptoms during the first year of life. From the time of onset they often suffer from rapid disease deterioration resulting in a fatal outcome [67]. The clinical pictures are also very variable from infantile Leigh-Syndrome, to MELAS (Mitochondrial Encephalomyopathy, Lactic Acidosis, and Stroke-like episodes), to MERRF (Myoclonic Epilepsy with Ragged Red Fibers) to adult-onset encephalomyopathic syndromes of variable severity (Figure 1.5, taken from [68]).

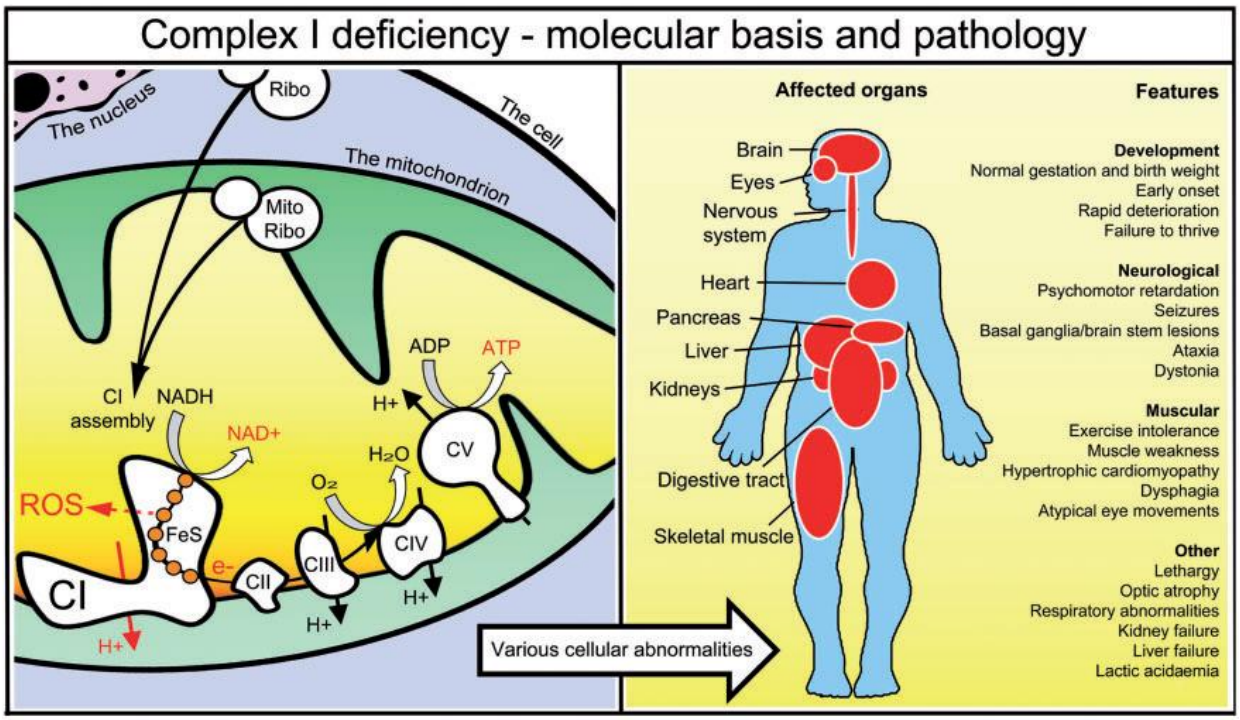

Figure 1.5: Molecular basis of complex I deficiency leading to a variety of affected organs and clinical features (taken from [68])

The most common phenotype of patients with a complex I-deficiency is Leigh or Leigh-like syndrome. Leigh syndrome is a progressive bilateral neurodegeneration mostly with symmetrical changes in the brain [69, 70]. It is characterized by degeneration of the basal ganglia, particularly the putamen, thalamus and brain stem, cerebellum and Dienzephalons, and the white and grey substance. Accordingly, the majority of patients showing a neuronal loss of function, in the psychomotor regression, individual seizures up to epilepsy, dystonia, ataxia, paralysis of the optic nerve, and a disorder of respiratory control (Hypopnea) manifests. Symptoms of the disease usually occur prenatal and in infancy [71, 72]. The disease progression is usually very severe, and the majority of patients die before reaching their fifth birthday [73].

1.4.3.2 Known disease-causing genes

Inherited isolated complex I deficiency can result from mutations in either nDNA-encoded complex I subunits, nDNA encoded complex I assembly factors or mutations in the mtDNA. Mutations in all seven mitochondrially encoded subunits ND1 [74, 75], ND2 [76], ND3 [77, 78], ND4 [79], ND4L [80], ND5 [81] and ND6 [82] were found. Mutations in nDNA-encoded complex I subunits are frequently inherited in an autosomal recessive fashion, meaning that both parents have to be heterozygous carriers with the exception of NDUFA1 which is an X-linked gene. Up to date pathogenic mutations were described in 21 nuclear encoded subunits: NDUFA1 [83], NDUFA2 [84], NDUFA6 [85], NDUFA9 [86], NDUFA10 [87], NDUFA11 [88], NDUFA12 [89], NDUFA13 [90], NDUFB3 [91], NDUFB8 [92], NDUFB9 [93], NDUFB10 [94], NDUFB11 [95] , NDUFS1 [96], NDUFS2 [97], NDUFS3 [73], NDUFS4 [98] , NDUFS6

[99], NDUFS7 [100], NDUFS8 [101], NDUFV1 [96] and NDUFV2 [102]. In addition to the structural components of complex I, there are a number of known and putative assembly factory, which chaperone the 44 subunits proteins, one FMN moiety and eight Fe-S clusters through the intricate process of assembling the final 980kDa holoenzyme [24, 103]. To date 11 such assembly factors have been linked to human disease: NDUFAF1 [104, 105], NDUFAF2 [106], NDUFAF3 [107], NDUFAF4 [108], NDUFAF5 [109], NDUFAF6 [110], NDUFAF8 [111], FOXRED1 [112], ACAD9 [113, 114] and TMEM26B [92].

Beside the complex I subunits and assembly factors more and more genes are discovered which have to do with the mtDNA transcription and translation, mtDNA maintenance, fission and fusion, protein import, homeostasis, substrates, inhibitors and mitochondrial co-factors. The following figure gives an overview of to date 320 known disease-causing genes for patients with mitochondrial disorders, including also subunits of respiratory chain complexes II-V, which will not be further described (Figure 1.6). The list was created within the mitoNET Salzburg-Munich collaboration and regularly updated by Dr. Johannes Mayr [115, 116].

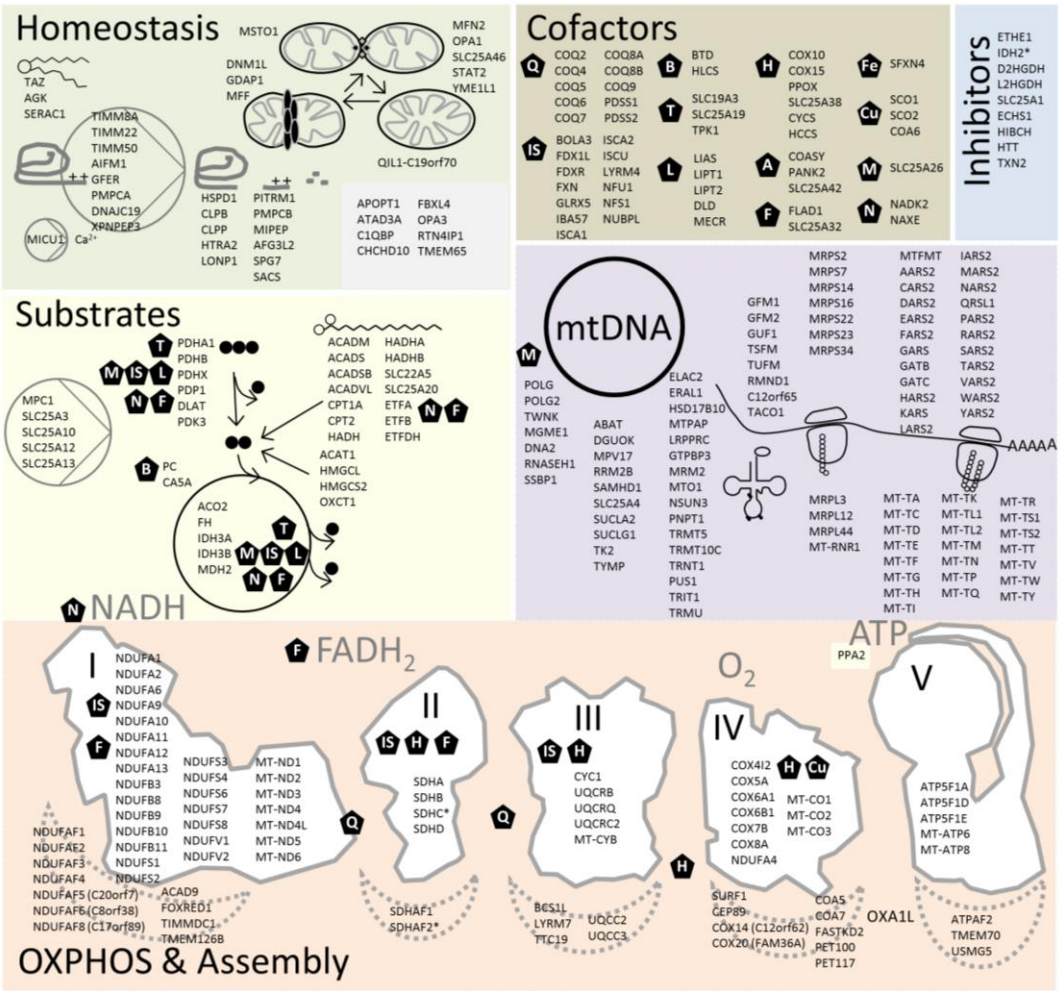

Figure 1.6: Overview of all known disease-causing genes for patients with mitochondrial disorder divided into their functional properties (modified from [116]) Abbreviations: coenzyme Q10 (Q), iron-sulfur clusters (IS), biotin (B), thiamine pyrophosphate (T), lipoic acid (L), heme (H), coenzyme A (A), riboflavin/FMN/FAD (F), iron (Fe), copper (Cu), S-adenosyl-methionine (M), NAD(P)H (N).

1.5 Diagnostic for mitochondrial disorder

1.5.1 General information

The diagnosis for patients with mitochondrial disorders is made by the combination of clinical observations (muscle weakness, seizures, growth retardation, cardiomyopathy and failure to thrive), laboratory evaluation (lactic acidosis, amino acids and organic acids), brain imaging (MRI symmetric lesions basal ganglia), detailed family anamneses and muscle biopsies. The analysis of the histology of the muscle fibers (ragged red fibers, cox negative fibers) is also a standard diagnostic method. The enzymatic analysis in muscle of the activity of different complexes of the respiratory chain can further give an indication which or which combinations of complexes are affected. Together with the muscle biopsy a fibroblast cell lines can be generated and used to measure enzyme activity as well. Nevertheless, the discovery of the genetic cause of the defect is difficult. An isolated reduction of complex II activity can be for example a sign of mutations in the complex II subunit genes *SDHA-D* or assembly factors *SDHAF1-2*. A combined respiratory chain complex defect can be caused by depletion or deletions of the mtDNA, in the case of a maternal family history due to mt-tRNA mutations, mutations in the nuclear mt-DNA translation genes (e.g. *TRMU, MTFMT*) or mutations in the CoQ10 defect genes. In the case of an isolated complex I defect far more genes have to be considered. The first screen is often the search for depletion, deletion and mutations in the mtDNA. The mtDNA analysis discovers the underlying disease-causing mutation in approximately 15% of patients with isolated complex I-defect [117]. But the majority of cases are caused by mutations in nuclear encoded proteins. The large number of known and probably even higher number of unknown disease genes makes the analysis of all potential disease genes one after the other very time and money consuming [118, 119]. Therefore, in pediatric patients, the molecular genetic cause of the disease often remains unclear. From the starting time point of my PhD thesis until the finalization big advances in diagnosis were achieved with the implementation of Next-Generation-Sequencing (NGS) technology.

1.5.2 Routine diagnostics

Sanger sequencing

Beside the big advantages and progress made in the use of NGS in research a lot of diagnostic laboratories still use the Sanger Sequencing technology (also called dideoxy chain termination sequencing). The method was invented in 1975 by Frederick Sanger and colleagues [120, 121], and was awarded with the Nobel Prize in 1980. It is mainly used to sequence single genes in order to identify DNA mutations. This

might be useful when a specific phenotype is associated with only a few genes. The process can be parallelized up to 384 DNA samples in a single run. The read length achieved by the Sanger biochemistry is up to 1,000 bp, and the per-base accuracies is as high as 99.99% [122]. In the case of a single gene disorder with clear clinical, biochemical indication and/or known mutation hot spots, Sanger sequencing of the target region is an accurate and cost-effective way to obtain a definitive molecular diagnosis. However, the selection of candidate gene(s) for sequence analysis is extremely difficult, as most inherited disorders exhibit genetic and clinical heterogeneity [123].

1.5.3 Next-Generation-Sequencing

The field of DNA sequencing in the research and diagnostics changed dramatically during the last ten years with the development of 'next-generation' sequencing methods. In contrast to Sanger Sequencing these methods rely on the massive parallel sequencing of very short DNA fragments [124]. By parallelizing millions of sequencing reactions, it is now possible, to read in an approximately 7-day run 300,000,000,000 bases (= 300Gb), which corresponds to 30 times the human genome. The principle of the new sequencing methods is based on the fact that millions of DNA fragments bound to a small surface are read simultaneously. This can be the DNA of an entire genome (whole genome sequencing), the DNA of all coding regions of a genome (Whole-Exome sequencing) or the DNA of some genes of interest (Targeted/Panel sequencing). During the past years the sequencing costs drop radically. The sequencing of the first human genome took about eleven years, was finished in 2001 and the costs amounted to approximately over $100,000,000 [125, 126]. Using next-generation sequencing instruments it is possible to obtain a complete human genome sequence for approximately $ 1,000 [127]. The Sequencing of the DNA of the patients described in this work was performed on the Illumina/Solexa technology and will be discussed briefly in the following part.

Whole-Genome/Exome Sequencing

The Illumina 'sequencing by synthesis' approach uses reversible terminator chemistry to sequence billions of short, fragmented DNA molecules covalently attached to a glass slide, the so-called flow cell [128]. The flow cell acts as reaction chamber and has eight distinct compartments, referred to as lanes. The sequencing is a stepwise process which subsequently alternates between incorporation of a single nucleotide, complementary to the base in the DNA template, and the detection of the incorporated base, the imaging. Sequencing is performed cycle-wise, where the cleavage of the terminator group marks the end of the cycle. Prior to the sequencing, the DNA sample has to be prepared for sequencing in the so-called library preparation. All steps involved in the library preparation and sequencing using the Illumina technology are now further discussed. The first step is the isolation of patient DNA from nucleated cells and the random fragmentation into 200-300 bases using sonification or mechanical shearing. Specific adaptors, which

supply as universal priming sites during the amplification and sequencing steps, are ligated to the fragmented DNA (Figure 1.7A taken from [129]). At this step the fragments can be enriched by hybridization to complementary sequences for specific genes of interest (Targeted sequencing) or all coding regions (Whole-Exome sequencing) in a physical capture step. It is further possible to mark the DNA fragments from different patients uniquely so that it is possible that they can be sequenced together in one run. This reduces the cost per sample and allows the simultaneous analysis of many samples. Without capture step all fragments will be sequenced (Whole-Genome sequencing) (Figure 1.7B taken from [129]). In order to get distinct clusters, the DNA fragments bound via adapters to surfaces (flow-cells) and are then clonally amplified by PCR (cluster amplification). After this step billion of surface-bound and amplified DNA segments are available for simultaneous sequencing. This starts through the provision of different color-coded fluorescence marked nucleotides (arginine, guanine, cytosine and thymine) to the surfaces. Nucleotides bind the base sequence corresponding to the DNA to be sequenced and are translated while the specific sections for the base color signal are released. The color signal is picked up by a laser scanner and noted. The release of nucleotides, the binding to the DNA fragments, the release of a color signal and the reading of the color signals are repeated up to a hundred times. Then the laser scanner reads for each DNA cluster a particular sequence of fluorescent signals (Figure 1.7C, [129, 130]). With these signals the base sequence of each DNA fragment can be determined (Figure 1.7D, taken from [129]).

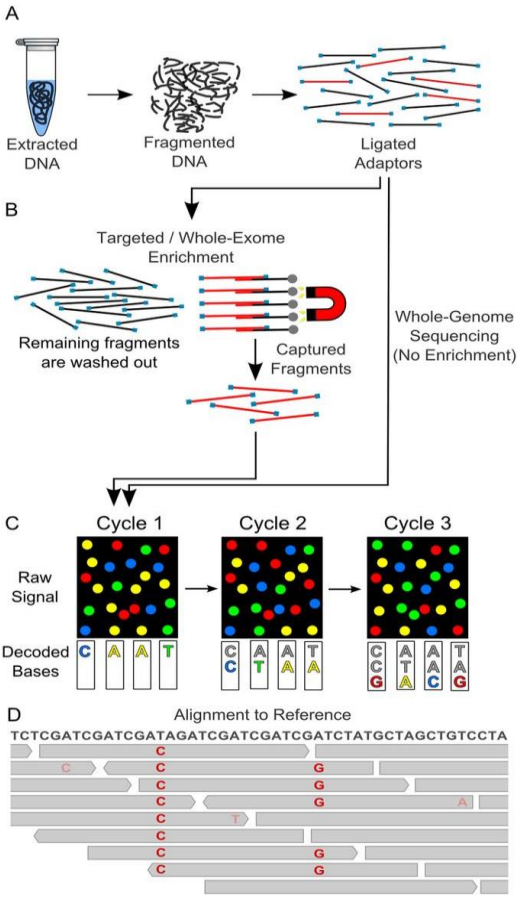

Figure 1.7: Workflow of Targeted/Whole-Exome and Whole-Genome-Sequencing (Picture taken from [129])

Before the data is analysed several million short nucleotide sequences (so called reads) are assigned to the individuals again. The raw sequencing data consist of large data sets in average between 10-100Gb and requires a good bioinformatic analysis. The first step is the mapping (alignment) of the millions of reads to the reference human genome. After the alignment, the reads should overlap to have a good coverage of each base. The next step is called variant calling: each single nucleotide is compared to the reference genome and recorded (Figure 1.7D, taken from [129]). Any difference to the reference is regarded as a variant. A homozygous change would be different from the reference genome in almost all the reads. A patient with a heterozygote mutation would lead to a change in around 50% of the reads. One of the first successful applications of Whole Genome Sequencing led to the discovery of cancer-initiating mutations in previously unidentified genes in one patient with acute myeloid leukaemia [131]. The application of Whole-exome sequencing led to the identification of *DHODH*, which encodes a key enzyme in the pyrimidine de novo biosynthesis pathway and is causative for Miller syndrome around 10 years ago [132]. This is followed by the identification of the first reported identified heterozygous de novo variants in *SETBP1* as causative for Schinzel-Giedion-syndrome [133] and *MLL2* as the cause for Kabuki Syndrome [134]. The average time from the blood sample to the diagnosis via Whole-Exome/Genome-Sequencing is about 2-4 weeks or in some cases even longer. But the time of waiting to get the diagnosis can be crucial in some patients. The knowledge of the genetic cause can help to find the right therapy for the patient [135]. A recent paper about NGS in diagnostics could show that it is possible to perform Whole-Genome-Sequencing in about 50 hrs [136]. In monogenic diseases the disease progression is extremely rapid and even when the phenotype is heterogeneous in new-borns, the molecular diagnosis must occur quickly to be relevant for the right therapy. This could also prevent treatments based on nonspecific or obscure symptoms, which can be unhelpful or dangerous.

Beside the big advantages of using next-generation sequencing as a diagnostic tool there are still some disadvantages. The read length (around 35-400bp) is significantly lower than Sanger sequencing. Second, the sensitivity and specificity of the detection of structural mutations like microlesions (small indels, tandem repeats) and macrolesions (deletions and duplications) are still challenging. During the last five years big progresses were made to improve the detection of copy number variations (CNVs) also from NGS data [137, 138]. Base calling errors or not-interpretable areas due to low coverage might be remediable to some extent by increasing coverage to achieve higher consensus accuracy [139]. The ethical consequences or how to deal with random findings are also not clear [140].

Targeted –Panel diagnostic

A part of the disadvantages using NGS for diagnostics can be overcome with the use of Targeted sequencing (or panel diagnostic). In this specific form of exome sequencing only a certain amount of genes are filtered out from the whole genome [141]. The coverage of the panel genes is normally higher, the cost and the duration of such an experiment are normally lower than in whole exome sequencing projects, which makes it even more attractive for clinicians. The random findings by classical exome and genome

sequencing are obviously also not possible. In the case of mitochondrial disorders, mutations in more than 320 genes have been identified to date, which are characterized by phenotypic and genetic heterogeneity. The group of Calvo et al. performed "MitoExome" sequencing of the mtDNA and exons of ~1000 nuclear genes encoding mitochondrial proteins and prioritized rare mutations predicted to disrupt function in 42 infantile patients [119]. They found in 24% of the patients' variants in genes, which were previously reported and in 31% variants, which were not reported so far. In 45% of all cases the molecular diagnosis remains still unclear. These percentages of successful diagnosis are comparable to other studies in which whole exome sequencing was used for patients with mitochondrial disorder [91].

1.6 Therapy for mitochondrial disorders

1.6.1 General information

In the last decade major advances in the biochemical and molecular diagnostics and the deciphering of complex I structure, function, assembly and pathomechanism have been made. But there are currently no satisfactory treatment options for patients with mitochondrial complex I defects. Different pharmacological agents have been tested, including vitamins, cofactors, quinone derivatives, artificial electron acceptors, or free radical scavengers, but despite clinical improvements observed in isolated cases, there is no hard evidence in support of these treatments. The strategies include gene therapy (replacement or repair), controlled regulation of specific transcriptional regulators, metabolic manipulation (ROS scavenging, normalization of the mitochondrial membrane potential), stimulation of mitochondrial biogenesis, bypassing of OXPHOS complexes or the alteration of the balance between wild-type and mutated mtDNA (e.g. by exercise training) [142]. Furthermore, most of them focus on symptoms rather than on the cause of the disease, and in particular do not target the respiratory chain enzyme deficiency. Some interventions were or are at the moment tested in clinical studies in humans, in animal models or are still at the level of in vitro research.

1.6.2 Bezafibrate treatment in vitro and in vivo

Bezafibrate is a drug of the group of fibrate drugs which belongs to the class of amphipathic carboxylic acids. It is a well-known drug which has been used for more than 40 years in the treatment of hyperlipidaemia. The main effect is the lowering of LDL cholesterol and triglyceride in the blood, and the increase of HDL. Bezafibrate binds to the peroxisome proliferator-activated receptor (PPAR) which binds to a specific DNA sequence (DNA response element) and later leads to the activation of gene transcription [143-145]. Bastin and Djuoadi provided evidence from in vitro studies that activation of the PPAR/PGC-

1-alpha pathway with bezafibrate could be a new therapeutic approach for patients with mitochondrial disorders. They treated five patient-derived cell cultures with genetically confirmed complex I deficiency (affecting the genes *NDUFS1*, *NDUFS3*, *NDUFS4*, *NDUFV1* and *NDUFV2*) with bezafibrate, in order to upregulate residual metabolic capacities. Cells were treated with 400µM bezafibrate for 72 hours, after which increased complex I activity was observed in three of the five cell lines. The bezafibrate effect was due to a stimulation of the transcription of the various genes confirmed by qPCR experiments. This upregulation was probably due to the stimulation of PGC1α-expression by bezafibrate [146]. The pivotal role of PGC1-α as the master regulator of mitochondrial biogenesis, makes it a particularly attractive therapeutic target to induce stimulation of residual metabolic capacities in patients with respiratory chain deficiencies. Another recent study has demonstrated an effect of bezafibrate on homoplasmic cybrids carrying the most common mtDNA mutations [147]. Bezafibrate strongly induces PGC1-α and TFAM mRNAs (two-three fold change) and increases oxygen consumption (32%) of fibroblasts in the presence of complex I substrates. Another in vitro study on patient fibroblast cell lines was performed in the group of Ann Saada. They screened patient cell lines with mutations in *NDUFS2*, *NDUFS4* or assembly factors *NDUFAF4*, *C20ORF7*, *FOXRED1* and *NDUFA12L*. The cell lines with mutations in *C20ORF7*, *NDUFS4* and *NDUFA12L* showed a mixed response in growth rate, ROS and ATP production. The cell line with FOXRED1 mutation showed no significant difference whereas the cell lines with the remaining mutations responded positive to the bezafibrate treatment [148]. In the study of Casarin et al. a positive effect of bezafibrate was observed in patient cell lines with mutations in *SCO2* and *SURF1* leading to a severe complex IV defect with fatal infantile cardioencephalomyopathy [149]. The treatment led to an increase of the remaining complex IV activity accompanied by an increase in ATP production. Interestingly they detected only an increase in enzymatic activities of complex I, complex III, and complex IV. Other mitochondrial proteins, like the matrix enzyme citrate synthase (CS) or other enzymes localized to the mitochondrial inner membrane, such as complex II and SCO2 protein itself, were unaffected by bezafibrate treatment. This findings militate against an overall effect of bezafibrate on mitochondrial biogenesis as a whole as postulated by [150]. The second exciting finding in this study was the synergy effect of copper and bezafibrate. Previous studies showed already a positive effect of copper in the treatment of patients with SCO2 mutations but had problems with the toxic side effects [151, 152]. The additive effect of bezafibrate and copper could lead to a decrease of the doses of each compound. The first investigation of the effect of bezafibrate in a mouse model for respiratory chain deficiency was performed by Wenz et al. [153]. They treated a mouse model of mitochondrial myopathy, caused by a cytochrome c oxidase deficiency with bezafibrate. The treatment led to a stimulation of residual respiratory capacity in muscle tissue. Mitochondrial proliferation resulted in an enhanced OXPHOS capacity per muscle mass and a delayed onset of the myopathy and a markedly prolonged life span. They found that the overall mitochondrial mass was increased due to increased mitochondrial biogenesis. In the case of a nuclear defect you still have mitochondria with a reduced OXPHOX activity per cell. But you have more mitochondria per cell and therefore an increased OXPHOS capacity per cell. Patients with mtDNA mutation have still some healthy mitochondria depending on the heteroplasmy grade. The increase of

mitochondria per cell would in this case also lead to an increase in OXPHOS capacity (Figure 1.8, taken from [150])

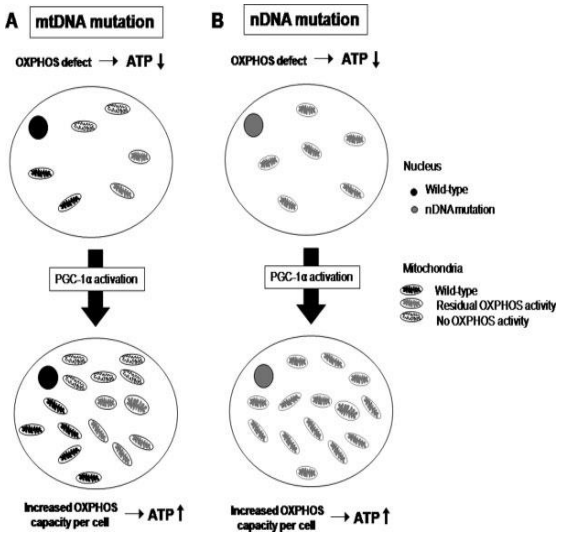

Figure 1.8: Model of effect of bezafibrate treatment via activation of PPAR/PGC-1-alpha pathway (Picture taken from [150])

A more recent publication from the group of Suomalainen reported a positive effect of bezafibrate in a muscle-specific knock-out of *COX10* but not in a constitutive knock-out of *Surf1*. Bezafibrate delayed significantly the accumulation of COX-negative fibers and multiple mtDNA deletions but mitochondrial biogenesis was not induced. Furthermore, bezafibrate induced severe lipid oxidation effects, with hepatomegaly and loss of adipose tissue [154]. These negative side effects in the liver were also observed in a study from Viscomi et al. in *SURF1* and *COX15* KO mice [155]. Another in vivo study was performed by Dillon et al. [156]. This group treated the mitochondrial DNA (mtDNA) mutator mouse (mouse model of aging that harbors a proofreading-deficient mtDNA polymerase γ) with bezafibrate for eight months. These mice develop many features of premature aging including hair loss, anemia, osteoporosis, sarcopenia, decreased lifespan and increased mtDNA mutations and marked mitochondrial dysfunction. The bezafibrate treatment delayed the hair loss and improved skin, spleen aging-like phenotypes, and resulted in an increase in markers of fatty acid oxidation in these tissues but no detection of a generalized increase in mitochondrial markers. They found no improvements in muscle function or lifespan, which we attributed to the rodent-specific hepatomegaly associated with fibrate treatment. In the latest in vivo study from Noe et al. a murine model with a forebrain-specific cytochrome *c* oxidase deficiency caused by conditional deletion of the *COX10* gene was treated with bezafibrate for six months [157]. They found an improved phenotype of the mice associated with an increase in mitochondrial proteins and mitochondrial ATP generating capacity. Interestingly they found a neuroprotectiv effect accompanied with attenuated astrogliosis and decreased levels of inflammatory markers in the affected tissues. Two older studies from the group of Bastin showed that bezafibrate treatment has also a positive effect in patient fibroblast cell lines harbouring mutations in the fatty acid oxidation pathway by upregulating of ß-oxidation enzymes. The first study was performed with patient cell lines having mutations in Carnitine palmitoyltransferase 2 (CPTII). The bezafibrate treatment in cell lines with a residual CPTII enzyme activity responded positive

and led to normalization of 3H-palmitate and 3H-myristate cellular oxidation rates [158]. The second study was performed on four cell lines with mutations in *VCADL*. Similar to the CPTII study only the cell lines with residual activity responded to the treatment with the almost complete restoration of VCADL activity [159]. This positive effect of the CPTII in vitro study was later confirmed in a clinical study from Bonnefont et al. [160]. After the three-year treatment the patients refer to an improvement in the overall condition with an increase in physical activity and a decline in muscular pain. In contrast to that, in a second clinical trial with ten patients with CPTII or ACADVL deficiencies bezafibrate treatment indeed lowered low-density lipoprotein, triglyceride and free fatty acid concentrations but failed to improve palmitate oxidation, to increase fatty acid oxidation (FAO) or to lower heart rate during exercise [161]. Nevertheless, the group of Prof. Sperl in Salzburg started with bezafibrate treatment of five patients with PDH or complex I defect respectively in the framework of individual curative trials. Some patients responded positively to the treatment with a prolonged exercise tolerance. These first positive results will be evaluated in a bigger clinical trial with children from different centres in Austria and Germany starting in the end of 2013.

1.6.3. Riboflavin treatment

Another potential substance which is already in use to treat patients with mitochondrial disorders is riboflavin, or vitamin B_2. It is a central component and precursor of flavin adenine dinucleotide (FAD) and flavin mononucleotide (FMN). FAD and FMN are essential cofactors of numerous dehydrogenases involved in fatty acid beta-oxidation, branched chain amino acid catabolism, mitochondrial electron transport chain, and in the tricarboxylic acid cycle [162]. Up to date four groups of patients are reported to be responsive to the riboflavin treatment: 1. Patients with multiple acyl-CoA dehydrogenase deficiency and mutations in electron transferring flavoprotein genes (*ETFA/ETFB*) and its dehydrogenase (*ETFDH*); 2. Patients with Brown-Vialetto-Van Laere and Fazio-Londe syndromes with mutations in the riboflavin transporter *SLC52A3* (*C20orf54*) [163] and *SLC52A2* [135]; 3. Patients with the haploinsufficiency of another riboflavin transporter gene *GPR172B* [164]; the fourth group are patients with mutations in *ACAD9* leading to an assembly defect of complex I [113, 165]. FAD is the catalytic cofactor of the ACADs. Riboflavin is known to foster their assembly and stability which might explain the beneficial effect of the treatment in some patients with complex I defect [166-169]. Recently Nouws et al. reported a patient with a new mutation in *ACAD9* who did not respond to riboflavin [170]. A review on the medical course of 15 patients with different mitochondrial disorders supplemented with a cocktail of different vitamins (Coenzyme Q10, Vitamine B10, Vitamine C and Riboflavin) was published in 2004. Nine patients responded to the therapy with the temporary attainment of developmental skills and five patients died. Two patients with recurrent seizures had a significant reduction of the severity of the seizures and one had no further seizures [171]. Nevertheless a bigger clinical study with follow-up data of a larger cohort of

individuals especially with ACAD9 mutations is needed to verify the clinical efficacy of a supplementation with riboflavin [113].

1.6.4 Further treatment options

Beside the mentioned small molecules bezafibrate and riboflavin, far more compounds were tested in vitro and in vivo. In the already mentioned in vitro study on patient fibroblast cell lines performed by the group of Ann Saada they evaluated, beside bezafibrate, ten further small molecules for their therapeutic potential. They revealed the compound 5-Aminoimidazole-4-carboxamide ribotide (AICAR) to be the most beneficial compound in improving growth and ATP content while decreasing ROS production. They observed an increased mitochondrial biogenesis without altering the mitochondrial membrane potential ($\Delta\psi$) and activation of the AMP activated protein kinase (AMPK). The other feasible compound was Oltipraz (1,2-dithiole-3-thione) [148]. This compound has antioxidant properties and it has been demonstrated to reduce apoptosis in cells with chemically inhibited complex I by exerting its cytoprotective effect through AMPK. All other polyphenolic phytochemicals (resveratrol, grape seed extract, genistein, sodium phenylbutyrate and epigallocatechin gallate) had a mixed response, failed to improve mitochondrial function or were detrimental [148]. Recently Djouadi and her group tested the effect of resveratrol on control and 16 different complex I or complex IV –deficient patients' fibroblasts (NDUFV1, NDUFV2, NDUFS1, NDUFS3, NDUFS6, C8orf38, COX10 and SURF1). They could show that resveratrol stimulates the expression of a panel of proteins representing structural subunits or assembly factors the respiratory chain [172]. Three out of six cell lines with NDUFV1 mutation and one cell line with COX10 and NDUFV2 mutation respectively significantly increased their protein levels and stimulated residual enzyme activity, whereas the treatment with resveratrol had no effect on cell lines with NDUFS1, NDUFS3 and SURF1 mutation. The cell lines with a positive effect presented also increased cellular O_2 consumption levels, a prevention of the accumulation of lactate and induced mitochondrial biogenesis. They could further prove that the increased mitochondrial function was mainly independent from SIRT1 and AMPK-pathway and was rather involved in the estrogen receptor and estrogen-related receptor alpha signalling pathway [172]. The positive effect of AICAR, found from the group of Ann Saada, was also observed in the *SURF1*, *SCO2*, and *COX15* KO mouse. They found a partial correction of COX deficiency in all three models, and a marked amelioration of motor performance up to normal in the *SCO2* KO mouse. This finding was supported by an unchanged Nrf1 and Nrf2 gene expression but a significant increase in Tfam and the COX subunit encoding genes [155]. In contrast to the study of Ann Saada in in vivo models such as on mice and rats resveratrol treatment led to an increase in running time and consumption of oxygen in muscle fibres indicating an increased anaerobic capacity. Genes associated with oxidative phosphorylation and mitochondrial biogenesis were induced, PGC-1alpha acetylation was decreased and PGC-1alpha activity was increased [173, 174]. Beside the relatively new compounds bezafibrate, riboflavin, AICAR and resveratrol, CoenzymeQ10 (CoQ10) has been used for more than 15

years for the treatment of mitochondrial disorders. The positive effect is well documented in patients with CoQ10 deficiency and especially patients with COQ2 mutation. Patients with mutations in *PDSS2* and *COQ9* and mutations causing a secondary CQ10 defect respond very heterogeneous to the treatment. This could be due to the poor bioavailability and delayed mitochondrial uptake of ubiquinone. The synthetic compound idebenone, a benzoquinone carrying exactly the same quinone moiety as CoQ_{10}, shows multiple activities in vitro and in vivo. One activity is its potent antioxidant capacity and the protection against ROS-induced damage in multiple systems. More important for patients with complex I-defect is the discovery that certain short-chain quinones are able to bypass the deficiency in complex I by shuttling electrons directly from the cytoplasm to complex III of the mitochondrial respiratory chain to produce ATP [175]. An improvement of brainstem and respiratory function was reported in a patient with Leigh-Syndrome after idebenone treatment [176]. Moreover the efficiency of idebenone was tested in a clinical study with a specific group of 85 patients with Leber's hereditary optic neuropathy (LHON) and was reported in single case reports of patients with MELAS [177-179]. An in vitro study was performed on cybrid cells harbouring the G3460A/MT-ND1 mutation of LHON and cells with a stop mutation in *ND1* that hampers complex I assembly. Both appendages report at least in part of an improvement. Patients with discordant visual acuities are the most likely to benefit from idebenone [180]. After the treatment the cybrid cells sustained membrane potential in intact cells and ATP synthesis in permeabilized cells and restored a good level of coupled respiration in complex I-deficient cells [181]. More recently another synthetic modification of the natural form of CoQ10 EPI-743 (para-benzoquinone) was tested in a cohort of 13 children and one adult with genetically-confirmed mitochondrial disease (polymerase γ deficiency, n = 4; Leigh syndrome, n = 4; MELAS, n = 3; mtDNA deletion syndrome, n = 2; Friedreich ataxia, n = 1).
EPI-743 was shown to be more than ten thousand times as potent as CoQ10 and idebenone in protecting cells from oxidative stress in patient fibroblasts assays [182]. 12 of the 14 cases survived and eleven of them demonstrated clinical improvement, with three showing partial relapse, and ten of the survivors also had an improvement in quality-of-life scores at the end of the 13-week emergency treatment protocol [183]. This positive effect was further validated in a group of ten children with genetically defined Leigh-Syndrome. All cases, independent from the genetic determinant or disease severity, in this open label design study showed a neurological and neuromuscular improvement [184]. Not only patients with Leigh-Syndrome also patients with LHON seem to benefit from EPI-743 supplementation. Four out of five patients with genetically confirmed LHON and acute loss of vision had an arrested disease progression and reversed vision loss [185]. Just recently it was shown that the treatment of ACAD9 deficient fibroblast cells with JP4-039, a novel mitochondrial-targeted antioxidant, lowered the levels of superoxide production and increased basal and maximal respiratory rate [186]. Two novel approaches, with complete other strategies, may offer hope for preventing and treating mitochondrial disease: mitochondrial replacement therapy and CRISPR/Cas9 [187]. Mitochondrial replacement or manipulation therapy uses two main techniques; the maternal spindle transfer or pronuclear transfer. [188]. The naked nucleus with the nuclear DNA from the mother could be transferred to a normal enucleated host oocyte from another donor with healthy mitochondrial DNA and then implanted to the woman uterus. The first successful

human pronuclei transfer was published in 2010. In this study they showed that only a minimum of mtDNA was carried from the donor to the acceptor. It was compatible with onward development to the blastocyst stage in vitro and were destroyed at six days of age [189]. This novel technique was permitted in the United Kingdom in 2015. The embryo generated using this technique is termed a "three-parent embryo" since its genome is derived from three sources: genetic characteristics of mainly its mother and father, but also some from the mitochondria of the egg donor [142, 190, 191]. The first three-parent baby was claimed to be born in Mexico in 2016 [192, 193]. The CRISPR/Cas9 technique (by genome editing) exploits the principles of bacterial immune function to target and remove specific sequences of mutated DNA [187]. It has been already successfully employed to produce mitochondrial sequence-specific cleavage. Furthermore the use of mitoCas9 (whose localization is restricted to mitochondria matrix) would reduce the risk of off-target mutations in the embryos and prospective children [194]. Although all these new techniques might help to prevent the inheritance of disease or treat individuals it raises a lot of ethical concerns and the safety of the techniques are yet to be established [192, 195].

The application of NGS revolutionized the research and diagnostics of mitochondrial disorders. During the last five years approximately more than 100 new genes responsible for OXPHOS defects were discovered; not only respiratory chain complex subunits but more and more defects in cofactors and substrates were identified. Each new gene might need a new therapeutic strategy.

1.7 Purpose of the work

Mitochondrial disorders are a heterogeneous group of diseases displaying a variable degree of dysfunction of the mitochondrial OXPHOS system. The use of NGS, especially Whole-Exome sequencing, offered new possibilities in the research and diagnostic area. Despite the big improvements made to find the genetic basis of the disease, treatment options are still very limited. This work is divided into two big parts. The aim of the first part of this study was to use NGS to detect new pathogenic variants in patients with mitochondrial disorders, particularly complex I deficiency. Beside the verification of the pathogenicity of the found variant, a better understanding of the underlying molecular pathomechanisms and genotype-phenotype correlations was achieved. Fibroblast cell cultures of patients with different mitochondrial disorders, together with good clinical information, were collected and established. In a second step new polarographic and biochemical methods were developed to measure oxygen consumption and enzyme activity in cells. During this work the DNA of six patients with unclear genetics, but clear biochemical defect, were used for WES. The potential pathogenic variants found via exome sequencing were verified with a lentiviral complementation assay. The wt-DNA of the affected gene was therefore expressed into the patient cell line and the effect was analysed with different methods. A focus was made on patients with mutations in *ACAD9*. The clinical, biochemical, and genetic spectrum of 70 patients with ACAD9 deficiency were analyzed in detail (Figure 1.9).

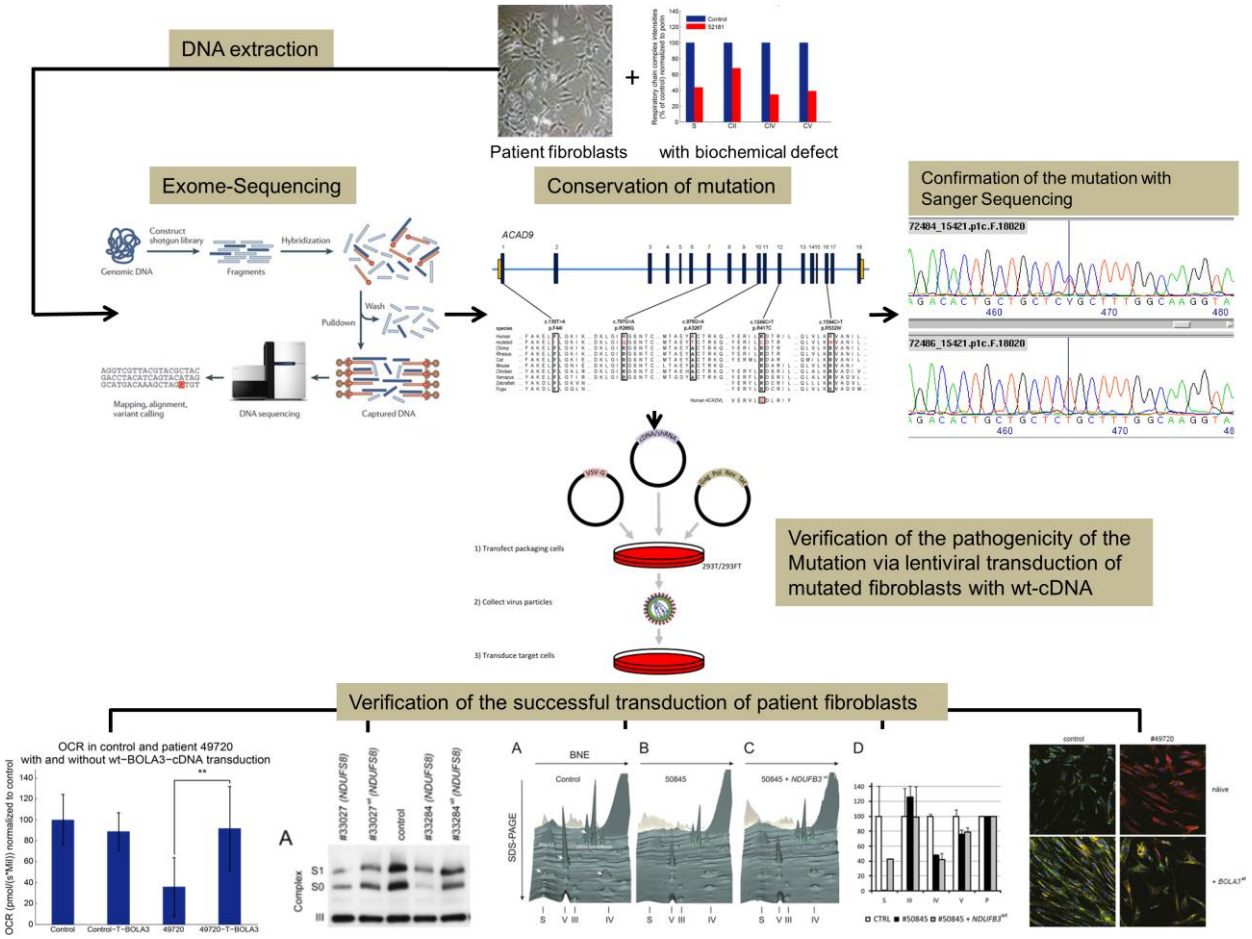

Figure 1.9: Overview of the experiments performed to identify and verify new gene variants detected in patients with mitochondrial disorders

The second part of the thesis aimed to identify new treatment options for patients with mitochondrial disorders. Based on previous studies the effect on the respiratory chain of four substances (bezafibrate, riboflavin, resveratrol and AICAR) was tested in vitro. The effect was tested on respiratory chain complex activity, gene expression and protein level. The different strategies used are illustrated in figure 1.10.

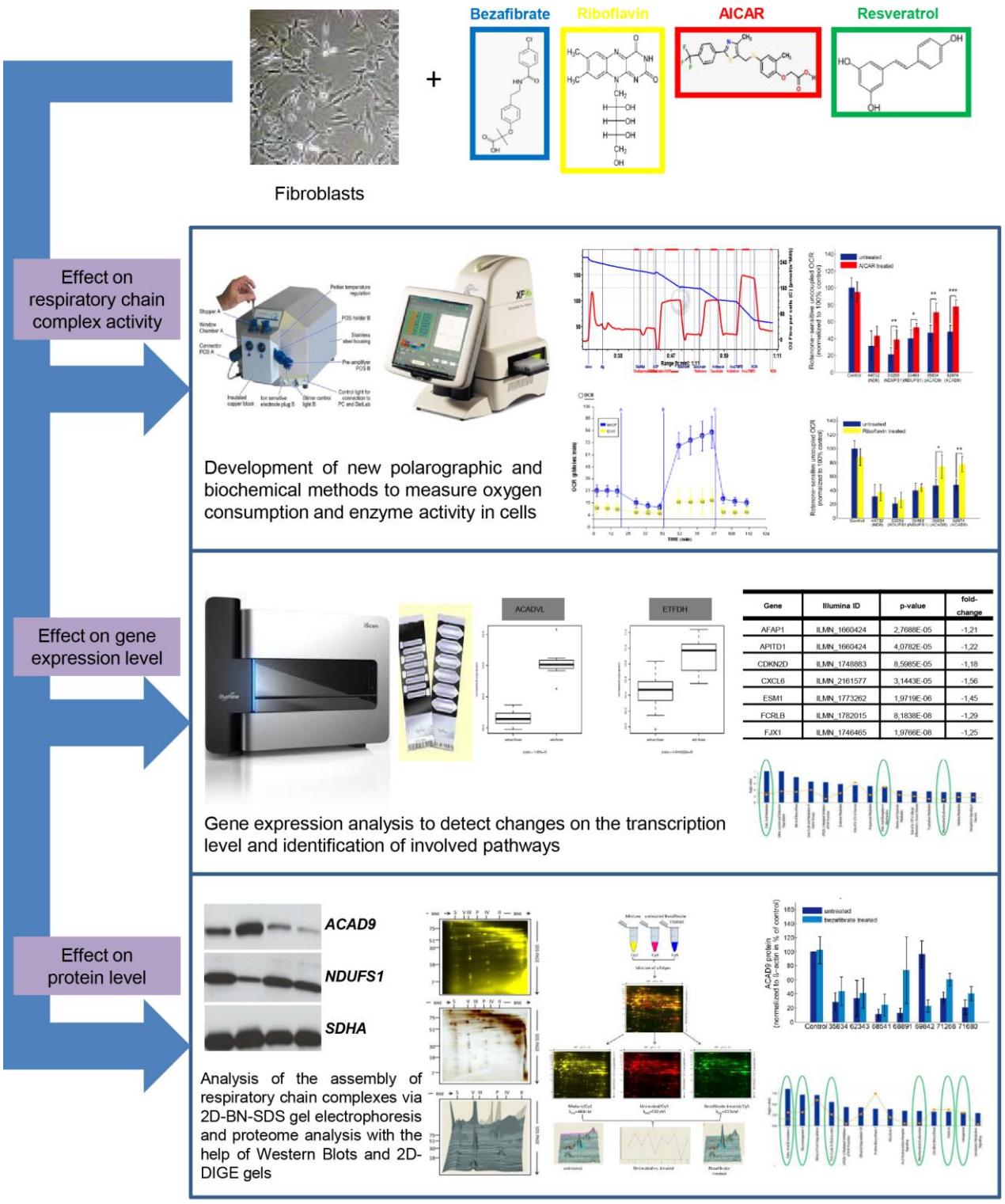

Gene	Illumina ID	p-value	fold-change
AFAP1	ILMN_1660424	2,7688E-05	-1,21
APITD1	ILMN_1660424	4,0782E-05	-1,22
CDKN2D	ILMN_1748883	8,5985E-05	-1,18
CXCL6	ILMN_2161577	3,1443E-05	-1,56
ESM1	ILMN_1773262	1,9719E-06	-1,45
FCRLB	ILMN_1782015	8,1838E-08	-1,29
FJX1	ILMN_1746465	1,9766E-08	-1,25

Figure 1.10: Overview of the experiments performed to test different treatment options on fibroblast cell lines from patients with mitochondrial disorder

2 Materials and Methods

2.1 Materials

2.1.1 Reagents, media and buffers

Compound	Company
Acetyl-Coenzym A	Sigma-Aldrich
Adenosine diphosphate	Sigma-Aldrich
Agar-Agar, Kobe I	Roth
AICAR	Sigma-Aldrich
Ampicilline	Sigma-Aldrich
Antimycin A	Sigma-Aldrich
Ascorbate sodium salt	Sigma-Aldrich
ATX Ponceau S red staining solution	Fluka
Bezafibrate	Sigma Aldrich
Bio-Rad Protein Assay	Bio-Rad Laboratories GmbH
Biozym DNA Agarose	Biozym
Blasticidin S HCL	Invitrogen
Blotting Grade Blocker Non-Fat Dry Milk	BioRad Laboratories
Boric acid	Sigma-Aldrich
Bovine Serum Albumin	PAA Laboratories GmbH
Bromophenol blue	Fluka
Calciumchlorid	Sigma-Aldrich
CHAPS	Sigma-Aldrich
Coomassie (R) Brilliant Blue R250	Fluka
Cytchrome c from horse heart	Sigma-Aldrich
D-(+)-Galactose, anhydrous	Sigma-Aldrich
D-Mannitol	Sigma-Aldrich
Decylubichinon	Sigma-Aldrich
Digitonin High Purity	Calbiochem
Dikaliumhydrogenphosphat	Merck

Dimethylsulfoxide	Sigma-Aldrich
Dinatriumhydrogenphosphat	Merck
DL-Dithiothreitol (DTT)	Sigma-Aldrich
DTNB	Sigma-Aldrich
ECL Plus Western Blotting Detection System	Amersham
EDTA	Sigma-Aldrich
EGTA	Sigma-Aldrich
Ethidium bromide	Roth
FCCP	Sigma-Aldrich
Fluorescein	Fisher Scientific
Formic acid	Sigma-Aldrich
G418 disulfate salt solution	Sigma-Aldrich
Gibco - 0,05%-Trypsin-EDTA	Invitrogen
Gibco - DMEM - No glucose	Invitrogen
Gibco - Dulbecco's Modified Eagle Medium – DMEM – High glucose	Invitrogen
Gibco - Dulbecco's Phosphate Buffered Saline	Invitrogen
Gibco - Fetal Bovine Serum	Invitrogen
Gibco - Pen Strep	Invitrogen
Glycerol	Merck
Glycine	Roth
HCl	Merck
HEPES	Sigma-Aldrich
Iodacetamid	Sigma-Aldrich
JC-1 dye	Life technologies
L-Glutamic acid	Sigma-Aldrich
L-Malic acid	Sigma-Aldrich
Lysine	Sigma-Aldrich
Monopotassium phosphate	Merck
Magnesium chloride	Sigma-Aldrich
Methanol	Merck
MitoSOX Red	Life Technologies
NADH	Roche
NP-40	Sigma-Aldrich
Orange G	Sigma-Aldrich
Oxalacetate	Sigma-Aldrich

Phenylmethylsulfonylfluoride	Sigma-Aldrich
PMP	Seahorse Bioscience
Potassium chloride	Merck
Potassium cyanide 97% (KCN)	Sigma-Aldrich
Riboflavin	Sigma-Aldrich
Rotenone	Sigma-Aldrich
Sodium chloride	Merck
Sodium deoxycholate	Sigma-Aldrich
Sodium dodecyl sulfate	Roth
Sodium dithionite	Merck
Sodium-Pyruvate	Sigma-Aldrich
Succinate	Sigma-Aldrich
Sucrose	Merck
Sypro Ruby	Sigma-Aldrich
Taurine	Sigma-Aldrich
Tetramethylphenylendiamin	Sigma-Aldrich
Thiourea	Sigma-Aldrich
Tris	Merck
Tris-HCl 1M pH = 7,8	Rockland
Tris-HCl 1M pH = 8,0	Rockland
Triton X-100	Merck
Trizma-Base	Sigma-Aldrich
Trypton/Pepton from Casein	Roth
Tween® 20	Sigma-Aldrich
Urea	Sigma-Aldrich
Uridine	Sigma-Aldrich
Yeast extract	Roth

Table 2.1: List of reagents, medias and buffers

2.1.2 Antibodies, ladders and enzymes

Name	**Company**
ACAD9 antibody	Sigma Aldrich, Kind gift from Prof. Vockley
ACADVL antibody	Kind gift from Prof. Vockley
ACADM antibody	Kind gift from Prof. Vockley

Anti-mouse	Amersham Bioscience
Anti-rabbit	Amersham Bioscience
ß-actin antibody	Sigma-Aldrich
CIII subunit core 2 antibody	Mitosciences
MTFMT antibody	Sigma-Adrich
NDUFA9 antibody	Abcam
NDUFB8 antibody	Mitosciences
NDUFB9 antibody	Santa Cruz Biotechnology, Inc.
NDUFS1 antibody	Abcam
NDUFS3 antibody	Mitosciences
OXPHOS antibody cocktail	Abcam
Porin antibody	Mitosciences
SDHA antibody	Abcam
GeneRuler 1kb DNA Ladder	Fermentas
PageRuler Prestained Protein Ladder	Fermentas

Table 2.2: List of antibodies, ladders and enzymes

2.1.3 Kits

Name	**Company**
6000 Nano LabChip reagent set	Agilent
AllPrep DNA/RNA Mini/Midi Kit	Qiagen
CyDye DIGE Fluor, minimal labelling dye (2nmol)	GE Healthcare
CyQuant Cell Proliferation Assay Kit	Invitrogen
Effectene® Transfection Reagent	Qiagen
First strand cDNA synthesis kit	Fermentas
Illumina TotalPrep-96 RNA Amp Kit	Ambion
Lipofectamine™ LTX and PLUS™ Reagents	Invitrogen
pLenti6.3⁄V5-TOPO® TA Cloning® Kit	Invitrogen
QIAGEN Plasmid Midi Kit	Qiagen
QIAPrep Spin Miniprep Kit	Qiagen
QuickChange™ XL Site-Directed Mutagenesis Kit	Stratagene
Taq Polymerase	Qiagen
ViraPower™ Bsd Lentiviral Support Kit	Invitrogen

Table 2.3: List of kits

2.1.4 Equipment and Software

Equipment/Software	Company
4800 MALDI-TOF/TOF analyzer	AB Sciex
Analysis scales BP221S	Sartorius
Autoclave Systec 5075 ELV	Systec
BioTools 2.2	Bruker Daltonik
CO_2 incubator	Sanyo
DeCyder™software version 7.0	GE Healthcare
EasyJect Plus	Wolf Laboratories
EasyWin 32	Herolab
Elctrophoresis chamber	Owl Seperation Systems Inc.
FACS-Canto II	BD
FACS-DIVA software	BD
Incubator (37°C)	Memmert
LTQ Orbitrap XL	Thermo Scientific
Liquid Nitrogen Tank	Chronos Messer
Magnetic stirrer RH basic	IKA Labortechnik
Mascot 2.2 search engine	Matrix Science
NanoDrop ND-1000 Version 3.5.2	Thermo Scientific Abgene
OROBOROS Oxygraph-2k	Oroboros Instruments
Oxygraph-2k: DatLab Software	Oroboros Instruments
Potter S, IKA Eurostar digital	IKA
Precision scales Basic Plus BP2100	Sartorius
PTC 225 Peltier Thermal Cycler	MJ Research
Rotanta 46 RS	Hettich Zentrifugen
Rotator SB3	Stuart Benchtop Equipment
Sanyo CO2 Incubator - MCO 17AIC	Sanyo
Scepter 2.0 Handheld Automated Cell Counter	Millipore
Shaker Duomax 1030	Heidolph Instruments
SIGMA Centrifuge 3K30	SIGMA Laborzentrifugen GmbH
SIGMA Centrifuge 4K15C	SIGMA Laborzentrifugen GmbH
SIGMA Centrifuge 6K15	SIGMA Laborzentrifugen GmbH
Spektrophotometer Jasco V-550	Jasco
Typhoon™ 9400 Imager	GE Healthcare
Ultra-low temperature freezer VIPTM	Sanyo Scientific

Ultraspec 3300 pro UV/Vis photometer	GE Healthcare
UVT-40-M	Herolab
Vortex Genie 2 Scientific Industries	VWR
Water bath HRB 4 digital	IKA Labortechnik
XF 96 Extracellular Flux Analyzer	Seahorse Bioscience

Table 2.4: List of equipment and software

2.1.5 Material

Name	**Company**
96 well microplate	Ratiolab
96 well plates (perforated)	Thermo Scientific
ABgene® PCR Plates	Thermo Scientific
Adhesive PCR Film	Thermo Scientific
Cell culture plates 6-well/10cm/14cm	Nunc
Cell Scraper 25cm	Greiner Bio One
Eppendorf Safe-Lock tubes (0,2-2ml)	Eppendorf
FACS tubes	BD Bioscience
Falcon conical tubes 15/50 mL	BD Bioscience
Filter Tips 10-1000µl	Greiner Bio One
Filtertop cell culture flask (25, 75, 175cm^2)	Greiner Bio One
Gel loading pipetting tips	Greiner Bio One
Hot-sealable aluminium foil	Pierce
Hybond™ Blotting Paper	GE Healthcare
HybondTM-P	GE Healthcare
Hyperfilm™ ECL High performance chemiluminescence film	GE Healthcare
Insulin syringe U-100 (0,5ml, 0,3mm x 8mm)	BD Bioscience
MILLEX GP; syringe filter unit, 0.22/0.45 µm	Millipore
NativePAGE™ Bis-Tris Gel (4-16%)	Life Technologies
PAGEr GELS (4-12%T-G, 10-20%T-G, 15%)	LONZA
QIAshredder	Qiagen
Safe lock reaction tubes 0.5/1.5/2.0 ml	Eppendorf
Scepter Sensors, 60 µm	Millipore
Serological Pipettes 1 to 50 ml	Greiner Bio One
Steritop-GP filter unit, 0.22/0.45 µm	Millipore

TC Dish 140x20	Nunc
TC Dish 60x15	Nunc
TC Dish 92x17	Nunc
Trap column	Agilent
Universal pipette tips (0,5-1000µl)	Greiner Bio One
XF-96 2 port FluxPaks	Seahorse Biosience
XF-96 4 port FluxPaks	Seahorse Biosience

Table 2.5: List of material

2.2 Molecular biology methods

2.2.1 DNA/RNA isolation

2.2.1.1 DNA and RNA isolation from cells

The isolation of RNA and DNA from human fibroblasts was performed with the AllPrep DNA / RNA mini kit from Qiagen. The isolation was done according to the manufacturer's protocol. Fibroblasts were collected and resuspended in 700µl RLT Plus buffer. After homogenization using a QIAshredder column, the sample was applied to an AllPrep DNA spin column and centrifuged at 14000rpm for 30s. The column with the bound DNA was placed for subsequent DNA isolation into a new Eppendorf tube and stored at 4°C. For the isolation of the RNA, 700µl of 70% ethanol was added to the flow through of the DNA column and transferred to the RNeasy column and centrifuged for 15s at 14000rpm. The flow through was discarded and the membrane was washed with 700µl RW1 washing buffer followed by centrifugation for 15s at 14000rpm. After removal of the flow-through, 500µl buffer RPE was transferred onto the membrane and the column was centrifuged at 14,000rpm for 15s. For complete removal of the wash buffers an additional centrifugation for 2min at 14,000rpm was performed. In order to elute the RNA from the membrane, the column was placed in a new Eppendorf tube and 50µl of RNAse free water was added and centrifuged for one minute at 14000rpm. The obtained RNA was kept at -80°C until further use.
For DNA isolation 500µl buffer AW1 was applied to the AllPrep DNA spin column mentioned above and centrifuged for 15s at 14000rpm. The flow through was discarded and 500µl buffer AW2 was added to the column followed by centrifugation at 14000rpm for 2min to wash the membrane. The column was placed into a new Eppendorf tube and 100µl buffer EB was pipetted onto the membrane. After incubation for 1min at room temperature (RT) the DNA was eluted by centrifugation at 14000rpm for 1min. The resulting DNA was stored until use at 4°C.

2.2.1.2 Isolation from plasmid-DNA from bacteria

The extraction of plasmid DNA was performed with the Midiprep kit form Qiagen according to the manufacturer's protocols. The bacteria were collected by alkaline lysis and absorbed on a silica gel membrane. After several washing steps the plasmid DNA was eluted. In brief: a 100ml overnight culture supplemented with 100µl ampicillin was inoculated with 100µl of bacterial culture and gently shaken at 37°C. By centrifugation at 6000g and 4°C for 15min, the bacteria were pelleted. The pellet was resuspended in 10ml of buffer P1, mixed with 10ml of buffer P2 and incubated for 5min at RT. Thereafter, 10ml of buffer P3 was added and mixed. After incubation time for 20min on ice the mixture was centrifuged (30min, 4°C, 10000g) and the supernatant decanted into a new Falcon tube followed by a second centrifugation for 15min at 4°C and 10000g. During this time, the Qiagen-tip 500 was equilibrated by adding 10ml QBT buffer. The supernatant obtained after the second centrifugation was transferred to the Qiagen-tip. After complete soakage the Qiagen-tip was washed twice with 30ml of buffer QC. The plasmid DNA was then eluted with 15ml of buffer QF. To precipitate the DNA, 10,5 ml of isopropanol was added to the eluate and then centrifuged for 60min at 4°C and 5000g. The supernatant was carefully decanted and the DNA pellet washed with 5ml of 70% ethanol and again centrifuged at 5000g and 4°C for 60min. After removal of the supernatant, the pellet was air dried and finally resuspended in EB buffer.

2.2.2 Determination of DNA and RNA purity and concentration

The concentration and purity of isolated DNA and RNA samples were determined using the ND-1000 UV-Vis Spectrophotometer NanoDrop (Thermo Scientific). The NanoDrop measures the absorbance of light of RNA and DNA photometrically at 260 and 280 nm respectively. The software NanoDrop ND-1000 version 3.5.2 was used.

2.2.3 Reverse transcription of RNA

For the reverse transcription from previously isolated RNA to cDNA the First strand cDNA synthesis kit from Fermentas was used. 1µg of RNA was mixed with 1µL of random hexamer primers and DEPC treated water was added up to a total volume of 11µl. Afterwards 4µl of 5X reaction buffer, 1µl RiboLock RNase inhibitor, 2µl 10mM dNTP mix and 2µl M-MuLV reverse transcriptase were added. The mixture was centrifuged and incubated: 5min at 25°C, followed by incubation at 37°C for 60min. To terminate the reaction, the sample was heated to 70°C for 5min and then cooled for 10min at 4°C. The resulting cDNA was either used immediately or stored at -20°C.

2.2.4 Polymerase chain reaction (PCR)

The polymerase chain reaction (PCR) was used to amplify DNA sequences. It consists mainly of three steps that are repeated for several cycles. In the first step the DNA is denaturized by heating. In the subsequent step the primers hybridize to the complementary DNA sequence. In this step the annealing temperature depends on the base sequence and the length of the primers used. In the last step, the desired piece of DNA is synthesized by a thermostable polymerase.

2.2.4.1 Amplification of DNA sequences by PCR

The amplification of the DNA sequences was performed following the protocol of Qiagen. The 10X PCR buffer, dNTP mix, Q-Solution, the Taq polymerase and sequence-specific primers were thawed on ice. A master mix was prepared by mixing H_2O, Q-Solution, dNTP mix, 10X PCR buffer and Taq polymerase in a ratio of 26,8:10:5:5:2:0,2. The required volume was distributed on PCR plates or tubes and the DNA was added. The tubes or plates were placed in a thermal cycler and the PCR program (Table 2.6) was started.

Temperature	**Time**	**Amount of cycles**
95 °C	5min	1
95 °C X °C (primer specific annealing-Temperature) 72 °C	0,5min 0,5min 1min	35 – 40x
72 °C	10min	1
4 °C	10min	1

Table 2.6: Typical PCR program

The primers were designed using the Institute's program “ExonPrimer”, designed by Dr. Tim M. Strom. All used primers can be found in Table S1.

2.2.4.2 Agarose gel electrophoresis

The size of the obtained PCR products was determined by agarose gel electrophoresis. To prepare a 1 or 1,5% agarose gel (depending on the size of the expected DNA fragment), 4 or 6g of agarose were dissolved in 400ml TBE buffer and stored at 65°C. The fluorescence dye ethidium bromide (8µl) was added to the solution which intercalates into the DNA which can be visualized when excited by UV light (366nm/254nm). 5µl of the PCR product were mixed with 5µl Orange G and loaded onto the gel. TBE was

used as the electrode buffer. The electrophoresis was carried out at a voltage of 130V for 30min. The DNA bands became visible under UV light and could be photographed. The lengths of the fragments were compared to a DNA ladder.

2.3 Cell biological methods

2.3.1 Cultivation of HEK 293T cells

HEK293T cells were routinely grown in High glucose Dulbecco's modified eagle medium (DMEM), containing 10% fetal bovine serum (FBS), 1% penicillin-streptomycin) in 14cm cell culture dishes at 37°C and 5% CO_2 in a cell culture incubator. The medium of the cells was changed every 2-3 days. The cells were splitted at a confluence of 70-80% at a ratio of 1:4. The medium was removed; cells were washed once with pre-warmed PBS and incubated with 2,5ml of trypsin/EDTA solution (0.5mg/ml trypsin, 0.22mg/ml EDTA in PBS) for 2-4 minutes. Double amount of growth medium was added and the cell suspension was centrifuged for 3,5 minutes at 500g. Cells were resuspended in 20ml of growth medium and 5ml of the suspension was added to 15ml fresh medium in new cell culture dishes.

2.3.2 Growth and maintenance of Human fibroblasts

Human Fibroblast cell cultures were grown in high glucose DMEM (supplemented with 10% FBS, 1% penicillin-streptomycin and 200µM uridine). Due to the impaired activity of the respiratory chain in the patient's cells sufficient uridine synthesis cannot be ensured, but this is necessary for DNA replication. Therefore, uridine was added to ensure that the respiratory chain defect can still be measured even after several passages. The cultures were maintained at 37°C and 5% CO_2. The medium change and splitting of the cells was performed analogous to the HEK-293-T cells. Stocks were prepared in culture medium supplemented with 10% DMSO and left over night at -80°C before they were transferred into liquid nitrogen for long-term storage.

2.3.2.1 Contamination test for mycoplasma

New cell lines were routinely tested for mycoplasma contamination with the MycoAlert Kit from LONZA according to the manufactures protocol. Briefly 2ml of the cell culture medium were taken and centrifuged for 5min at 1500rpm. Viable mycoplasmas were lysed and the enzymes reacted with the MycoAlert™ Substrate, catalysing the conversion of ADP to ATP. By measuring the level of ATP in a sample both

before (read A) and after the addition of the MycoAlert™ Substrate (read B), a ratio can be obtained which is indicative of the presence or absence of mycoplasma. Mycoplasma is present with a ratio >1 and absence at a ratio <1.

2.3.2.2 Contamination tests for HBV, HCV and HIV

Prerequisite for lentiviral gene transfer is the exclusion of infection with hepatitis B (HBV) and C virus (HCV) and human immunodeficiency virus (HIV) of the cell line. HBV and HIV were detected by PCR and HCV RNA virus by RT-PCR; in each case a highly conserved region of the infecting virus was amplified.
A PCR with Patient's DNA and control DNA was carried out with the primers-mentioned in table S1, and the product is applied onto the agarose gel. For the HCV test, RNA was initially isolated from the fibroblasts and transcribed into cDNA. Then, the PCR was carried out, and also applied on the agarose gel conditions. All cell lines were negative in terms of the tested viruses.

2.4 Diagnostics in patients with mitochondrial disorders

2.4.1. Sanger Sequencing

The sequencing of a single gene by Sanger sequencing was done whenever the patient presented a clear clinical phenotype corresponding to a single gene. This method was also used to verify variants found by exome sequencing. In brief the gene of interest was amplified by PCR as described in chapter 2.2.4, followed by the filtration on a Millipore plate. By applying a vacuum, the liquid is sucked through the membrane. The DNA remains in the membrane and is subsequently eluted by adding 20µl HPLC water and transferred to a new 96-well plate. The DNA sequencing was done with the BigDye-Terminator v3.1 Sequencing Kit. Sequence specific primers were used to amplify the DNA by DNA polymerase. The dNTP mixture includes 4 dideoxynucleotides (ddNTPs), labelled with four different fluorescent dyes, one for each nucleotide. This results in one label for each amplified DNA fragment. The label is dependent on the ddNTP that leads to disruption of the polymerase reaction. The fragments are separated by capillary electrophoresis and the fluorescence is detected. The emission of the fluorescence of the particular base leads automatically to the determination of the nucleotide sequence. The following reagent set-up and cycling parameters were used (Table 2.7 and 2.8)

Reagents	Volume
Filtrated PCR product	1µl
Forward/Reverse primer	1µl
BigDye	0,5µl
BigDye buffer	1,5µl
H_2O	1µl
Total Volume	5µl

Table 2.7: Reagent set-up for Sanger sequencing

Temperature	Time	Amount of cycles
96°C	5min	1
96°C	10sec	35x
50°C	5sec	
60°C	4min	
20°C	1min	1

Table 2.8: Cycling parameter for Sanger sequencing

After the sequencing reaction, the DNA was precipitated using ethanol. 25µl of 100% ethanol was added to each well and incubated for 1 hour in the dark, followed by a centrifugation step of 30min at 20°C and 3000g. The plate was inverted and tapped slightly. Than 125µl of 70% ethanol was added to each well and again centrifuged for 30min at 20°C and 2000g. During the last minute the plate was inverted and centrifuged at 600g. After evaporation of the ethanol 50µl HPLC water was added to each well and 25µl were used for sequencing with the ABI sequencers.

2.4.2 Whole Exome Sequencing

Exome sequencing of patients with respiratory chain complex deficiency was performed in our institute as previously described [91]. The patients who fulfil the following criteria were selected: 1. Clear diagnosis based on established diagnostic criteria, 2. No mutations in the entire mtDNA (excluded by Sanger sequencing), 3. Good clinical data and 4. Fibroblasts available. The bioinformatic analysis was done by the group of Dr. Strom. The exomes of all individuals were sequenced as 54bp or 76 bp paired-end runs using two lanes of a flowcell on a Genome Analyser IIx system (Illumina, San Diego, CA, USA) after in-solution enrichment of exonic sequences using the SureSelect Human All Exon 38 or 50 Mb kit (Agilent, Santa Clara, CA, USA) [91]. The average coverage was 120x corresponding to 9–12 Gb of sequence data. Read alignment was performed with BWA (version 0.5.8 or 0.5.9) to the human genome assembly hg19.

Single nucleotide variants and small insertions and deletions were detected with SAMtools (V.0.1.7). Due to the fact, that mitochondrial disorders are rare, all variants with a frequency of >0.4% in 879 control exomes were excluded. Assuming an autosomal recessive mode of inheritance, homozygous or compound heterozygous variants were searched for. We further applied three sequential filters. The first filters for disease known respiratory chain defects according to Human Gene Mutation database. The second filter is based on the identification of novel homozygous or compound heterozygous variants affecting genes encoding respiratory chain complex subunits or known assembly factors. The third filter looks for genes encoding known or predicted mitochondrial proteins in MitoP2 [57, 91].
The following table gives a short overview of the patients whose exome was sequenced.

Patient ID	Clinical features	Biochemical defect in fibroblasts
35834	Lactic acidosis, cardiomyopathy	CI 63%
58045	Muscular hypotonia, developmental delay, lactic acidosis in blood	CI 21%
33284	Muscular hypotonia, respiratory insufficiency	CI 52%
33027	Muscular hypotonia, dyskinesia, epilepsy, lactic acidosis, MRI changes	CI 54%
49720	progressive muscular hypotonia, respiratory insufficiency and severe lactic acidosis	CI 67%, CII/III 62%
52181	development delay, Lactic acidosis, increased alanine in serum	CI 60%, CIV 59%

Table 2.9: Clinical features and biochemical information of patients chosen for exome sequencing

2.5 Determination of the pathogenicity of the founded variants via lentiviral gene transfer

Exome sequencing is on the way to become the standard approach in routine molecular diagnostic. A big challenge for the analysis of exome sequencing data remains the distinction between causal mutation and other DNA sequence variants in each patient. One approach we used is the cellular rescue assay as described in a publication of a former medical PhD student in our group Katharina Danhauser [196]. The assay is based on the lentiviral-mediated expression of the wildtype form of the obtained variants in the appropriate patient cell line.

2.5.1 Cloning of cDNA

The wild-type cDNA (wt-cDNA) was either ordered from the company and sub-cloned into the lentiviral vector or directly cloned from a healthy control sample. The cloning was carried out analogue to the protocol pLenti 6.3/V5-TOPO TA Cloning Kit. The first step is the amplification of the gene of interest by the following PCR reaction (Table 2.10).

Reagents	**Quantity**
cDNA template	10-100ng
10x PCR buffer	5µl
50mM dNTPs	0,5µl
forward/reverse primer	100-200ng each
Sterile H_2O	Up to 49 µl
Taq Polymerase (1 Unit/µl)	1µl
Total Volume	50µl

Table 2.10: Reagent set-up for cloning PCR

The next step was the TOPO cloning reaction for the transformation into chemically competent OneShot Stb12 Competent *E. coli*. (Table 2.11):

Reagents	**Quantity**
Fresh PCR product	0,5-4µl
Salt solution	1µl
Sterile H_2O	Up to 5µl
pLenti-TOPO vector	1µl

Table 2.11: Reagent set-up for cloning reaction

The reaction mix is incubated for five minutes at RT and then placed on ice. One Shot Stbl3 chemically competent *E. coli* cells were thawed on ice and 4µl of TOPO cloning reaction added and gently mixed. The mixture was incubated for 30 minutes on ice. Afterwards a heat shock at 42°C for 30s was performed followed by two minutes on ice. 225µl pre-warmed SOC medium was added to the mixture and gently shaken at 37°C, 225rpm for one hour and finally plated on pre-warmed LB-Ampicillin plates. The next day, the resulting *E. coli* colonies were picked and each dissolved in 20µl dH_2O. With this suspension a colony PCR, to check the right size and orientation of the cDNA insert, was performed. The clones which presented the right size and orientation were further sequenced to exclude additional undesired mutations. For the isolation of the plasmid DNA the protocol described in chapter 2.2.1.2 was used.

2.5.2 Lentiviral transduction

The lentiviral transduction was performed as previously described [196]. The advantage of the use of lentiviral vectors in gene transfer is the ability to integrate the DNA into the human genome, and thus to allow a permanent expression of the transgene. The lentiviral system is based on the Feline immunodeficiency virus or Human Immunodeficiency Virus. A large part of the FIV and HIV gene is deleted and the information necessary for the production of lentiviral vector genes are distributed on three constructs (one expression vector and two/three packaging plasmids). The FIV lentiviral system was ordered from the company GeneCopoeia and performed accordingly to the manufacturers protocol. Prior to the start of the transduction all medium was required to be filtered through a 45µM protein filter to reduce precipitation. HEK 293-T cells were cultured for several days in DMEM (+10% FBS, 1%Pen/Strep). One day before the transfection approximately $4x10^6$ cells were plated on a small plate (∅ 10 cm) and grown in DMEM + 10% heat-inactivated FBS to reach a confluence between 70-80% at the day of the transfection. On the next day 10µg of packaging plasmids was mixed with 2µg of the expression vector, 400µl normal DMEM and 20µl PLUS Reagent (from Lipofectamine Transfection Kit) and incubated for 15min at RT. Meanwhile, 30µl Lipofectamine reagent was gently mixed with 400µl of normal DMEM. Subsequently, the diluted Lipofectamine reagent was added dropwise to the plasmid PLUS Reagent mixture and again incubated for 15min at RT. In the meantime, HEK-293T cells were washed and 4ml of DMEM +2% FBS were added. After the incubation time the DNA/Lipofectamine complex was carefully dropped onto the cells and the plate was swung gently. Thereafter, the cells were incubated overnight at 37°C. The supernatant containing the virus was collected after 48hrs, centrifuged for 5min at RT, 3000rpm and filtered through a 45µM filter. The supernatant was mixed 1:2 with normal medium and was used directly for the transduction of the selected fibroblasts cell lines. The medium was changed the following day and after 48hrs the selection with 2µl/ml of the antibiotic G418 was started. The selection was completed approximately after two weeks. Nevertheless, the G418 selection was kept during all experiments to ensure a pure cell line. The other lentiviral transduction kit used, was the pLenti6.3/V5-TOPO® TA Cloning® Kit from Invitrogen. The transduction was performed according to the manufacturers protocol and was similar to the procedure described above. Nevertheless, two main differences in the protocol are important. The kit from Invitrogen is based on HIV and uses as a selection marker Blasticidin. The exact composition of the expression vectors and packaging plasmids can be found in Figure S3 in the supplementary material.

2.6 Cell culture treatment

Potential new therapeutic agents for patients with mitochondrial disorders were tested in vitro in control and patient primary fibroblasts. To exclude altering effects, all experiments were carried out between cell passages 3-20.

2.6.1 Bezafibrate

An initial dose-dependent experiment was performed to figure out the best concentration of bezafibrate. Patient and control cells were splitted 1:4. The next day the medium was changed and concentrations between 0-500µM of bezafibrate (dissolved in DMSO) were added. After 72hrs the cells were harvested and the oxygen consumption rate was measured. The concentration with the biggest increase in RCC activity was used in the following experiments [146]. Another experiment was used to find out the right time points. Again patient and control cell lines were treated with bezafibrate for 24hrs, 48hrs, 72hrs and 96hrs and the oxygen consumption rate was analyzed. The time point with the highest response was used.

2.6.2 Riboflavin

Several patients with complex I defect could profit from the supplementation with riboflavin [167, 197]. A concentration of 530nM (diluted in ddH_2O) was used, which was reported to be most efficient *in vitro* [198-200]. The most effective treatment time reported was 72hrs and therefore used for all experiments.

2.6.3 Resveratrol

Another potential substance which might increase the respiratory chain complex activity via the activation of the SIRT1 pathway is resveratrol. Resveratrol was added to the cell culture medium in a concentration of 75µM for 72 hrs [173, 201].

2.6.4 AICAR

AICAR is a pharmacological activator of AMP activated protein kinase (AMPK). This heterotrimeric protein complex plays a key role in the regulation of energy homeostasis. First reports in mouse models

and in vitro studies demonstrated some positive effects [155]. To test the potential defect in our patient cell lines the best reported concentration (500µM AICAR for 72hrs) was used.

2.7. Oxygen consumption measurements in cells

2.7.1 Buffer and medium preparation

The following substrates, inhibitors and buffers for Oxygraph and Seahorse measurement were prepared. All substances were aliquoted, shock frozen in liquid nitrogen and stored at -20°C. ADP and KCN were stored at -80°C (Table 2.12).

Substance	**Stock concentration**	**Final concentration**
Glutamate/Malate	2M (in ddH_2O)	10mM/5mM
ADP	50mM (in ddH_2O)	1mM
Succinate	1M (in ddH_2O)	10mM
Asc/TMPD	200mM/100mM (in ddH_2O)	2mM/0,5mM
Oligomycin	5mM (in DMSO)	1µM
Digitonin	10% (in DMSO)	2,1µl/10^6 cells
PFO	10mM (in DMSO)	1-3nM
FCCP	10mM (in DMSO)	0,4µM
Rotenone	0,5mM (in EtOH abs)	0,5µM
Antimycin A	1mM (in EtOH abs)	2,5µM
KCN	1M(in ddH_2O)	1µM

Table 2.12: Reagent set-up for oxygen consumption measurement in cells

Respiration medium B

EGTA (0,5mM), $MgCl_2$*$6H_2O$ (3mM), taurine (20mM), KH_2P0_4 (10mM), HEPES (20mM), BSA (1g/l), potassium-lactobionate (60mM, 120ml of 0,5M K-lactobionate stock solution), mannitol (110mM) and dithiothreitol (0,3mM) were dissolved in ddH_2O, the pH adjusted to 7,2 with 5N KOH and the solution was sterilized by filtering through a 0,45µM filter.

Unbuffered Seahorse Medium

Unbuffered DMEM was dissolved in sterile ddH_2O and supplemented with 25mM glucose and 1mM NaPyruvate. The pH of the medium was adjusted to 7,4 and filtered through a 0,45µM filter.

2.7.2 High-resolution respirometry

One of the most important experiments to measure mitochondrial function in cells is the measurement of oxygen consumption rate (OCR). The high resolution respirometer (Oroboros-2k oxygraph) allows the measurement of oxygen consumption in two closed chambers, following the protocol (with miner corrections) as previously described [202]. A special substrate/inhibitor titration approach allows the step-by-step analysis of several mitochondrial complexes.

2.7.2.1 Sample preparation

The day before the measurement, the medium of the cells was changed to ensure exponential growth. Before the experiment the chambers were washed three times with ddH_2O, EtOH, ddH_2O and filled with 2ml of respiration medium B. The Oxygraph was turned on and the oxygen consumption was recorded for at least 1h to ensure a stable background calibration. For each Oroboros-2k chamber two big dishes (∅ 14 cm) of 70-80% confluent cells were harvested and once washed with respiration medium B. After centrifugation for 3,5min at 500rpm the supernatant was aspirated and the cell pellet dissolved in the required amount of respiration medium to achieve a final amount of $1\text{-}3*10^6$ cells/2ml in the chamber.

2.7.2.2 Measurement

Shortly before the measurement started 10µl of the cell suspension was recovered for counting the cells and later normalization of the experiment. By closing the chamber, the oxygen consumption was recorded. Depending on the number of cells, the amount of digitonin was determined and added to the cell suspension to permeabilize the cells. The polar heads of digitonin interacts with the polar heads of cholesterol, which is abundantly present in plasma membrane, leading to the loss of membrane integrity. All solutes in the cytosol were washed out and the intracellular space was equilibrated with the respiration medium (Figure 2.1 taken from [202]).

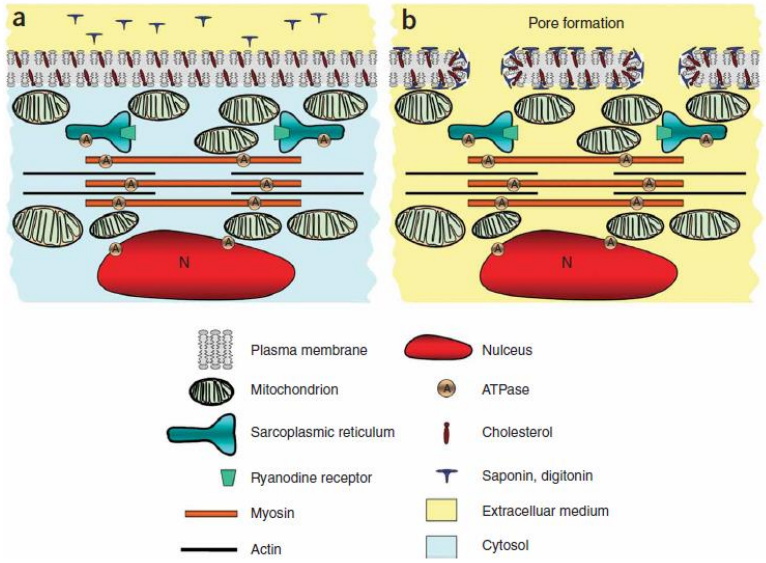

Figure 2.1: Principle of the digitonin permeabilization (taken from [202])

The next injections were Glutamate/Malate and ADP to observe the maximum complex I activity. After the addition of rotenone, the complex I (CI) activity was blocked and only non-mitochondrial oxygen consumption was observed. The next substrate/inhibitor (Succinate followed by Antimycin A) injection led to maximum complex II/III (CII/III) activity. The complex IV (CIV) activity was stimulated and later inhibited by the addition of Ascorbate/TMPD and KCN (Figure 2.2).

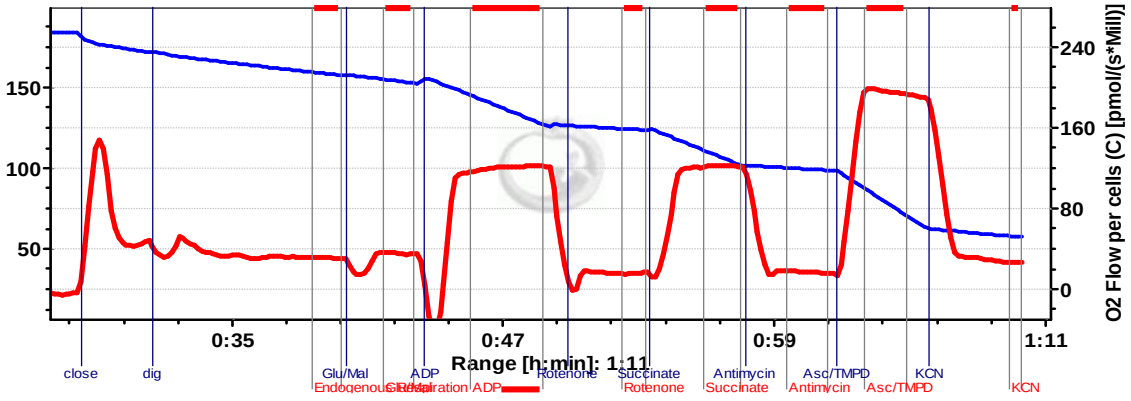

Figure 2.2: Typical output of the oxygen consumption measurement with the Oroboros instrument

2.7.2.3 Analysis of data

The software DatLab (Version 4.3.1.15) was used for the analysis of the data. The blue line presents the decreasing oxygen concentration over time. The red line describes the oxygen flow per cells over time [pmol/(s*Mill)]. The red marked areas were used for analysis (Figure 2.2). The non-mitochondrial oxygen consumption rate was subtracted prior to the analysis. For the specific complex I activity the stable values after the addition of its substrate Glu/Mal/ADP minus the oxygen consumption after the injection of rotenone was used. Complex II/III activity was calculated from the difference in OCR after the addition of

succiante and antimycin A. Accordingly the complex IV activity was determined (OCR Asc/TMPD-OCR KCN).

2.7.3 Seahorse measurement

An advancement of analysis of mitochondrial function is the XF Extracellular Flux Analyzer from Seahorse Bioscience. It allows the measurement of oxygen consumption and extracellular acidification on a 96-well format. For one experiment compared to the oxygraph only around 1% of cells are required. Another advantage is that far more probes and different set-ups can be measured in parallel. The assay kits contain a disposable sensor cartridge, including 96 immobilized (solid-state) dualfluorescent biosensors. This allows the measurement of oxygen and pH in parallel. Each sensor cartridge is also equipped with 2 or 4 drug injection chambers for delivering substances into the wells during the assay.

2.7.3.1 Sample preparation

On the day before the experiment 10.000-30.000 cells/per well were seeded in the 96-well plate XF Cell Culture Microplate. The appropriate cell concentration had to be determined in advance. The cells were grown in normal DMEM for 24hrs at 37°C and 5% CO_2. The 2/4-Port XF Sensor Cartridge was hydrated with 200µl XF Calibrant and left over night at 37°C without CO_2. On the day of the experiment the medium was changed to 180µl unbuffered DMEM and incubated for at least 30min at 37°C without CO_2. In the meantime, the 2/4-Ports of the Flux Plate were loaded with 25µl of the stock substances necessary for the planned experiment. To start the experiment the Seahorse instrument was programmed and the Flux plate loaded.

2.7.3.2 Measurement cycle

The following measurement cycle was used (Table 2.13):

Command	Time (min)	Port	#Repeat
Calibrate	30		
Equilibrate	15		
Mix	2		3x
Wait	2		
Measure	3		
Inject		A	
Mix	2		3x

Wait	2		
Measure	3		
Inject		B	
Mix	2		3x
Wait	2		
Measure	3		
Inject		C	
Mix	2		3x
Wait	2		
Measure	3		
Inject		D	
Mix	2		3x
Wait	2		
Measure	3		

Table 2.13: Cycling protocol for oxygen consumption measurement with the Seahorse Bioscience Instrument

Upon completion of cartridge calibration, the cell culture plate was loaded into the instrument. The following steps were fully automated and were completed in about 110min. After the run was finished the cells were washed once with PBS and all assay medium aspirated. The remaining medium may interfere with the fluorescence of the CyQuant GR dye, necessary for the normalization. Afterwards the cell plate was frozen for at least 24hrs at -80°C.

2.7.3.3 CyQuant Assay

The CyQuant Assay from Invitrogen to determine the number of cells in each well, which was later used for normalization of the OCR obtained from the above experiment. This step is important to adjust potential different cell amounts at the day of the measurement, especially between patient and control cell lines. The cell plate, buffers and fluorescence dyes were thawed and allowed to equilibrate to RT. 20ml of cell lysis buffer b was mixed with 200µl CyQuant GR dye. 200µl of the mixture was pipetted into each well and gently mixed with the cell lysates by pipetting up and down several times. The fluorescence measurements were performed in a microplate reader with excitation at 485nm and emission detection at 530nm. The measurement of a standard curve allowed the exact calculation of the number of cells.

2.7.3.4 Analysis of the data

The oxygen consumption rate was normalized by the number of cells. The maximum uncoupled respiration could be used as a measure of electron transport chain (ETC) integrity and mitochondrial functional capacity. Oxygen consumption was measured under basal conditions, in the presence of oligomycin (1µM,

ATP coupler), FCCP (0,4µM, mitochondrial uncoupler) or antimycin A (2,5µM, complex III inhibitor) and/or rotenone (0,5µM, complex-I inhibitor). Antimycin A and/or rotenone blocked all mitochondrial respiration and the OCR after addition of these substrates was subtracted from all values (Figure 2.3).

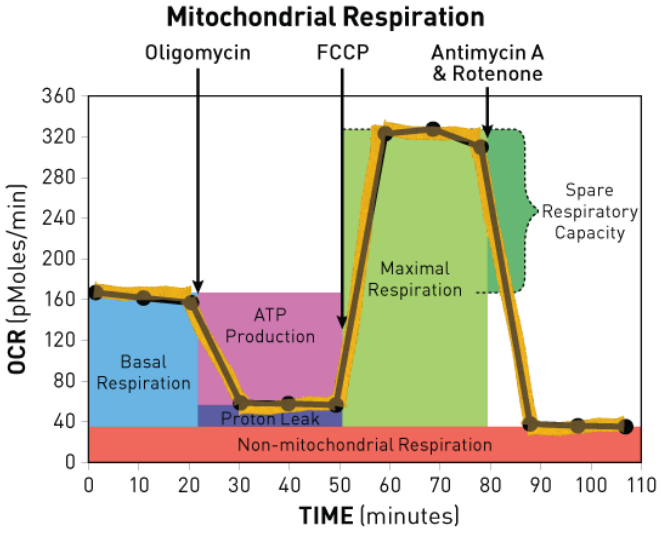

Figure 2.3: Experimental regime of a typical uncoupled respiration measurement with the Seahorse instrument

Another set-up to measure mitochondrial function in cells allowed the analysis of the specific activity of single respiratory chain complexes. The oxygen consumption rate was measured under basal conditions as well after permeabilization with PFO. The addition of Glu/Mal/ADP followed by the addition of rotenone allowed the measurement of the specific complex I activity. Succiante/Antimycin A were used for complex II/III activity and Asc/TMPD/KCN for complex IV activity.

The example shows the measurement of the specific complex I activity after the permeabilization with PFO (Port A), substrate injection Glu/Mal/ADP (Port B) and the inhibition of complex I activity with rotenone (Port C). The graph shows the clear difference between the control (NHDF) and patient (52181) cell line. (Figure 2.4)

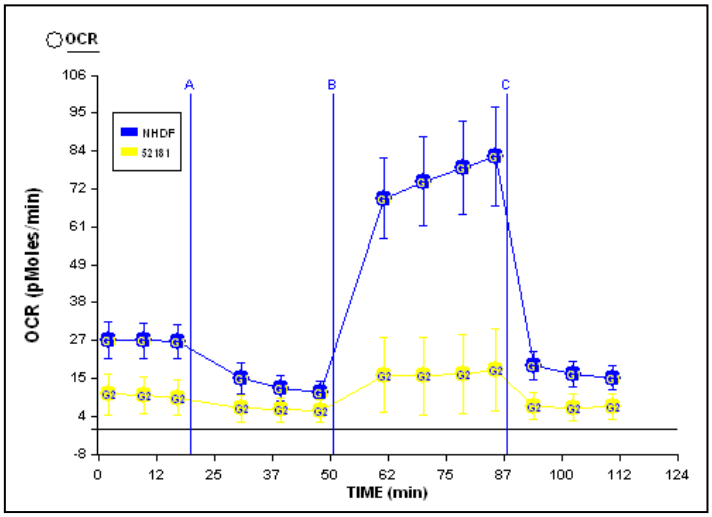

Figure 2.4 Typical output of complex I activity measurement with the Seahorse instrument

2.7.4 ROS measurement

The ROS measurement was performed in cooperation with the group of Dr. Ilka Wittig and Valentina Strecker in Frankfurt. Fibroblasts from patients and control were incubated in galactose media at 37°C and 5% CO_2 1h before staining. D-DMEM w/o phenol red, w/o glucose was supplemented with 10mM D-galactose, 10% FCS, 2mM L-glutamine and 1mM sodium pyruvate. For mitochondrial superoxide measurements MitoSOX Red was applied to the cell number of 1.5 x 10^5 per sample at final dye concentration of 5µM in media not containing FCS. For a positive control rotenone (1µM) was used. After 20min of incubation the cells were washed with PBS and trypsinized, transferred into the FACS tubes and washed again with PBS. The red fluorescence (Ex/Em: 514/51-630nm) was detected with FACS-Canto II (BD) via BD FACS-DIVA software. For analysis of mitochondrial membrane potential the cationic dye JC-1 was applied. First the cells were trypsinized, counted and transferred into FACS tubes: 5 x 105 in 250µl media w/o FCS. Then 2µM of JC-1 was added for 30 minutes at 37°C. FCCP (1µM) served as a negative control. JC-1 accumulates potential-dependent in mitochondria, where it forms concentration-dependent J-aggregates. These aggregates are characterized by a fluorescence emission shift from green to red (Ex/Em: 514/529 and 590nm). The decreased red/green fluorescence intensity ratio points to depolarization of mitochondrial membrane potential.

2.8 Gene expression analysis

2.8.1 3-day treatment

14 different fibroblast cell lines (three healthy age-matched controls and eleven patients with complex I defect measured in fibroblasts, see table 2.14) were treated with bezafibrate for 72hrs as described in chapter 2.6.1.

Cell line	Defect	Mutation
NDHF-neo	no	none
NDHF-neo + Bezafibrate	no	none
47041	no	none
47041 + Bezafibrate	no	none
45863	no	none
45863 + Bezafibrate	no	none
33545	Complex-I	NDUFA1

33545 + Bezafibrate	Complex-I	NDUFA1
33255	Complex-I	NDUFS1
33255 + Bezafibrate	Complex-I	NDUFS1
33023	Complex-I	NDUFS3
33023 + Bezafibrate	Complex-I	NDUFS3
18699	Complex-I	MELAS
18699 + Bezafibrate	Complex-I	MELAS
33460	Complex-I	NDUFS1
33460 + Bezafibrate	Complex-I	NDUFS1
33464	Complex-I	ND3
33464 + Bezafibrate	Complex-I	ND3
45157	Complex-I	ND1
45157 + Bezafibrate	Complex-I	ND1
33461	Complex-I	unknown
33461 + Bezafibrate	Complex-I	unknown
33281	Complex-I	unknown
33281 + Bezafibrate	Complex-I	unknown
33008	Complex-I	unknown
33008 + Bezafibrate	Complex-I	unknown
35791	Complex-I	unknown
35791+Bezafibrate	Complex-I	unknown

Table 2.14: Overview of all samples used for the gene expression experiment

Total RNA was extracted from 28 treated and untreated fibroblast cell lines according to the manufacturer's instructions using the AllPrep RNA/DNA Mini Kit (see chapter 2.2.1). Purity and integrity of the RNA was assessed on the Agilent Bioanalyzer with the 6000 Nano LabChip reagent set. The RNA was quantified spectrophotometrically and then stored at -80°C.

Using the Illumina TotalPrep-96 RNA Amp Kit 500ng of RNA were reverse transcribed into cRNA and biotin-UTP-labeled. 3000ng of cRNA were hybridized to the Illumina Human-12 v3 Expression bead chip, followed by washing steps as described in the Illumina protocol (P/N IL1791M Revision B). The raw data were exported from the Illumina GenomeStudio software to the statistic program “R” and converted into logarithmic scores. The “Bioconductor” package “lumi” was used to perform quantile normalization. A total of 48,781 probes were analyzed. For all probes a paired t-test was calculated to compare the cell lines with and without bezafibrate treatment. The data was adjusting for multiple testing using Benjamini-Hochberg correction.

2.8.2 Time course experiment

A second gene expression experiment was performed to detect genes which respond shortly after the treatment with bezafibrate and might be overseen by the 3-day experiment. Therefore, three different control cell lines were treated with 400µM bezafibrate and harvested after 0, 2, 4, 6, 8, 12, 24, 48, 72 and 96 hrs. The analysis of the data was performed as described in the previous chapter.

2.8.3 Pathway analysis

The significantly up-or downregulated genes were analyzed with the help of the pathway analysis software Ingenuity.

2.9 Proteomic analysis

2.9.1 Sample preparation

Whole cell lysates

The cells of 1-3 big flasks/plated of 70-80% confluent cells were harvested according to chapter 2.3.2. The cell pellet was washed once with PBS and centrifuged for 5min 2000rpm at 4°C. The cell pellet was resuspended in 200-400µl RIPA buffer (50mM Tris-HCL pH 7.4, 1% NP-40, 0.5% Na-deoxycholate, 0.1% SDS, 150mM NaCl) by pipetting up and down and agitated on a rotating wheel (35rpm) for 1hr at 4°C. The suspension was pressed through a 1ml insulin syringe and centrifuged for 10min at 16000rpm and 4°C. The supernatant was further processed or frozen in liquid nitrogen and stored at -20°C.

Isolated mitochondrial membrane proteins

For protein analysis 1-2 large cell plates/flasks of 70-80% confluent cells were washed with phosphate buffered saline (PBS) and harvested by scraping in PBS and sedimented by centrifugation 3min 2000g. After the determination of the wet weight, the cell pellet was homogenized in 500µl diluted sucrose buffer (83mM sucrose, 10mM Sodium phosphate buffer, pH 7.5, 1mM EDTA, 2mM aminocaproic acid) using a motor-driven, tight-fitting 2ml glass/Teflon-Elvehjem homogenizer, 30x at 2,000rpm at 4°C. The homogenate was then centrifuged for 10min at 600g to sediment nuclei and unbroken cells. The resulting supernatant was divided into portions to obtain aliquots of mitochondrial membranes from initial 20mg

cell wet weight and centrifuged for 10min at 22,000g, at 4°C. Aliquots for proteomic analysis were either used immediately or shock frozen in liquid nitrogen and stored at -80°C [203-205].

2.9.2 SDS-PAGE

Protein samples were separated according to their molecular weight by SDS-PAGE (sodium dodecyl sulfate-polyacrylamide gel electrophoresis) for downstream analysis such as Western blot or protein staining. In order to load equal amounts of protein for each sample to compare to other samples protein concentration was determined by the Bradford method. A standard curve with different concentrations of bovine serum albumin served as a reference. Before the proteins were separated by application of an electric field in a polyacrylamide gel, Laemmli buffer (8% SDS, 40% glycerol, 0.02% bromphenol blue, 250mM Tris-HCl pH = 6.8, 0.1M DTT) was added. SDS binds to the proteins and adds negative charges, which mask the intrinsic charge of the proteins. This leads to a charge-to-mass ratio that is almost constant for all proteins. In combination with the reduction of disulfide bonds by a reducing agent such as DTT a migration speed relative to the mass of the protein is achieved. In most applications of SDS-PAGE sample boiling for 5 min was used to denature proteins. Depending on the size of analyzed protein of interest, 4-12% or 10-20% acrylamide gradient gels or 15% continuous acrylamide precast gels from Lonza were used. The gels were first rinsed with ddH_20 and then clamped into the electrophoresis chamber. The inner and outer chamber was filled with running buffer (25mM Tris, 200mM glycine, 1% SDS, pH = 8.9) and each gel well was washed carefully with running buffer. Amounts of 5, 10 or 15µg of enriched mitochondria membrane proteins and a size-specific protein ladder an electric field with a voltage of 130V were applied. The run was completed approximately after 120-180min.

2.9.3 2D-BN-SDS Gels (mitoGELs)

The 2D-BN-SDS Gels (mitoGELs) were performed in cooperation with the group of Dr. Ilka Wittig in the mitoNET subproject mitoPROT. The first dimension of the mitoGELs was a blue native (BN) gel, which allowed the analysis of the assembly state of respiratory chain complexes. The second dimension was a 13% SDS-Gel which further allowed the analysis of the subunits of the mitochondrial complexes. The native polyacrylamide gradient gels were composed of two solutions: 3% T, 3% C and 13% T, 3% C (T is the percentage of total acrylamide, C gives the percentage of bisacrylamide of T). A 3-13% T native acrylamide gradient gel was casted at 4°C using a gradient mixer (CBGM-20 gradient maker from C.B.S. Scientific). The polymerization was initiated with APS and TEMED. The special gel system for enhanced resolution of large mitochondrial complexes with a native mass from 1-2MDa includes a stacking step at 5.3% in the gradient gel. Native gels were placed to RT for polymerization about 30min. After the polymerisation a large-pore stacking gel (3% T, 20% C) was casted on top and comb was set. The

polymerization was complete in 1-2 h. After removal of the comb 1x gel buffer was added. 10mg of mitochondrial membrane pellets were resuspended in 20µl diluted sucrose buffer and 2µl N-Hydroxysuccinimide (NHS)- fluorescein- (10nmol/µl in DMSO, Thermo Scientific) was added for fluorescence labelling and incubated for 2h at 4°C and additional 30min at RT in the dark. Free non bound reactive fluorescent dye was stopped with 10mM lysine in the same dye volume for 10min on ice. Labeled mitochondria were sedimented by 10min centrifugation at 22,000g at 4°C. Cell pellets were resuspended in solubilization buffer (50mM NaCl, 2mM 6-aminohexanoic acid, 1mM EDTA, 50mM imidazole/HCl, pH 7.0) and solubilized by digitonin (2 and 5g/g of protein) for 5min on ice. After centrifugation (10min, 22,000g, 4°C) the supernatant was used for analysis. The BN-PAGE was carried out at 4-7°C. The separation of the proteins in an electric field was achieved out by means of the cathode buffer (50mM Tricine, 7.5mM imidazole (pH 7.0-7.5) and 0.02% Coomassie Blue G-250), and the anode buffer (25mM imidazole/HCl, pH 7.0). The initial voltage was 100V and 15mA. Once the proteins have reached the separating gel, the voltage was increased to 500V. After the blue running front had travelled over a third of the desired distance the cathode buffer was replaced by 1/10 of cathode buffer. The entire run was completed after 2-4hrs. Subsequent 0.5cm strips from the 1-D BNE gel were placed on glass slides and incubated in 1% SDS for 15min. The second dimension 13% SDS-gel was casted to 5mm below the strip and the gap was filled with water. After polymerization, the strip was pushed down to the separation gel. On the left- and right-hand side of the native stripe a 10% acrylamide SDS gel was casted. Electrophoresis was carried out at RT and covered from light. The gel was running with a maximum of 200V and 50mA overnight [204].

Data analysis

The mitoGELs were scanned with a Typhoon 9400 scanner (excitation 488nm, emission filter 520nm to detect fluorescein and analysed by DIA modul (Differential In-Gel Analysis) of the DeCyderTM 2D 7.0 software for densitometric quantification of fluorescence intensities of selected clearly visible protein spots. Mitochondrial complexes were quantified by densitometry, normalized to porin complexes and expressed as percentage of healthy control cells.

2.9.4 Silver staining

The silver staining of the gels was used for a better visualization of the protein spots. The gels were incubated in a fixing solution (50% methanol, 10% acetic acid, 100mM ammonium acetate) for 30min. Thereafter, they were rinsed 2x15min with water, followed by sensitization with 0.005% sodium thiosulfate ($Na_2S_2O_3$), and incubation with 0.1% silver nitrate for 15min. Prior to the development in the solution of 0.036% formaldehyde, 2% sodium carbonate, the gels were washed briefly with water. The

reaction was stopped by the addition of 50mM EDTA. After 15min the gels were washed twice with water and documented with a photo camera [206].

2.9.5 Western Blot

After the separation of the proteins by their specific size, some gels were transferred to a PVDF membrane for further western blotting analysis. The PVDF membrane was incubated for 10min in 100% methanol for its activation. The gel with the separated proteins, as well as the PVDF membrane and Whatman blotting paper were gently shaken for 10min in blotting buffer (25mM Tris, 190mM Glycine, 20% MeOH). The PVDF membrane and the gel were placed in the blotting chamber surrounded by soaked Whatman blotting paper. Protein transfer was completed after 90 min setting current to 5mA/cm^2. The efficiency of the protein transfer was checked with Ponceau Red (0.1% in 0.1% acetic acid). In order to prevent unspecific antibody binding the membrane was blocked for 1 hour in 5% skimmed milk powder. This was followed by the decoration of the membrane with the specific antibodies at 4°C overnight. The specific antibody dilutions can be found in table 2.15. The next day, the membrane was washed three times for 10min with 0.1% TBS-Tween, followed by the incubation with the secondary antibody for one hour at RT. After repeated washing with TBS-Tween (0.1%), the proteins were visualized with enhanced chemiluminescence (ECL).

Antibody	Dilution	Second antibody (dilution)
NDUFS1	1:200	Anti-goat (1:7500)
NDUFS3	1:1000	Anti-mouse (1:1000)
NDUFB3	1:1000	Anti-mouse (1:1000)
NDUFB9	1:200	Anti-rabbit (1:1000)
NDUFA9	1:1000	Anti-mouse (1:1000)
ACAD9	1:500 1:1000	Anti-mouse (1:1000) Anti-Rabbit (1:10000)
ACADM	1:1000	Anti-Rabbit (1:10000)
ACADVL	1:1000	Anti-Rabbit (1:10000)
Porin	1:1000	Anti-mouse (1:1000)
SDHA	1:1000	Anti-mouse (1:1000)
ß-actin	1:1000	Anti-mouse (1:1000)
CIII subunit core 2	1:1000	Anti-mouse (1:1000)

Table 2.15: Primary and secondary antibodies

2.9.6 2D-DIGE-Gels

Difference-gel electrophoresis combines the isoelectric focusing (IEF) with SDS-PAGE for the separation of complex protein mixtures labelled by fluorescent dyes. This method is used to analyze different protein samples within one gel. It was used to find out post-transcriptional effects of the fibroblast cell lines untreated and treated with bezafibrates and differences in the proteasome of patients versus healthy controls [207, 208].

DIGE work-flow

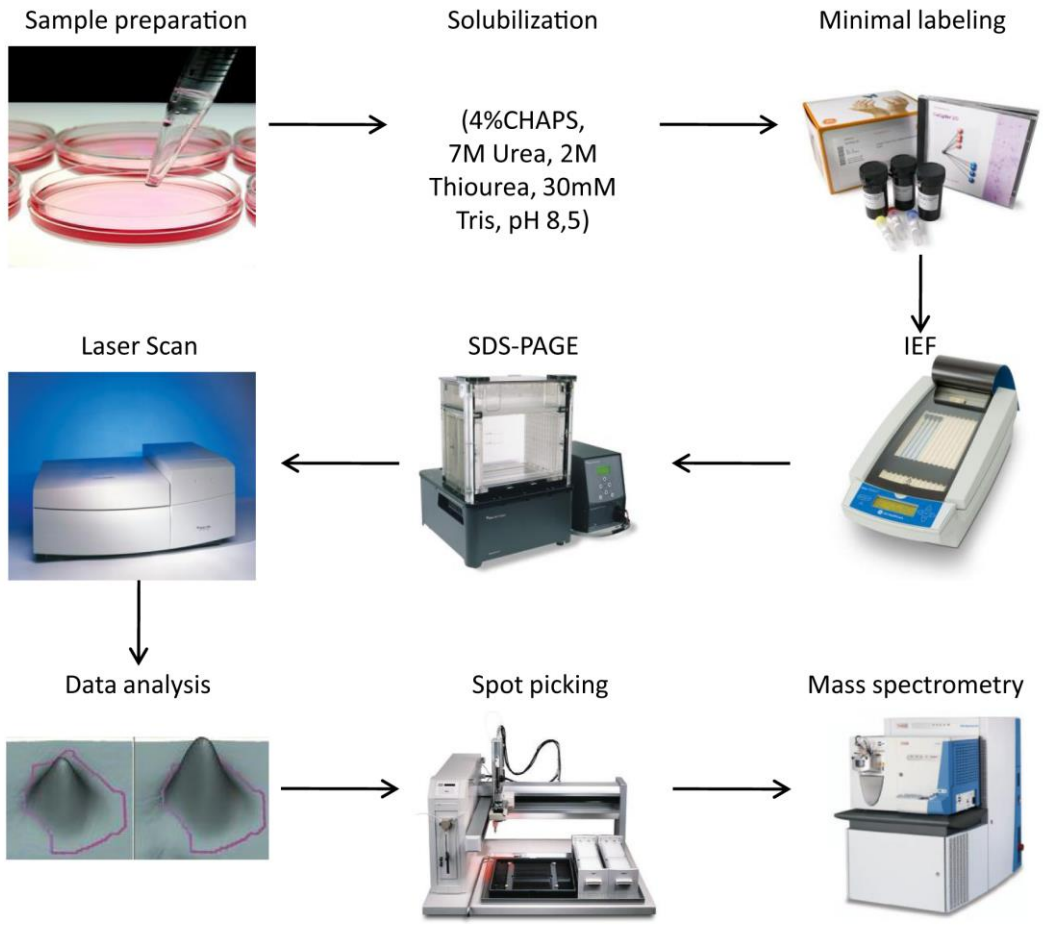

Figure 2.5: Workflow of DIGE experiments

Sample preparation

For this experiment four different fibroblast cell lines with mutations in the *ACAD9* gene and one healthy control cell lines were used (Table 2.16). These cells were treated with bezafibrates as described in chapter 3.6.1. After 72hrs treatment the cells were washed once with PBS and scraped from the plate with a cell scraper, imbibed in PBS and centrifuged for 3min at 2000g and 4°C. The pellet was resuspended in mito

buffer (250mM Sucrose, 10mM Tris pH 7.4, protease inhibitor PMSF). For the isolation of mitochondria, the cell suspension was pressed three to five times through a syringe with a needle thickness of 25µM on ice. The cell suspension was again centrifuged for 10min at 600g and 4°C. The supernatant contained the enriched mitochondrial fraction and was pelleted for 10min at 10000g and 4°C. The mitochondrial pellet was shock frozen in liquid nitrogen and stored at -80°C.

Cell line	**Mutations in *ACAD9***	**Biological replicates**
NHDF-neo	no	3
NHDF-neo+Bezafibrate	no	3
35834	p.Phe44Ile, p.Arg266Gln	3
35834+Bezafibrate	p.Phe44Ile, p.Arg266Gln	3
52933	p.Arg266Gln, p.Arg417Cys	3
52933+Bezafibrate	p.Arg266Gln, p.Arg417Cys	3
52935	p.Phe44Ile, p.Arg266Gln	2
52935+Bezafibrate	p.Phe44Ile, p.Arg266Gln	2
52674	p.Ala326Pro, p.Arg532Trp	1
52674+Bezafibrate	p.Ala326Pro, p.Arg532Trp	1

Table 2.16: Patient cell lines used for the DIGE experiment

Experimental Set-Up

For the 2-D DIGE experiment, a minimal labeling technique was performed according to the protocol from GE Healthcare. To compare untreated and bezafibrate treated samples an experimental plan was designed in which two biological samples were labeled with the fluorescent dyes Cy3 or Cy5 (CyDye; GE Healthcare). A dye swap was applied for each pair to exclude labeling errors. In total 24 samples (Table 2.16) were applied to 12 analytical gels. In order to allow normalization of all samples for quantitative biological variance analysis an internal standard (comprised of a mixture of equal amount of all samples used in the experiment labeled with Cy2) was applied to each gel.

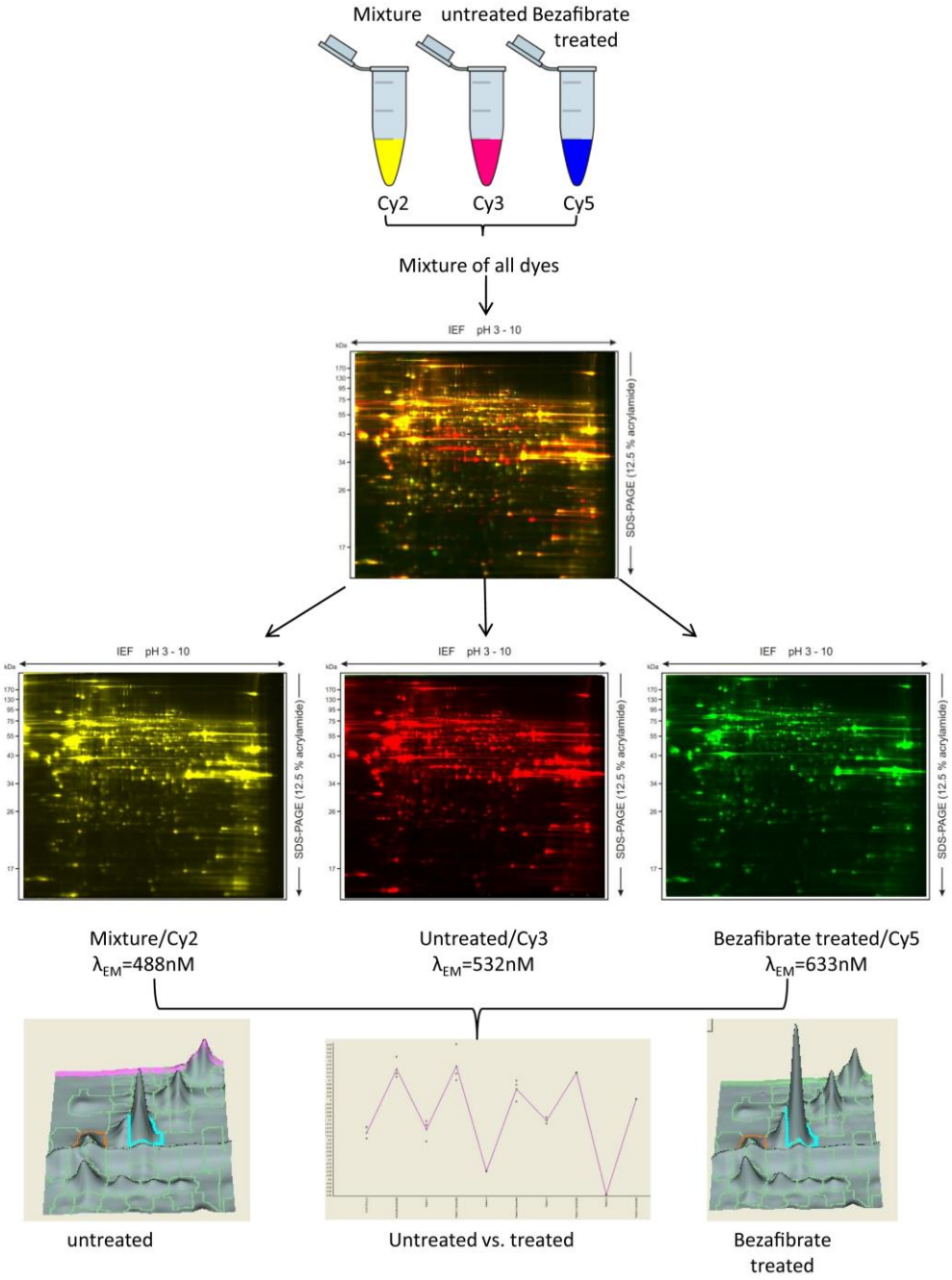

Figure 2.6: Experimental procedure and analysis of DIGE gels

2mg/ml mitochondria were denaturated in DIGE labeling buffer (30mM Tris-HCl, 7M urea, 2M thiourea, 4% CHAPS, pH 8.6) on ice. After 30min the samples were centrifuged at 22,000g for 10min to remove insoluble material. For analytical gel 25µg of protein were labeled with 100pmol of Cy3 or Cy5. The labeling reaction was stopped after 30min incubation in the dark by the addition of 1% lysine. After an additional 10min of incubation, 12 sample-sets (one sample of untreated, one sample of bezafibrate treated and one sample of internal standard) were mixed in 100µl rehydration buffer (7M Urea, 2M Thiourea, 2% CHAPS, 18mM DTT, 0.5% IPG ampholyte pH 3-10, GE Healthcare,). Nonlinear immobiline Dry strips (pH 3–10, 24cm, GE Healthcare) were rehydrated with 450µl rehydration buffer (+0.002%, bromphenol blue) overnight. Samples were loaded onto the IEF strips with cup loading and isoelectric focusing was

performed using an Ettan IPGphor 3 IEF unit (Multiphor; GE Healthcare) according to standard procedures. The second dimension was performed by separation on SDS-PAGE gels (12%) using an Ettan DALT twelve electrophoresis system (GE Healthcare). Electrophoresis was started at 0.5W/gel for one hour followed by 1.5W/gel for 16hrs at 20°C in the dark. Additionally to the analytical gels, two preparative gels were designed for protein identification by mass spectrometry. For the preparative gels a pool of control, patient, untreated and bezafibrate treated samples were mixed and 100µg of protein was loaded (Figure 2.6 [208]).

Data acquisition and protein quantification

After the SDS-PAGE, the analytical gels were scanned in a Typhoon™ 9400 Imager (GE Healthcare) at a resolution of 100µm using the emission wavelengths of the fluorescent dyes (Cy2–488nm; Cy3–532nm; Cy5–633nm). For visualization of the preparative gels, they were stained with SYPRO Ruby according to the standard protocols. Analysis of the gel images was performed with the DeCyder™ software version 7.0 according to the manufacturer's recommendations. The estimated number of spots was set at 3000 per gel and the spots were first matched automatically using the batch function, then checked and manually corrected as needed. The data was then exported to BVA (biological variance analysis) module of the software and a normalization step with the internal standard was performed. For statistical analysis, Student's t-test was used to detect significant differences between spot volumes from patient and healthy controls as well as untreated versus bezafibrate treated samples. Protein spots with an increase or decrease of more than 1.2-fold with a p-value$\leq$0.05 between different groups were picked of the gel using an Ettan™ Spot Picker supplied with 2.0mm picker head and placed in perforated 96 well plates.

In-gel tryptic digestion and MALDI-MS

The first round of picked gel spots were subjected to an automated tryptic in-gel digestion protocol [209, 210] in cooperation with the group of Prof. Michael Karas (Institute of Pharmaceutical Chemistry, University of Frankfurt) from Benjamin Müller employing a ML Star liquid handling Robot (Hamilton, Bonaduz, Switzerland). MALDI-MS/MS measurements were performed on a 4800 MALDI-TOF/TOF analyzer. Data were analysed using BioTools 2.2 and the Mascot 2.2 search engine. MS/MS queries were performed against the human UniProt database (from April 2011, 20406 sequences). False discovery rates (FDR) were estimated by running a search against an internal Mascot decoy database. Significance thresholds were set to $p<0.05$, so that individual ion scores < 14 indicate identity or extensive homology. By mischance only 30% of the picked spots were identified by MALDI-MS. A second pick-gel was prepared and the protein identification was performed with the help of nanoLC/MS.

In gel tryptic digest and nanoLC/MS

The second round was performed by nanoLC/MS in cooperation with Dr. Ilka Wittig, Mirco Steger, and Heinrich Heide from the Institute of Molecular Bioenergetics at the University of Frankfurt. Prior to the mass spectrometry analysis an in-gel trypic digestion was performed as previously described [208, 210, 211]. In brief the gel spots were washed twice with 50% acetonitrile/25mM ammonium bicarbonate buffer, the cysteines reduced with 5mM DTT and alkylated with 15mM Iodacetamid. After washing and drying of the spots, trypsin solution was added and the spots were allowed to take up the solution. Subsequently enough ammonium bicarbonate buffer was added to cover the spots and the proteins were digested overnight at 37°C. The buffer solution and a subsequent 2nd elution solution (50% acetonitrile/3% formic acid were collected in a 96 well microplate and the liquid evaporated in a speed vac concentrator. The peptides were resolved in the starting buffer of the subsequent HPLC separation (5% acetonitrile/5% formic acid), then the microplate was sealed with hot-sealable aluminium foil. The chromatographic run was performed with an Agilent 1200 HPLC systemequipped with an autosampler, a capillary pump and a nanopump. First the sample that was drawn by the autosampler was loaded onto a trap column (300µm x 5mm) at 100% buffer A (5% acetonitrile/0.1% formic acid) and a flow of 5µl/min delivered by the capillary pump to concentrate and desalt the peptides. The peptides were then separated on a picotip emitter tip (75µm id x 10cm, 15µm tip id, new objectives) packed in house with reprosil-pur C_{18} silica beads (3µm, Dr. Maisch) by a gradient up to 50% buffer B (95% acetonitrile/5% formic acid) in 40min with a flow of 200nl delivered by the nanopump. The peptides eluting from the column were electrosprayed into the entrance capillary of the mass spectrometer at a positive voltage of 1800V. The mass spectrometer (LTQ Orbitrap XL) was operated in a data dependent aquision mode. First a survey scan at 30000 resolution is performed in the Orbitrap analyser (MS scan) to determine the exact precursor m/z values.
Subsequently the ten most abundant ions with a charge of at least two are selected and are consecutively fragmented in the linear ion trap by collision induced dissociation (CID) to get the fragment spectra (MS/MS mode). An exclusion list with all precursors that have already been fragmented ensures that every precursor is only fragmented once.
To identify the peptides and with it the proteins the fragment spectra are matched against theoretical spectra generated through an in silico digest of all protein sequences of the respective fasta database (human reviewed UniProt database, from March, 8th 2012, 20248 sequences) and a score is generated. This step was done by in an in house mascot server (matrixscience). The software delivers a html-file with all protein hits and the corresponding peptide sequences.

2.9.7 Pathway analysis

The pathway analysis of the gene expression and DIGE experiment data was performed with the Ingenuity Pathway Analysis (IPA) software from Ingenuity Systems.

3 Results

3.1 Identification and verification of novel variants in patients with mitochondrial disorder

My PhD Thesis is divided into two big parts. The first part of the thesis focuses on the identification and verification of new and known disease-causing genes in six patients with mitochondrial disorder with the help of WES. The second part focuses on possible treatment options, tested on patient-derived fibroblast cell lines. From the beginning of my PhD time until the end round 1000 exoms from patients with isolated and combined complex I defect were successfully sequenced in the Institute of Human Genetics. The selection of the very first patients was made on the following criteria:

1. Clear complex I defect in muscle and fibroblasts
2. Good clinical data
3. No mutation in mtDNA

The results of six different patients will be described in the next chapters.

3.1.1 Patient overview

This table 3.1 provides an overview of six patients with their main clinical phenotype, respiratory chain complex activities in fibroblasts and the affected gene.

Patient ID	Clinical features	Biochemical defect in fibroblasts (% of control)	Affected gene	Reference
35834	Lactic acidosis, hypertrophic cardiomyopathy	CI 63%	ACAD9	Haack et al. 2010
58045	Muscular hypotonia, developmental delay, lactic acidosis in blood	CI 21%	NDUFB3	Haack et al. 2012
33284	Muscular hypotonia, respiratory insufficiency	CI 52%	NDUFS8	Haack et al. 2012

33027	Muscular hypotonia, dyskinesia, epilepsy, lactic acidosis, MRI changes	CI 54%	NDUFS8	Haack et al. 2012
49720	progressive muscular hypotonia, respiratory insufficiency and severe lactic acidosis	CI 67%, CII/III 62%	BOLA3	Haack et al. 2013
52181	development delay, lactic acidosis, increased alanine in serum	CI 60%, CIV 59%	AIFM1, MTFMT	Haack et al. 2014

Table 3.1: Overview of all patients chosen for Exome Sequencing and the results

3.1.2 ACAD9

3.1.2.1 Results Exome Sequencing

The DNA of the first patient (35834) we used for exome sequencing was a girl with cardiorespiratory depression, hypertrophic cardiomyopathy, encephalopathy and lactic acidosis. The phenotype was present from birth on and the girl died with 46 days of age. Her brother presented a similar phenotype and is now ten years old. The biochemical analysis of the muscle, liver and fibroblasts showed a severe complex I defect with a milder involvement of complex V. The brother of the 35834 presented also a clear complex I defect in fibroblasts. At this time the protocols for WES were not completely established in our Institute. Therefore, the DNA sample was sent for exome sequencing to the company CeGAT. The following analyses were performed in our Institute by Dr. Tobias Haack. The big number of SNVs was reduced by filtering against dbSNP, HapMap and in-house SNP data. The only homozygote or compound heterozygote variants, with a predicted mitochondrial localisation, were found in acyl-CoA dehydrogenase 9 (ACAD9, c.130T>A het, p.Phe44Ile, c.797G>A het, p.Arg266Gln) (Table 3.2) [113].

Filter	Number of SNVs / genes
Total SNVs	14,167
Synonymous SNVs	3,921
NS/SSV	4,928
Novel NS/SSV	533
Homozygous NS/SSV	23
Heterozygous NS/SSV	510
Compound heterozygous NS/SSV	25
With predicted mitochondrial localization	1

Table 3.2: Identification of candidate genes for complex I deficiency by exome sequencing (Table taken from [113])

Sanger sequencing of patient 35834, performed by our technical assistant, her affected brother and her parents confirmed the compound heterozygous state of the mutations, with each parent being heterozygous for one variant. This gene was previously not associated with complex I defect. Additional high-resolution melting-curve analysis (performed by our technical assistants), in 120 patients with isolated complex I deficiency revealed two additional individuals carrying compound heterozygous variants and one case harboring a homozygous variant. The sequence alignment of *ACAD9* to mammalian orthologues could show that the altered positions are highly conserved (Figure 3.1, [113]).

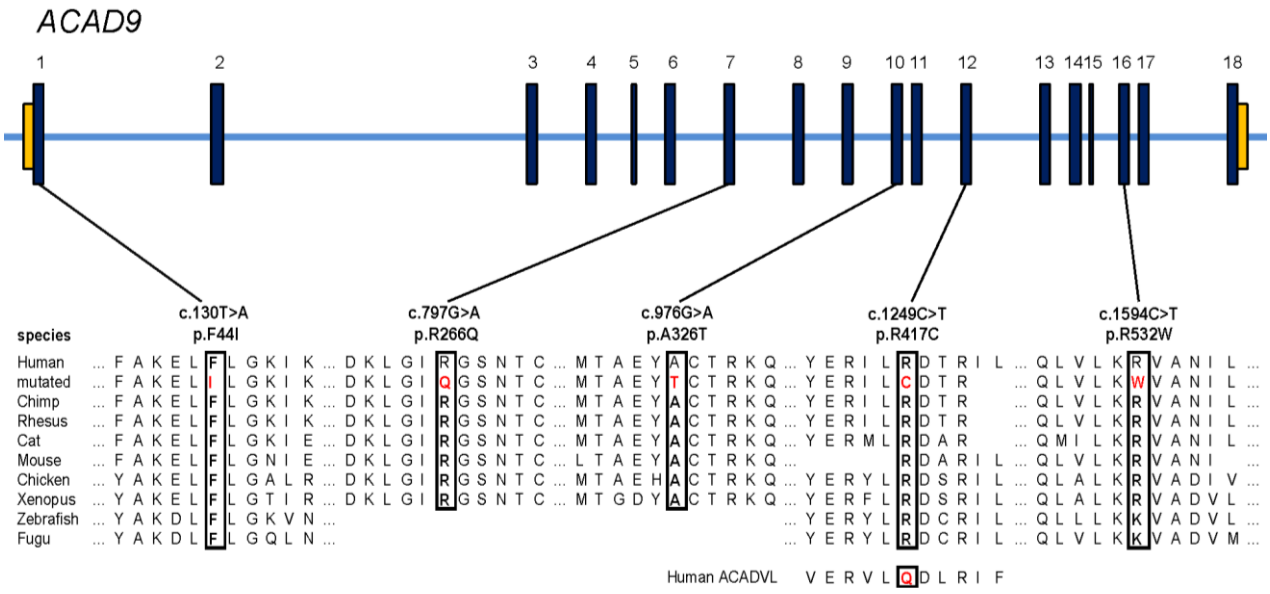

Figure 3.1: *ACAD9* gene structure and conservation of affected amino acid residues of identified mutations of patient 35834, her brother and two additional patients found by melting-curve analysis (shown in red)

3.1.2.2 Lentiviral complementation

In order to confirm the pathogenicity of the ACAD9 variant, complementation experiments in the patient fibroblast cell line to test for functional rescue of impaired enzyme activities was performed by a former medical student in our lab Katharina Danhauser. Part of the results are already published in her PhD thesis [212]. The mutant and the control cell line were transduced with a lentiviral vector expressing the wild-type ACAD9 complementary DNA (wt-ACAD9-cDNA). Spectrophotometrically analysis of complex I, complex IV and citrate synthase (performed by Katharina Danhauser) showed a significant increase in complex I, but not complex IV and citrate synthase activities.

I measured the oxygen consumption in the patient cell line 35834 untransduced and transduced with the wt-ACAD9-cDNA with the oxygraph as described in chapter 2.7.2 (Figure 3.2). The complex I activity increased significantly from 48% rest activity to 82% (p-value<0.01). The complex II/III and complex IV activity did not increase significantly. The measurement was performed in three biological independent experiments. These results supported the pathogenic significance of the mutations found in *ACAD9*.

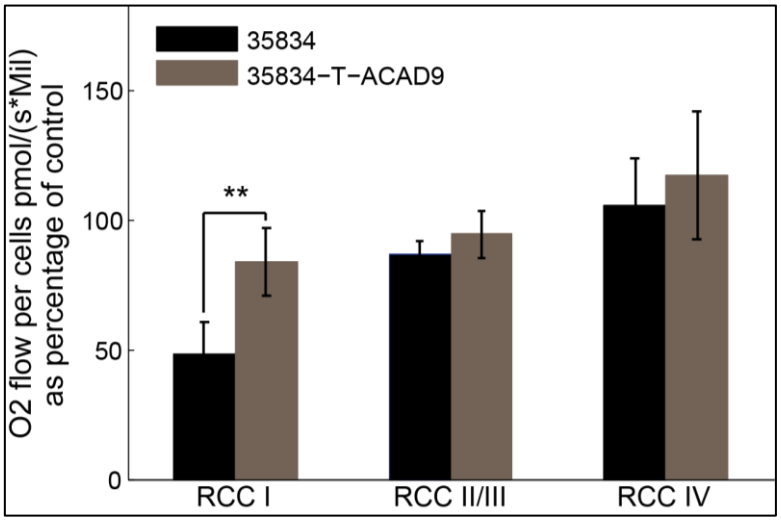

Figure 3.2: Oxygen consumption measurement of patient 35834 with and without wt-ACAD9-cDNA transduction Data are expressed as average of > 3 technical replicates and normalized to control. ±SD (p-value <0,01,**)

A further experiment was made to find out, if the reduction of complex I activity caused by the ACAD9 mutation, lead to a reduced or abnormal complex I assembly. This was determined with the help of mitoGELs in cooperation with Dr. Ilka Wittig and Valentina Strecker. I prepared the samples, the mitoGELs were performed by Valentina and the quantification and data analysis was done together. Mitochondrial proteins were labelled with Fluorescin, followed by one-dimensional BNE and two-dimensional SDS-PAGE. It was found that the complex I in supercomplexes of complex I, III and IV, is assembled. However, quantifying the amount, a reduction of the complex I holoenzyme in the patient's cells to 35% was observed, which can be either due to instability of the complex or an impaired assembly process. After transduction of cells with wt-ACAD9-cDNA a comparable amount of the supercomplex can be detected compared to the control. This confirmed the pathogenicity of the mutations found also on protein level ([113], Figure 3.3).

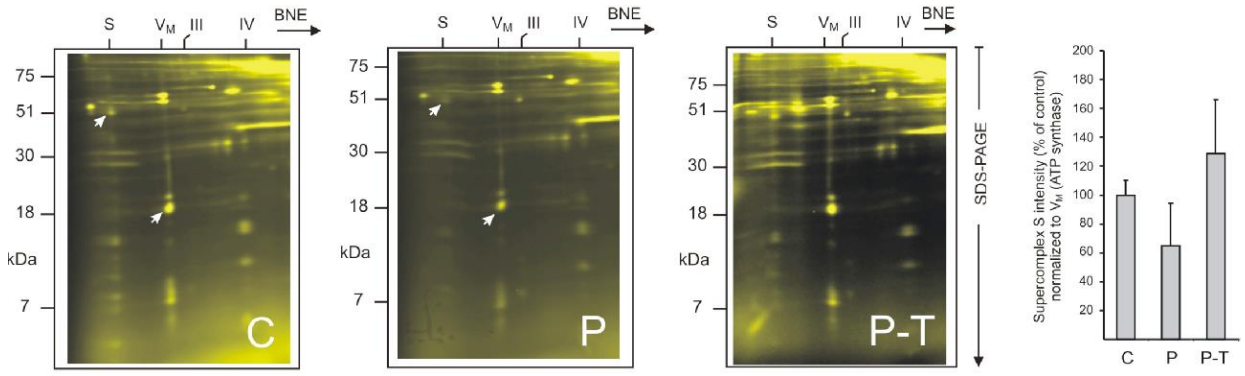

Figure 3.3: Complex I assembly in fibroblasts of patient 35834. 2D-BN-SDS Gel showed the increased supercomplex assembly after wt-ACAD9-cDNA transduction in patient 35834. Data are expressed as average of > 3 technical replicates and normalized to control. ±SD (C = healthy control, P = Patient 35834, P-T = Patient 35834 transduced with wt-ACAD9-cDNA, white arrows indicate proteins used for quantification)

3.1.2.3 Further patients with mutations in *ACAD9*

Whole Exome sequencing with our cohort of unsolved complex I patients and samples sent from different co-operation partners or specific ACAD9 sequencing led to the identification of 29 additional patients with mutations in the *ACAD9* gene (Table 3.3 and Figure 3.4). 41 other patients were already described in literature by other groups [92, 114, 119, 165, 170, 213-219]. Within this group of 50 families (70 patients), 52 different variants were found (18 previously unreported; indicated in bold, Figure 3.4 taken from [220]): 42 missense, one frame shift, one nonsense, seven splice site and one start codon mutation. No individual was found with two predicted loss of protein (LOF) function. This indicates that a complete loss of ACAD9 function might be incompatible with life. To estimate the incidence of ACAD9 deficiency in the European and worldwide population the minor allele frequency of LOF variants contained in GnomAD and causal ACAD9 variants present in the ACAD9 cohort was used. Based on the total allele frequency it can be assumed that approximately 59 children in Europe and 689 children worldwide will be born with ACAD9 deficiency every year (Calculation done by Elisa Mastanuono, Table 3.3) [220].

		Formula	
ACAD9 LoFs* in GnomAD**	(A)	Allele count – n homozygous carrier/ 1/2* allele number	European 0,000666345 Total 0,000689169
Causal ACAD9 missense and LoF variants (ACAD9 cohort)	(B)	Allele count – n homozygous carrier/ 1/2* allele number	European 0,002762796 Total 0,001618123
Total allele frequency (missense + LoF) in GnomAD and ACAD9 cohort	(C)	$(A+B)^2$	European 0,00001176 Total 0,0000053236
Estimated prevalence	(D)	1/C	European 1:85041 Total 1:187842
Estimated incidence in Europe# Worldwide extrapolation §	(E) (F)	$5.1*10^6$/D 129.596 *106/D	59 689

Table 3.3: Calculation of European and worldwide incidence of ACAD9 deficiency (Table taken from [220])

To further investigate this big cohort of ACAD9 patients, Dr. Saskia Wortmann, Elisa Mastantuono and me created an online survey which was completed by the responsible clinician (www.surveymonkey.com [221]). The survey included questions about age of onset, biochemical abnormalities, current age or age at death, prenatal and neonatal findings, most frequent clinical findings, neurological findings, neuroradiological findings, activities of daily life and medication (Table 3.4). The cardiac and neurological phenotype and the effect of riboflavin on the outcome of the patients was analysed in detail in the PhD work of Elisa Mastantuono [222]. I used the data to analyse any genotype-phenotype correlation, remaining complex I activity measured in muscle and/or fibroblasts correlated to the severity of the disease, correlation between effect of riboflavin in vivo and vitro and correlation between severity of the disease and remaining FAO capacity.

Table 3.4 Overview of all known and new discovered patients with ACAD9 mutation

Patient ID	Family ID	Addition patient ID, #FirboID	Gender	Origin	Diagnosed through	Mutation Nucleotide	Mutation Amino Acid	Measured tissue	Complex I activity	Lactate acidosis	Age at first symptoms	Current age/age of death	Main clinical symptoms	Riboflavin treatment	Reference
1	1a	Pat.1 #35834	f	Italy, Caucasian	WES	c.130T>A c.797G>A	p.Phe44Ile p.Arg266Gln	muscle liver fibroblasts	14% 1% 32%	yes	neonatal	death 7 w	HCM, ME, MM	No	Haack et al. 2010
2	1b	Pat.2 #52935	m	Italy, Caucasian	WES	c.130T>A c.797G>A	p.Phe44Ile p.Arg266Gln	fibroblasts	38%	yes (>4)	neonatal	alive 10 y	HCM, ME, MM	Yes, with beneficial effect	Haack et al. 2010
3	2	Pat.3 #52933	f	Italy, Caucasian	CS	c.797G>A c.1249C>T	p.Arg266Gln p.Arg417Cys	muscle fibroblasts	13% 37%	yes	early infancy	death 12 y	HCM, ME, MM	Yes, with beneficial effect	Haack et al. 2010
4	3	Pat.4 #52674	f	Great Britain, Caucasian	CS	c.976G>C c.1594C>T	p.Ala326Pro p.Arg532Trp	muscle fibroblasts	26% 48%	yes	1 w	death 2 y	HCM, ME, MM, mild ID	n.a.	Haack et al. 2010
5	4a	Pat.1 CB, VII:11	f	Netherlands, Caucasian	HM	c.1594C>T c.1594C>T	p.Arg532Trp p.Arg532Trp	muscle fibroblasts	11% 40%	yes (6.5)	4 y	alive 43 y	MM	Yes, with beneficial effect	Gerards et al. 2010 Scholte et. al. 1995
6	4b	Pat.2 #49591, MJ, VII:6	f	Netherlands, Caucasian	HM	c.1594C>T c.1594C>T	p.Arg532Trp p.Arg532Trp	fibroblasts	38%	yes (3)	4 y	alive 34 y	MM, mild ID	Yes, with beneficial effect	Gerards et al. 2010 Scholte et. al. 1995
7	4c	Pat.3 JJ, VII:8	m	Netherlands, Caucasian	HM	c.1594C>T c.1594C>T	p.Arg532Trp p.Arg532Trp	muscle fibroblasts	72% 50%	yes (3)	4 y	alive 41 y	MM	Yes, with beneficial effect	Gerards et al. 2010 Scholte et. al. 1995
8	5	Pat.4 CV	f	Netherlands, Caucasian	CS	c.380G>A c.1405C>T	p.Arg127Gln p.Arg469Trp	muscle	9%	yes (9)	early childhood	alive 30 y	HCM, MM, mild DD	Yes, with beneficial effect	Gerards et al. 2010 Scholte et. al. 1995
9	6	Pat.1 #69842	f	Canada	AP	c.1553G>A c.1553G>A	p.Arg518His p.Arg518His	muscle fibroblasts	31% 60%	yes (7.6)	8 m	alive 18 y	HCM	Yes, with beneficial effect	Nouws et al. 2010
10	7a	Pat.2	f	Thai mother, German father	CS	c.187G>T c.1237G>A	p.Glu63X p.Glu413Lys	muscle fibroblasts	61% 58%	yes	4 m	death 6 m	HCM, ME	n.a.	Nouws et al. 2010
11	7b	Pat.3 (twin sister)	f	Thai mother, German father	CS	c.187G>T c.1237G>A	p.Glu63X p.Glu413Lys		n.d.	yes	6 m	death 8 m	HCM, ME	n.a.	Nouws et al. 2010
12	8a	Pat.1 #59029, 72545	m	Turkey	WES	c.1594C>T c.1594C>T	p.Arg532Trp p.Arg532Trp	muscle fibroblasts	3% n.r.	yes (5, during infection)	6 m	death 14 y	HCM, DCM, MM, mild DD	Yes, with beneficial effect	Haack et al. 2012
13	8b	Pat.2 #59033	f	Turkey	WES	c.1594C>T c.1594C>T	p.Arg532Trp p.Arg532Trp		n.d.	yes (4.4 during infection)	4.5 m	alive 6 y	HCM, DCM, mild DD	Yes, with beneficial effect	Haack et al. 2012
14	8c	Pat.3 #59036	f	Turkey	WES	c.1594C>T c.1594C>T	p.Arg532Trp p.Arg532Trp	muscle	reduced	yes (4.7)	4 m	alive 9 y	HCM, DCM, MM, mild DD	Yes, with beneficial effect	Haack et al. 2012
15	9	Sci Transl Med	m		MP	c.260T>A c.976G>A	p.Ile87Asn p.Ala326Pro	fibroblasts	severly reduced	yes	neonatal	neonatal death	HCM	n.a.	Calvo et al. 2012
16	10	JAMA Neurol	m	Italy, Caucasian	MP	c.1240C>T c.1240C>T	p.Arg414Cys p.Arg414Cys	muscle fibroblasts	15% 32%	yes (10)	1 y	alive 19 y	ME, MM, mild ID, mild DD	Yes, with beneficial effect	Garone et al. 2013
17	11	JIMD	f	Turkey	HM	c.659C>T c.659C>T	p.Ala220Val p.Ala220Val	muscle fibroblasts	≤11% 67%	yes (20)	neonatal	death 6 m	HCM, MM	Yes, with no effect	Nouws et al. 2014
18	12	JIMD Rep	m	France, Caucasian	CS	c.1030-1G>T c.1249C>T	acceptor splice site p.Arg417Cys	muscle	0.1%	yes (28)	prenatal	death 10 h	HCM, MM	No	Lagoutte-Renosi et al. 2015
19	13	F2	f	West Africa	CS	c.976G>A c.1595G>A	p.Ala326Pro p.Arg532Gln	muscle	severly reduced	yes (11)	neonatal	death 10 w	HCM, ME, MM	No	Collet et al. 2015
20	14	#62343 F3	f	France, Caucasian	WES	c.358delT c.1594C>T	p.Phe120fs p.Arg532Trp	heart muscle fibroblasts	40% 72% 79%	yes (7.4)	1 y	death 6 y	HCM, MM	No	Collet et al. 2015
21	15	#62340 F4	m	France, Caucasian	WES	c.976G>C c.1595G>A	p.Ala326Pro p.Arg532Gln	heart muscle fibroblasts	64% 54% 49%	yes (6.4)	18 m	alive 15 y	HCM, ME, MM	No	Collet et al. 2015
22	16	#62006 F5	f	France, Caucasian	WES	c.151-2A>G c.1298G>A	acceptor splice site p.Arg433Gln	heart muscle fibroblasts	68% 64% 78%	yes (4)	9 y	alive 35 y	HCM	n.a.	Collet et al. 2015
23	17	#62347 F6	m	France, Caucasian	WES	c.1237G>A c.1552C>T	p.Glu413Lys p.Arg518Cys	heart fibroblasts	43% 66%	yes (>3)	4 m	alive 22 y	HCM	No	Collet et al. 2015
24	18	F7	f	France, Caucasian	CS	c.1552C>T c.1564-6_15569del	p.Arg518Cys splice site	heart	severly reduced	yes (8)	15 m	death 21 m	HCM, MM	No	Collet et al. 2015

Table 3.4 continued

Patient ID	Family ID	Addition patient ID, #FirboID	Gender	Origin	Diagnosed through	Mutation Nucleotide	Mutation Amino Acid	Measured tissue	Complex I activity	Lactate acidosis	Age at first symptoms	Current age/age of death	Main clinical symptoms	Riboflavin treatment	Reference
25	19	F8	f	France, Caucasian	CS	c.1A>G c.796C>T	p.Met1? P.Arg266Trp	muscle fibroblasts	severly reduced mild	yes (14)	1 y	death 1.5 y	HCM, MM	No	Collet et al. 2015
26	20	PLoS Genet, Pt090	f	Japan	WES	c.1150G>A c.1817T>A	p.Val384Met p.Leu606His	muscle	severly reduced	yes	2 w	alive 2 w	HCM	n.a.	Kohda et al. 2016
27	21	PLoS Genet, Pt025	f	Japan	WES	c.811T>G c.1766-2A>G	p.Cys271Gly spilce site	muscle	reduced		14 y	alive 14 y	HCM, MM	n.a.	Kohda et al. 2016
28	22	Hum Pathol	m	Caucasian	WES	c.187G>T c.941T>C	p.Glu63* p.Leu314Pro	fibroblasts	53%	yes	neonatal	death 1 d	HCM, DCM, ME	n.a.	Leslie et al. 2016 Valencia et al. 2016
29	23	J Transl Med P1, #15	f	Polish	WES	c.514G>A c.803C>T	p.Gly172Arg p.Ser268Phe	muscle	39%	yes (12.9)	2 d	alive 8 y	HCM, MM, mild DD	Yes, with no effect	Pronicka et al. 2016
30	24	J Transl Med P2, #23	m	Polish	WES	c.1552C>T c.1553G>A	p.Arg518Cys p.Arg518His	muscle	28%	yes (8.9)	1 m	death 3 m	HCM, DCM, MM, mild DD	No	Pronicka et al. 2016
31	25	J Transl Med P3, #53	m	Polish	WES	c.728C>G c.1552C>T	p.Thr243Arg p.Arg518Cys	muscle	26%	yes (4.5)	2 y	alive 9 y	MM	n.a.	Pronicka et al. 2016
32	26a	BI-1	f	Morocco	MP	no confirmation du to lack of DNA				yes (17.4)	neonatal	death 5 m	HCM	n.a.	Dewulf et al. 2016
33	26b	BI-2	f	Morocco	MP	c.1636G>C c.1636G>C	p.Val546Leu p.Val546Leu	muscle	15%	yes (20.8)	2 m	death 10.5 m	HCM, ME, severe DD	Yes, with no effect	Dewulf et al. 2016
34	26c	BI-3	m	Morocco	MP	c.1636G>C c.1636G>C	p.Val546Leu p.Val546Leu	lymphocytes	reduced	yes (8.2)	15 d	death 9 m	HCM, ME, mild ID, severe DD	No	Dewulf et al. 2016
35	26d	BI-4	f	Morocco	MP	c.1636G>C c.1636G>C	p.Val546Leu p.Val546Leu	fibroblasts	n.r.	yes	15 m	alive 9 y	left ventricular hypertrophy, mild ID, mild DD	Yes, with beneficial effect	Dewulf et al. 2016
36	27a	BII-1	m	Belgium	MP	c.509C>T c.1687C>G	p.Ala170Val p.His563Asp	muscle	17%	yes (12.5, after exercise)	12 y	alive 29 y	HCM, MM, mild DD	n.a.	Dewulf et al. 2016
37	27b	BII-2	f	Belgium	MP	c.509C>T c.1687C>G	p.Ala170Val p.His563Asp	muscle	19%	yes (4.4, after exercise)	8 y	alive 26 y	HCM, MM, mild ID, mild DD	No	Dewulf et al. 2016
38	28a	BIII-3	f	Congo	MP	c.1240C>A c.1650_1672dup	p.Arg414Ser p.Leu558fs	muscle	reduced	yes (24.3)	2 d	death 9 d	HCM, ME	No	Dewulf et al. 2016
39	28b	BIII-6	f	Congo	MP	c.1240C>A c.1650_1672dup	p.Arg414Ser p.Leu558fs		n.d.	yes (60.9)	neonatal	death 2 d	HCM	No	Dewulf et al. 2016
40	28c	BIII-7	f	Congo	MP	c.1240C>A c.1650_1672dup	p.Arg414Ser p.Leu558fs		n.d.	yes (25.27)	neonatal	death 6 m	DCM, HCM, mild ID	Yes, with no effect	Dewulf et al. 2016
41	29	Muscle Nerve	f	Tunesia	CS	c.1240C>T c.1240C>T	p.Arg414Cys p.Arg414Cys	muscle	60%	yes (9.3, after excersise)	6 y	alive 34 y	MM	n.a.	Fragaki et al. 2016
42	30	#68891	m	Austria, Caucasian	WES	c.1690G>A c.1832A>G	p.Glu564Lys p.Tyr611Cys	muscle fibroblasts	64% 72%	yes (28.7)	pren.a.tal	death 2 d	DCM, ME	No	This study
43	31	#61980, UK1	m	Pakistani	CS	c.1553G>A c.1553G>A	p.Arg518His p.Arg518His	fibroblasts	34%		3 m	death 4 m	HCM	No	This study
44	32	#68541, UK2	f	Britain, Asian	CS	c.293T>C c.293T>C	p.Leu98Ser p.Leu98Ser	muscle fibroblasts	6% n.r.	yes (11)	7 y	alive 14 y	MM	Yes, with no effect	This study
45	33a	#63869, 71266	f	Sri Lanka	WES	c.1253A>G c.1253A>G	p.Asp418Gly p.Asp418Gly	muscle fibroblasts	9% 59%	yes (22)	4 m	death 1.5 y	DCM, mild ID, severe DD	No	This study
46	33b	#69297	m	Sri Lanka	WES	c.1253A>G c.1253A>G	p.Asp418Gly p.Asp418Gly	muscle	29%	yes (6)	9 m	alive 11 y	DCM, mild MM	Yes, with beneficial effect	This study
47	33c	SI-3	m	Sri Lanka	WES	c.1253A>G c.1253A>G	p.Asp418Gly p.Asp418Gly			yes (7.9)		alive 2 y	HCM, mild MM, mild ID, mild DD	Yes, with beneficial effect	This study
48	34	#71680, RaAn	f	Italy	CS	c.857T>C c.1240C>T	p.Leu286Pro p.Arg414Cys	muscle fibroblasts	7% 85%	yes	neonatal	alive 8 y	HCM, DCM, mild ID, mild DD	Yes, with no effect	This study
49	35	#71265	f	France	WES	c.976G>C c.1651A>G	p.Ala326Pro p.Ser551Gly	muscle liver fibroblasts	14% 38% n.r.	yes (7)	1 y	death 11 y	HCM, ME, MM, mild ID, mild DD	n.a.	This study

Table 3.4 continued

Patient ID	Family ID	Addition patient ID, #FirboID	Gender	Origin	Diagnosed through	Mutation Nucleotide	Mutation Amino Acid	Measured tissue	Complex I activity	Lactate acidosis	Age at first symptoms	Current age/age of death	Main clinical symptoms	Riboflavin treatment	Reference
50	36	#54900	m	Bahrain	WES	c.1684G>A c.1684G>A	p.Asp562Asn p.Asp562Asn	muscle	slightly reduced	no (2.2)	neonatal	alive 3 y	ME, MM, mild DD	n.a.	This study
51	37a	#75826	f		MP	c.1805C>T c.1805C>T	p.Ser602Phe p.Ser602Phe	mucle fibroblasts	severly reduced	yes (5.8)	2 m	death 6 m	HCM, DCM, ME, MM	No	This study
52	37b	#75827	m		MP	c.1805C>T c.1805C>T	p.Ser602Phe p.Ser602Phe		n.d.	yes (5)		alive 13 y	HCM, MM, mild DD	Yes, with beneficial effect	This study
53	38a	B1a	m	Nigeria	WES	c.868G>A c.1237G>A	p.Gly290Arg p.Glu413Lys	muscle	19%	yes (13, post cardiac arrest)	9 m	death 9.5 m	HCM, ME	No	This study
54	38b	B1b	m	Nigeria	WES	c.868G>A c.1237G>A	p.Gly290Arg p.Glu413Lys		n.d.	yes (5, CSF)	9 m	alive 8 y	HCM, ME, MM, severe ID, mild DD	Yes, with beneficial effect	This study
55	38c	B1c	m	Nigeria	WES	c.868G>A c.1237G>A	p.Gly290Arg p.Glu413Lys		n.d.	yes (2.9)	pren.a.tal	alive 7 y	HCM, MM, mild ID, mild DD	Yes, with beneficial effect	This study
56	39	UK3	f	UK, Caucasian	MP	c.976G>C c.1594C>T	p.Ala326Pro p.Arg532Trp	heart	1%	n.d.	neonatal	death 2 h	HCM	No	This study
57	40a	UK4a	m	UK, Caucasian	MP	c.665T>A c.1249C>T	p.Ile222Asn pArg417Cys	muscle	59%	yes (23.6)	neonatal	death 13 d	ME	Yes, with no effect	This study
58	40b	UK4b	m	UK, Caucasian	MP	c.665T>A c.1249C>T	p.Ile222Asn pArg417Cys		n.d.	n.d.	6 m	death 6 m	sudden death	No	This study
59	41a	UK5a	m	UK, Caucasian	MP	c.1150G>A c.1168G>A	p.Val384Met p.Ala390Thr	muscle	23%	y (7.2)	2 y	alive 38 y	HCM, MM, mild DD	Yes, with no effect	This study
60	41b	UK5b	m	UK, Caucasian	MP	c.1150G>A c.1168G>A	p.Val384Met p.Ala390Thr		n.d.	y (6.3)	9 y	alive 44y	HCM, MM	Yes, with no effect	This study
61	42	UK6	f	UK, Caucasian	MP	c.1552C>T c.1715G>A	p.Arg518Cys p.Cys572Tyr	muscle	30%	y (20)	2 m	death 3 m	HCM, ME	n.a.	This study
62	43	B2	f	Belgium, Caucasian	CS	c.976G>C c.1552C>T	p.Ala326Pro p.Arg518Cys	muscle	50%	y (11.6)	2 y	alive 3 y	HCM, MM	No	This study
63	44	I1	m	Italy, Caucasian	WES	c.1240C>T c.1646G>A	p.Arg414Cys p.Arg549Gln	muscle	65%	y (2.5)	neonatal	alive 9 y	HCM, MM, mild DD	Yes, with beneficial effect	This study
64	45	M12188	f	Germany, Caucasian	MP	c.569C>T c.1405C>T	p.Ala190Val p.Arg469Trp	muscle	severely reduced	y (12.5)	1 y	alive 16 y	MM, HCM, Deafness, mild DD	Yes, with beneficial effect	This study
65	46a	I2a	m	Italy, Caucasian	WES	c.1240C>T c.1240C>T	p.Arg414Cys p.Arg414Cys	muscle	n.a.	n.d.	infancy	death 44 y	HCM, DCM, MM	n.a.	This study
66	46b	I2b	m	Italy, Caucasian	WES	c.1240C>T c.1240C>T	p.Arg414Cys p.Arg414Cys	n.a.	n.a.	y (37)	neonatal	alive 16 y	HCM, MM	Yes, with no effect	This study
67	47	I3	m	Italy, Caucasian	WES	c.555-2A>G c.1168G>A	splice site p.Ala390Thr	muscle	2%	y (<13)	neonatal	death 2 m	HCM, severe DD	Yes, with no effect	This study
68	48	C1	m	China, Asian	WES	c.797G>A c.1359-1G>A	p.Arg266Gln splice site		n.a.	n.a.	2 y	alive 3 y	HCM, DCM, mild DD	Yes, with beneficial effect	This study
69	49	C2	f	China, Asian	WES	c.1737T>G c.1240c>T	p.Asn579Lys p.Arg414Cys		n.a.	n.a.	10 m	alive 3 y	HCM, DCM, mild DD	Yes, with beneficial effect	This study
70	50	C3	f	China, Asian	WES	c.988A>C c.988A>C	p.Lys330Gln p.Lys330Gln		n.a.	n.a.	4 m	alive 6 y	mild ID, mild DD	Yes, with beneficial effect	This study

Table 3.4: Overview of all known and newly discovered patients with mutations in *ACAD9*. Complex I rest activity is expressed as percentage of the lowest control level, HCM: Hypertrophic cardiomyopathy, CM: cardiomyopathy, LA: lactic acidosis, n.r.: normal range, n.a.: not available

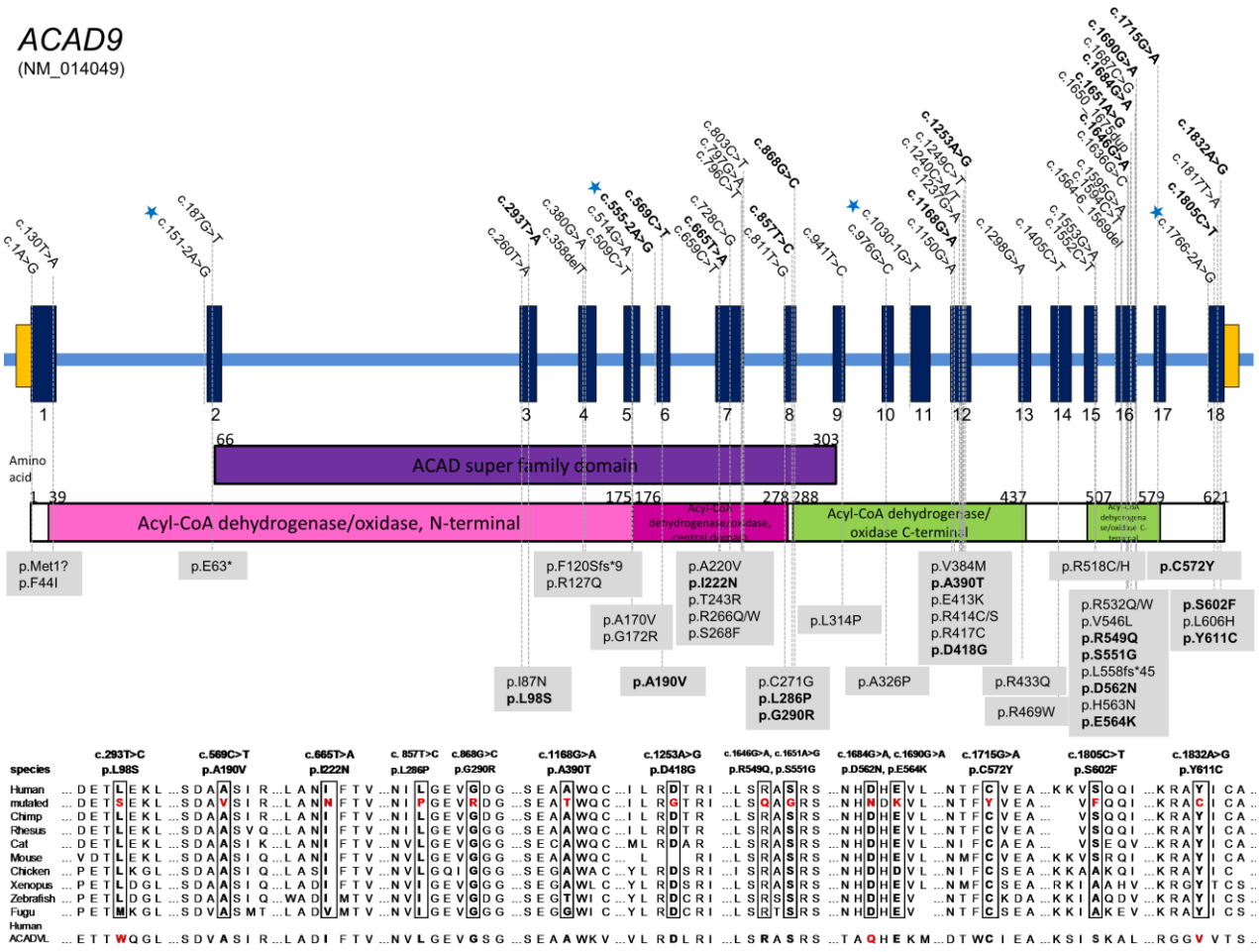

Figure 3.4: Gene structure of *ACAD9* with localization of mutations in 70 patients and conservation of affected amino acid residues. Blue asterisks indicate splice site mutations. Newly identified mutations are shown in bold. Conservation of amino acid residues affected by missense variants (Figure taken from [220])

3.1.2.4 ACAD9 cohort

The main clinical findings are summarized in Table 3.4. A detailed description, including clinical data, clinical course and treatment of all 70 patients in 50 families can be found in the supplements (Table S2, S3 and S4).

Together with reported cases a cohort of 70 patients (41 female, 29 male) from 50 families will be described. Parental consanguinity was present in seven families. 34 patients were of Middle and South European (five siblings), twelve of African (seven siblings), four Turkish (two siblings), seven Asian (one sibling), two Asian/European (one sibling) and one each of American, Pakistani and Arabian descent. Ethic background was unknown for four cases.

Clinical spectrum

The age of onset ranges from prenatal to 14 years (median four months, Figure 3.5A). Prenatal symptoms, occurring in four patients, were intrauterine growth retardation and revealed cardiomegaly. 22% of the

patients (n = 15) showed first symptoms directly after birth. The main neonatal symptoms were lactic acidosis, failure to thrive, hypoglycemia and hypertrophic cardiomyopathy. 18 patients (30%) developed first symptoms before the age of six months. These patients were conspicuous through growth retardation, recurrent infections, dyspnea, elevated blood pressure or abnormal fatigue. Only six patients showed an onset at the age >5 years. These six patients presented signs of dyspnea, exercise intolerance, myotonia and milder forms of hypertrophic cardiomyopathy. At the time of the study 37 individuals were alive (median 14 years, range 24 days-44 years) and 33 patients already deceased (median three months, range 1 day-44 years). Most patients (n = 50) develop the first symptoms before one year of life and the majority of them do not survive the first two years of life. In contrast to that, most patients with an onset >1 year (n = 20) survive the more than ten years. The main clinical findings were cardiomyopathy (n=56/66, 85%), muscular weakness (n = 37/49, 75%), exercise intolerance (n = 34/47, 72%) and mild developmental delay (n = 23/51, 45%) (Figure 3.5D).

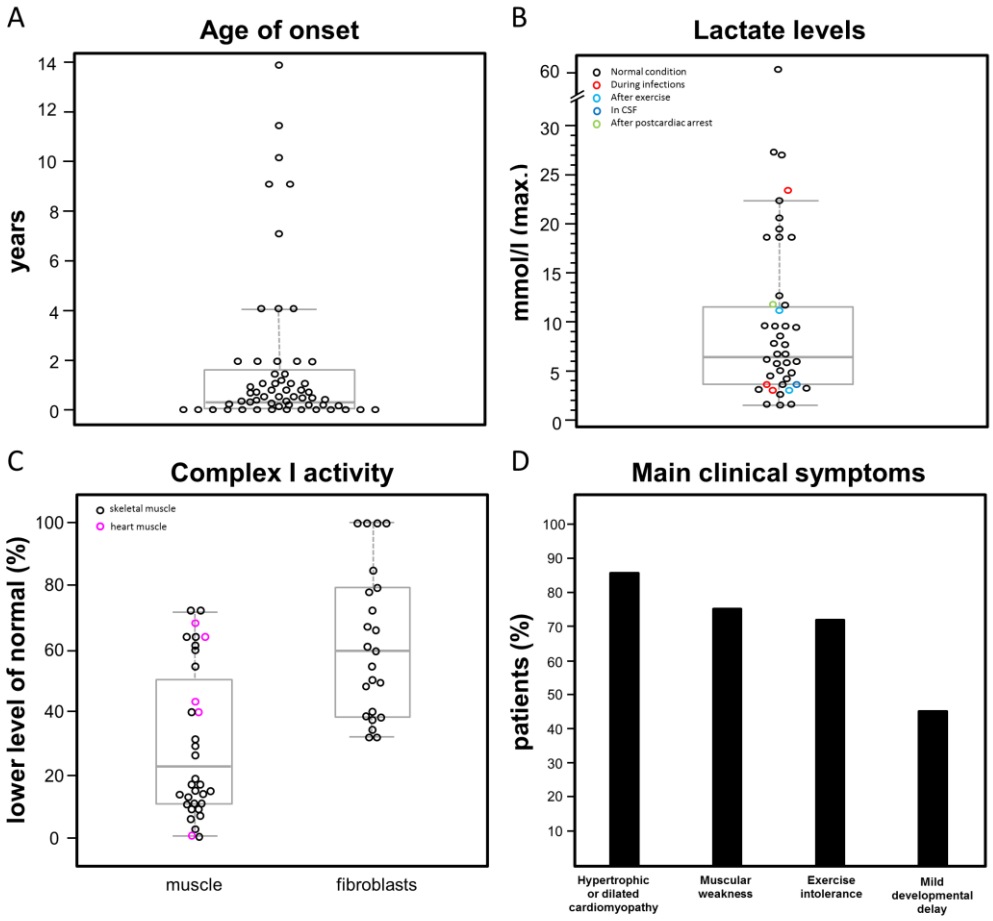

Figure 3.5: (A) Age of onset, (B) lactate levels, (C) complex I activity (measured in muscle and fibroblasts) and (D) main clinical symptoms of our cohort of 70 patients with mutations in *ACAD9*

Cardiac disease was reported in 85 % of the patients (n = 56/66). 42 patients developed a hypertrophic, seven patients dilated and six patients hypertrophic and dilated cardiomyopathy. In three patients, heart problems were already recognized during pregnancy. Ultrasound examination revealed cardiomegaly, cardiac insufficiency or cardiac arrhythmia. Six patients revealed a patent ductus arteriosus, and one patient present a scimitar syndrome. Cardiac failure was the main cause of death in 50% of the patients (n = 14).

Interestingly four patients received heart transplantation at the age of 1 month, 1 year, 9 years and 18 years respectively. Unfortunately the two young patients died despite all efforts at the age of 3 months and 4 years respectively, whereas the other two patients are alive and currently 15 and accordingly 35 years old [63]. Only nine patients presented without cardiac involvement. From these nine patients seven are still alive to date. The second most frequent clinical finding was muscular weakness (75%, n = 37/49), followed by exercise intolerance with a frequency of 72% (n = 34/47). Seven individuals were reported to have only muscular problems, without cardiac or brain involvement, defining a relativity mild group of patients. The fourth main clinical feature was mild developmental delay, observed in almost half of the patients (45%, n = 23/51). Only one patient was reported to have a severe intellectual disability and mild intellectual disability was present in 29% of the patients (n = 14/48). The majority of patients currently alive are able to perform the same activities of daily living compared to children of the same age.

Metabolic findings

Elevated blood lactate levels were reported in 98% of all cases (n = 56/57, median 8.6mmol/l, range 2.5-60.9mmol/l, normal range < 2.2mmol/l) (Figure 3.5B). Blood alanine concentrations were measured in 22 cases and exceed the reference range in 15 cases (68%). Analysis of respiratory chain complex activities in skeletal muscle revealed a clear complex I defect in all patients analyzed (n = 44, median 26%, range 0-72% of the lower range of normal). The analysis of heart muscle in seven patients showed a clear reduction of complex I activity as well (median 40%, range 1-61% of the lower range of normal). The complex I defect was also present, but less pronounced in 82% of the analyzed fibroblast cell lines (n = 26, median rest activity 60%, range 32-100% of the lower range of normal, Figure 3.5C). Five patients presented an additional defect in complex V, one patient in complex II and IV; the other complexes were reported to be normal or slightly increased.

Disease course variations between families

Due to the broad spectrum of different ACAD9 mutations predictions for genotype-phenotype correlations are very limited. Within the cohort of 50 families five times two families have the same mutations in *ACAD9*. One example for a similar disease course between families, are members of the family 4 and 8. They all have a homozygous mutation at position p.Arg532Trp. At the time of the study all members (n = 6) were alive and were reported to have mitochondrial myopathy, exercise intolerance, no or mild hypertrophic cardiomyopathy, no encephalopathy and in general only minor restrictions. An example of different disease course between patients sharing the same mutation (p.Arg518His) is patient 9 and 43. The first symptoms occurred in patient 9 at the age of eight months with failure to thrive and hepatomegaly due to congestive heart failure. At the age of 18 years she has a short stature, exercise intolerance, mild hearing loss, and mild hypertrophic cardiomyopathy. Patient 43 developed at the age of three months

respiratory distress and a hypertrophic obstructive cardiomyopathy was diagnosed. His disease course worsened and he died one month later due to cardiac failure.

Disease course variations within families

One example for disease course variation within siblings is family 37: The younger child presented from the age of two months on with persistently elevated lactate levels, hypertrophic cardiomyopathy, mitochondrial encephalopathy and mitochondrial myopathy. She finally died at the age of six months due to respiratory, cardiac and metabolic decompensation. mitoPANEL diagnostics discovered a homozygous mutation (p.Ser602Phe) in *ACAD9.* The older brother was first reported to be healthy, but is sharing the same mutation as the affected sister. In retrospection the parents report that he has since a long time marginally movement disorders and light exercise intolerance. Cardiac examination revealed mild hypertrophy of the left ventricle and blood lactate levels were also increased (5mmol/l, normal <2mmol/l). He is now 13 years old presenting mild exercise intolerance and learning difficulties.

Taken together, the analysis of the data leads to the assumption, that there are two subgroups pf patients with mutations in *ACAD9*. Patients with a disease onset of <1 year have poor survival rate compared to patients with a disease onset >1 year of age. The overall frequency of cardiomyopathy in patients with *ACAD9* mutations was found to be four times higher than in other patient cohorts with isolated complex I deficiency [63], whereas severe developmental delay and intellectual disability was present only in a minority of (surviving) patients. There was no clear genotype-phenotype correlation.

3.1.2.5 Studies on ACAD9 patient-derived fibroblasts

In order to study the effect of the different mutations and test new treatments we collected fibroblast cell lines from 17 of the 70 ACAD9 patients. 13 out of 17 examined patient cell lines showed a significant reduction of OCR (Figure 3.6). The cell line with the mutations on position c.293T>C leading to the amino acid change from leucine to serine at position 98 showed no complex I defect (FibroID 68541). In most cases the complex I defect was more pronounced in muscle than in fibroblasts (Table 3.3, Figure 3.5C). The OCR measurements of two patients harbouring the same mutation (p.Arg532Trp) homozygote in patient 12 (FibroID 72545) and heterozygote with an additional frame-shift mutation in patient 20 (FibroID 62343) showed only mildly reduced levels.

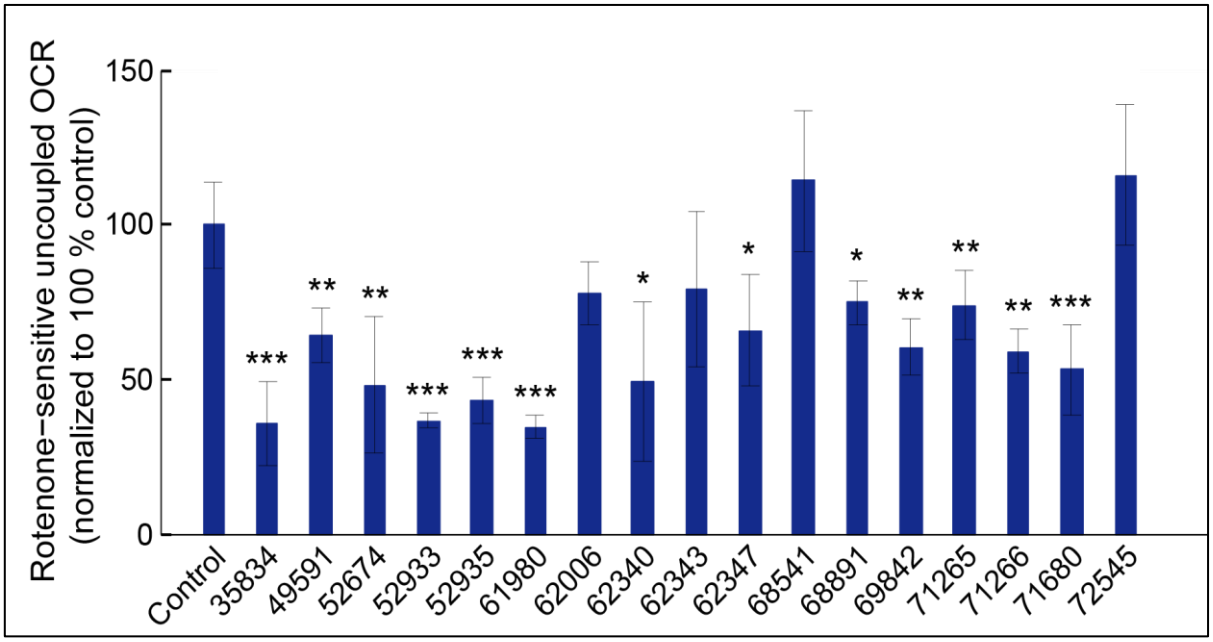

Figure 3.6: OCR in fibroblasts of patients with mutations in *ACAD9*. Data are expressed as average of > 10 technical replicates and normalized to control. ±SD, (p-value<0,05 *, p-value<0,01**, p-value<0,001,***).

3.1.2.6 Western Blot analysis of patients with ACAD9 mutation

The consequences of the different mutations on the ACAD9 protein stability were determined with Western Blots.

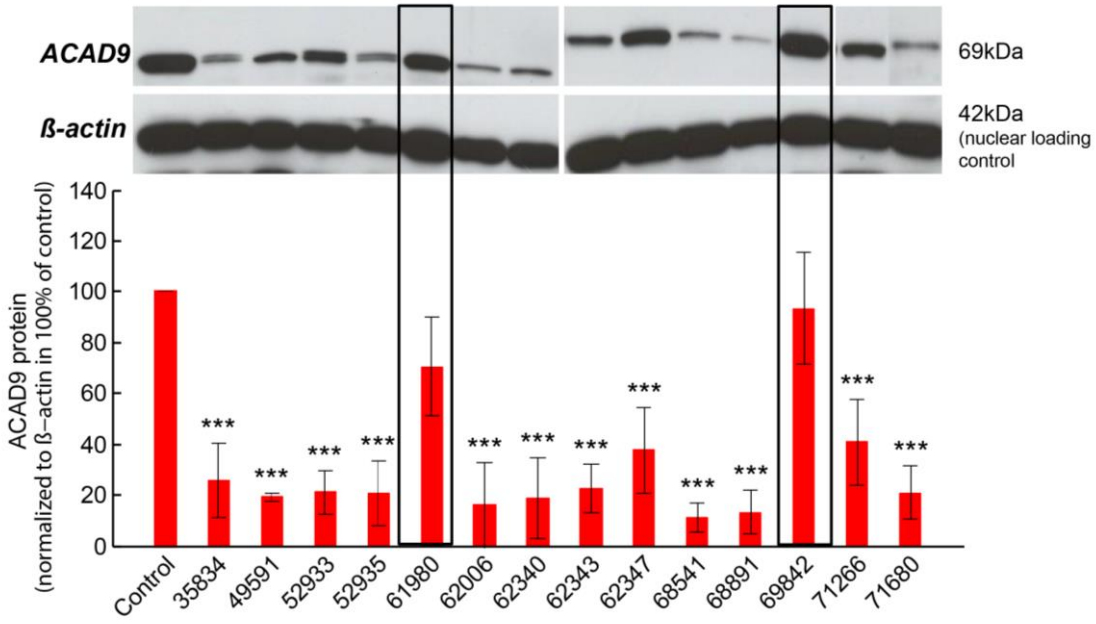

Figure 3.7: Western Blot analysis of patients with different ACAD9 mutations. Average of three technical replicates, ±SD. Amount of ACAD9 protein was normalized to ß-actin in % of control (p-value<0,001,***).

The amount of ACAD9 is significantly reduced in all cell lines except patients with mutations leading to the amino acid change from Arginine to Histidine at position 518 (FibroID 61980 and 69842, Figure 3.7).

Interestingly patients with mutations in p.Arg266Gln showed a double band of ACAD9. The analysis of two other complex I subunits (NDUFS1 and NDUFA9) showed also a reduction in some cases whereas the amount of SDHA (complex II subunit) remained almost unchanged. The protein of the very long form of the ACAD family ACADVL is only slightly reduced in some patients (Figure 3.8)

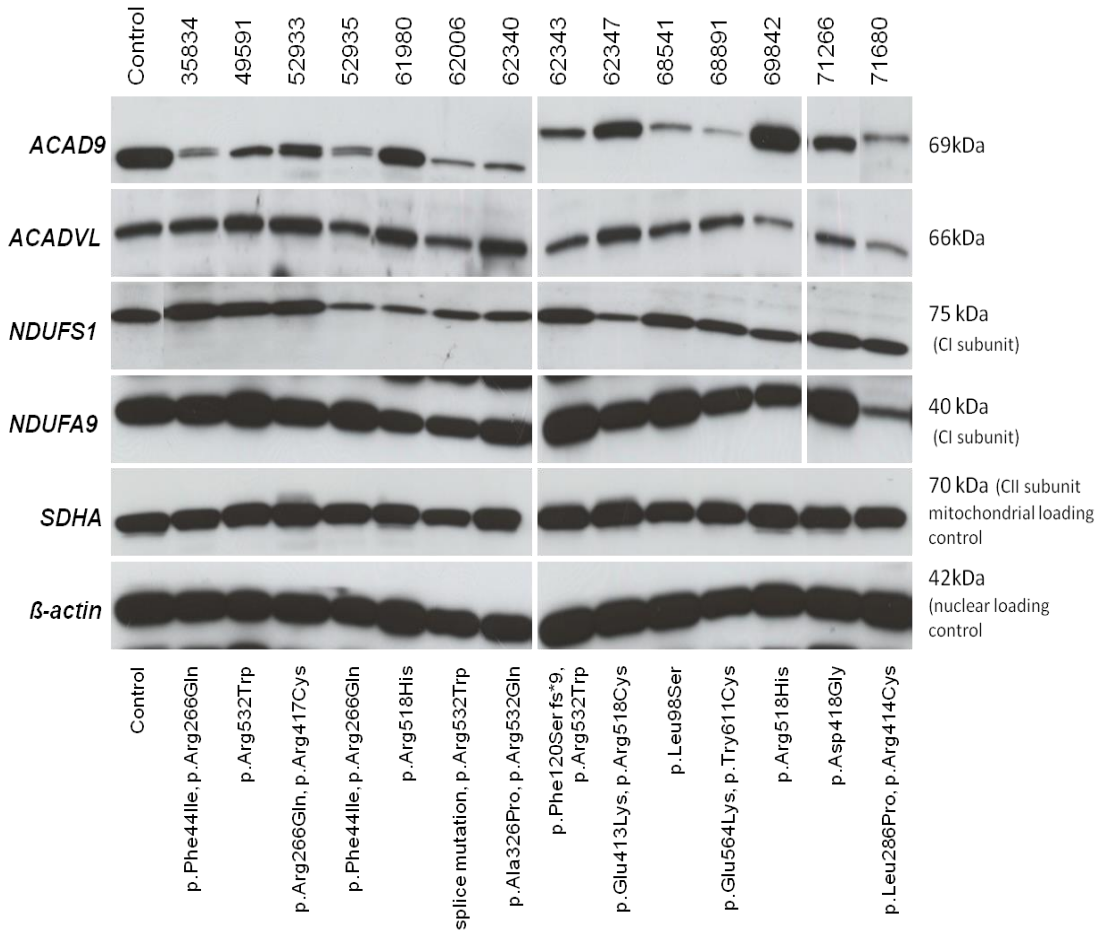

Figure 3.8: Western Blot analysis of patients with different ACAD9 mutations. SDS-gels were decorated with ACAD9, ACADVL two different complex I subunits (NDUFS1, NDUFA9), complex II subunit (SDHA) and ß-actin as a loading control.

The next point was to see if there is any correlation between the complex I activity and the amount of remaining ACAD9 protein (Figure 3.9).

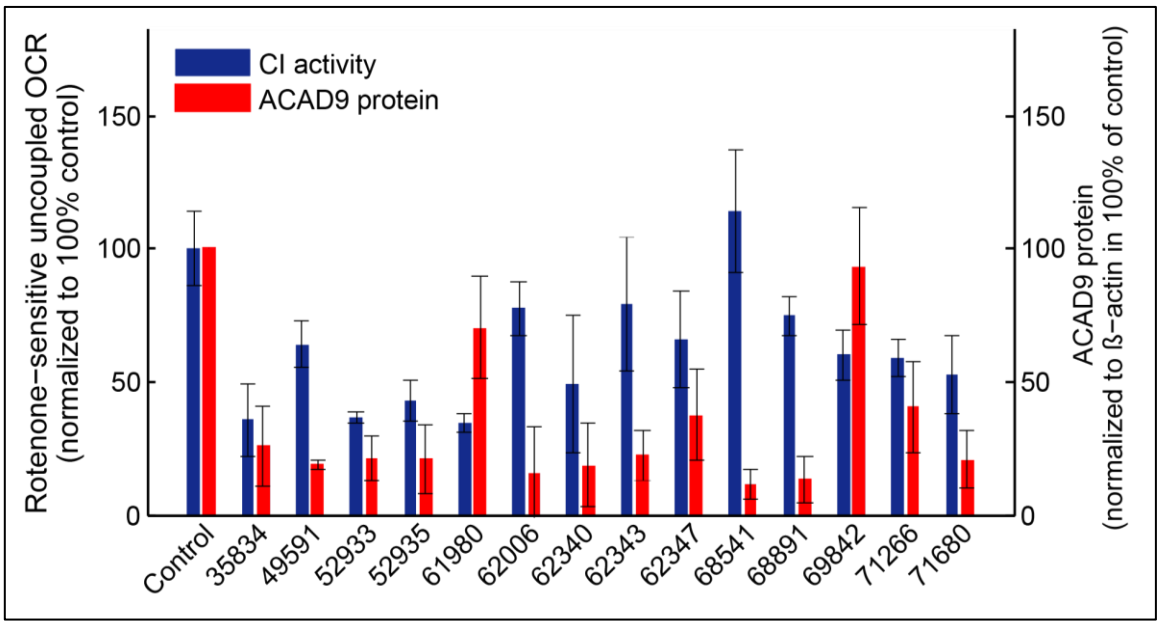

Figure 3.9: Comparison of complex I activity (blue bars) and remaining ACAD9 protein levels (red bars) Data expressed as average of three independent Western Blots and average of >10 technical replicates (OCR) ±SD

The cell lines with the homozygote p.Arg518His mutation have still a quite normal amount of ACAD9 but a low complex I activity (FibroID 61980 and 69842). These observations direct to the assumption that this mutation leads to a reduction of the ACAD9 activity rather than protein stability. Ten cell lines show a low amount of ACAD9 protein resulting in a clear reduction of complex I activity. The cell lines with the homozygous mutation p.Leu98Ser (FibroID 68541) and the compound heterozygote mutations p.Glu564Lys and p.Try611Cys (FibroID 68891) respectively have a very low amount of ACAD9 protein but a high complex I activity. In this case the remaining ACAD9 chaperone activity might be high enough to result in a correct assembly of complex I and consequently an almost normal complex I activity (Figure 3.9).

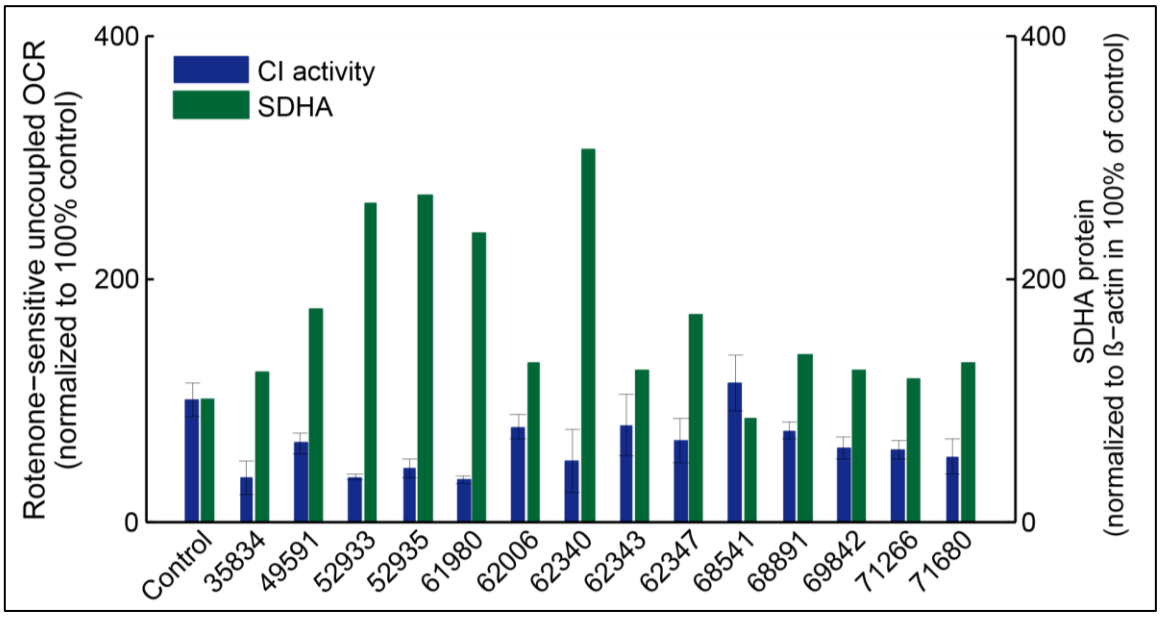

Figure 3.10: Comparison of complex I activity and the amount of SDHA protein. (Blue bars: complex I activity, green bars: amount of SDHA protein) Data expressed as average of >10 technical replicates (OCR) ±SD

Due to the compensatory effect, known from other mitochondrial complex I deficient cell lines, the amount of SDHA (complex II subunit) in fibroblasts increased in most cases compared to the control (see figure 3.10). The patient cell lines with the lowest complex I activity presented the highest amount of SDHA protein (FibroID 52933, 52935, 61980 and 62340).

ACAD9 is a member of the big acyl-CoA dehydrogenase family. Prof. Jerry Vockley and his group from Pittsburgh are experts on the metabolism of short chain acyl-CoAs and its deficiency as well as on the molecular characterization of acyl-CoA dehydrogenases. In order to get more information about the consequences of the different ACAD9 mutations and their influence on the ß-oxidation pathway we started a collaboration. They were able to model different ACAD9 mutations in *E. coli* to look for ACAD9 expression and to measure the residual C16-CoA dehydrogenase activity (Figure 3.11).

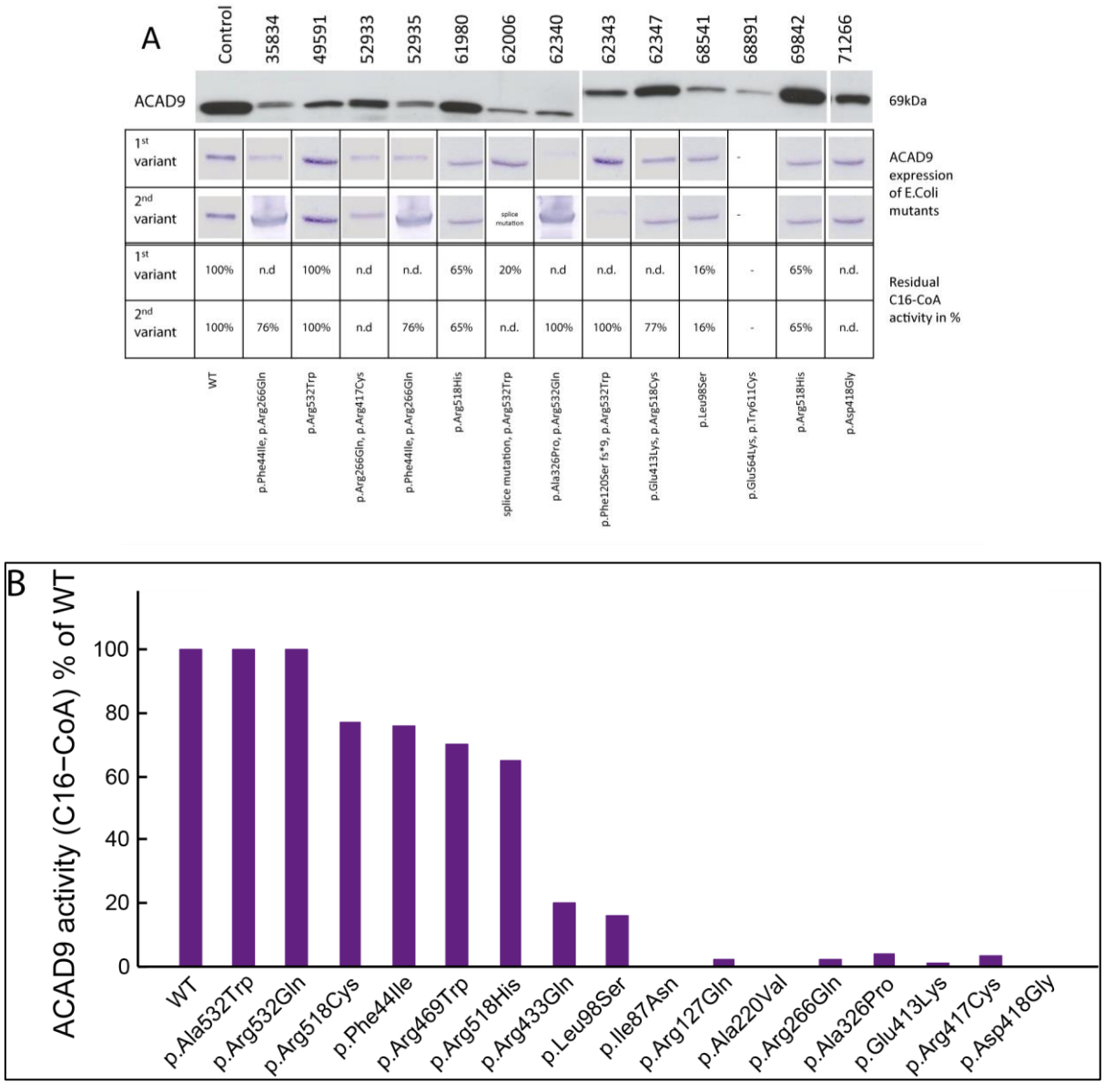

Figure 3.11: (A) Comparison of *ACAD9* expression in fibroblasts, *E. coli* and residual C16-CoA activity. (n.d. not detectable), (B) Graphical view of all *ACAD9* activity of all modeled ACAD9 variants in *E. coli*

The residual ACAD enzyme activity of mutant proteins varied from not detectable to normal compared to the control and did not correlate with the complex I defect [223]. This shows that ACAD9 mutations cause complex I deficiency independent of their effects on ACAD enzyme activity. Molecular modeling of ACAD9 point mutations was further used to identify their location in the enzyme structure. Interestingly all mutations with little or no impact on ACAD activity are located in the C-terminal domain of the protein, while inactivating mutations were observed to be located in the catalytic portion of the molecule [223].

The next interesting question was if the different residual ACAD enzyme activity, the amount of protein and complex I activity have an influence on the severity of the phenotype of the different patients.

3.1.2.7 Correlation analysis

Influences of ACAD enzyme activity on the severity of the phenotype

The clinical phenotypes of all described patients with mutations in *ACAD9* range from neonatal death to mild exercise intolerance. Great variations in complex I activity, the remaining ACAD9 protein level and the FAO capacity were observed. But the influence of complex I activity, ACAD9 protein level and fatty acid oxidation capacity on the severity of the phenotype remains ambiguous.
Therefore, we classified the phenotype of the patients in two groups. The first group included patients with only mild exercise intolerance and/or cardiomyopathy. The second group included all patients with death before the age of two years and/or encephalopathy. The median of complex I measured in muscle was 21% in the mild group and 15% in the more severe group ($p = 0.971$). The median complex I activity measured in fibroblasts was a little bit but not significantly higher in the group of patients with a milder phenotype (72% to 49%, p-value = 0,09). The median of the remaining ACAD9 protein level was similar in both groups (19 to 21%, p-value =0,89). The only significant influence on the severity of the phenotype seems to have to the mean of both alleles` ACAD9 dehydrogenase activity. The median ACAD9 dehydrogenase activity, as determined in the prokaryotic expression system, was 77% in the milder group. The median of the group with patients with more severe phenotype was only 19% (p-value: 0,0022) (Figure 3.12).

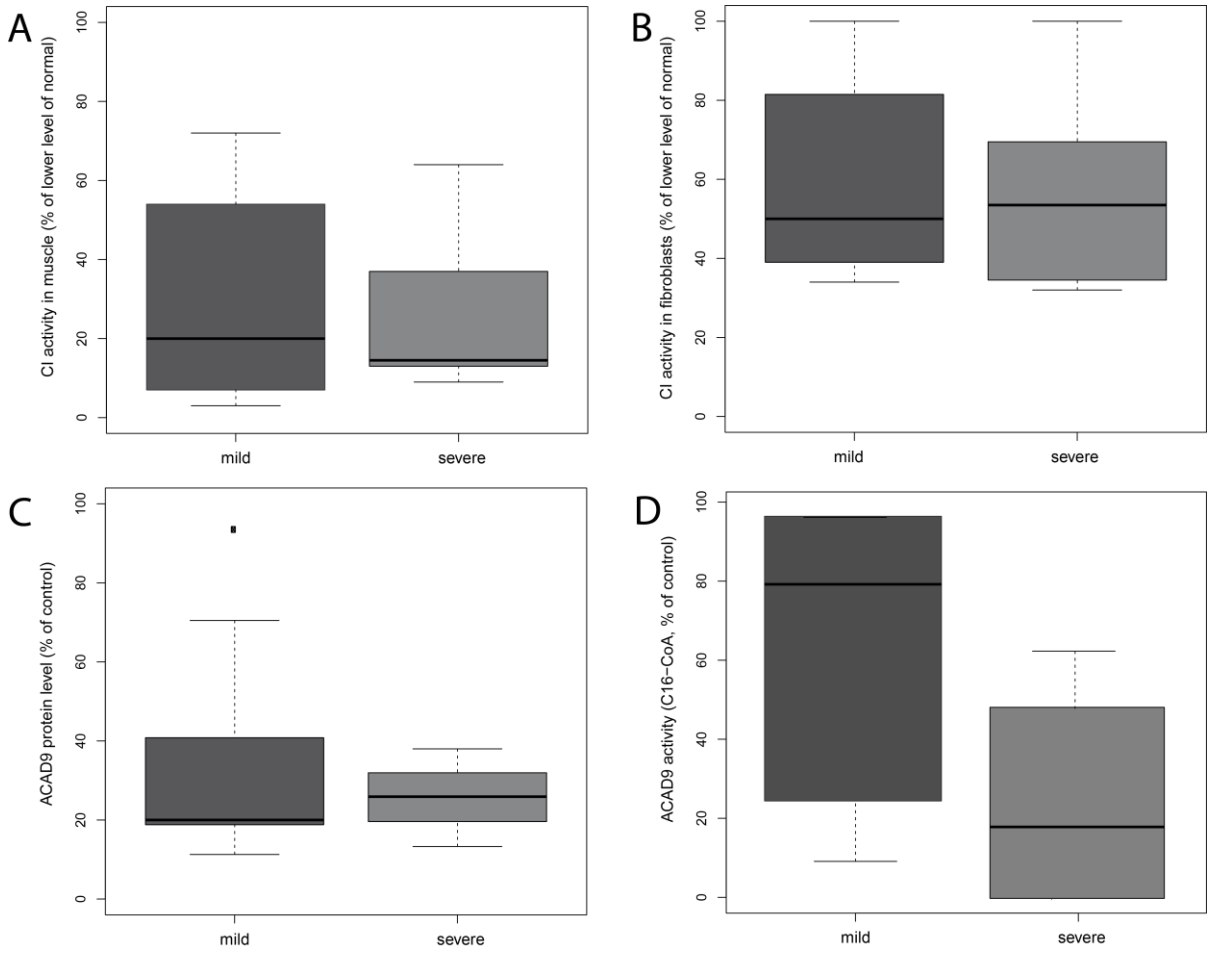

Figure 3.12: Correlations between the severity of the phenotype and the complex I activity in muscle (A), in fibroblasts (B), the remaining amount of ACAD9 protein (C) and ACAD9 dehydrogenase activity (D).

These results demonstrate that ACAD9 mutations can impact ACAD9 chaperonin function in the respiratory chain independent of its ability to function as a fatty acid oxidation enzyme. The complex I activity (measured in muscle and fibroblasts) and remaining ACAD9 protein levels seem to be not a good predictor of clinical severity. It seems that patients, who have a complex I defect and low levels of ACAD enzyme activity have a much higher risk to die early or develop encephalomyopathy. In terms of treatment possibilities the counteracting of the dysfunction of complex I and simultaneously fatty acid oxidation dysfunction should be taken into account [223].

3.1.3 Further examples

3.1.3.1 NDUFB3

The DNA of the next patient (50845) used for exome sequencing was a girl with mitochondrial encephalopathy; mitochondrial myopathy, muscular hypotonia, developmental delay and blood lactic acidosis. The biochemical analysis of the respiratory chain in fibroblasts showed a clear complex I defect

with a rest activity of only 17%. The other complexes were also reduced to a rest activity of 42% (complex II/III) and 57 % (complex IV). The data filtering, performed by Dr. Tobias Haack, revealed the following results (Table 3.5):

Filters	**Number of SNVs/genes**
NSV (frequency <0.4% in controls)	246
Genes with ≥ 2 NSV	9
Known disease alleles	0
Known complex I subunits and assembly factors	1 (NDUFB3)
Mitochondrial localization	1 (NDUFB3)

Table 3.5: Filtering steps to identify candidate genes for complex I deficiency by exome sequencing of patient 50845, NSV = nonsynonymous genetic variants

In this patient a compound heterozygote mutation in the complex I subunit *NDUFB3* was found (c.64T>C het, p.Trp22Arg, c.208G>T het, p.Gly70X). These variants were not described previously. Therefore, the pathogenicity was tested with the complementation assay followed by functional and protein level investigation. Complementation experiments, the oxygen consumption measurement and Western Blot analysis were performed together with a former medical student Eva-Maria Frisch. Patient derived skin fibroblast cell line was transduced with a lentiviral system overexpressing the wt-NDUFB3-cDNA and in this case also the cDNA with the NDUFB3 missense mutation and an additional cDNA with a NDUFB3 stop mutation. The oxygen consumption rate was measured using the Seahorse XF 96 extracellular flux Analyzer following the standardized uncoupling protocol (Chapter 2.7.3). Uncoupled complex I activity was calculated as rotenone-sensitive OCR. OCR increased significantly from 17% to almost 90% of the lower level of normal after the transduction with the wt-NDUFB3-cDNA. The overexpression of NDUFB3-cDNA carrying either the p.Trp22Arg (missense-NDUFB3-cDNA) or the p.Gly70X (stop-NDUFB3-cDNA) mutations into the patient cells did not increase the low levels of complex I activity. The transduction of the control cells with the stop-NDUFB3-cDNA dropped complex I activity down to 35% of control whereas the transduction of the control cells with the missense-NDUFB3-cDNA did not change complex I activity significantly (Figure 3.13, [91]).

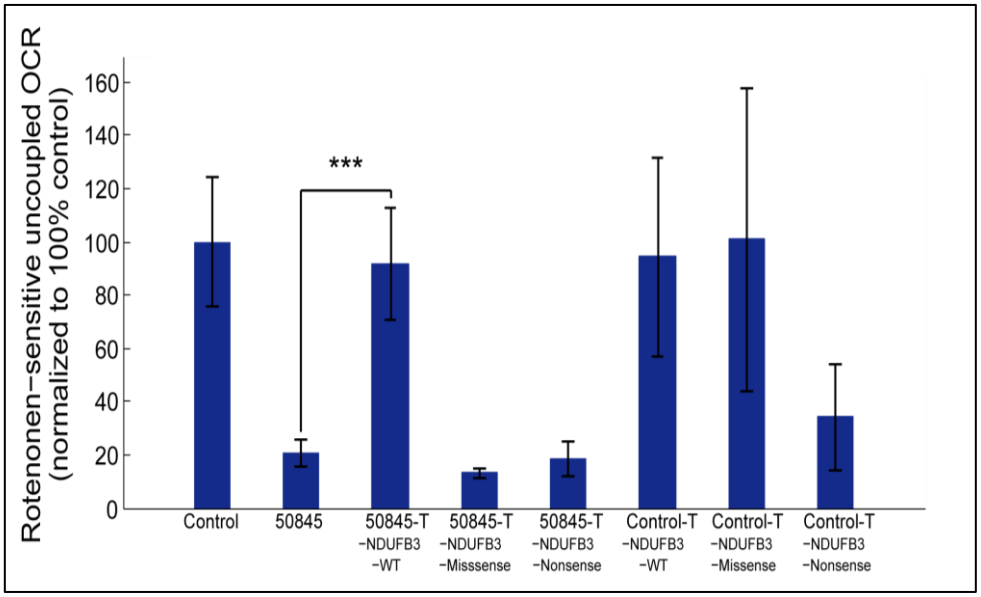

Figure 3.13: Rotenone-sensitive uncoupled oxygen consumption rate of patient 50845 and control before and after wt-NDUFB3-cDNA, missense-NDUFB3-cDNA and stop-NDUFB3-cDNA transduction. Data are expressed as average of > 10 technical replicates and normalized to control. ±SD, (p-value<0,05,*, p-value<0,01,**, p-value<0,001,***)

The analysis of the patient cell line on the protein level showed that the NDUFB3 protein was absent in naïve cells, but re-established after transduction with wt-NDUFB3-cDNA, but not after the transduction with the stop-NDUFB3-cDNA. The identical effect was detected in two other complex I subunits (NDUFB8 and NDUFS3), indicating a general assembly and/or stability defect of complex I (Figure 3.14A, taken from [91]).

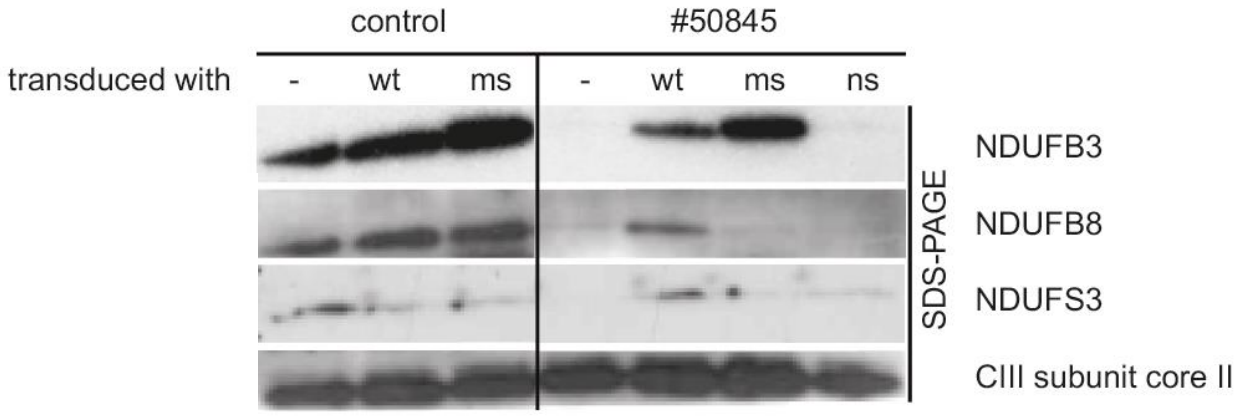

Figure 3.14A: Expression of mitochondrial complex I subunits/complex I assembly. For Western-blot analysis 20mg of total cell protein from patient 50845 and control skin cultured fibroblasts with and without overexpressing of the wt-NDUFB3-cDNA or stop-NDUFB3-cDNA were separated and immuno-decorated with antibodies specific for subunits of the respiratory chain complex I (NDUFB3, NDUFB8,NDUFS3) and subunit core II of complex III as control (figure taken from [91])

The impaired complex I assembly or stability due to NDUFB3 mutations was further confirmed by two-dimensional blue-native/SDS-PAGE separation and in-gel quantification of fluorescein-labelled mitochondrial complexes (mitoGELs). Comparing patient and control fibroblasts, the signal intensity of complex III was not altered. Complex IV and V of patient fibroblasts were reduced to 48% and 76%, respectively compared to the control cell line. The supercomplexes were not detectable in the patient. After the transduction of the patient cell line with wt-NDUFB3-cDNA, the amounts of mitochondrial

supercomplexes in patient fibroblasts increased up to 43% of the control. The amounts of complexes III, IV, and V did not change significantly (Figure 3.14B) [91].

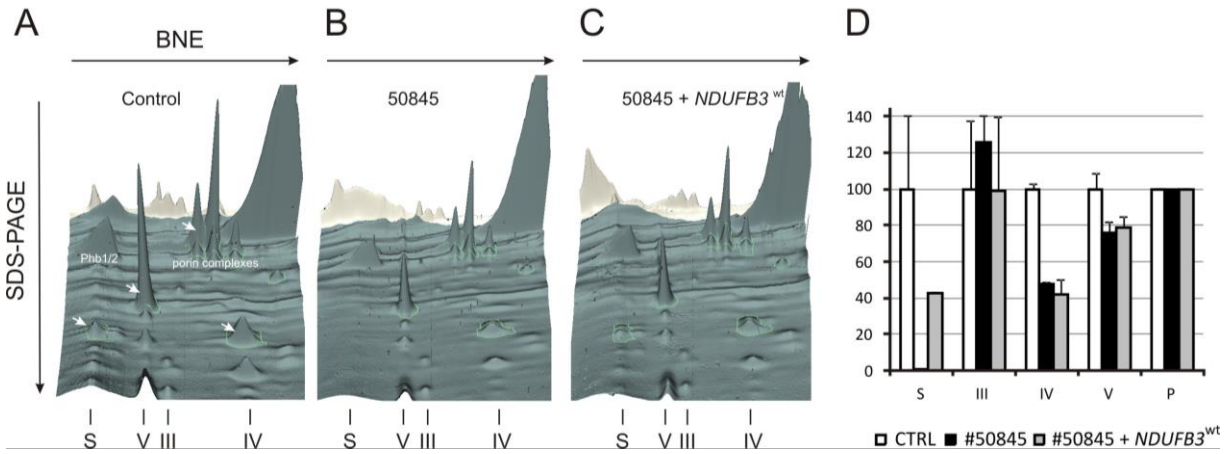

Figure 3.14B: mitoPanorama of a 2D- BN/SDS-PAGE separation and quantification of fluorescent-labelled mitochondrial complexes and supercomplexes. Control (A) and patient #50845 fibroblasts before (B) and after (C) transduction with the NDUFB3-wt construct (D), densitometric quantification of mitochondrial complexes in 2D BN/SDS-PAGE from human fibroblasts, expressed as per cent of healthy control cells, ±SD (two technical replicates). Arrows indicate proteins used for quantification.

In conclusion, these results provide a functional validation of the pathogenicity of the newly identified mutations in the complex I subunit *NDUFB3* [91].

3.1.3.2 NDUFS8

The next two patients (33027, 33284), whose exome was sequenced, presented with the following clinical and biochemical features. Both patients had an isolated complex I defect (present in muscle and skin fibroblasts) and muscular hypotonia. Patient 33027 had additionally a diagnosed Leigh-Syndrome, accompanied with dyskinesia, epilepsy, lactic acidosis and MRI changes. Patient 33284 presented with mitochondrial encephalopathy, hypertrophic cardiomyopathy and respiratory insufficiency. After analysing and filtering the whole-exome result (performed by Dr. Tobias Haack) the following variants were found in the two patients [91] (Table 3.6):

Filters	**33027**	**33284**
NSV (frequency <0.4% in controls)	2523	231
Genes with ≥ 2 NSV	588	13
Known disease alleles	0	0
Known complex I subunits and assembly factors	2 (NDUFS7/8)	1 (NDUFS8)
Mitochondrial localization	14	1

Table 3.6: Filtering steps to identify candidate genes for complex I deficiency by exome sequencing of patient 33027 and 33284

In patient 33027 two mutations in two genes encoding for complex I subunits *(NDUFS7* c.124C>T het, p.Pro42Ser; c.514C>A het, p.Arg172Ser and *NDUFS8* c.187G>C homo, p.Glu63Gln) were found. The NDUFS7 variant could be excluded, because his affected sister carried only the homozygous mutation in *NDUFS8*. Patient 33284 had only one variant in a complex I subunit with mitochondrial localization (NDUFS8 c.229C>T het, p.Arg77Trp, c.476C>A het, p.Ala159Asp). All variants were not reported before. That's why the disease character of all variants was verified with the complementation assay. The effect of the wt-NDUFS8-cDNA transduction in patient cell lines was measured with the Seahorse XF 96 Flux Analyzer (Figure 3.15) and BN gels.

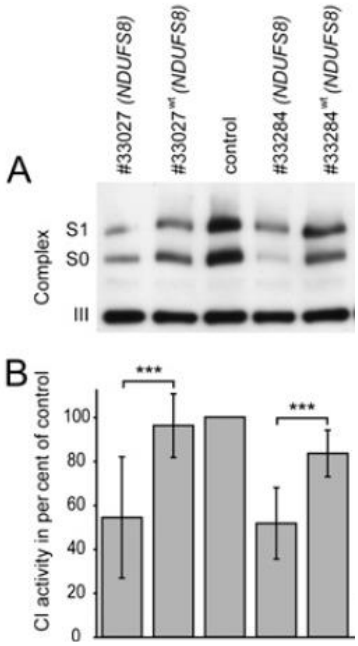

Figure 3.15: The mutations in *NDUFS8* result in decreased activity and amount of complex I Introduction of wt-NDUFS-cDNA rescues both amount and activity of complex I in subject fibroblasts measurement (A) BN-Gel, (B) Uncoupled oxygen consumption. Data are expressed as average of > 8 technical replicates and normalized to control. ±SD, (p-value<0,001,***) (Figure taken from [91])

The rotenone-sensitive uncoupled respiration increased significantly in patient 33027 and 33284 up to almost normal level (Figure 3.15B). An increase in the amount of assembled supercomplexes can be seen in the BN-Gel (Figure 3.15A). These results confirmed the pathogenicity of the variants [91].

3.1.3.3 BOLA3

Exome sequencing was further used to identify the disease-causing variant in two siblings with multiple mitochondrial disorders (MMDS) associated with an early onset fatal course of the disease leading to death within the first year of life. Both children showed a combined deficiency of respiratory chain complexes I, II, and II+III accompanied by a defect of the pyruvate dehydrogenase complex. The defect was also confirmed by mitoGEL analysis. The quantification demonstrated a clear decrease of complex I containing supercomplexes and a milder decrease of complex IV (Figure 3.16).

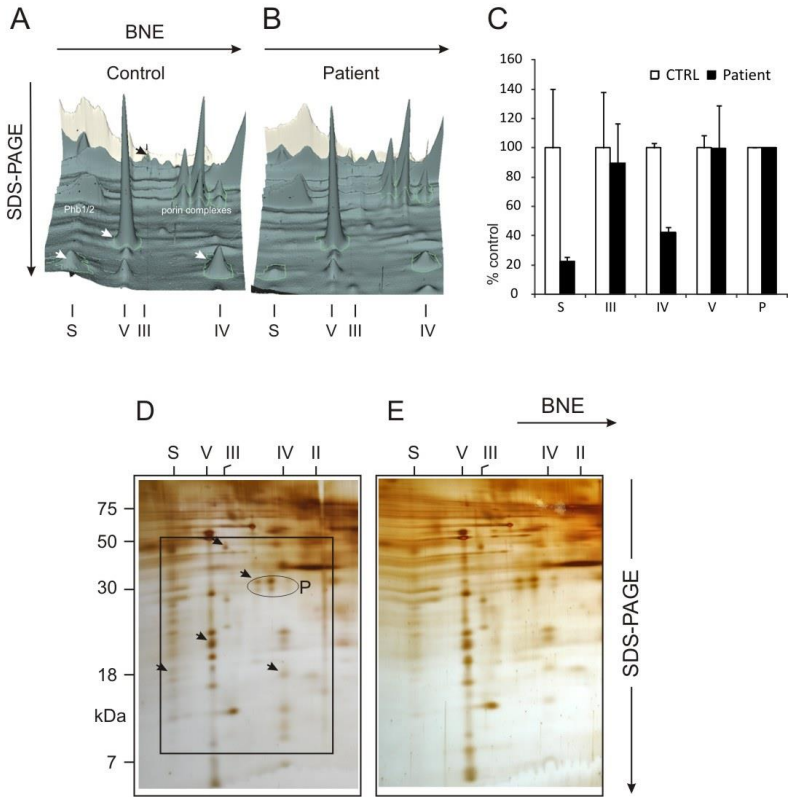

Figure 3.16: Separation and quantification of fluorescent-labelled mitochondrial complexes by 2D BN/SDS-PAGE. 3D visualization of quantified mitochondrial membrane complexes from control (A) and patient #49720 (B). (C) Quantification of fluorescence intensities of selected clearly visible protein spots. Mitochondrial complexes were quantified by densitometry, normalized to porin complexes and expressed as percent of healthy control cells ±SD (two technical replicates). Silver stained 2D-gels from (D) control and (E) patient fibroblasts are shown for comparison. Rectangle shows a representative gel area of the 3D view in (A and B). Arrows indicate proteins used for quantification. Assignment of complexes: S, supercomplexes composed of respiratory chain complexes I, III, and IV; V, complex V or ATP synthase; III, complex III or cytochrome c reductase; IV, complex IV or cytochrome c oxidase; Phb1/2, prohibitincomplex and P for porin complexes (Figure taken from [224]).

The analysing and filtering of the results of the exome sequencing was performed by Dr. Tobias Haack as previously described [91, 224]. The following variants were identified (Table 3.7):

Patient ID	#49720	#56712	present in both
Synonymous	8,761	11,015	6,985
NSV	8,058	10,824	6,264
NSV not present in 818 controls	201	294	72
≥2 NSV / gene	8	16	2 (*BOLA3, GCSI*)
Mitochondrial localization	1	1	1 (*BOLA3*)

NSV = missense, nonsense, stop loss, splice site disruption, insertions, deletions; mitochondrial localization refers to proteins with a MitoP2-score ≥1.0.

Table 3.7: Filtering steps to identify candidate genes for combined OXPHOS deficiency by exome sequencing of patient 49720 and 56712 (Table taken from [224])

The only variant present in both siblings with mitochondrial localization prediction was BOLA3. Cameron et al. recently identified a homozygous BOLA3 nonsense mutation in a patient with MMDS. The clinical and biochemical findings and progress of the disease were remarkably similar to our patients [225]. In order to confirm the deleterious impact of the BOLA3 variant, we performed complementation experiments in patient fibroblast cell lines to test for functional rescue of impaired enzyme activities.
OCR was measured using the Seahorse XF 96 extracellular Flux Analyzer. Uncoupled complex I activity was calculated as rotenone-sensitive OCR. It showed a significant increase from 32 % to 82 % residual activity upon expression of wt-BOLA3-cDNA. The transduction of wt-BOLA3-cDNA in control cell lines did not change the activity significantly [224] (Figure 3.17).

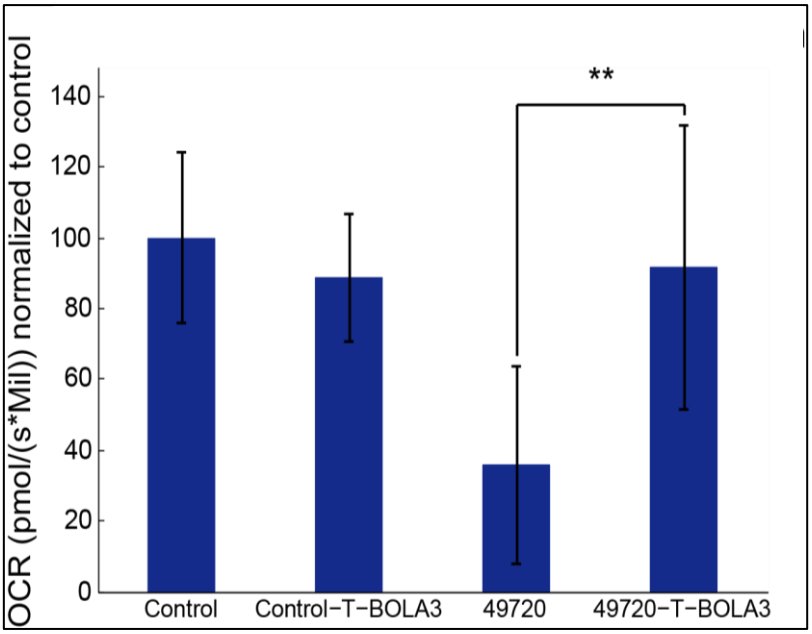

Figure 3.17: Rotenone-sensitive uncoupled oxygen consumption rate of patient 49720 and control before and after wt-BOLA3-cDNA transduction. Data are expressed as average of > 8 technical replicates and normalized to control. ±SD, (p-value<0,01,**)

Immunohistochemical staining

The immunohistochemical investigation by confocal microscopy was performed in cooperation with the group of Dr. Hans Mayr and Franz Zimmermann at the "Universitätsklinik für Kinder-und Jugendheilkunde" in Salzburg. Immunohistochemical staining demonstrates an increase of SDHA protein upon BOLA3-wt expression in patient fibroblasts. The complex II subunit SDHA was stained with green, VDAC1 with red and DAPI with blue. The immunohistochemical analysis of lipoic acid levels in patient and control fibroblasts demonstrated reduced lipoic acid levels in the patient cell lines which were clearly increased upon expression of wt-BOLA3-cDNA. VDAC1 (green), lipoic acid (red), DAPI (blue) (Figure 3.18)

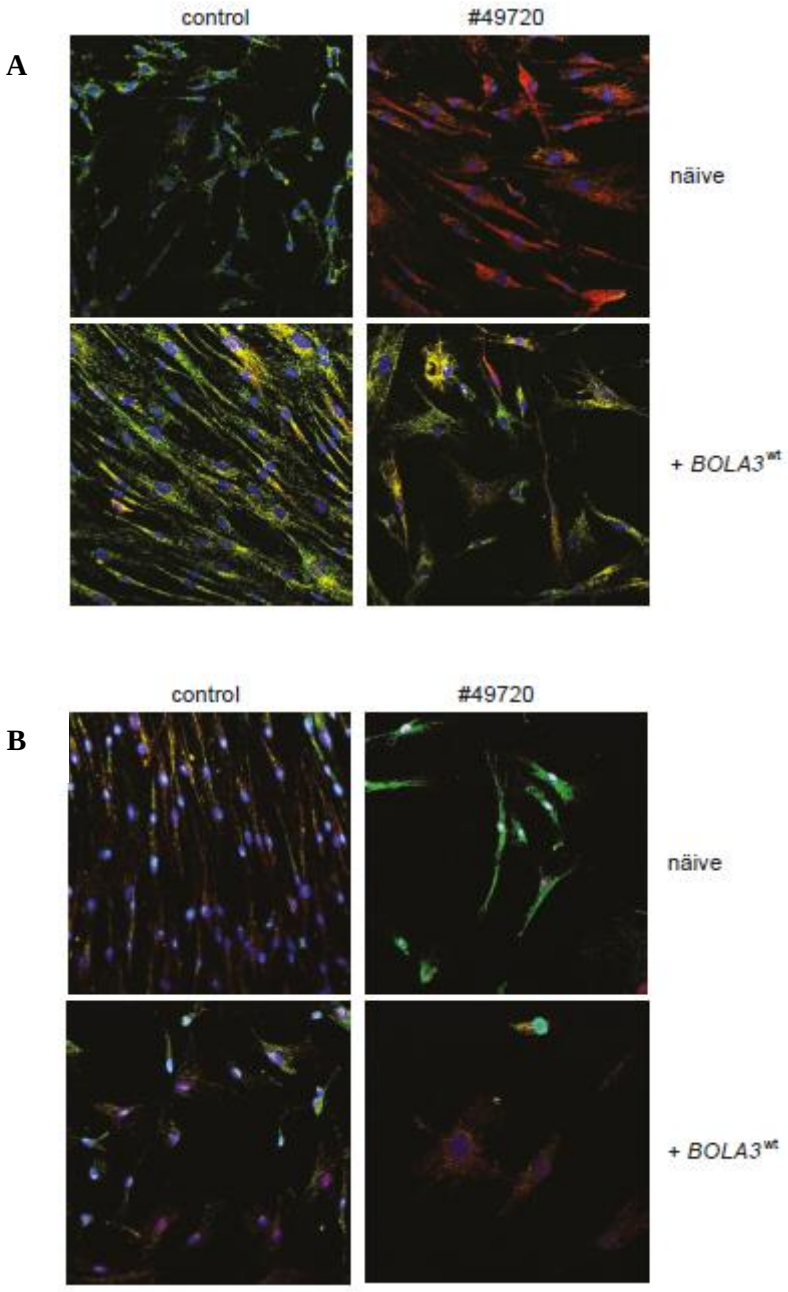

Figure 3.18: (A) Immunohistochemical investigations before and after wt-BOLA3-cDNA transduction of patient 49720. The staining demonstrates an increase of SDHA protein upon wt-BOLA3-cDNA expression in patient fibroblasts. Complex II, SDHA (green), VDAC1 (red), DAPI (blue). (B) Immunohistochemical analysis of lipoic acid levels in patient and control fibroblasts. Reduced lipoic acid levels were clearly increased in patient cell lines upon expression of wt-BOLA3-cDNA. VDAC1 (green), lipoic acid (red), DAPI (blue) (Figure modified from [224]).

All together the BOLA3 variant found via exome sequencing is most likely the cause of the disease. Patients with similar biochemical pattern and clinical course should be tested for mutations in the *BOLA3* gene.

3.1.3.4 AIFM1/MTFMT

We next applied exome sequencing to investigate a girl with pronounced microcephaly, accompanied by severe muscular hypotonia and developmental delay. At six months of age the development stopped and she regressed. Despite all efforts she died at the age of 19 months due to pneumonia with respiratory insufficiency [226]. Biochemical analysis of the respiratory chain revealed a 70% and 45% reduction of complex I activity in muscle and fibroblasts, respectively, compared to controls. In fibroblasts an additional complex IV defect was detected. The number of identified variants at different levels of prioritization filters is given in table 3.8 (Exome analysis performed by Dr. Tobias Haack):

Filters	**52181**
synonymous variants	8493
nonsynonymous variants	7258
Genes with het. rare (<4 controls)	182 (AIFM1)
Genes with comp. het + homo rare	3 (APEX1, LRRC37B, TYW1)
known mitochondrial disease variants	0

Table 3.8: Filtering steps to identify candidate genes for combined OXPHOS deficiency by exome sequencing of patient 52181

The analysis of known structural subunits and assembly factors of complex I, the search for two mutated alleles in genes coding for mitochondrial proteins and the screen for two loss of function alleles in any gene did not succeed. The identified compound heterozygous mutations or homozygous mutations in two (*APEX1*, *LRRC37B*) of the three genes were predicted to be neutral (Reference: MutationTaster/Polyphen2) [227]. The mutation in *TYW1* was predicted to be deleterious; however, the corresponding gene product has not been linked to mitochondria. TYW1 is responsible for the synthesis of Wybutosine, which is involved in the decoding of ribosomes.

As in some cases the second mutation might be missed due to poor coverage of the targeted region, we next expanded our filters to include genes affected by heterozygous mutations. This analysis identified missense mutations in three genes previously associated with respiratory chain defects, *NUBPL*, *POLG*, and *AIFM1*. Manual inspection of the coverage of the genes in the exome sequencing experiment and Sanger sequencing of uncovered regions did not indicate any additional rare variants. However, *AIFM1* (NM_004208.3) is located on the X chromosome and the heterozygous mutation (c.952G>A, p.Ala318Thr) together with an unfavorable pattern of X-inactivation, a mechanism previously reported for another complex I disease gene, *NDUFA1*, could explain the disease phenotype in our patient [228]. Reanalyzing the data, one of the 182 heterozygote mutations was a mutation in the x-linked gene Apoptosis-inducing factor 1, mitochondrial (AIFM1 c.952>A het, p.Ala318Thr). The main function of AIFM1 is the maintenance of the electron transport chain, reactive oxygen species regulation, cell death, and neurodegeneration [229]. Due to the fact, that AIFM1 is located in mitochondria and the mutation is

predicted deleterious the variant seemed to be the best candidate. The mother was also examined and presented the same mutation. X-inactivation in the patient and her mother was examined. The mother had an activation of 80% of the wild-type allele and 20% of the mutated allele. The daughter presented inverted levels. An existing mouse model with a proviral insertion of the *AIFM1* gene caused a partial decrease of the AIF protein to about 20% compared to wild-type mice. The phenotype of this mouse model was very heterogeneous in disease expression and severity and time progression. Most animals showed a correlation between the reduction level of the 20kDA subunit of complex I and the severity of the phenotype and pace of disease progress [230]. The mice are characterized with progressive cerebellar ataxia, early fur abnormalities, optic tract dysfunction with retinitis pigmentosa and a higher risk of cardiomyopathy. Recently two case reports from Ghezzi and Berger [169, 231]; showed that hemizygous mutations in *AIFM1* cause a mitochondrial encephalomyopathy and other mitochondrial deficiency syndromes. All cases had a clear reduction of complex I and complex IV activity in muscle and fibroblasts.

In order to test if this variant is responsible for the complex I/IV defect of the patient we transduced a patient-derived fibroblast cell line displaying the enzymatic defect with wt-AIFM1-cDNA. The Seahorse oxygen consumption measurement showed an increase of OCR by about 30%. The transduction of the wt-cDNA into control cells did not change OCR significantly (Figure 3.19).

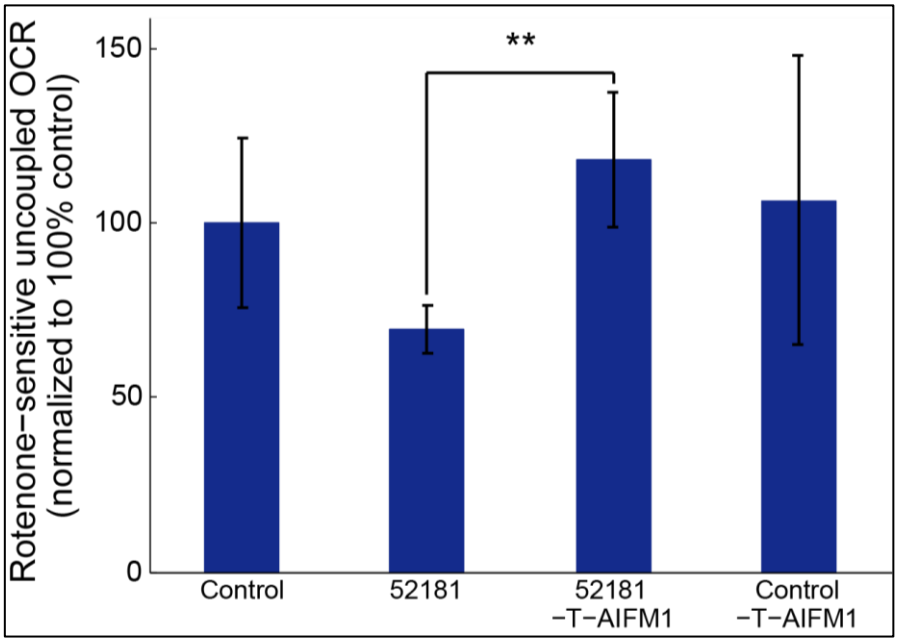

Figure 3.19 Rotenone-sensitive uncoupled oxygen consumption measurement of patient 52181 and control before and after wt-AIFM1-cDNA transduction. Data are expressed as average of > 8 technical replicates and normalized to control. ±SD, (p-value<0,01,**)

The next step was to look on the assembly of the respiratory chain complexes with mitoGELs. The gels showed a reduction of supercomplexes, complex II, complex IV and complex V of the patient compared to the control. After transduction the amount of the respiratory chain complexes did not change significantly (Figure 3.20).

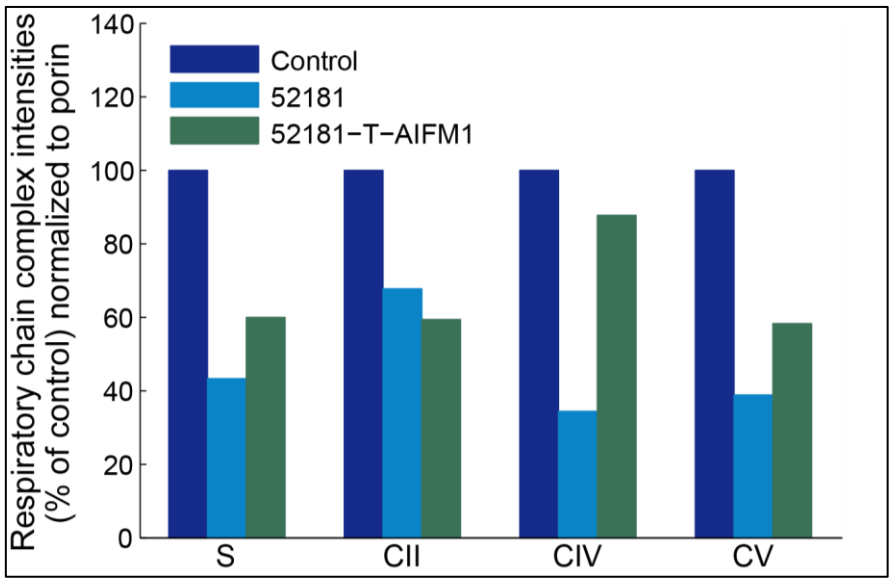

Figure 3.20: Quantification of 2D-BN-SDS Gels of control, patient 52181 and patient 52181 transduced with wt-AIFM1-cDNA in % of control normalized to porin

The results were still not clear. The Harlequin mouse model showed a correlation between the severity of the disease and the amount of the complex I subunit NDUFB8 (20kDA). The Western Blot in our patient showed a strong decrease of NDUFB8 compared to the control. But the amount of NDUFB8 in the transduced cell line was almost unchanged (Figure 3.21).

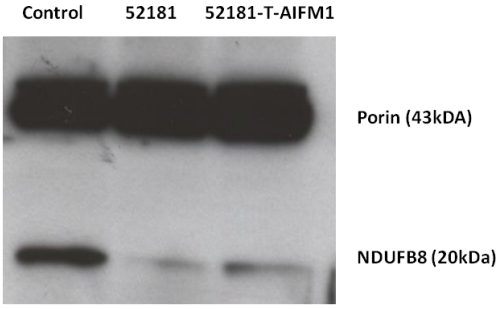

Figure 3.21: Western Blot of control, patient 52181 and patient 52181 transduced with wt-AIFM1 cDNA (Porin was used as a loading control)

This result let us doubt more and more that the found AIFM1 mutation is causative in that patient. An intensive analysis of male family members showed that the grandfather of the patient also carried the variant in the *AIFM1* gene. This was the point to exclude AIFM1 as the cause for the disease. Therefore the genetic background remained unclear. More recently mutations in a gene called *MTMFT* (Methionyl-tRNA formyltransferase, mitochondrial) were discovered to be responsible for impaired mitochondrial translation, leading to combined OXPHOS defects [232]. The phenotype of our patient was also quite similar to the patient described by Tucker et al. Consequently this patient has also been included in a high resolution melting curve (HRMA)-based candidate screen to test for genetic variation in *MTFMT* (performed by our technical assistants) [232]. HRMA was performed essentially as described previously, with intronic primers covering all coding exons of *MTFMT* [233]. This analysis also identified MTFMT mutations in patient #52181. In fact, both mutations in *MTFMT* (c.[219_222del]+[626C>T];

p.[Glu74Lysfs*3]+[Arg181Serfs*5]) were missed by exome sequencing due to poor coverage of the entire gene. The mother was a heterozygous carrier of the mutation c.626C>T and the father of mutation c.219_222del.

An additional Western Blot against MTFMT confirmed the impaired MTFMT protein (Figure 3.22). Patient 52181 had an additional shorter MTFMT protein band appeared which was absent in the controls. This shorter band can be seen as the consequence of the frame-shift mutation. The complex II subunit SDHA was used as a loading control. The same Western Blot showed in addition the CI defect.

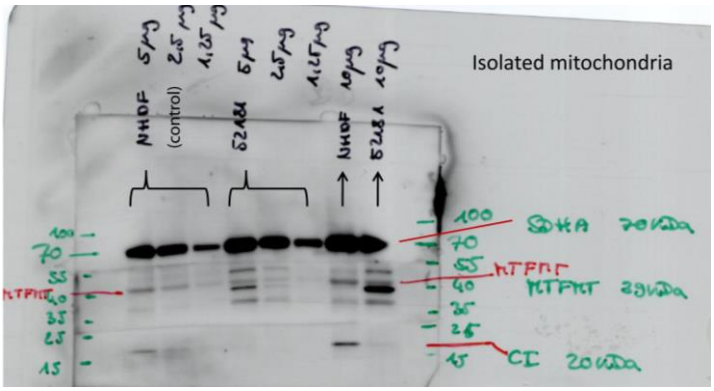

Figure 3.22: Western Blot of control (NHDF-neo) and Patient 52181. MTFMT (39kDa), SDHA (70kDa) and NDUFB8 (20kDA) expression in isolated mitochondria from fibroblasts

All together the MTFMT variants seem to be the cause of the disease. The increase of OCR after transduction with the wt-AIFM1-cDNA in the patient cell line might be due to the over expression of AIFM1. The melting curve analysis (performed by our technical assistants) in 350 OXPHOS patients identified pathogenic mutations in *MTFMT* in three other cases resulting in decreased activities of multiple or isolated respiratory chain complexes. During the last six years additional five patients with causal mutations in *MTFMT* were identified by exome sequencing [226]. Further functional analysis (qPCR, immunoblot investigation of steady state levels of MTFMT and other respiratory chain complexes) was performed by another PhD student Matteo Gorza and Valentina Strecker (Group Dr. Ilka Wittig, University of Frankfurt) to confirm the pathogenicity of all variants found. A short overview of all variants and the clinical features of the patients and the results of the functional analysis can be found in the supplements (Table S5, Figure S1).

In summary, NGS coupled with functional validation of new disease alleles was successfully used to identify disease-causing variants in known and new complex I associated disease genes in six patients. ACAD9 was identified as a new complex I assembly factor and seems to be a quite frequent cause of complex I deficiency. In total data of 70 patients with mutations in *ACAD9* were collected and studied in detail. WES discovered new variants in an already described disease-causing gene *NDUFS8* and for the first time in the complex I subunit *NDUFB3*. New disease-causing variants in the gene *BOLA3* were also found in a patient presenting a combined respiratory chain deficiency. The identification of the disease-

causing gene in the last patient was trickier. In the end the analysis of more family members revealed *MTFMT* as the right gene and excluded the first considered gene *AIFM1*.
Nevertheless, the identification of the disease-causing gene is just the first step. A deep understanding of the function of the identified gene, the involved pathomechanisms and pathways is crucial to find new therapy options. Therefore, the second big part of this thesis is the evaluation of different treatment options for patients with mitochondrial disorders.

3.2 Therapy

The second part of my PhD thesis addresses the evaluation of different treatment options for patients with mitochondrial disorders. The effect on respiratory chain complex activity level was analysed polarographically with the oxygraph or Seahorse XF 96 Flux Analyzer. Genome wide expression level experiments were used to detect changes on the transcription level and identify involved pathways. Changes in on the protein level were analysed with the help of mitoGELs and Western Blot analysis. Possible post-transcriptional effects were examined with 2D-DIGE gels.

3.2.1 Bezafibrate treatment

Bastin et al. (2008) provided evidence from in vitro studies that activation of the PPAR/PGC-1-alpha pathway with bezafibrate could be a new therapeutic approach for patients with mitochondrial disorder [146]. Djouadi et al. (2010) showed in a clinical study, that bezafibrate increased the resting activity of ß-oxidation enzymes in patients with inherited ß-oxidation disorders leading to a significant improvement in the condition of the patients [234]. The positive effects, like increased RCC activity, increased mutated mRNA and RC protein levels, which were reported in these papers, were the starting point to verify these effects in our big skin fibroblast collection of patients with mitochondrial disorders. Complex I activity measurements, genome wide expression profiles, investigations on protein level (Western Blots, mitoGELs, 2D-SDS-DIGE Gels) and pathway analysis were performed on control and patient-derived fibroblasts before and after bezafibrate treatment.

3.2.1.1 Complex I activity measurement

In the first group, fibroblasts from three controls and 35 patients with isolated complex I defect and molecular diagnosis were examined. A first time-and dose-dependent experiment revealed 400µM bezafibrate for 72hrs as the best conditions and was used in all further experiments. The OCR was measured with the oxygraph or Seahorse XF 96 Flux Analyzer as described in chapter 2.7.2 and 2.7.3

respectively. The complex I activity was calculated as % of the lower level of the normal range. The average of at least three independent measurements is given in the following table 3.9:

FibroID	Mutation	Complex I activity (% of normal range)	Complex I activity after bezafibrate treatment	Change (in %)	p-value
NDHF-neo	WT	100,0	112,0	+12,0	<0,01
47039	WT	100,0	109,8	+9,8	>0,05
35028	WT	100,0	114,5	+14,5	<0,01
35834	ACAD9	35,7	67,6	+ 89,5	<0,001
49591	ACAD9	64,2	92,8	+ 44,6	<0,001
52933	ACAD9	36,6	88,2	+ 141,0	<0,001
52935	ACAD9	43,1	66,1	+ 53,4	<0,01
52674	ACAD9	48,0	68,4	+ 42,5	<0,05
61980	ACAD9	34,6	33,0	- 4,5	>0,05
62006	ACAD9	77,5	97,9	+ 26,2	<0,05
62340	ACAD9	49,3	70,4	+ 42,8	<0,01
62343	ACAD9	79,1	124,5	+ 57,4	<0,05
62347	ACAD9	65,8	86,7	+ 31,7	<0,01
68541	ACAD9	114,1	147,0	+ 28,7	>0,05
68891	ACAD9	74,8	110,1	+ 47,3	<0,001
69842	ACAD9	60,1	49,6	- 17,4	>0,05
71265	ACAC9	74,0	73,6	- 0,55	>0,05
71266	ACAD9	59,0	64,0	+ 8,5	<0,05
71680	ACAD9	53,0	68,5	+ 29,5	<0,001
72545	ACAD9	116,0	115,0	- 0,86	>0,05
33545	NDUFA1	78,8	91,1	+ 15,5	<0,05
50845	NDUFB3	14,2	13,1	-7,7	>0,05
47103	NDUFB9	18,2	20,4	+ 12,0	>0,05
49732	NUBPL	29,8	27,3	-8,4	>0,05
33255	NDUFS1	43,4	73,3	+ 68,8	<0,001
33460	NDUFS1	37,3	70,3	+ 88,6	<0,01
37796	NDUFS1	60,3	71,2	+ 18,0	<0,05
33254	NDUFS2	73,2	99,2	+ 35,5	<0,001
33027	NDUFS8	71,3	80,1	+ 12,4	n.a.

33284	NDUFS8	64,9	79,3	+ 22,3	<0,05
35791	NUDFV3	63,9	61,2	- 4,1	>0,05
54373	PDHA1	62,3	100,4	+ 61,2	<0,01
61846	PDHA1	77,3	109,6	+ 41,7	<0,05
61819	PDHA1	90,2	97,3	+ 7,9	>0,05
44732	ND6	57,4	62,3	+ 8,5	>0,05
18699	tRNA	80,4	85,1	+ 5,9	>0,05
45157	ND1	85,7	87,8	+ 2,4	>0,05
33464	ND3	67,2	75,7	+ 12,6	<0,05

Table 3.9: Results of the complex I activity measurement of patient derived fibroblast cell lines (with molecular diagnosis) with and without bezafibrate treatment, n.a.= not available

The complex I activity in fibroblasts ranged from 14% to 116% in comparison to the lower level of normal (Table 3.9). After bezafibrate treatment complex I activity increased between 9 and 15% in the control cell lines. In three out of four cell lines with mtDNA mutations no significant improvement of complex I activity was found. The cell lines with mutations in *NDUFB3* and *NDUFB9* had strong reduction of complex I activity to around 15-30% of the lower level of normal, which was also almost unchanged after the bezafibrate treatment. Patients with mutations in *NDUFS1*, *NUDFS2* and *NDUF8* responded to the treatment with an increase of complex I activity between 12 and 89%. The increase was significant in five out of six cases. Patients with mutations in *PDHA1*, which led to a secondary complex I defect, had a quite mild reduction of complex I activity which was in two out of three cases significantly restored to normal levels. Patients with mutations in *NUBPL* and *NDUFV3* did not respond to the bezafibrate treatment.

The largest effect was observed in a homogeneous group of missense and frame-shift mutations in the same gene, *ACAD9*. In this large group of 17 patients cell lines the complex I activity increased in all cell lines except three. The increase (9 to 141%) was significantly in 12 out of 17 patient cell lines. Five patient cell lines reached almost normal levels. The treatment was ineffective in five cell lines (FibroID 61980, 68541, 69842, 71265 and 72545). The treatment seems to be ineffective if complex I activity was already within the normal range (FibroID 68541, 71265 and 72545). Interestingly the two cell lines sharing the homozygous mutation at position p.R518H, presenting the lowest levels of complex I activity, did also not respond to the treatment (Figure 3.23).

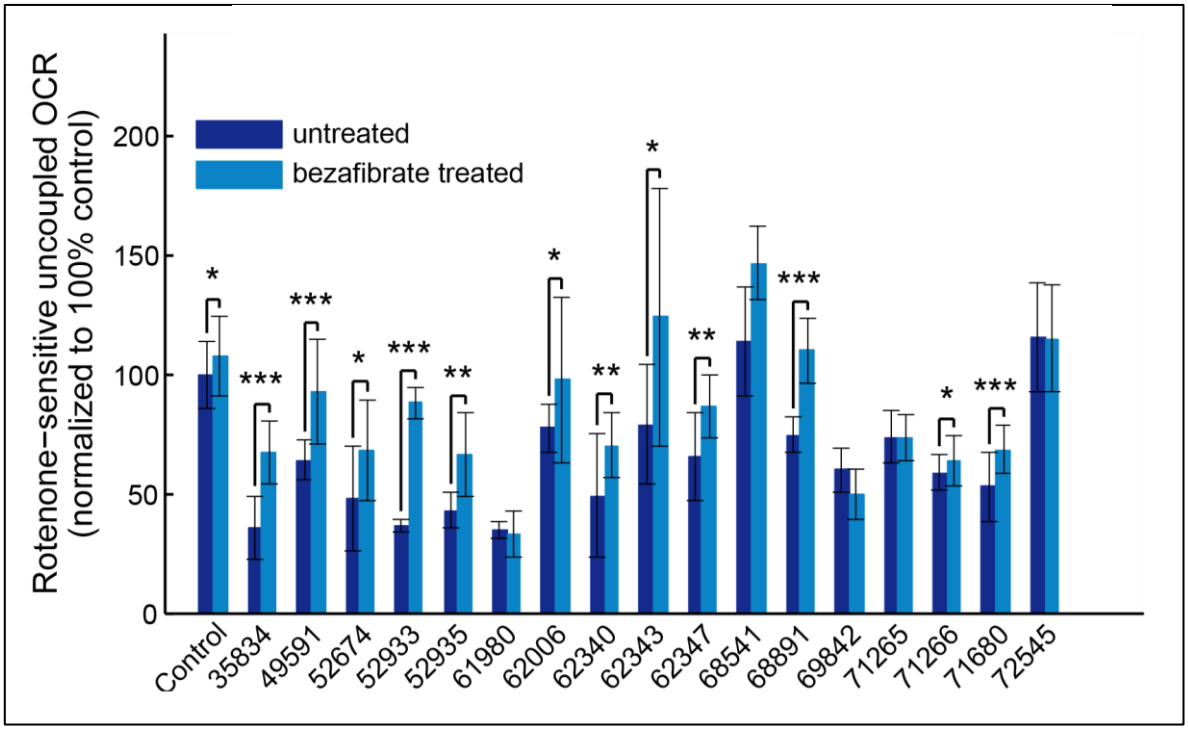

Figure 3.23: Rotenone sensitive uncoupled oxygen consumption rate of control and all ACAD9 patient derived cell lines untreated and bezafibrate treated patient and control values are means ± SD of at least three different experiments (p-value 0,05,*, p-value<0,01,**, p-value<0,001,***)

The second group included eight patients with complex I defect without molecular diagnosis. The results can be seen in the following table (Table 3.10):

FibroID	Mutation	Complex I activity (% of normal range)	Complex I activity after bezafibrate treatment	Change (in %)	p-value
33281	unclear	52,2	70,4	+ 34,9	<0,05
35791	unclear	63,9	61,2	-4,1	n.a.
33254	unclear	74,2	117,2	+57,9	<0,001
37796	unclear	75,0	85,4	+13,8	<0,05
33004	unclear	86,8	102,2	+17,7	<0,01
33008	unclear	92,8	101,9	+9,8	>0,05
35814	unclear	93,3	102,	+9,3	<0,05

Table 3.10: Results of the complex I activity measurement of patient derived fibroblast cell lines (without molecular diagnosis) with and without bezafibrate treatment, n.a.= not available

In conclusion we could see, that bezafibrate treatment increased complex I activity significantly in 28 out of 42 examined cell lines. The overall increase was significant (p-value=0,0024). Within the subgroup of patients with mutations in *ACAD9* the overall increase was significant as well (p-value=0,018)

Due to the fact, that cell lines with a rest activity of <20% did not respond to the treatment it can be assumed that a certain amount of RCC activity is needed to respond to the treatment. Control cells and cells with almost normal levels of complex I activity increased in average between 10 and 20%. In general patient cell lines with mutations in *ACAD9*, *NDUFS1* or *NDUFS8* seem to be more responsive than others.

3.2.1.2 Gene expression experiment

3.2.1.2.1 3-day experiment

Genome wide expression profiles were performed to determine the effect of bezafibrate treatment on the mRNA level as described in chapter 2.8. We selected 11 patient cell lines with known but also unknown genetic background as well as bezafibrate responsive and unresponsive cell lines. We included also three different age-matched control cell lines. In total 14 different cell lines were treated with bezafibrate for 72hrs and analysed as described in chapter 2.6.1 (Patient selection can be found in Table S6). After correction for multiple testing 97 genes were found which were differentially regulated between patients and controls. A list of ten genes with the highest up-and downregulation as well as the complete list can be found in the supplements (Table S7 and S8). Due to the fact, that the sample size was quite small and the genetic background quite heterogeneous there was no clear gene detected which could be used as a marker to detect mitochondrial disorder patients.

The analysis of the different gene expression between untreated and bezafibrate treated cells detected, after correcting for multiple testing, 92 genes. The 14 most interesting genes can be found in figure 3.24. The complete list can be found in the supplements (Table S10 and S11). Eight significantly upregulated genes are involved in the fatty acid metabolism (*ACCA2*, *ACADVL*, *CPT1A*, *CPT1B*, *ECH1*, *ETFA*, *ETFB* and *HADHB*). The gene ACADVL (acyl-Coenzyme A dehydrogenase very long chain) is responsible for the catalyzation of the first step of the mitochondrial fatty acid beta-oxidation pathway, whereas ACAA2 (acetyl-CoA acyltransferase 2) catalyses the last step of the mitochondrial fatty acid beta-oxidation spiral. Especially the significant upregulation of *ACADVL* and *ACAA2* is very interesting. Some studies suppose an interaction and reciprocal stabilisation of FAO and OXPHOS proteins. They gave evidence for the existence of a multifunctional FAO complex within mitochondria that is physically associated with OXPHOS supercomplexes [235-237]. The increase of complex I activity which was seen in most cell lines could be also explained by the stabilisation of supercomplexes due to the increased amount of FAO protein. This possible effect was further analysed on the protein level and described in chapter 3.2.1.3. Another interesting gene which was found to be significantly upregulated was PDK4 (pyruvate dehydrogenase kinase 4). The protein of the gene PDK4 is located in the matrix of the mitochondria and inhibits the pyruvate dehydrogenase complex by phosphorylating one of its subunits, thereby contributing to the regulation of glucose metabolism. This upregulation of *PDK4* led consequently to the down regulation of the glycolysis, resulting in a metabolic shift. Fatty acid metabolism and OXPHOS pathway are increased

to produce enough energy to maintain cellular function. This could explain the increased complex I activity we found after bezafibrate treatment as well. The genes *ALDH1A3*, *ETFDH*, *PDGDH*, *ARK1C2* are involved in the electron transport system, lipid peroxidation and amino acid biosynthesis.

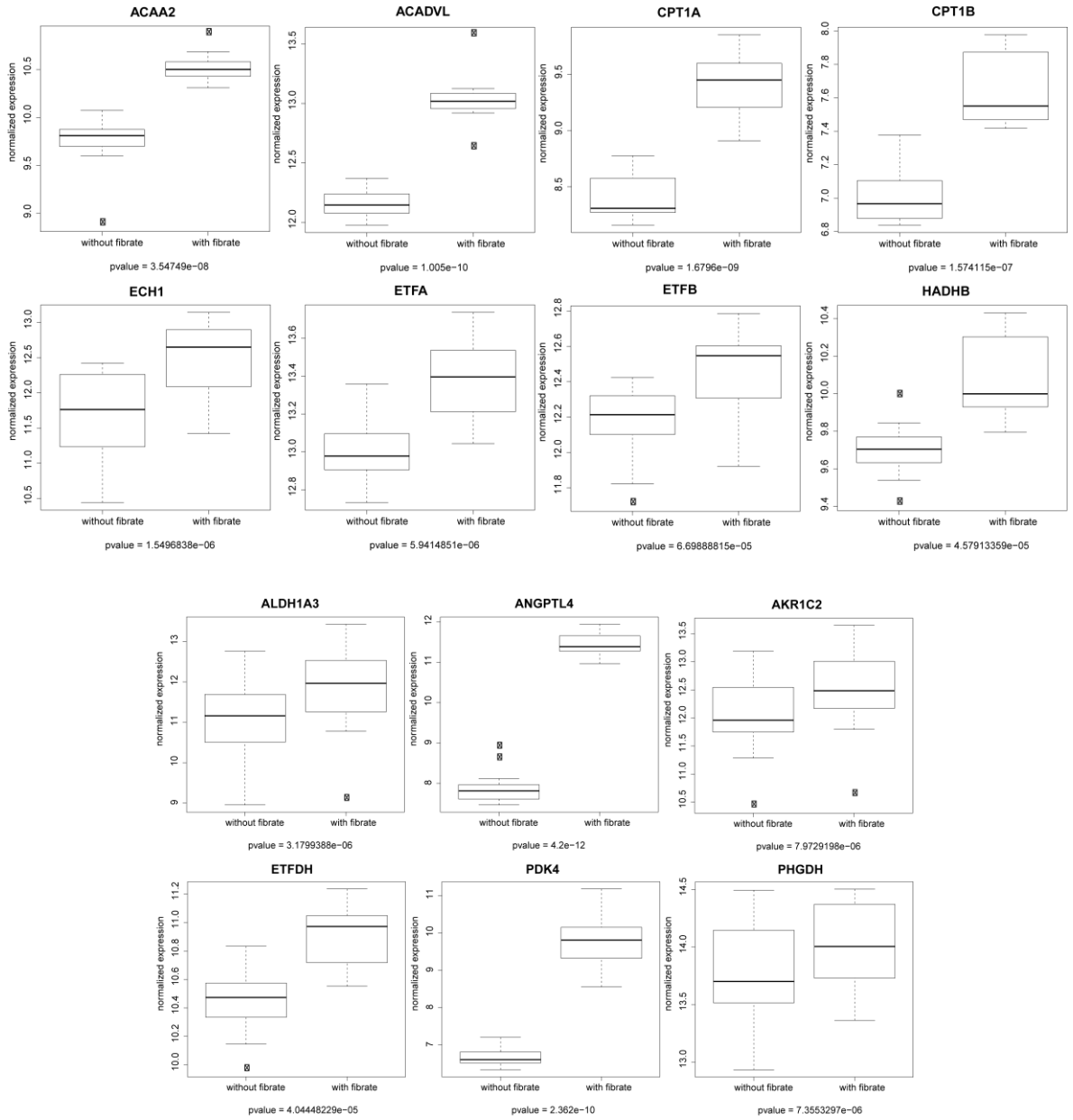

Figure 3.24: Boxplots of the most interesting genes changed after 3-day bezafibrate treatment

An overall upregulation of genes coding for respiratory chain complex subunits was not found. Furthermore, known mitochondrial biogenesis genes (like NRF1, PPARG, Tfam or PGC-1-alpha) were not significantly changed after 72hrs overall patient and control cell lines after bezafibrate treatment. Nevertheless, a closer look to the changes in expression of NRF1, PPARG and PGC-1-alpha showed an upregulation in some cell lines. Expression levels of PPARG and NRF1 for example was increased in nine and eleven out of 14 cell lines respectively. PGC-1-alpha expression increased in ten cell lines whereas Tfam remained unchanged after 72hrs bezafibrate treatment (Figure 3.25). Unfortunately, there was no

correlation between bezafibrate responsive cell lines (seen in the activity measurement) and unresponsive cell lines.

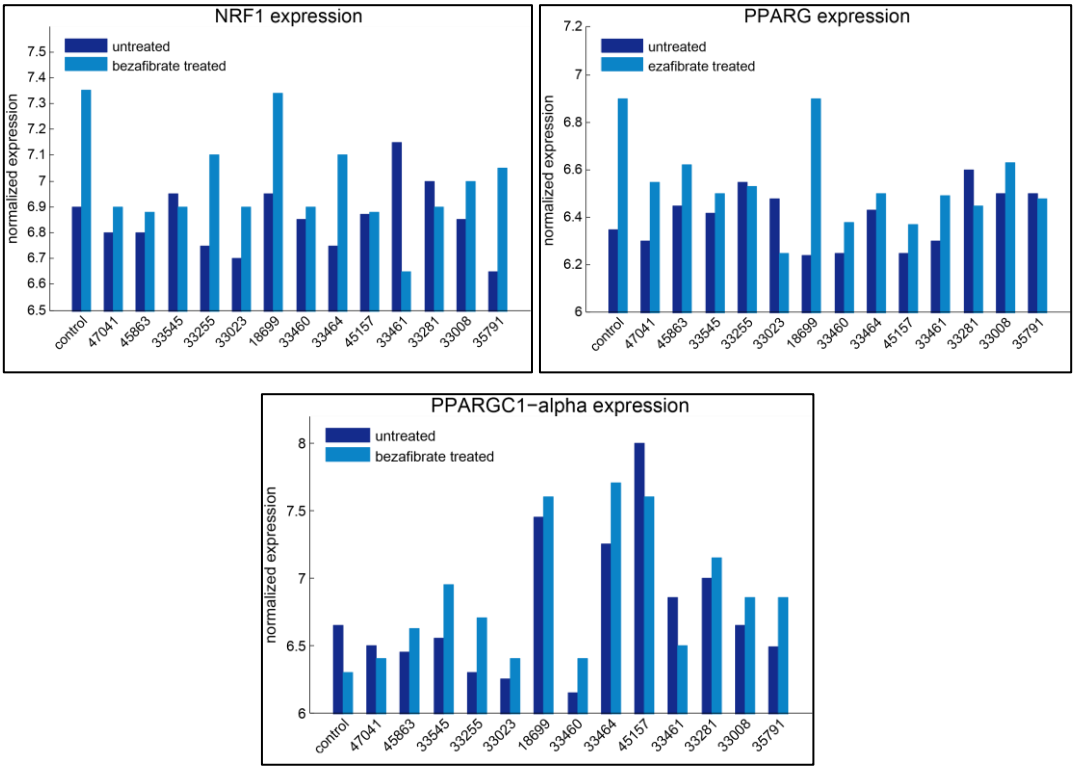

Figure 3.25: Gene expression data from mitochondrial biogenesis genes *NRF1, PPARG, PGC-1-alpa*

Taken together, the gene expression experiment could clearly show that mainly genes involved in the fatty acid oxidation pathway and genes leading to a metabolic shift towards increased OXPHOS are significantly changed upon bezafibrate treatment. In contrast to other studies we could not detect any upregulation of subunits of the RC or other mitochondrial biogenesis genes. A limitation of the study was, that the gene expression was analysed only after 72hrs bezafibrate treatment. But it is possible that the changes in the mitochondrial biogenesis or other involved pathways due to the treatment happen earlier. Therefore, another gene expression experiment with different time points was performed.

3.2.1.2.2 Time course experiment

During the second gene expression experiment RNA samples after 0, 2, 4, 8, 12, 24, 48 and 72hrs of bezafibrate treatment were taken. In order to reduce the sample size and to analyse a more homogeneous group only three different control cell lines were included into the experiment. Each time point was measured in triplicate. After the correction for multiple testing no mitochondrial biogenesis genes were significantly up- or downregulated. Therefore, the idea to perform the time-course experiment also with patient cell lines was discarded.

3.2.1.3 Protein analysis

3.2.1.3.1 mitoGELs

The effect of bezafibrate treatment on protein level was examined in ten different fibroblast cell lines (three control cell lines and seven cell lines with isolated complex I defect). In all seven cases the genetic cause of the defect was known (five nuclear and two mtDNA mutations, Table 3.11). Six cell lines (two controls and four patient cell lines) were already used in the gene expression experiment. In order to gain more insight, why some cells responded to the bezafibrate treatment and others not, we selected cell lines with different levels of complex I rest activity and different responses to the bezafibrate treatment on the RCC activity level. The samples were prepared in our institute and the gels and the analysis was performed in cooperation with Dr. Ilka Wittig and Valentina Strecker as described in chapter 2.9.3.

Number	Cell line	Mutation	Complex I activity (% of normal range)	Response to the bezafibrate treatment on complex I activity measurement
1	NHDF	WT	100,0	+12,0
2	47039	WT	100,0	+9,8
3	35028	WT	100,0	+14,5
4	35834	ACAD9	35,7	+ 89,5
5	33545	NDUFA1	78,8	+ 15,5
6	47103	NDUFB9	18,2	+12,0
7	33460	NDUFS1	37,3	+88,6
8	33254	NDUFS2	73,2	+35,5
9	45157	ND1	85,7	+2,4
10	44732	ND6	57,4	+8,5

Table 3.11: List of cell lines used to detect differences in the amount of supercomplex after bezafibrate treatment with mitoGELs

The biggest increase in assembled supercomplexes was observed in the cell line 35834 (compound heterozygote mutation in *ACAD9*). The amount of assembled supercomplexes increased from 60% to normal level. The significant increase was measured in three biological independent experiments (Figure 3.26).

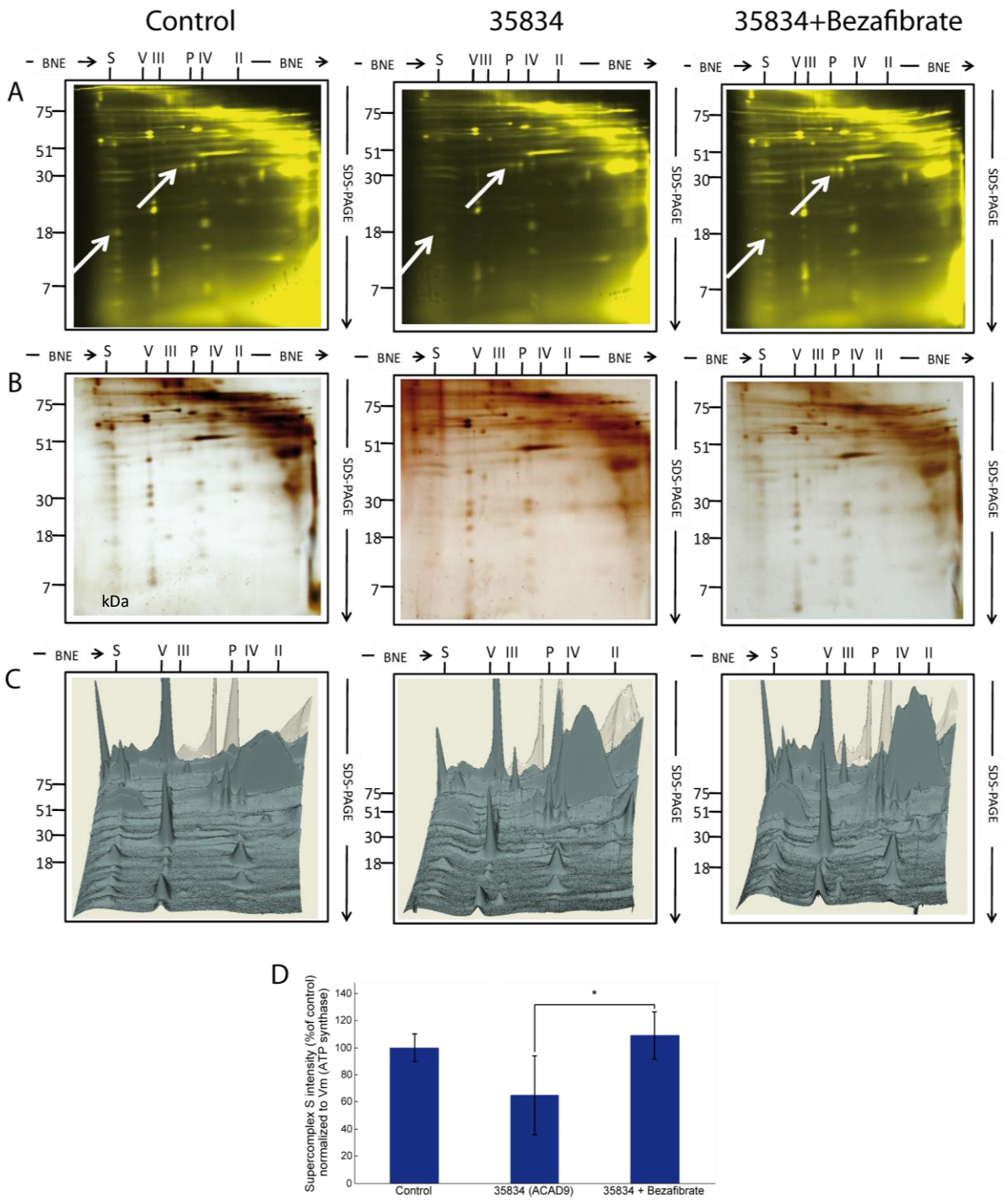

Figure 3.26: 2D-BN-SDS Gel of control and patient 35834 with and without bezafibrate treatment, (A) fluorescence gel, and white arrows indicate signals used for quantification, (B) silver-stained gel, (C) mitoPanorama and (D) quantification. Values are means ± SD of at least three different experiments (p-value<0,05,*). Assignment of complexes: V, complex V or ATP synthase, III, complex III or cytochrome c reductase, P, Porin, IV, complex IV or cytochrome c oxidase, S, supercomplexes composed of chain complexes I, III and IV

The increased amount of supercomplexes was consistent with the increased OCR. The positive effect of the complex I activity measurement in this patient cell line could be therefore explained by an increased assembly of supercomplexes (in which complex I is included). In cell line 6 (FibroID 47103, homozygote NDUFB9 mutation) a complete loss of assembled supercomplexes was observed and was unchanged after bezafibrate treatment (Figure 3.27). This finding was also consistent with OCR measurement, in which

complex I activity was not significantly increased. In this patient it can be assumed, that a certain amount of assembled complex I is necessary to respond to the proposed stabilizing effect of bezafibrate treatment.

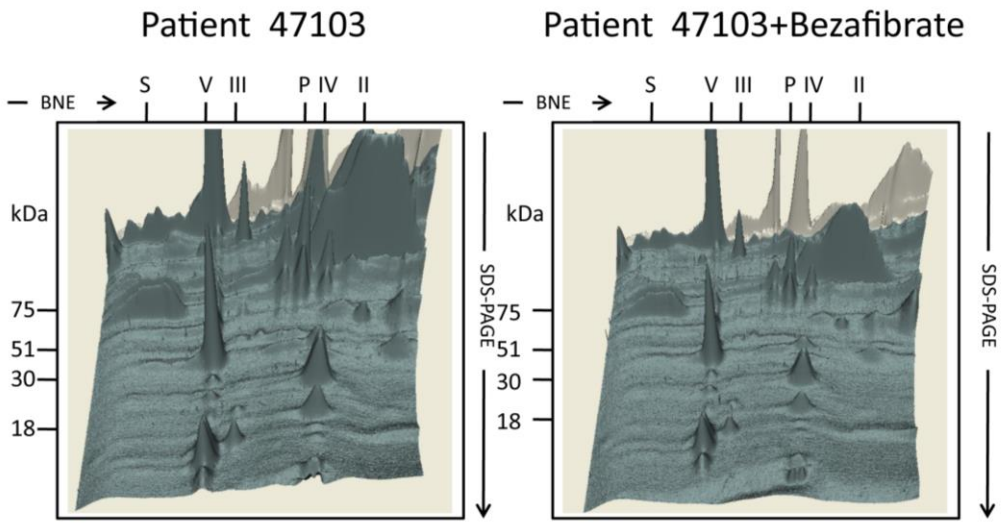

Figure 3.27: mitoPanorama of patient 47103 with and without bezafibrate treatment. Assignment of complexes: V, complex V or ATP synthase, III, complex III or cytochrome c reductase, P, Porin, IV, complex IV or cytochrome c oxidase, S, supercomplexes composed of chain complexes I, III and IV

The cell line 5, 7 and 8 with mutations in *NDUFA1* (FibroID 33545), *NDUFS1* (FibroID 33460) and *NDUFS2* (FibroID 33254) showed also a big increase in the amount of supercomplexes (+100, +80 and +16% of the control). This was also consistent with the OCR measurement. In contrast to the results of the oxygen consumption measurement the two cell lines with the mtDNA mutation showed an increase of 35 to 55% and 88 to 117% compared to the control. All control cell lines responded to the treatment as well with an increase of all complexes between 5-40% (Figure 3.28).

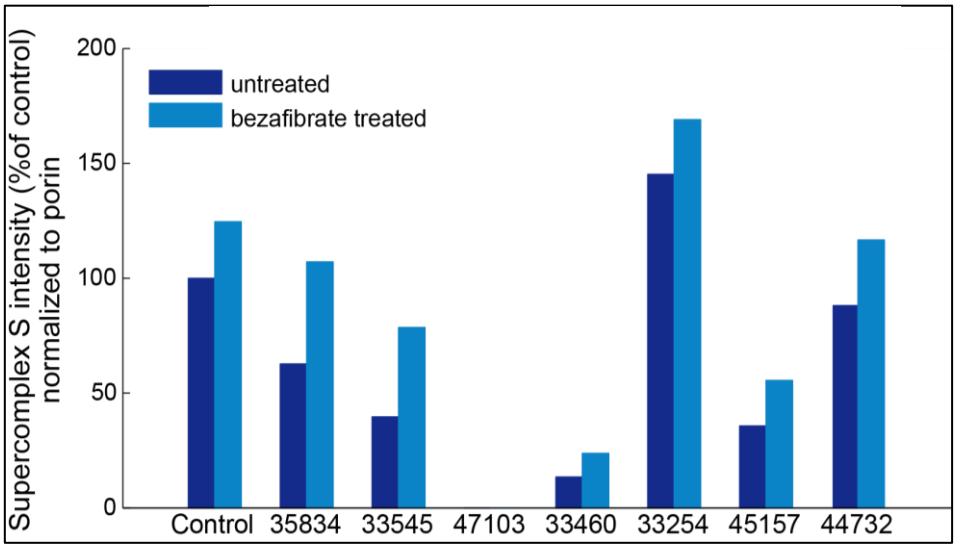

Figure 3.28: Quantification of the supercomplexes of control (average of three control cell lines) and seven patients with and without bezafibrate treatment (average of two technical replicates)

Taken together, the analysis of ten mitoGELS revealed an increased assembly of supercomplexes in the control cell lines and in 6 out of 7 patient cell lines. This finding was consistent with the OCR measurement in all cell lines with nDNA mutation but not in the cell lines with mtDNA mutation.

It can be assumed, that cell lines with mutations in *ACAD9*, leading to a complex I assembly defect, could especially profit from the bezafibrate treatment. In the gene expression experiment a clear upregulation fatty acid oxidation pathway was observed. One of the top hits with the highest increase in gene expression was *ACADVL*. *ACADVL* and *ACAD9* shares considerable sequence homology (47% identical and 65% similar amino acids).
Therefore, the positive response of the patient cell line 35834 with the ACAD9 mutation was further validated in other cell lines with ACAD9 mutation (FibroID 62006, 62347, 68541 and 69842). The cell lines were again treated for 72 hrs with bezafibrate and mitoGEL analysis was performed (Figure 3.29).

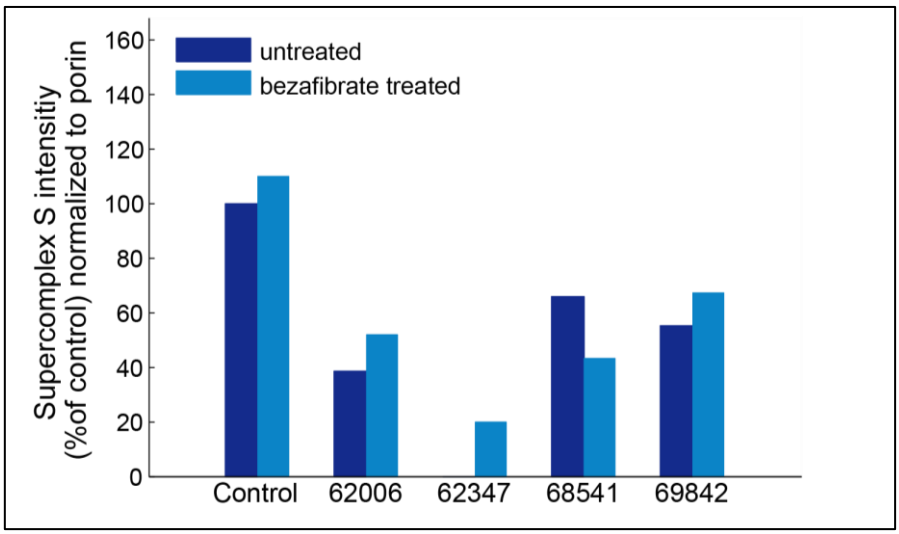

Figure 3.29: Quantification of the supercomplexes of one control and four patients with ACAD9 mutation with and without bezafibrate treatment (average of two technical replicates)

The cell line 62006 is harbouring one splice site variant and one missense mutation. All other cell lines (Fibro ID 62347, 68541 and 69842) have compound heterozygote or homozygote missense mutations. The mutations in cell line 62006 and 68541 lead to a severe reduction of ACAD9 protein whereas cell line 62347 and 69842 presented only a small reduction of ACAD9 protein (Figure 3.6). Nevertheless, all cell lines had a clear reduction of assembled supercomplexes, but the amount of remaining ACAD9 protein seems to be not crucial for the correct supercomplex assembly. In this case, cell line 62347 with almost normal amount of ACAD9 protein, presented a complete loss of supercomplexes whereas the cell line 68541 (with nearly absent ACAD9 protein) presented a quiet high amount of assembled supercomplexes. An increase in the assembled amount of supercomplexes was found in three cell lines after bezafibrate treatment. The cell line 68541 showed no increase or even a destructive effect. This finding was consistent to the OCR measurement.

Summing up, bezafibrate treatment led to an increase in assembly of supercomplexes in four out of five patient cell lines with mutations in *ACAD9*. The findings were consistent with the RCC activity measurement.

3.2.1.3.2 2D-DIGE Gels

The biggest response to the bezafibrate treatment was observed in the patient cell lines with ACAD9 mutation. To detect further post transcriptional effects and find out more about the mode of action, 12 2D-DIGE gels with one control (NHDF-neo) and four different patient cell lines with mutations in *ACAD9* were performed (as described in chapter 2.9.6, sample list can be found in table S12). Two representative examples of the gels obtained can be seen in figure 3.30.

Gel A is an example of the differences in the proteasome of control ("C") and patient 35834 (spots appearing in green: control, red: patient and yellow: present in both). Gel B is an example of the effect of the bezafibrate treatment in patient cell line 52674 (spots appearing in green: untreated, red: bezafibrate treated and yellow present in both).

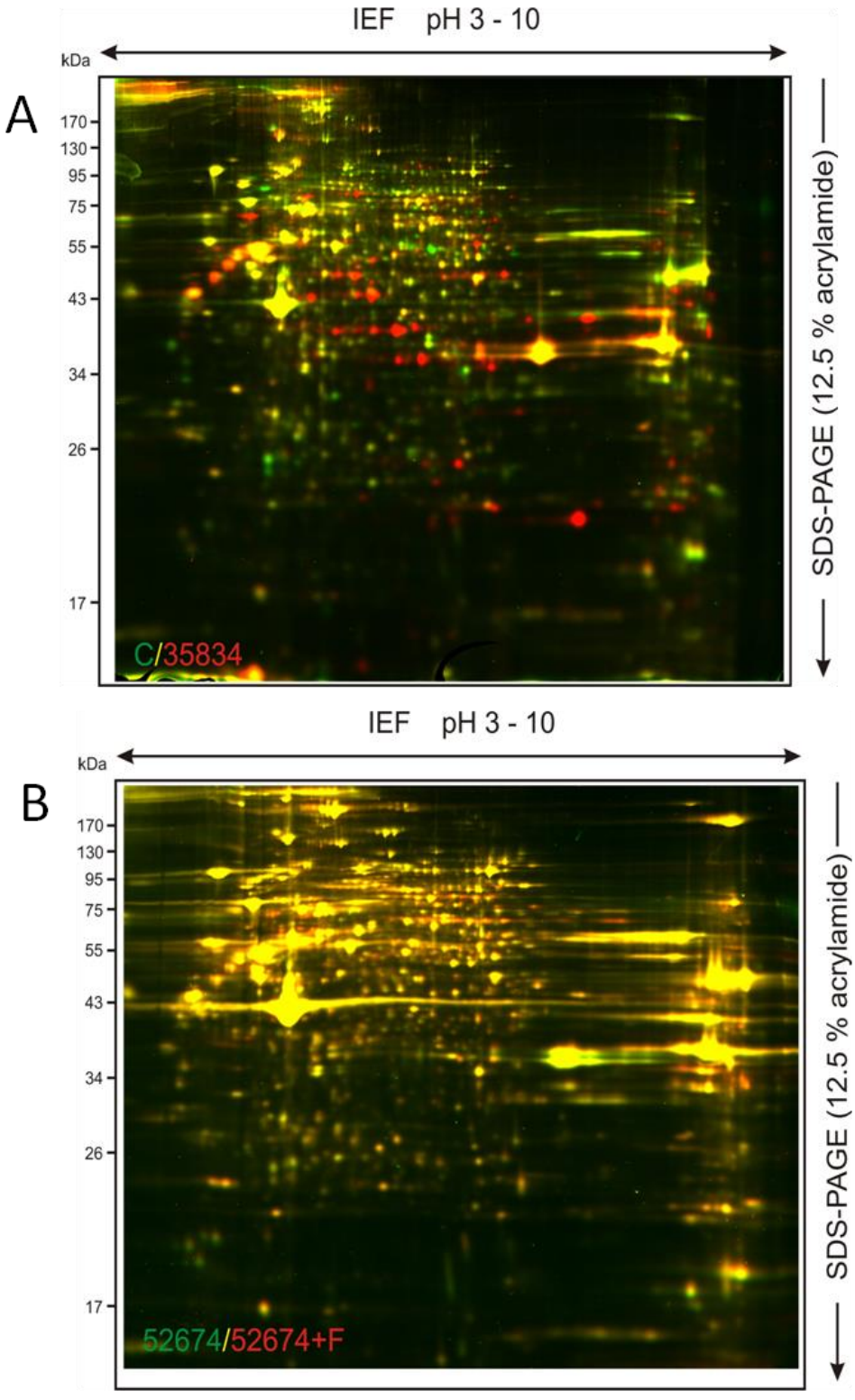

Figure 3.30: Examples of DIGE gels, control vs. patient (A) and untreated vs. bezafibrate treatment (B)

Significantly changed spots were picked of the gel and analysed with mass spectroscopy. From 200 picked spots 95 could be determined without any doubt (Figure 3.31).

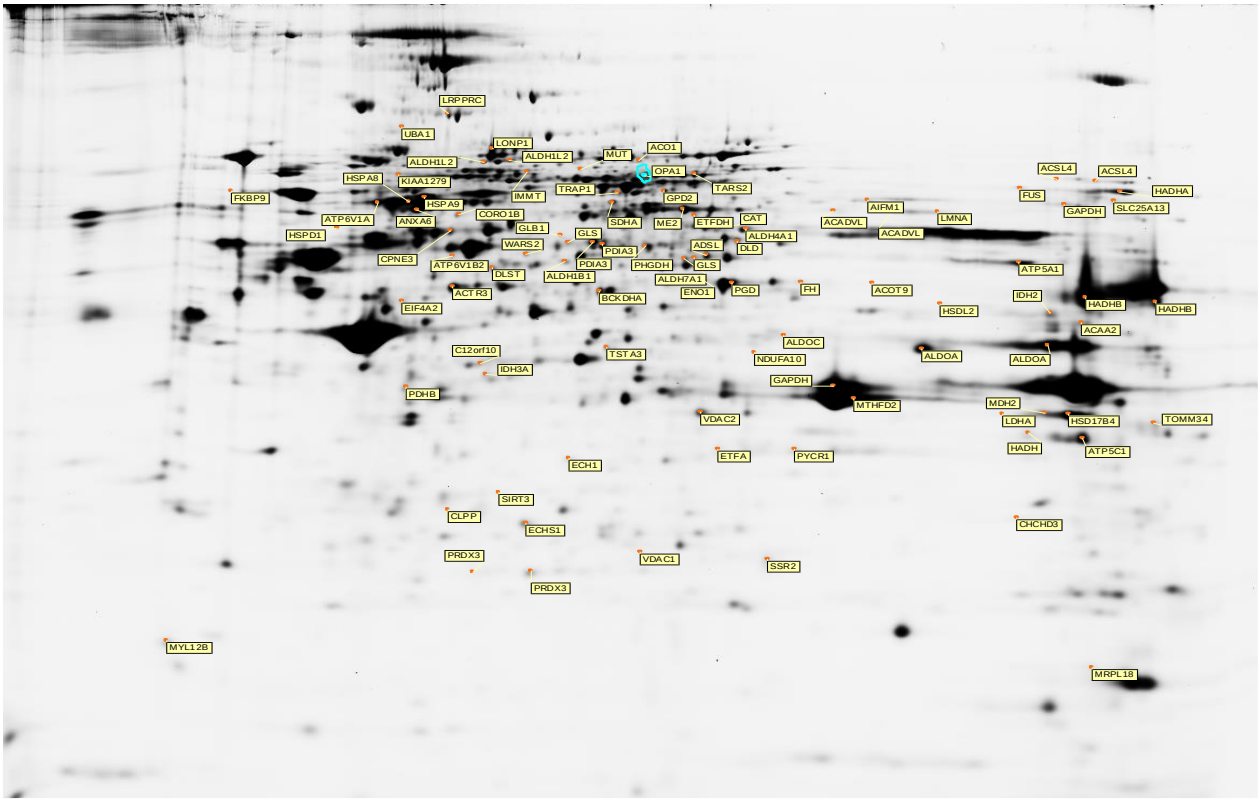

Figure 3.31: Position of 95 significant spots picked and later determined by mass spectrometry

58 proteins were significantly downregulated between ACAD9 patients and control and 13 showed higher levels. Unfortunately it was not possible, due to technical reasons, to detect a downregulation of ACAD9 protein (which was clearly seen in the Western Blots, chapter 3.1.2.6) itself. The proteins with the highest fold-changes between control and patients can be found in the next table (3.12). These results suggest, that impaired ACAD9 function (due to the mutations found in the patient) cause further disturbance in mitochondrial function and assembly of the respiratory chain. AIFM1 (known to maintain the electron transport chain, participate in the assembly of the respiratory chain and regulation of reactive oxygen species) and NDUAA (Accessory subunit of the mitochondrial membrane respiratory chain NADH dehydrogenase (Complex I)) for example are both significantly downregulated. It is already known from other studies, that impaired complex I assembly led to a decrease of other complex I subunits or assembly factors. Interestingly ACADVL (65% similarity to ACAD9) was significantly upregulated, speculating a compensatory effect. A compensatory effect can be also assumed by the upregulation of MDH2. MDH is essential for the reversible oxidation of malate to oxaloacetate, using the NAD/NADH cofactor system in the Krebs cycle. The complete list can be found in the supplements (Table S13).

Protein	Function	Fold-change	p-value
AIFM1	Apoptosis-inducing factor 1, mitochondrial precursor	-1,56	0,036
IMMT	Mitochondrial inner membrane protein	-2,06	1,10E-05
LRPPRC	Leucine-rich PPR motif-containing protein, mitochondrial	-1,27	0,0004

NDUAA	NADH dehydrogenase [ubiquinone] 1 alpha subcomplex subunit 10, mitochondrial	-1,82	0,00038
PDPR	Pyruvate dehydrogenase phosphatase regulatory subunit, mitochondrial	-2,06	1,10E-05
PHGDH	D-3-phosphoglycerate dehydrogenase	-3,62	0,0021
ACADVL	Acyl-Coenzyme A Dehydrogenase	1,27	0,024
GPD2	Glycerol-3-Phosphate Dehydrogenase 2	2,1	0,00035
MDH2	Malate dehydrogenase, mitochondrial	1,61	0,0095

Table 3.12: List of the most interesting proteins with the highest fold-change between patient and control

The treatment with bezafibrate led to the upregulation of 55 and downregulation of eleven proteins. Eight exciting proteins, which responded mostly to the treatment, can be found in the figure below (3.32). The picked and analysed spots are circled in turquoise. The Top-Hits ACAA2, ACADVL and ACSL4 are all involved the fatty acid oxidation pathway. ALDH4A1, CHCHD3, ETFA, IDH2 and SLC25A13 play a role energy production within the respiratory chain and proper mitochondrial function. It can be speculated, that the upregulation of the fatty acid metabolism, due to the bezafibrate treatment lead to a stabilisation of the supercomplexes and as a consequence to improved mitochondrial function, seen by increased complex I activity.

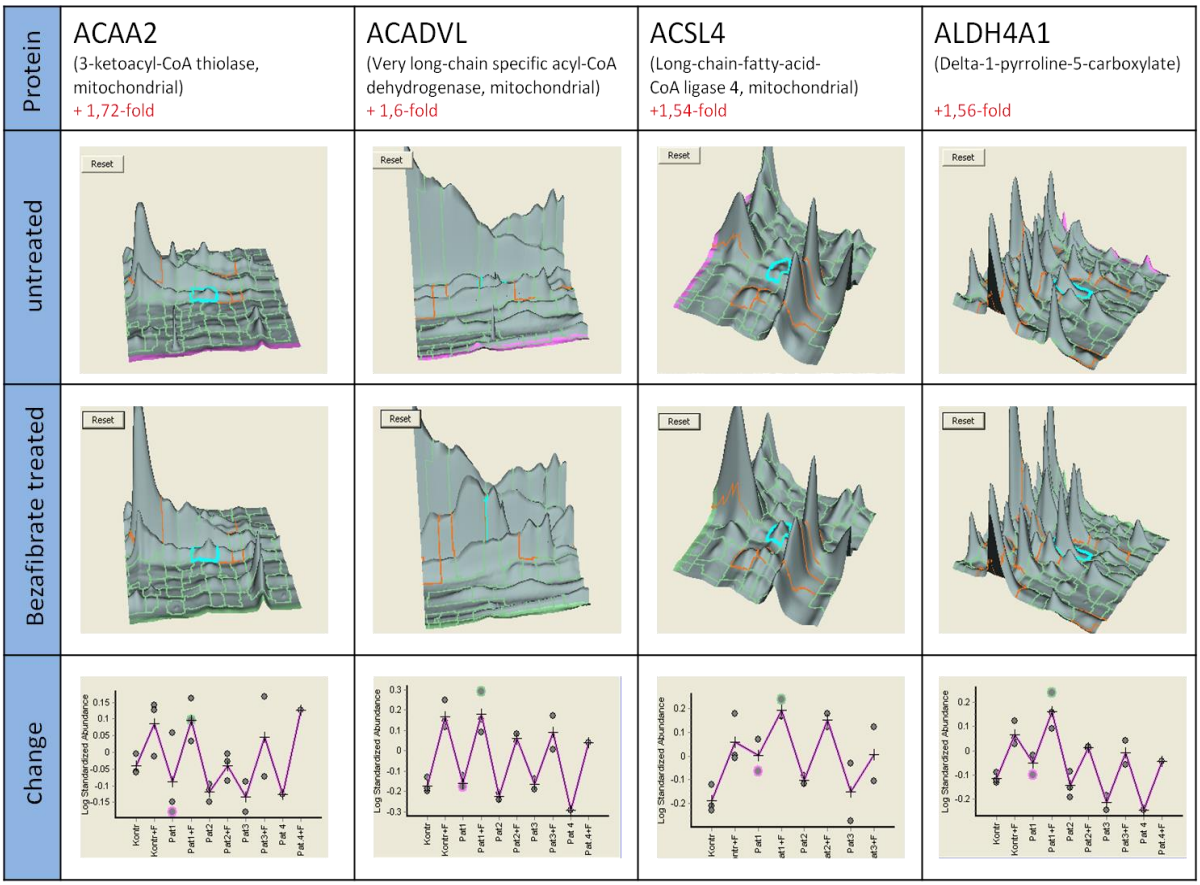

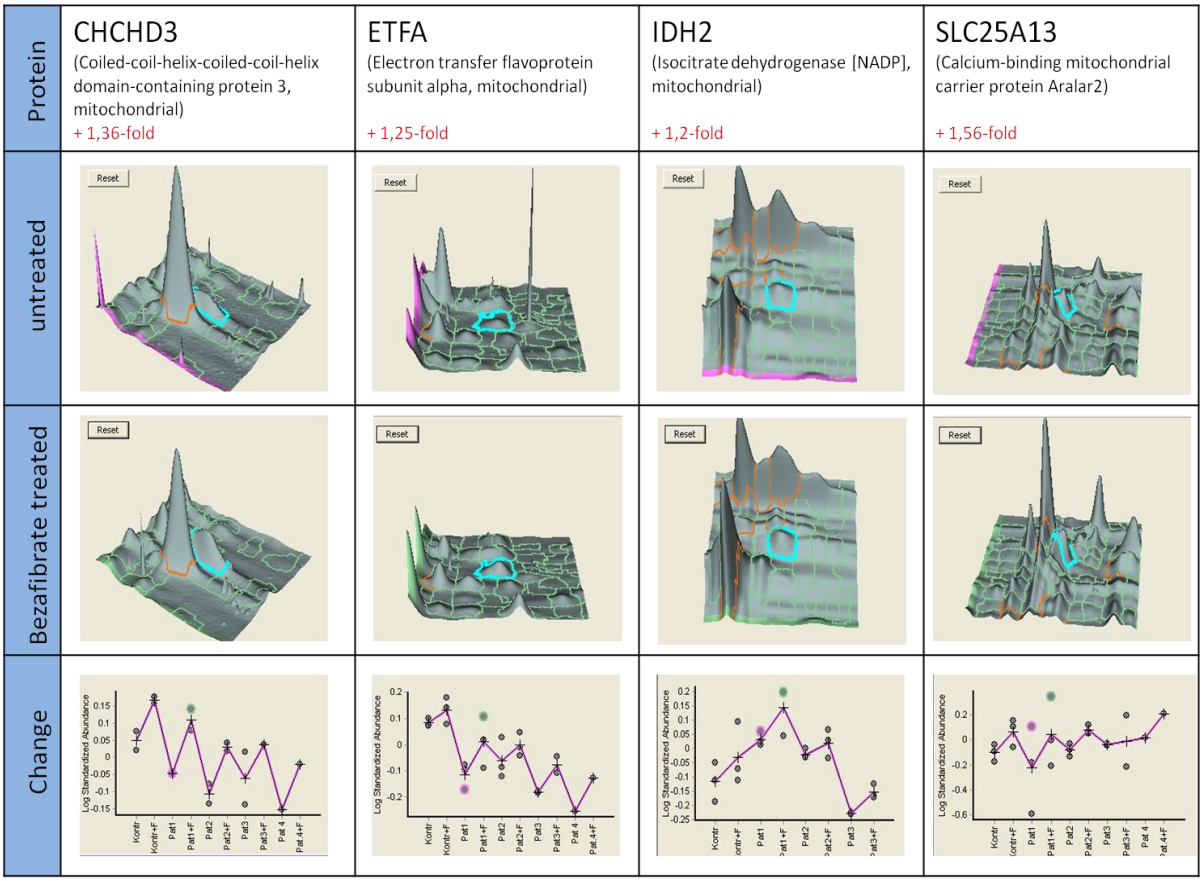

Figure 3.32: Overview of the proteins with the biggest respond to the bezafibrate treatment

The list of further significantly changed proteins can be found in the supplemental material (Table S14). Interestingly, the proteins ACAA2, ACADVL, CAT, ECH1, ETFA, ETFDH and HADHB, which are mainly associated with lipid and fatty acid metabolism, were also upregulated in the gene expression experiment. Similar to the in the gene expression experiment no significant upregulation of proteins involved in mitochondrial biogenesis was found.

In summary we could detect significant differences in the proteasome of control and patient cell lines with mutations in *ACAD9* and bezafibrate treated and untreated cell lines. As expected, and already shown in other studies, the impaired function of complex I led to degradation of other complex I subunits and might cause compensatory effects like the upregulation of MDH2 and ACADVL. The analyses of the differences in the proteasome of untreated versus bezafibrate treated cells revealed eight upregulated proteins involved in fatty acid oxidation pathway and no respiratory chain subunits or proteins involved in mitochondrial biogenesis. This was consistent to the gene expression experiment, supporting the theory of increased complex I activity due to stabilized supercomplexes with the help of different FAO proteins.

3.2.1.3.3 Western Blot analysis

In order to detect effects on protein level, which might be missed by the DIGE experiment due to experimental design and technical limitations seven different patients with mutations in *ACAD9* were

selected for further Western Blot analysis. Untreated and bezafibrate treated whole cells lysates were loaded on 4-12% precast SDS-gels and immune-decorated with different antibodies as described in chapter 2.9.5 (Figure 3.33).

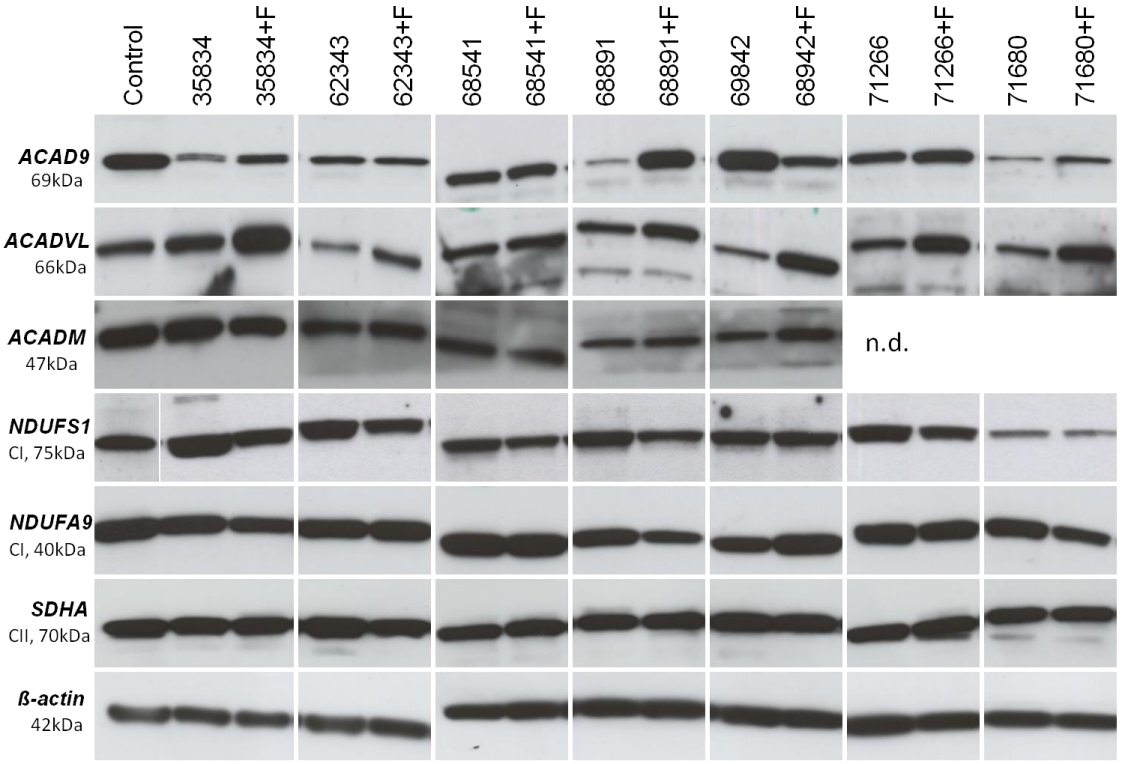

Figure 3.33: Western Blot Analysis of selected patients with ACAD9 mutation with (+F) and without bezafibrate treatment

In 6/7 cases the amount of ACAD9 protein (as mean of three technical replicates) was increased after bezafibrate treatment. The cell line 69842 did not respond to the treatment and even showed a reduction of ACAD9 protein (Figure 3.34A), the control was unchanged. The increase of ACAD9 protein varied from 18-83%.

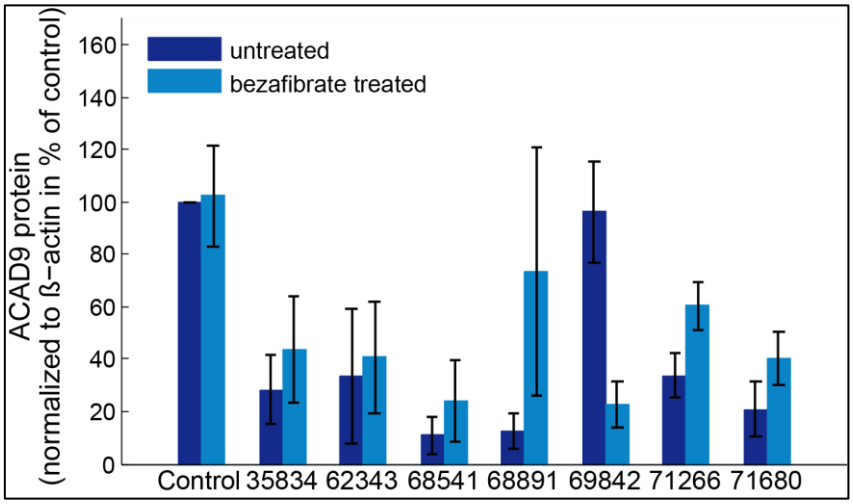

Figure 3.34A: Quantification of ACAD9 protein of one control and seven selected ACAD9 patients with and without bezafibrate treatment normalized to β-actin. Data shown are mean of three biological replicates ± SD.

Due to the fact that the variation between the three replicates was quite high, the increased ACAD9 protein level seen in 6/7 cell lines was not significant in the cell line itself. Nevertheless, the overall increase between the two groups (untreated and bezafibrate treated, excluding patient 69842) was significant (p-value: 0,011).

The enormous increase of ACADVL, already seen in the gene expression experiment on the transcriptional level and in the DIGE experiments on protein level, was confirmed with Western Blots. All patient cell lines showed a big increase between 22 and 209% (Figure 3.34B). Interestingly the cell line 69842 which did not show any increase of ACAD9 after bezafibrate treatment showed anyhow the biggest increase in ACADVL.

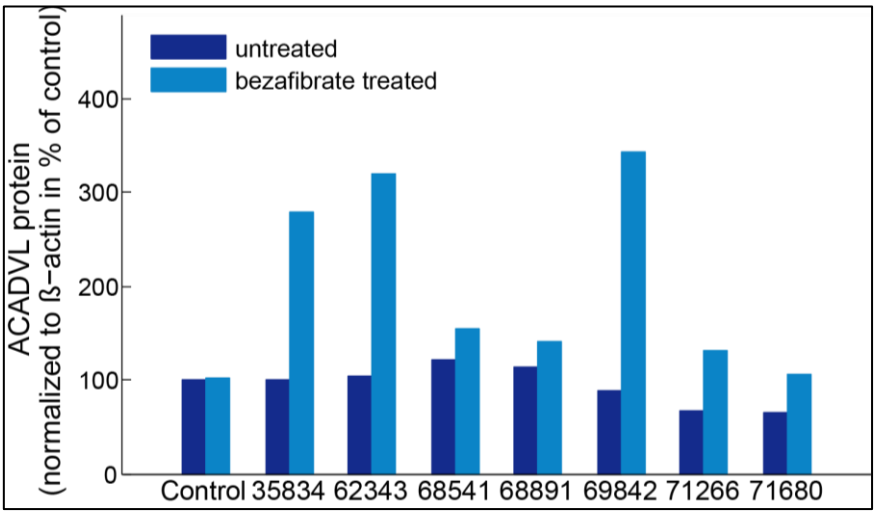

Figure 3.34B: Quantification of ACADVL protein of one control and seven selected ACAD9 patients with and without bezafibrate treatment.

In contrast to ACADVL, another examined acyl-CoA dehydrogenase family member, medium-chain specific acyl-CoA dehydrogenase (ACADM), was unchanged after bezafibrate treatment. Analogous to ACADM, the amount of protein of the complex I (NDUFS1 and NDUFA9) and complex II (SDHA) subunits was unaffected. This finding is contrary to previously publications which saw an upregulation of all mitochondrial proteins [146] (Figure 3.34C).

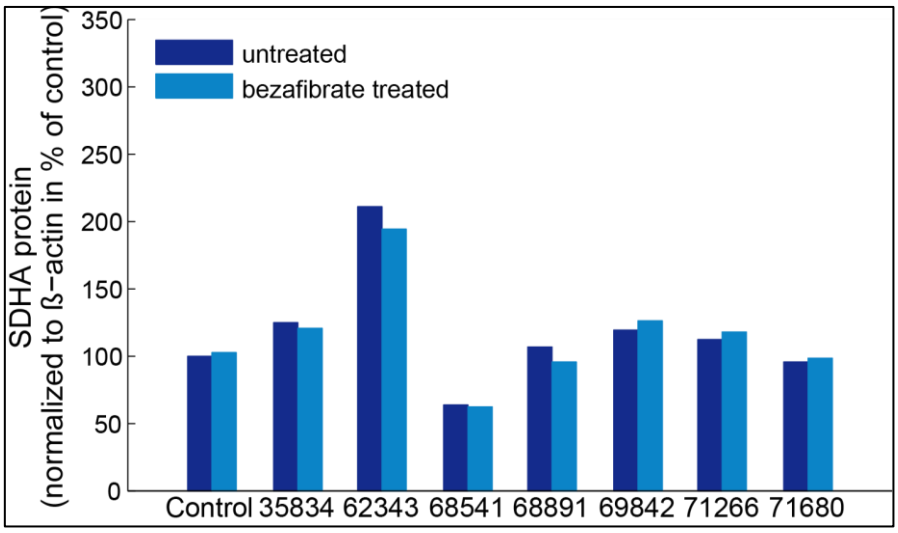

Figure 3.34C: Quantification of SDHA protein of one control and seven selected ACAD9 patients with and without bezafibrate treatment.

In order to answer the question why some cell lines respond to the treatment and others not, a deeper look to the kind of mutation was done. These results could be interesting for the treatment in patients as a primary stage of personalized medicine. First, I looked to the position of the mutation within the *ACAD9* gene. The "responsive" mutations were distributed over the whole *ACAD9* gene and no clear correlation was found (Figure 3.35). The mutations of responsive as well as unresponsive cell lines were found within the Acyl-CoA dehydrogenase/oxidase N-terminal, the central, C-terminal domain and close and far away from the FAD binding site and substrate binding pockets. This observation might be limited due to the small amount of cell lines and needs to be verified within a bigger cohort of cell lines.

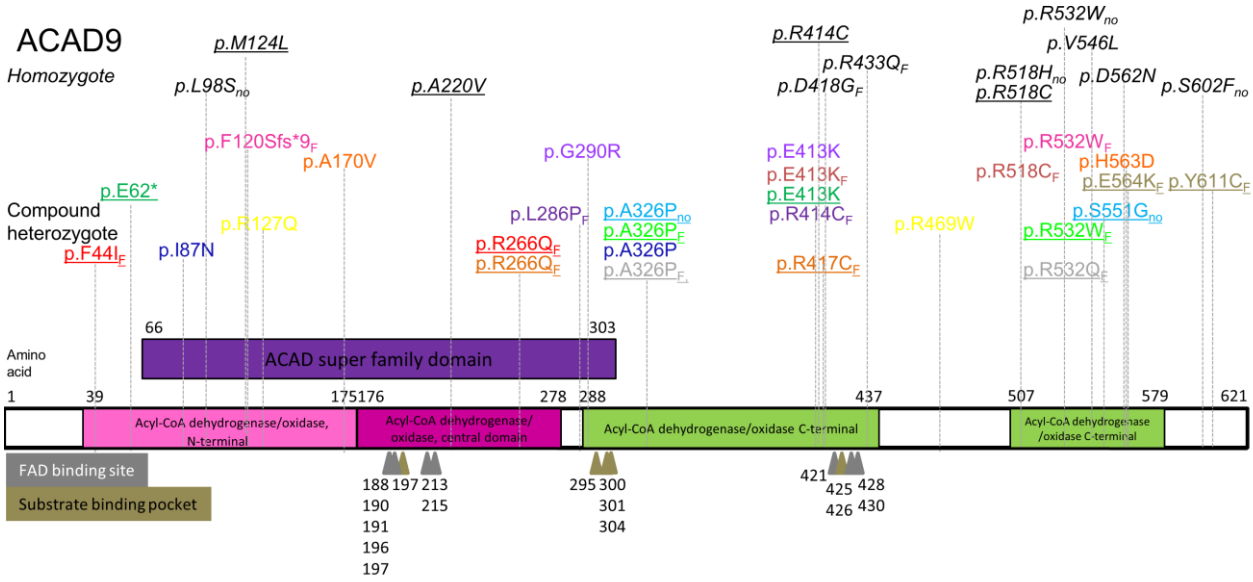

Figure 3.35: Domain structure of *ACAD9* with all known pathogenic mutations and their response to bezafibrate treatment in fibroblasts (significant increase: index F, no response: index no), no treatment performed (no index). Mutations with the same colour belong to the same patient

Another reason why some cell lines responded to the treatment and others not could be if the mutation lies in a domain which is identical, similar or different to its family member ACADVL. ACAD9 shares considerable sequence homology to ACADVL with 47% identical and 65% similar amino acids [114]. In all examined cell lines with at least one mutation in ACAD9 within an identical sequence domain of ACADVL and a clear reduction of complex I activity in fibroblasts the bezafibrate treatment was effective. This finding was observed in five cell lines, highlighted in yellow (Table 3.13).

Patient	Mutation	Similarity to ACADVL	Complex I rest activity	Effect of bezafibrate treatment in vitro
35834	c.130T>A, p.Phe44Ile c.797G>A, p.Arg266Glnc	Identical similar	Muscle: 14% Fibroblasts: 33%	89,5%
49591	c.1594C>T, p.Arg532Trp	Identical	Fibroblasts: 38%	44,6%
52933	c.797G>A, p.Arg266Gln c.1249C>T, p.Arg417Cys	Similar identical	Muscle: 13% Fibroblasts: 37%	140,5%
52935	c.130T>A, p.Phe44Ile c.797G>A, p.Arg266Gln	Identical similar	Fibroblasts: 38%	53,4%
52674	c.976G>C, p.Ala326Pro c.1594C>T, p.Arg532Trp	Identical Identical	Muscle: 26% Fibroblasts: 46%	42,5%
61980	c.1553G>A homo, p.Arg518His	similar	Fibroblasts: 50%	-4,4%
62006	c.151-2A>G, c.1298G>A, p.Arg433Gln	identical	Heart: 68% Muscle: 64% Fibroblasts: 78%	26,4%
62340	c.976G>C het, p.Ala326Pro, c.1595G>A het, p.Arg532Gln	Identical Identical	Heart: 64% Muscle: 54% Fibroblasts: 49%	42,8%
62343	c.358delT, p.Phe120Serfs*9 c.1594C>T, p.Arg532Trp	Identical	Heart: 40% Muscle: 72% Fibroblasts: 79%	57,4%
62347	c.1237G>A, p.Glu413Lys c.1552C>T, p.Arg518Cys	Identical Similar	Heart: 44% Fibroblasts: 66%	31,7%
63869	c.1253A>G, homo, p.Asp418Gly	Identical	Muscle: 9% Fibroblasts: 59%	8,5%
68541	c.293T>C, homo, p.Leu98Ser	different	Muscle: 6% Fibroblasts: n.r	28,7% (n.s.)
68891	c.1690G>A, p.E564K c.1832A>G, p.Y611C	Identical Different	Muscle: 64% Fibroblasts: 72%	47,3%
69842	c.1553G>A, homo, p.Arg518His	similar	Muscle: 31% Fibroblasts: 60%	- 17,4%
71265	c.976G>C, p.Ala326Pro c.1651A>G, p.Ser551Gly	Identical Identical	Muscle: 14% Liver: 28% Fibroblasts: n.r.	-0,55%
71680	c.857T>C, p.Leu286Pro c.1240C>T, p.Arg414Cys	Identical Identical	Fibroblasts: 53%	29,2%
72545	c.1594C>T homo, p.Arg523Trp	Identical	Muscle: 3% Fibroblasts: n.r	-0,86%

Table 3.13: Overview of the collection of ACAD9 mutation, their similarity to ACADVL, complex I activity and their response to bezafibrate treatment, n.s.= not significant

In three cell lines complex I activity was already within the normal range and bezafibrate treatment did not increase complex I activity significantly. Contrary to the control cell line, in which a significant increase of complex I activity was always observed between 10-15%. The reason for that is not clear. But it can be speculated, that in cell lines in which ACADVL sequence is identical to ACAD9 at the position of the mutation, ACADVL (which upregulation was clearly seen in the gene expression as well as in the experiments performed on protein level) could overtake the function of ACAD9, and therefore led to an increase in complex I activity.

3.2.1.4. Pathway analysis

The next point was to use the results of the gene expression and DIGE experiment to perform a pathway analysis with Ingenuity software. The idea behind the pathway analysis was to identify different patterns between patient and control. The complete lists with significantly changed proteins or genes and fold-changes were uploaded to the software and further analysed with IPA as described in chapter 2.9.7.
The first figure shows the identified pathways which were differently regulated between eleven complex I patients and three controls in the gene expression experiment (Figure 3.36A) and between five ACAD9 patients and one control in the DIGE experiment (Figure 3.36B):

Figure 3.36: Results of the pathway analysis of gene expression (A) and DIGE (B) experiment between control and patients. Most interesting pathways were marked in red.

The pathway analysis of the gene expression experiment revealed only five pathways above the significance level. At first view they have nothing to do with mitochondrial disorders. This finding could be explained due to the selection of patients in the gene expression experiment. All patients selected for the gene expression experiment had a clear complex I defect in fibroblasts, but the disease-causing mutation was different in all cell lines. Five cell lines hat mutations in complex I subunits, one assembly factor, two in the mtDNA, one in tRNA and two have no molecular diagnosis yet. Assuming that every mutation causes the observed complex I defect in different ways, it is not surprising, that the pathway analysis revealed no pathway which was differentially regulated in all patient cell lines compared to the controls. In contrast to that, the pathway analysis of the DIGE experiment (in which only patient cell lines with mutations in *ACAD9* were selected) showed more than 20 affected pathways above significance level. The amount of 16 proteins (ACSL4, ANXA6, DECR1, DLD, ECHS1, HADHA, HADHB, HSD17B10, IMMT, LRPPRC, HSPA8, MDH2, PDHB, PHGDH, SDHA) involved in fatty acid metabolism were 1,2-3,8-fold lower in the ACAD9 patients compared to the control. Furthermore, six proteins implicated in mitochondrial dysfunction (DLD, LRPPRC, NDUFA10, SDHA, HADHA, HADHB) were also detected by the DIGE experiment. All together the DIGE experiment could clearly show the differences between ACAD9 patients and control. The results could be used to help to find a diagnosis for unsolved patients (with suspected mitochondrial disorder and clear complex I defect) by comparing the whole mitochondrial proteasome in order to find similar pattern.

The next pathway analysis was performed with the gene expression data from up-and downregulated genes between untreated and bezafibrate treated samples (Figure 3.36C). In total 21 different pathways were affected above significance level. The well-known function of bezafibrate, upregulation of fatty acid metabolism, was the most significant hit. The analysis of the data of the DIGE experiment revealed also the upregulation of fatty acid metabolism as the most significant hit. The gluconeogenesis I, TCA cycle II, ketolysis and ketogenesis pathways were also affected after bezafibrate treatment (Figure 3.36D).

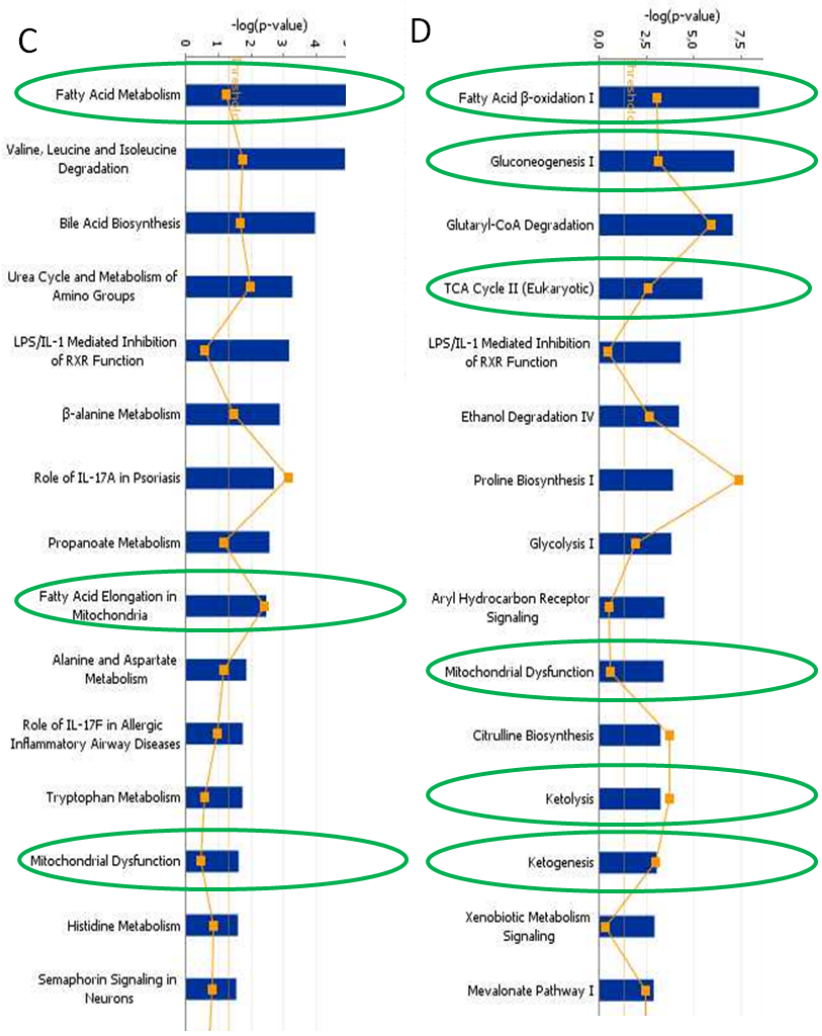

Figure 3.37: Results of the pathway analysis of gene expression data (C) and DIGE (B) experiment from up-and downregulated genes untreated and bezafibrate treated samples. Most interesting pathways were marked in green.

Further analysis with the IPA program identified the following upstream regulators. Bezafibrate treatment acts as a pan-PPAR activator (Table 3.14).

Upstream Regulator	Molecule Type	Predicted Activation State	Activation z-score	p-value of overlap	Target molecules in dataset
PPARA	ligand-dependent nuclear receptor	Activated	3,538	5,27E-12	ABCA1, ACAA2, ACADVL, ANGPTL4, ASS1, CAT, CD36, CPT1A, CPT1B, ECH1, HADHB, LPCAT3, MMD, PDK4, PLIN2, SLC25A20
PPARG	ligand-dependent nuclear receptor	Activated	2,860	1,07E-12	ABCA1, ACAA2, ANGPTL4, CAT, CD36, CFD, CPT1A, CPT1B, CXCL6, FST, HADHB, IL8, KRT19, PDK4, PLIN2, SLC25A20

PPARD	ligand-dependent nuclear receptor	Activated	2,583	1,28E-08	ACADVL, ANGPTL4, CD36, CPT1B, ECH1, PDK4, PLIN2, SLC25A20, ZBED5
PPARGC1A	transcription regulator	Activated	2,580	2,85E-06	ACADVL, CAT, CD36, CPT1A, CPT1B, PDK4, SLC25A20

Table 3.14: Most significant targeted regulators after bezafibrate treatment

In summary, the pathway analysis with the gene expression and DIGE experiment data confirmed the upregulation of the fatty acid oxidation pathway accompanied by the upregulation of ketogenesis due to the bezafibrate treatment. An increase of other mitochondrial biogenesis pathways (including NRF1, NRF2) was not observed.

3.2.1.5 Proposed mechanism of bezafibrate treatment

In the beginning three mechanisms seemed to be possible why bezafibrate could be beneficial for patients with complex I defect. Improved respiratory chain activity could be achieved through:

1. Increase of fatty acid oxidation pathway, leading to an increase of acetyl-CoA and subsequently an increase of energy in form of ATP.
2. Bezafibrate could lead to an increase of other acetyl-CoA family members (e.g. ACADVL, ACADM, ACAD9), which help to stabilize respiratory chain super complexes.
3. Bezafibrate could lead to an upregulation of mitochondrial biogenesis pathways by increased expression of Tfam, NRF1, NRF2 leading to an increase of mtDNA replication and transcription and finally more mitochondrial mass.

In order to verify or neglect the different mechanisms, experiments on activity, gene expression and protein level were performed. Bezafibrate treatment on patient-derived fibroblasts increased complex I activity significantly in 28 out of 42 cell lines. The treatment was especially successful in patient cell lines with mutations in the complex I assembly factor *ACAD9* (significant increase in 12 out of 17 patient cell lines). The gene expression as well as the DIGE experiment showed an increase in fatty acid oxidation pathways and no increase in mitochondrial biogenesis. Further protein experiments confirmed the increase on fatty acid-CoA family members (ACADVL and ACAD9). No increase in other respiratory chain complex subunits was observed and no increase in total mitochondrial mass. 2D-SDS-Gels showed an increase of assembled supercomplexes in the controls and six out of seven patient cell lines.

Taken together, bezafibrate acts most likely as a pan-PPAR-activator, leading to an upregulation of fatty acid oxidation pathway and increase of acid-CoA family members. The upregulation of fatty oxidation pathway leads to a metabolic shift from glycolysis to fatty acid oxidation in order to produce more energy. The increases of acid-CoA family members are probably responsible for the improved stability of respiratory supercomplexes followed by an increase of complex I activity and not an increase of mitochondrial biogenesis. It has been already shown, that FAO proteins form a multifunctional FAO

complex that interacts physically with OXPHOS super complexes and endorses metabolic channelling [235, 237]. Further experiments to understand the exact protein interactions will be crucial for the comprehension of the pathogenesis involved. But so far Bezafibrate seems to be a promising new treatment option for patients with complex I deficiency, especially patients with mutations in *ACAD9* (Figure 3.38).

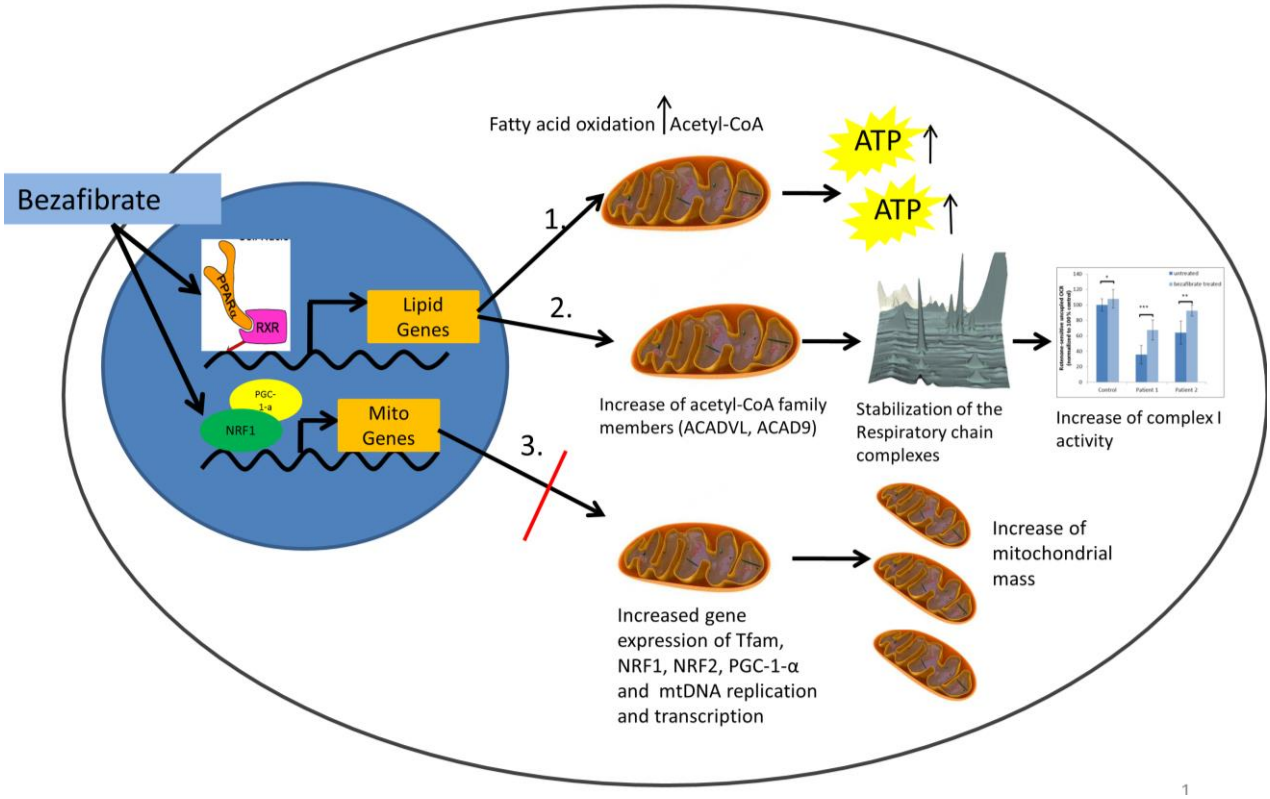

Figure 3.38: Proposed mechanism of bezafibrate treatment

3.2.2 Riboflavin treatment

The next drug which was tested in vitro as a possible treatment option for patients with complex I defect was riboflavin. Riboflavin is already routinely used in the treatment of patients with mitochondrial disorders. Riboflavin is a vitamin precursor of the flavin mononucleotide (FMN) and flavin adenine dinucleotide (FAD), cofactors in complex I. Gerards et al. reported nine years ago about a family with complex I defect and mutations in *ACAD9*. After the administration of riboflavin, the symptoms alleviated, but the mode of action remains elusive. It is suggested, that riboflavin increases FAD concentration and supports FAD binding. This binding could be necessary for the catalytic activity of ACAD9, or could improve folding and stability of the remaining protein. That's why riboflavin might be especially useful for patients with mutations in *ACAD9*. Since that, several anecdotal reports from riboflavin-responsive and unresponsive patients were published [113, 170, 238]. But the reason, why some patients respond to riboflavin and others not is still not clear. To address this question, complex I activity measurements and

investigations on protein level were performed on control and patient-derived fibroblasts before and after riboflavin treatment.

3.2.2.1 Oxygen consumption measurement

One control and five different patient cell lines were treated for three days with riboflavin as described in chapter 2.6.2 (Figure 3.39). The five cell lines had all an isolated complex I defect and mutation in the mtDNA (*ND6*) or nuclear gene (*NDUFS1*, *ACAD9*). The OCR in the cell lines with mutations in *ND6* and *NDUFS1* increased not significantly between 10-24%.

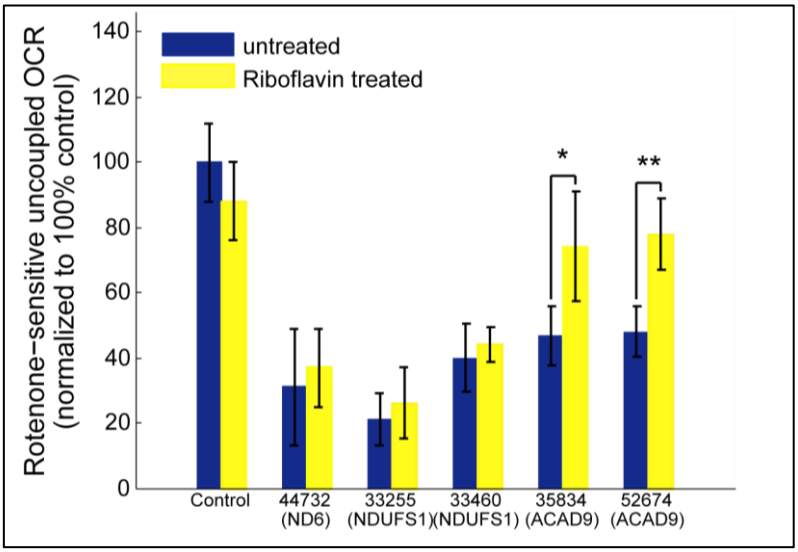

Figure 3.39: Rotenone sensitive oxygen consumption rate with and without riboflavin treatment in control and four complex I deficient cell lines. Values are means ± SD of at least three different experiments (p-value<0,05,*, p-value<0,01,**)

The biggest significant response to riboflavin treatment was observed in the patient cell lines with ACAD9 mutation (with an increase of 58% and 62% of complex I activity, normalized to the control) (Figure 3.39). This positive effect was further analysed in our collection of patients with ACAD9 mutation. 9/15 patient cell lines showed a significant increase ranging from 14-109%. The control cell line showed no improvement (Figure 3.40).

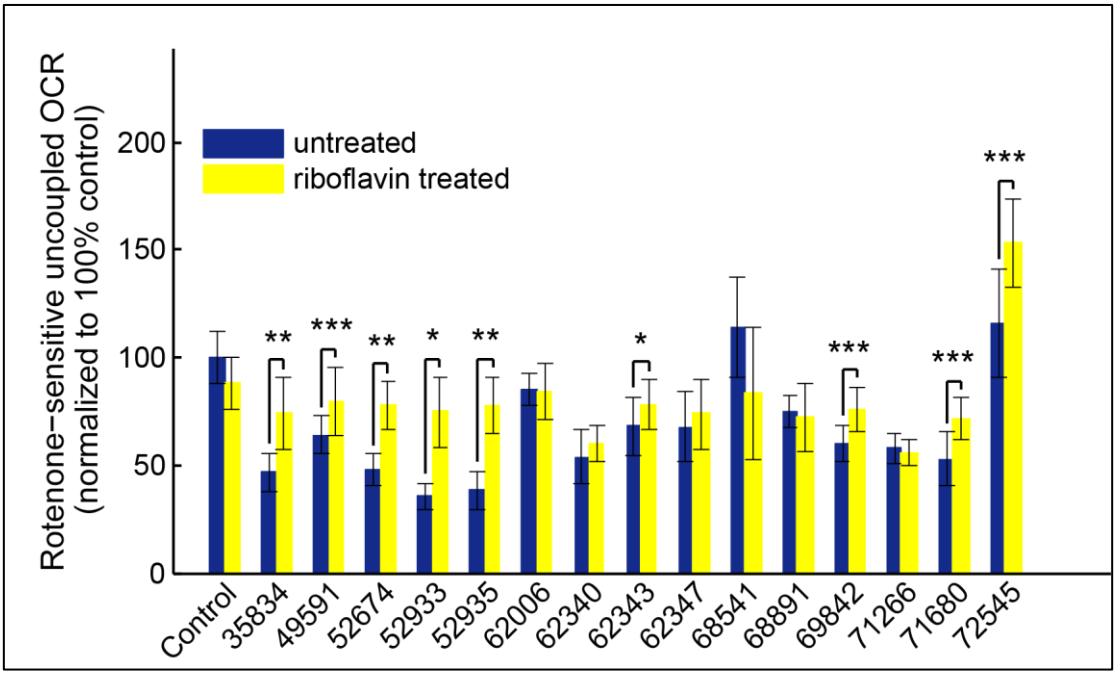

Figure 3.40: Rotenone sensitive oxygen consumption rate in all patients with ACAD9 mutations with and without riboflavin treatment (data shown are means ± SD of > three biological replicates, p-value< 0,05,*, p-value<0,01,**, p-value<0,001,***)

To address the question why some patient cell lines responded to the treatment and others not a deeper look to the kind of mutation was done. Interestingly 4/5 cell lines with at least one mutation at the position p.R532W (FibroID 49591, 52674, 62434 and 72545) responded significantly to the riboflavin treatment (Figure 3.41). In contrast to that, patient cell lines with mutations close to FAD binding site seem to be unresponsive to riboflavin treatment (p.A220V, p.R418G, p.R433Q). All other mutations were distributed over the whole gene and no clear correlation was found.

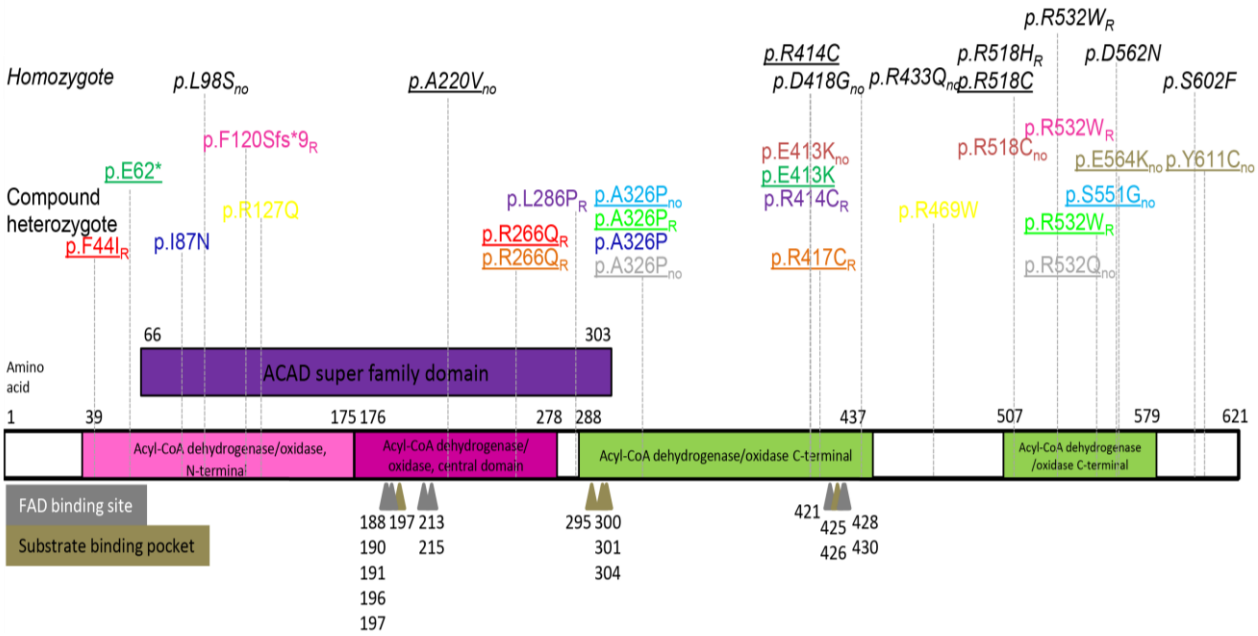

Figure 3.41: Domain structure of *ACAD9* with all known pathogenic mutations and their response to riboflavin treatment in fibroblasts (significant increase: index R, no response: index no, no treatment performed: no index). Homozygote variants in black, same colour indicate two heterozygote variants in one patient

These results could be interesting for the treatment in patients as a primary stage of personalized medicine. This observation might be limited due to the small amount of cell lines and needs to be verified within a bigger cohort of cell lines.

3.2.2.2 Western Blot analysis

The effect of the riboflavin treatment was further analysed on protein level. In contrast to the bezafibrate treatment no increase of ACAD9 or ACADVL protein was detectable. The amount of complex I subunits NDUFS1 and NDUFA9, CII subunit SDHA and ACADM remained also unchanged. The increase of OCR in 9/15 patients could not be explained with more ACAD9 protein itself. Riboflavin might stabilize the remaining ACAD9 protein and therefore increased the OCR in a majority of patients examined (Figure 3.42).

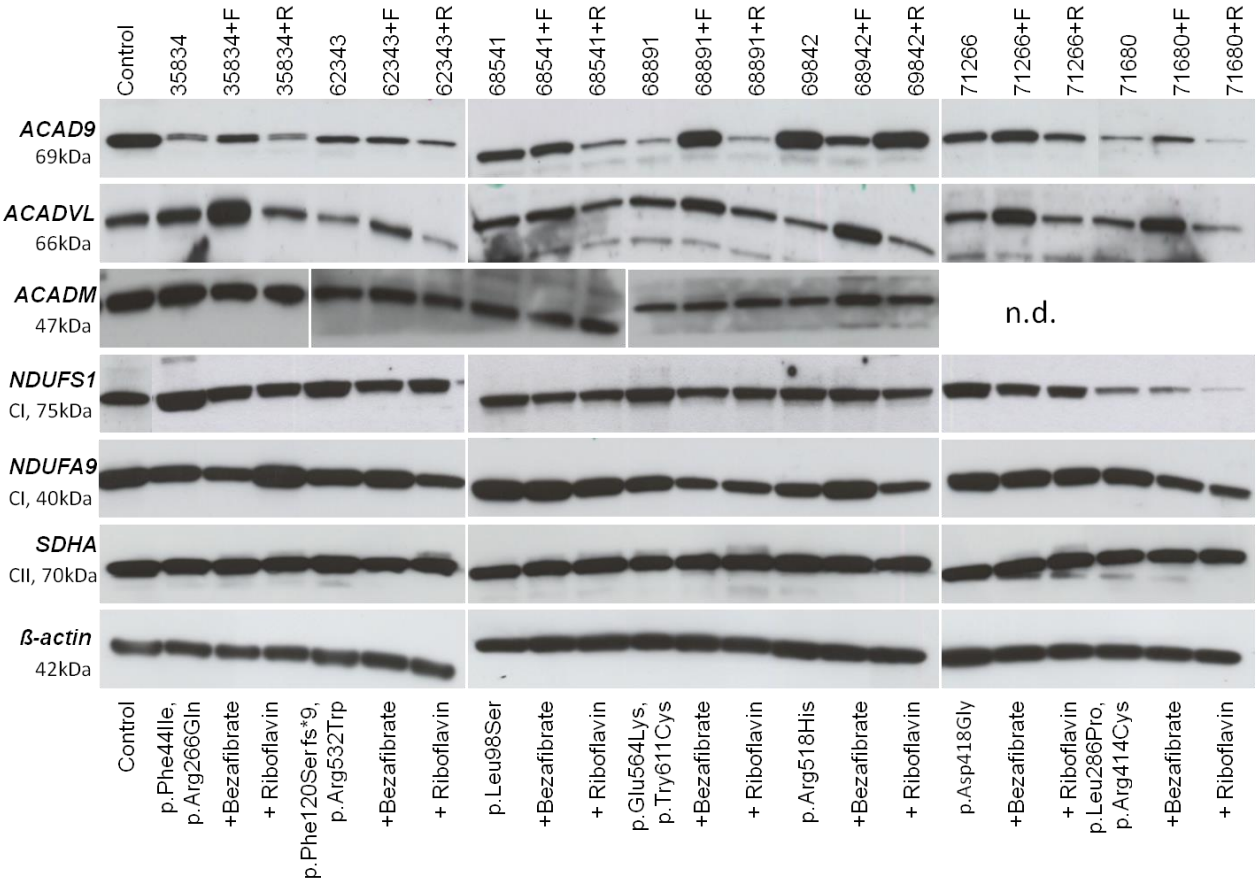

Figure 3.42: Western Blot Analysis of selected patients with ACAD9 mutation with (+F) and without bezafibrate and riboflavin (+R) treatment

3.2.2.3 mitoGELs

The effect of riboflavin treatment on the assembly of supercomplexes was further analysed with the help of mitoGELS as described in chapter 2.9.3. In total one control and four different ACAD9 patient cell lines were selected (Table 3.15). Riboflavin responsive as well as unresponsive ones were selected.

Number	Cell line	Mutation	Complex I activity (% of normal range)	Response to the riboflavin treatment on complex I activity measurement
1	NHDF	WT	100,0	+12,0
2	62006	ACAD9	85,4	-1,29
3	62347	ACAD9	67,9	+8,38
4	68541	ACAD9	114,1	-26,8
5	69842	ACAD9	60,1	+ 26,9

Table 3.15: List of cell lines used to detect differences in the amount of supercomplex after riboflavin treatment with mitoGELS

The control and two patient cell lines (FibroID 62006 and 685414) showed no improvement in the assembly of supercomplexes (which was concordant to the complex I activity measurement). The other two cell lines responded positive to the riboflavin treatment. Supercomplexes in fibroblasts of patient 62347 were first not detectible and then restored to 12 % compared to the control upon riboflavin treatment. In cell line 69842 the amount of assembled supercomplexes increased from 76% to normal levels (Figure 3.43). These positive findings were also consistent to the OCR measurement.

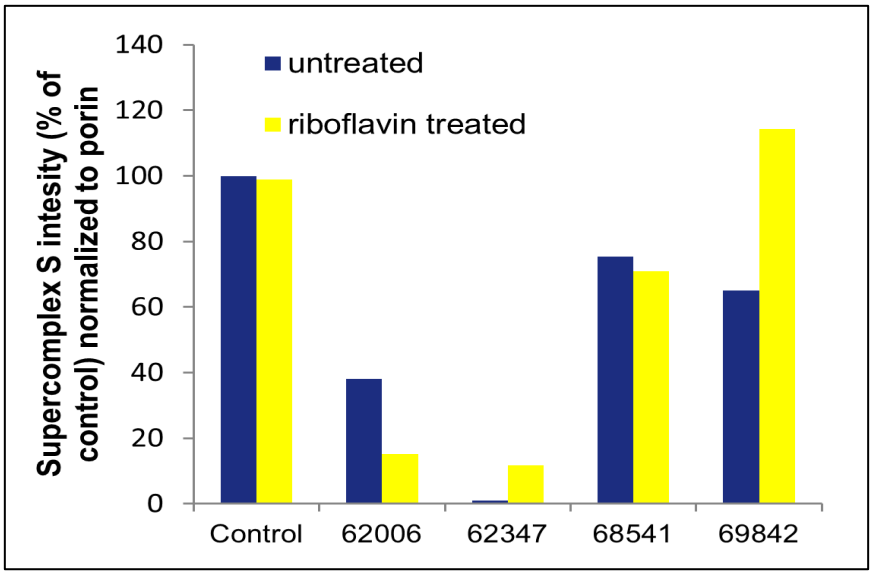

Figure 3.43 Quantification of the supercomplexes of one control and four patients with ACAD9 mutation with and without riboflavin treatment (average of two technical replicates)

Taken together, the analysis of five mitoGELs revealed an increased assembly of supercomplexes in two out of four patient cell lines but not in the control cell line. This finding was consistent with the OCR measurement in the corresponding cell lines.

3.2.2.4 Riboflavin treatment in patients

The online survey was further used to collect data about the effect of riboflavin treatment in patients with mutations in *ACAD9*. From the entire cohort of 70 patients, information about riboflavin treatment was unavailable for 15 patients and 21 patients were reported to be not treated. Of the remaining 34 patients the responsible clinician reported about general clinical effect. Due to the lack of detailed information about onset of riboflavin treatment, dosage, duration and clinical effect in most patients, a more detailed analysis was not possible.

In general, for 23 patients (23/34 = 68%) a beneficial effect was reported by the physicians. No effect was reported for 11 patients (11/34 = 32%) [220]. In order analyse the effect of the riboflavin treatment on the survival rate, the focus was made on patients with a diseases onset during the first year of life. These patients present the biggest subgroup (n = 52) and the group with the shortest survival, suggesting the most severe course (Figure 3.44A). For 41 of these 52 patients data on the riboflavin treatment was available (n = 17 untreated, n = 24 treated). Kaplan-Meier curve significantly indicates a better survival rate for patients with oral riboflavin treatment (deceased n = 7/24) in contrast to untreated patients (deceased n = 16/17) (Figure 3.44B) [220]. One restriction of this observation could be that most of the deaths in this subgroup occurred at the end of the first year of life. This might indicate that our analysis is susceptible to survivor treatment selection bias [220].

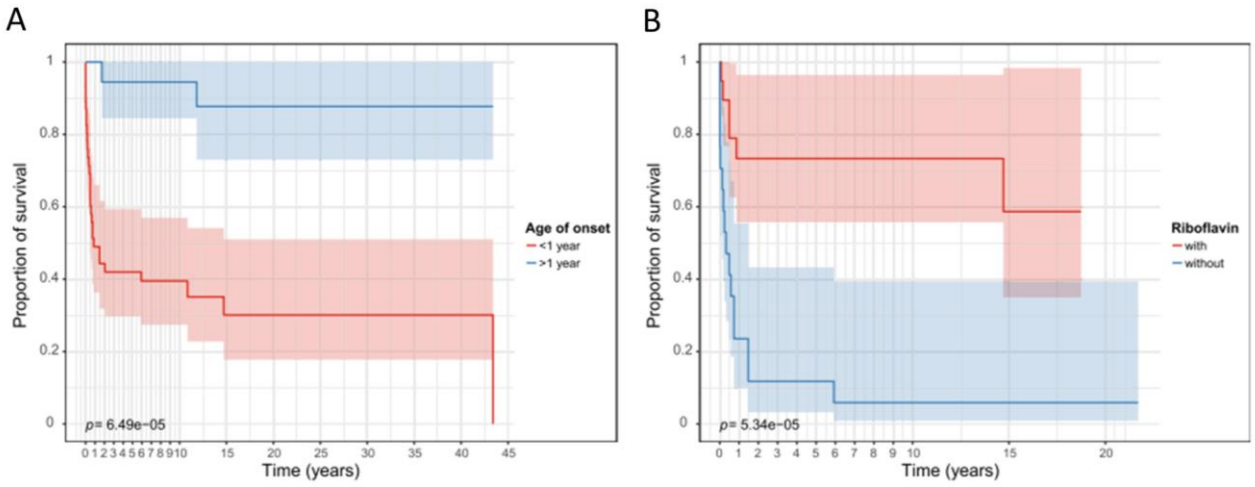

Figure 3.44: (A) Kaplan-Maier survival rates. In red, patients with a disease presentation in the first year of life. In blue, patients with a later presentation. ($p = 6.49e^{-05}$). (B) In red, patients with a disease presentation in the first year of life and treated with riboflavin. In blue, patients of the same age category but untreated with riboflavin ($p = 5.34e^{-05}$, confidence 95%)

Similar to the cell culture analysis the question was asked, if the position of the ACAD9 mutations has an influence on the success of the riboflavin treatment. Indeed six patients harbouring the variant

p.Arg532Trp, concordant to the cell culture experiment, reported a beneficial effect (Figure 3.44). Most patients with mutation at the position p.Arg532 have a milder phenotype with no brain or severe heart involvement. After the administration of riboflavin an increase in exercise intolerance and a clinical improvement was observed [91, 165]. The observation (mutations close to the FAD binding site prevent a beneficial riboflavin treatment) already seen in vitro was partly seen in the patient data. Two patients with mutations close to the FAD binding site p.215 did not respond to the treatment, whereas patients with mutations close to p.421 showed variable outcome. Further correlations between the beneficial effect of riboflavin treatment and the position of the mutation were not found (Figure 3.45). One reason could be that the limited number of patients sharing the same mutation. Another reason could be the start of the riboflavin treatment, which might have been too late in some patients to show a beneficial effect. Altogether the preliminary results are promising but further studies in vitro and in vivo are needed to verify the effect.

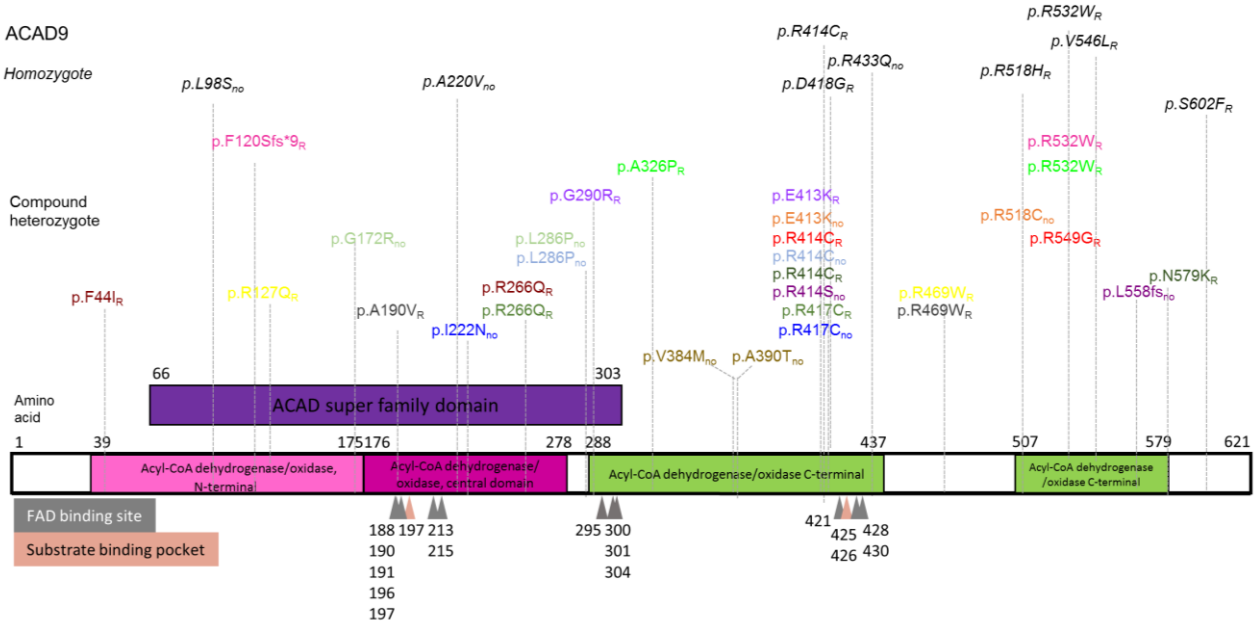

Figure 3.45. *ACAD9* domain structure. Position of causal variants and outcome of riboflavin treatment in patients with mutations in *ACAD9*. (Beneficial effect: index R, no response: index no, no treatment performed: no index). Homozygote variants in black, same colour indicate two compound heterozygote variants in one patient

3.2.2.5 Effect in cell culture versus clinical effect in patients supplemented with riboflavin

Within our cohort of 70 patients, data for riboflavin treatment of paired cells and patients were available for eight patients. In seven pairs the effect measured in cell culture was also concordant to the clinical response (six pairs: FibroID 52935, 52933, 52674, 49591, 69842, 72545 showed a beneficial effect, whereas one pair did not show any response: 68541). One individual did not respond the treatment whereas the cells did (FibroID 71680) [220].

3.2.2.6 Proposed mechanism of riboflavin treatment

Taken together, the experiments in vitro as well as the outcome of the patient survey revealed riboflavin as a promising drug especially for patients with mutations in *ACAD9*. Mutations in *ACAD9* probably lead to misfolded proteins or disturbance of the catalytic activity and FAD binding pocket. The mode of action is still not clear, but previous studies suggested, that riboflavin supplementation increases intra-mitochondrial FAD concentration followed by an increased FAD binding. This increased binding is important for the catalytic activity of all flavoproteins as well as for their right assembly, folding and stability [165, 166, 239]. The upregulation of intra-mitochondrial FAD concentration due to the riboflavin supplementation may compensate for a decreased folding capacity and could help to stabilize the protein [240]. Another additional effect might be the enhancement of the assembly of supercomplexes [241]. Enhancement of supercomplex formation could be hypothesized to complement the proposed negative effect of ACAD9 mutations on the function of the supercomplexes. This stabilized protein could be responsible for the increase of complex I activity in 9 out of 15 patient cell lines, increased supercomplex assembly in two out of four examined patient cell lines and beneficial effect reported in 65% of the patients (Figure 3.46). These promising results suggest further studies, both in vivo and in vitro, on riboflavin treatment in patients with complex I deficiency due to ACAD9 mutations to establish the effect of the treatment. Moreover, a riboflavin administration could be considered for phenotypically-consistent patients whilst their genetic investigations are underway. It is furthermore important to initiate next generation sequencing techniques promptly, accompanied by studies in affected tissue (if available). For these patients, early molecular diagnosis and start of the right therapy could be the difference between life and death [220, 242].

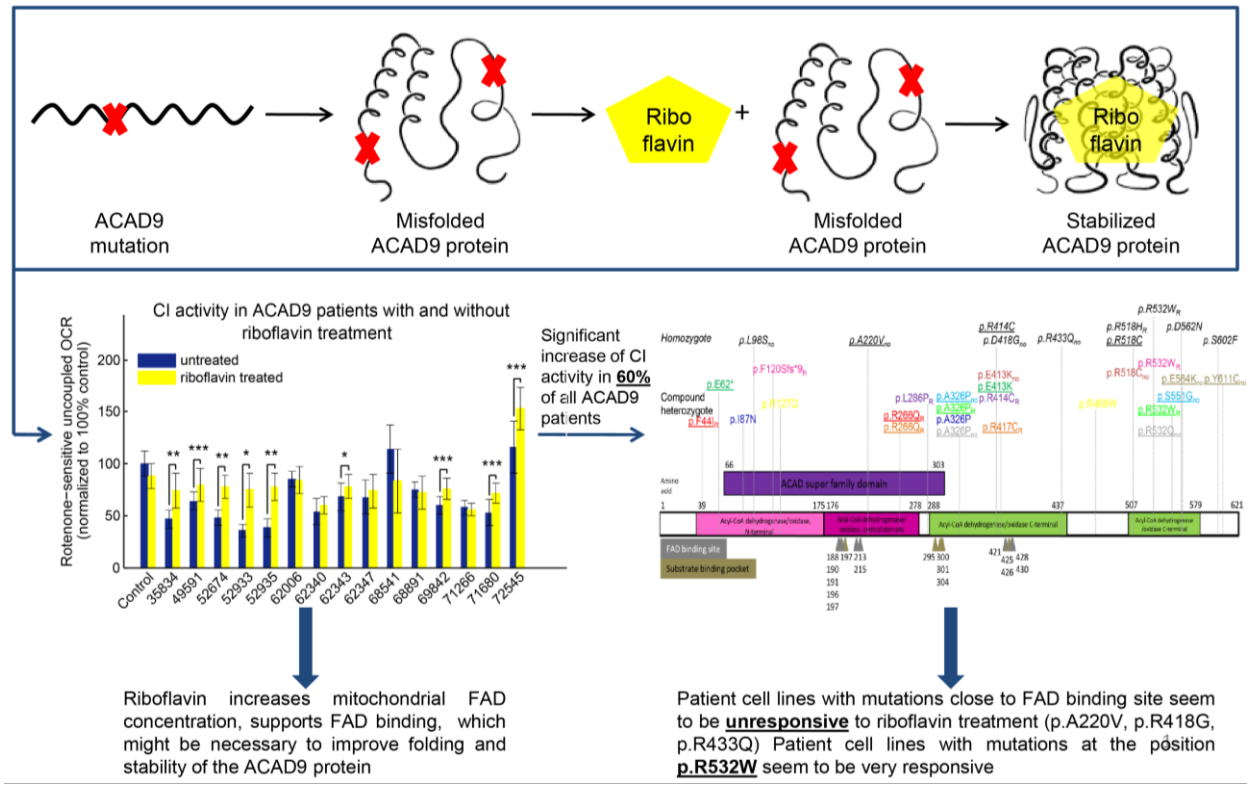

Figure 3.46: Proposed mechanism of riboflavin treatment in patients with mutations in *ACAD9*

3.2.3 Resveratrol treatment

The next substance, which was tested if there is any improvement in the patient fibroblasts, was resveratrol. The same cell lines than in the initial riboflavin treatment experiment were used. OCR seemed to be decreased in five out of six cases after the 3-day treatment with 75µM resveratrol (Figure 3.47). The only cell line which presented a little (but not significant) increase was patient 35834 harbouring two compound heterozygote mutations in *ACAD9*.

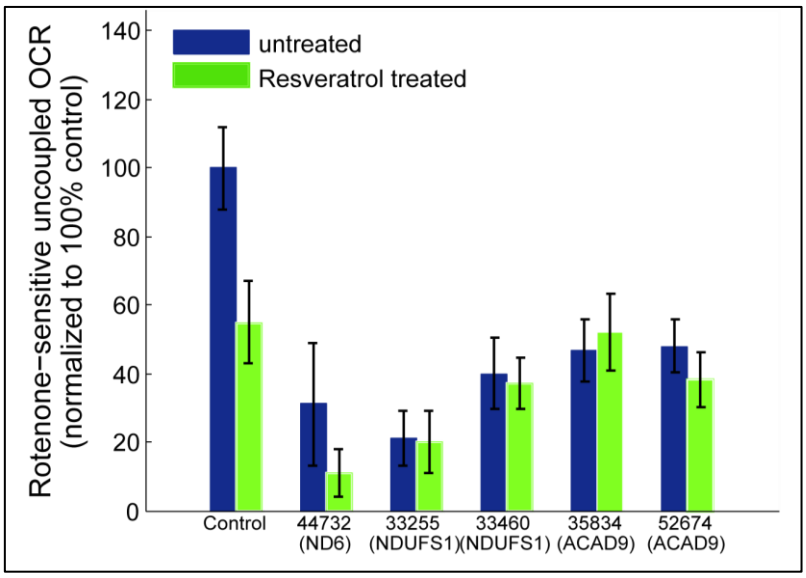

Figure 3.47: Rotenone sensitive oxygen consumption rate with and without resveratrol treatment in control and four complex I deficient cell lines. Data are expressed as average of > 8 technical replicates and normalized to control. ±SD

In this particular experiment no significant improvement was observed. To have a complete answer if resveratrol has any effect on patients with complex I defect more patients must be studied. Due to limited time no further experiments were performed.

3.2.4 AICAR treatment

Another substance which was shown previously to have a positive effect in vitro in patients with mitochondrial disorders is AICAR. On our five patients with complex I defect it seemed to improve OCR in all cases. OCR was not changed in the control cell line. The positive effect was observed in the cell line with mtDNA mutation as well as in the cell lines with nDNA mutation. (Figure 3.48)

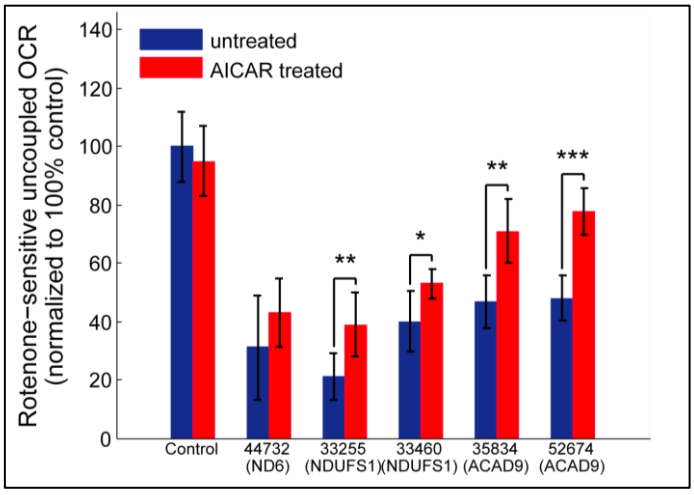

Figure 3.48: Rotenone sensitive oxygen consumption rate with and without AICAR treatment in control and four complex I deficient cell lines. Data are expressed as average of > 8 technical replicates and normalized to control. ±SD, (p-value<0,05,*, p-value<0,01,**, p-value<0,001,***)

This first positive effect needs to be verified in a bigger cohort of patients.

In summary, patient-derived fibroblast and control cell lines were used to test different treatment options for patients with respiratory complex I deficiency in vitro. The effects of resveratrol and AICAR on respiratory chain activity levels need to be verified in a larger set-up. Detailed studies on the effect of bezafibrate and riboflavin in patient fibroblasts were performed. Bezafibrate seems to act as a pan-PPAR-activator, leading to an upregulation of fatty acid oxidation and acid-CoA family members (e.g. ACADVL). The upregulation of acid-CoA family members is probably responsible for the observed improved stability of respiratory supercomplexes followed by an increase of complex I activity. Therefore, bezafibrate could be especially helpful for patients with complex I assembly defects (e.g. ACAD9). Riboflavin treatment seems to be also beneficial in patients with mutations in *ACAD9*. Our data supports the assumption that riboflavin increases mitochondrial FAD concentration, supports FAD binding, which might be necessary to improve folding and stability of the ACAD9 protein. The promising data in vitro encourages the next steps: Verification of the results in a bigger set of cell lines and initiation of a clinical trial.

4. Discussion and Outlook

4.1 Exome sequencing as diagnostic tool

In this thesis six patients with different biochemically diagnosed complex I or combined defect were selected for WES to provide a molecular diagnosis for these patients. The phenotype of these patients was quite heterogeneous. Most patients presented the classical symptoms of mitochondrial disorders (lactic acidosis, muscle hypotonia and developmental delay). Moreover, some patients had respiratory insufficiency, brain deformity, encephalopathy or cardiomyopathy. Exome sequencing led to the identification of a new gene (*ACAD9*) responsible for complex I deficiency. The function of ACAD9, beside the oxidation of long-chain fatty acids with an optimum activity toward unsaturated species, remains poorly understood. Previous papers reported three cases with metabolic and clinical features resembling a β-oxidation and reduced levels of ACAD9 mRNA but no mutations in *ACAD9* [243]. In contrast to that, our patients had no biochemical abnormality of β-oxidation which doubts the primary reported role of ACAD9 in metabolic diseases. In order to get more information about the function of ACAD9, patient-derived fibroblasts cell lines were established. The in vitro experiments were essential to confirm the pathogenicity of the mutation, get insights about the pathomechanism and test new treatment options. We demonstrated that mutations in *ACAD9* are associated with a mitochondrial disorder dominated by severe and generalized complex I deficiency. With the help of 2D-BN-SDS Gels we were able to show that ACAD9 is essential for the correct assembly of complex I. The correct assembly of respiratory chain supercomplexes (in which complex I is embedded together with complex III and complex IV) was disturbed as well. After the lentiviral transduction of the wt-ACAD9-cDNA into patient fibroblast cell lines the assembly of complex I was restored and the decreased complex I activity (48% rest activity) increased to 82%. During the last eight years 29 more patients (in 21 families) with ACAD9 mutation were identified either through WES or an IDAHO Screen of unsolved complex I patients [220]. This assumes ACAD9 mutations are a quite common cause of isolated complex I deficiency. Pathogenic variants were distributed throughout the entire gene, but none of the patients harboured tow loss of function alleles, indicating, that this might be incompatible with life. No clear genotype-phenotype correlation for mutations based on specific regions of the gene or functional domains of the protein was found [220]. There was also no correlation between the remaining complex I activity or the remaining ACAD9 protein level measured in fibroblasts or muscle respectively. The only tendency which could be detected was, that patients, who have a complex I defect and additionally low levels of ACAD enzyme activity have a higher risk to die early or develop encephalomyopathy. It seems that ACAD9 plays a dual role: one role related to β-oxidation and the other to complex I stability. The interaction of ACAD9 with two other complex I

assembly factors, NDUFAF1 and ECSIT, has been shown through complexome profiling [114] [244]. In this paper they found that, beside ACAD9, TMEM126B is an additional assembly factor of complex I. Another possible role of ACAD9 is, that is involved the biochemical dynamics of the lipid milieu in the inner mitochondrial membrane. Complex I is embedded in the inner mitochondrial membrane and its stability and activity depends on the composition of the surrounding lipid compounds. To further investigate this big cohort of 70 ACAD9 patients an online survey was performed and completed by the responsible clinician. The survey involved questions about age of onset, biochemical abnormalities, current age or age at death, prenatal and neonatal findings, most frequent clinical findings, neurological findings, neuroradiological findings, activities of daily life and medication. The main clinical findings were cardiomyopathy, muscular weakness and exercise intolerance. More than 70% of the patients were able to perform age adequate activities of the daily life. Interestingly only four patients suffer from a severe developmental delay and only one patient was reported to have severe intellectual deficits. This percentage is less than reported in other patients cohorts with isolated complex I deficiency (Frequency of 25% [64]). Interestingly one of our initial patients responded very well to a multivitamin scheme including daily riboflavin treatment (100 mg). In vitro supplementation of riboflavin to patient fibroblasts, derived from the initial two patients, let also to an increase of complex I activity. This encouraged us to analyse the effect in vivo within our big patient cohort with ACAD9 mutations and also in vitro in patient-derived fibroblasts. The results will be discussed in chapter 4.2.

The next successful use of NGS as a diagnostic tool was the identification of new potentially pathogenic variants in the complex I subunits *NDUFB3* and *NDUFS8* as a cause of complex I deficiency. The Exome of three patients with typical symptoms of mitochondrial disorders and biochemically identified isolated complex I defect was sequenced. The identified missense mutations in *NDUFB3* and *NDUFS8* affected amino acid residues conserved in >85% of at least 39 vertebrates. The verification of the pathogenicity was proven with complementation experiments followed by functional and protein level investigations. The expression of wt-NDUB3-cDNA and wt-NDUFS8-cDNA in the corresponding fibroblasts led to a significant increase of complex I activity and more amount of fully assembled complex I. The additional expression of NDUFB3-cDNA carrying either the p.Trp22Arg or the p.Gly70X mutation did not change the low activity of complex I (17% of control). The assembly/stability impairment in patients with NDUFB3 mutations was also seen by the absence of NDUFB3, NDUFB8 and NDUFS3 proteins in naïve cells which was increased after transduction to almost normal levels. This was furthermore confirmed by 2D-BN-SDS-PAGE separation and quantification of fluorescein-labelled mitochondrial complexes. The supercomplexes which were not detectable in the patient increased up to 43% of the control, whereas the amounts of complexes III, IV, and V did not change significantly. It is known that NDUFB3 is a single transmembrane domain subunit localised in the β arm of the p-module of complex I. It is a complex I accessory subunit and plays a role in regulation, assembly and stability of the 14 subunit catalytic core of complex I, possibly protecting it from reactive oxygen species damage [245]. Another variant in *NDUFB3* was identified recently in a screen of 42 patients with infantile onset mitochondrial disorders. Other studies

with even bigger cohorts of patients with mitochondrial disorders failed to discover rare variants in *NDUFB3* suggesting that mutations in that gene are quite rare [93, 246]. Taken together, these results demonstrate the causal role of the mutations identified in *NDUFS8* and *NDUFB3* [91].

The third application of WES was performed in two siblings presenting with severe neonatal lactic acidosis, hypotonia, and intractable cardiomyopathy. Both died within the first months of life. Biochemical analysis of the muscle biopsy revealed a combined deficiency of respiratory chain complexes I, II, II+III and complex IV accompanied by a defect of the pyruvate dehydrogenase complex and decreased levels of lipoic acid levels. The observed decrease in levels of lipoic acid suggests an impairment of the lipoic acid synthetase. Prioritized filtering uncovered one homozygous missense mutation in *BOLA3* in the two siblings. Recently a homozygous nonsense mutation in *BOLA3* was identified in a patient with multiple mitochondrial disorders (MMDS) by chromosome transfer. [225]. The phenotype of this patient was quite similar to our patient. The lentiviral mediated expression of the mitochondrial isoform of wildtype BOLA3 in patient fibroblasts validated the pathogenicity of the founded variant. After successful complementation the residual enzyme activities and lipoic acid levels increased significantly. BOLA3 is a poorly understood member of the mammalian BolA-like protein family, but the exact function of BOLA3 is not clear. In Saccharomyces cerevisiae it is shown that the BolA homologue Fra2 together with the monothiol glutaredoxins Grx3 and Grx4 play a key role in iron regulation [247]. The role in humans is still speculative. BOLA3 might interact with glutaredoxin 5, which is involved in the biogenesis of 2Fe-2S and 4Fe-4S clusters [225]. One of the two patients had also a decreased complex IV activity in the muscle biopsy. This is surprisingly, because complex IV does not contain Fe-S clusters and was also normal in the other patients. Therefore, the complex IV defect might be an indirect effect. In the study from Cameron et al. she also found another mutation in another gene involved in Fe-S cluster biogenesis (NFU1) in patient with MMDS. Two out of three siblings showed also an impaired complex IV. One clinical symptom which had all patients with BOLA3 and NFU1 mutations in common were elevated glycine levels. This symptom was also present in patients with defective lipoic acid synthesis due to mutations in *LIAS* [248, 249]. The reduced levels of lipoic acid could provide an explanation for impaired glycine cleavage thereby explaining the increased levels of glycine in patients with BOLA3 mutations. The disease nonketotic hyperglycinemia (NHK) is associated with defects in the mitochondrial glycine cleavage system, including the gene coding for the lipoic acid-containing H-protein GCSH [250]. Patients with NHK have, beside other clinical manifestations like lethargy, hypotonia and progressing apnea, intractable seizures and mental retardation. Stubborn seizures were observed in our patients as well as in the patients described by [225] and [251]. However, it remains provisional whether secondarily impaired glycine metabolism contributes to the phenotype of mutant BOLA3. All together these results suggest that BOLA3 plays a crucial role in the biogenesis of iron-sulfur clusters necessary for the proper function of respiratory chain and 2-oxoacid dehydrogenase complexes. Patients with MMDS, a fast progression of disease and eventually elevated glycine levels should be tested for BOLA3 mutations [224].

The next patient used for Exome sequencing was a girl with leukodystrophy and clear complex I defect in muscle and fibroblasts and an additional complex IV defect in fibroblasts. The first analysis of the Exome

data revealed one heterozygote mutation on the x-linked gene *AIFM1* as a good candidate. It is known that mutations in *AIFM1* in boys led to a mitochondrial encephalomyopathy and other mitochondrial deficiency syndromes. An existing mouse model presented a heterogeneous phenotype with progressive cerebellar ataxia, early fur abnormalities, optic tract dysfunction with retinitis pigmentosa and a higher risk of cardiomyopathy. One thing all mice had in common was the fact, that the degree of reduction of complex I subunit NDUFB8 (20kDa) corresponds to the severity of the disease. Even though the mother of the patient was also carrying the mutation, the phenomenon of x-inactivation could explain the deleterious effect of this heterozygote mutation. The complementation assay with the wt-AIFM1-cDNA and subsequent measurement of the OCR in the fibroblast cell line of the patient showed an increase of respiration. The analysis of the respiratory chain complexes with mitoGELs confirmed the combined respiratory chain complex defect but was unchanged after transduction. The analysis of the 20kDa subunit of complex I before and after transduction of the wt-AIFM1-cDNA showed also no significant change. The inconsistent results let us question if we have the right gene. Due to the fact that *AIFM1* lies on the x-chromosome, one male family member carrying the same mutation would exclude mutations found in *AIFM1* as the disease-causing variants. That was in fact the case. The grandfather of our patient had the same mutation. This analysis of male family members should be done always when candidate genes are lying on the x-chromosome and x-inactivation might assume a role. The reanalysis of the exome data demonstrated that the gene *MTMFT* was not covered very well. Therefore, only one frame-shift mutation was found and was consequently excluded during the filtering process. The sequencing of the entire gene detected a second heterozygote missense mutation in the area of the gene which was not well covered. Recently it was discovered that mutations in the *MTFMT* gene are responsible for impaired mitochondrial translation, leading to combined OXPHOS defects [232]. The phenotype of our patient was also quite similar to the described patient by Tucker et al. This is a good example that it is very essential to check the coverage of the known mitochondrial disease-causing genes in the exome data before concentrating on other genes. The average coverage with more than 40-fold which is necessary to detect mutations fluctuates between 85-95%. That means that you always have areas in which you might miss causative mutations. The other thing is to be careful with mutations on the x-chromosome, even when the x-inactivation could explain the pathogenicity of the one heterozygote mutation. The early analysis of male family members (not only the father) would have saved a lot of work and time to solve this case. During the last six years eight more patients with isolated or mostly combined respiratory chain complex defect with mutations in *MTFMT* were detected. This makes *MTFMT* also to a quite frequent disease-causing gene within the group of patients with mitochondrial disorders.

With the work done during this thesis it was possible to provide an assured molecular diagnosis for six patients via WES. The use of a cellular rescue assay together with continuative biochemical analysis is a powerful method to verify the pathogenicity of the found variants. All variants were found in new genes (*ACAD9*) or were new variants in known disease-causing genes (*NDUFB3*, *NDUFS8*, *BOLA3* and *MTFMT*). In some cases, the identification of the disease-causing gene could offer the pathophysiological basis for promising therapeutic interventions. Another example in which Exome Sequencing helped to find

the right therapy was the identification of the gene SLC52A2 in our group [135]. The gene *SLC52A2* causes the Brown-Vialetto-Van Laere syndrome which is characterized by an impaired riboflavin transport. The supplementation with high doses of riboflavin in our patient let to a moderate clinical improvement. Furthermore, the identification of the gene helps the clinicians to give a good genetic consultation to parents in case of their desire to have another child. In most cases the disease has an autosomal recessive mode of inheritance and the parents of the sick child are unaffected carrier of the heterocygote mutation. Pre-implantation diagnostic can help to minimize the risk to have another affected child. Beside the already mentioned advantages (therapy options and possibility to offer pre-implantation and prenatal diagnostic) of NGS another point would be time and money. The sequencing costs dropped tremendously during the last ten years. With the use of the latest sequencing machines more and more probes can be sequenced in parallel. The old-fashioned method to sequence in one patient one possible gene after each other seems to be a discontinued model. In a first study from Saunders et al. they report about a Whole-Genome analysis within 50hrs [136]. The invasive muscle biopsy with subsequent biochemical analysis of the OXPHOS system would be dispensable. Small blood samples would be sufficient. This is especially important in very young patients. The next advantage of the use of NGS in diagnostics for mitochondrial disorders is the fact, that you have the sequences from all genes. Every time a new mitochondrial disorder gene will be discovered it is possible to look into all unsolved cases for the new mutation. Up to date more than 320 genes are known to be involved in mitochondrial disorders. In total around 1100-1400 proteins are located to mitochondria. It is just a question of time when new studies about new genes will be published [252]. The advantages of NGS are unquestionable. But next to all the successful cases a lot of cases are still unsolved. In about 40-50% of the cases no causative mutation is found. The reason for this can be insufficient gene coverage, like in the patient with MTFMT mutation, and is therefore kicked out during filtering process. Other reasons could be too stringent filtering, mutations in non-coding regions or non-annotated exons, heterozygote mutations of whole exons or a non-autosomal recessive mode of inheritance [91]. In these cases, reanalysis of the data or in case of more than one good candidate gene, additional experimental evidence is required. The application of whole genome sequencing (WGS) could help to overcome these problems. In principal all genetic variants are detected, but often remain as variants of unknown significance (VUS) or they are missed due to the inability to prioritize them. Many of these VUS are synonymous or non-coding variants that may affect RNA abundance [253]. Therefore, another promising approach is transcriptome sequencing. Laura Kremer from our lab successfully used this approach for patients with suspected mitochondrial disease for which WES based variant prioritization did not yield a genetic diagnosis. In 10% (5 out of 48) a molecular diagnosis could be provided, including for the first time a disease-causing variant in the complex I assembly factor TIMMDC1 [253]. On the one hand it is good to minimize invasive handling by only blood sampling to get the right diagnosis. On the other hand information you get for example from the morphology or the activity of single respiratory complexes of the muscle can help to find the right gene. Moreover, the parallel setting up of a fibroblast or myoblast cell culture is essential for the verification of the pathogenicity of the found variant through for example lentiviral transduction. In general, NGS is a powerful tool to find the right diagnosis in patients

with mitochondrial disorders. It is unquestionable an advantage to know the causative gene, but the next step would be to provide a helpful therapy. The identification of the riboflavin transporter gene SLC52A2 is one example where the identification of the gene provided a basis for a successful therapy approach. Although in the majority of cases with mitochondrial disorders no causative therapy is available.

4.2 Therapy options for patients with complex I defect

In the second part of the thesis new therapy approaches were tested. The first and most intensive drug studied was bezafibrate. Ten years ago it was reported that the activation of the PPAR/PGC-1-alpha pathway could be a promising approach for patients with mitochondrial disorders [146, 153]. Furthermore Bonnefont et al showed in a clinical study that bezafibrate treatment increased the resting activity of ß-oxidation enzymes in patients with inherited ß-oxidation disorders leading to a significant improvement in the condition of the patients [254]. To verify this effect, to find out the mode of action and ideally predict the efficiency in humans, fibroblast cell lines from patients with mitochondrial disorders were collected. In the first initial experiment 35 patients with biochemically proven isolated complex I defect and clear molecular diagnosis was treated with bezafibrate for 72hrs. The first observation was that all four cell lines with mtDNA (ND1, ND6, tRNA) mutations showed only a small and not significant increase between 2,4-12,6% in complex I activity. This finding is in some extent contrary to other previous studies. (e.g. [147] and [156]). In the study from Wenz et al. they could show that bezafibrate treatment in cybrids homoplasmic for different mitochondrial tRNA mutations led to an increase in mitochondrial mass, tRNA steady state levels and enhanced mitochondrial protein synthesis. They concluded that these findings increase residual OXPHOS capacity. Following this theory our patient cell lines with mtDNA mutations should profit from more “still limited” mitochondria, but the overall increase in mitochondrial mass should consequently increase OXPHOS capacity. But in case of mtDNA mutations grade of heteroplasmy could also be crucial. It could be that in our patient cell lines the grade of heteroplasmy (more than 90%) is more important than the increase in mitochondrial mass itself. However, to confirm our finding a bigger group of patients with mtDNA mutations would have been necessary. Furthermore Dillon at al. showed that the bezafibrate treatment in the mtDNA mutator mouse improved among other things the skin and further aging-like phenotypes [156]. Beside the positive effect in skin and aging they did not see a generalized increase in mitochondrial markers and no improvement in muscle function or life span. The response of the other cell lines tested was promising in 24 out of 29 cases. The five cell lines with mutations in *NDUFA1*, *NDUFB3*, *NDUFB9*, *NUBPL* and *NDUFV3* did not respond to the treatment. The NDUFB3 and NDUFB9 cell lines had a very severe reduction of complex I activity. Due to the fact, that they did not respond it can be ascertained that a distinct rest activity might be necessary. In contrast to that cell lines with mutations in *NDUFS1* and *NDUFS8* benefit from the bezafibrate treatment with an increase in complex I activity ranging from 12 to 89%. Interestingly also the cell lines with the PDHA1 mutation

which we believe cause a secondary complex I defect benefit from the bezafibrate treatment. After bezafibrate treatment the mild reduction of complex I activity was restored in the fibroblasts. It is known that some patients with PDH defect respond to a ketogenic diet. With the increased supplementation of fatty acids, the body is able to use this second source of energy. The administration of bezafibrate could have the same effect by increasing the β-oxidation pathway. The biggest response was seen in our big group of missense and frame-shift mutations in the same gene, *ACAD9*. In this large group of 17 patients the complex I activity increased in all patients except one. The increase was significantly in 12 out of 17 cases with an increase between 20 and 141%. Five cell lines reached almost normal levels. Overall the oxygen consumption measurement showed that bezafibrate has the potential to be helpful in a certain group of patients with mitochondrial disorders. The exact mechanism, mode of action and the answer why some cell lines seem to respond more than the other remained unclear. In order to get more answers to these questions by looking on the transcriptional level gene expression experiments were performed. 14 different cell lines (control and complex I patients) were selected and treated for 72hrs with bezafibrate. The analysis of the data revealed 94 differentially regulated genes between patient and controls. Unfortunately, no clear down-or upregulation of a gene was found which could be used as a marker for mitochondrial disorders. Only the genes *CDA* and *UCK2* which were significantly down regulated in the patients compared to the control might be interesting to look at. CDA and UCK2 are involved in the pyrimidine metabolisms. UCK2 uses ATP or GTP to phosphorylate uridine and cytidine to uridine monophosphate and cytidine monophosphate. The patient cell lines used in the gene expression analysis had all a clear complex I defect assuming as a consequence also reduced levels of ATP. This could explain the reduced activity of CDA and UCK2 in this pathway. The differences in gene expression from untreated versus bezafibrate treated cell lines are more exciting. In total the expression of 97 genes was changed significantly. Eight upregulated genes were found, which are involved in the fatty acid metabolism confirming the known function of bezafibrate in the treatment of hypercholesterol. One of the mostly upregulated genes (p-value: 10^{-10}, fold-change: +2,05) was the gene *ACADVL* which is responsible for the catalysis of the first step of the mitochondrial fatty acid β-oxidation pathway. Another gene involved in the β-oxidation is the gene *ACAA2* which catalyses the last step of the mitochondrial fatty acid beta-oxidation spiral. Furthermore, the genes *CPT1a* and *CPT1b* which catalyse the transfer of the acyl group of long-chain fatty acid-CoA conjugate onto carnitine. This is another essential step for the mitochondrial uptake of long-chain fatty acids prior to the β-oxidation and plays a role in the triglyceride metabolism. Another interesting finding was the upregulation of *PDK4* (Pyruvate dehydrogenase kinase isozyme 4, mitochondrial). PDK4 inhibits the pyruvate dehydrogenase complex by phosphorylating one of its subunits and consequently downregulates the glycolysis. This is another hint that the energy metabolism is switched from glycolysis to fatty acid oxidation by the administration of bezafibrate. Further significantly upregulated genes were *ALDH1A3*, *ETFDH*, *ECH1*, *PDGDH* and *ARK1C2*, which are involved in the electron transport system, lipid peroxidation and amino acid biosynthesis. Moreover, no upregulation of genes coding for respiratory chain complex subunits was found. This is in contrast to previous publications from [146] and [153]. Bastin reported an upregulation of the mRNA level of the disease-causing genes *NDUFS3*, *NDUFV1*, *NDUFV2*,

BCS1, *SURF1* and *COX10* in patient and control cell lines. mRNA levels of NDUFS1 and NDUFS4 increased in the control but remained unchanged in the affected patient. Moreover he could show that PGC1-α, NRF1, NRF2α and Tfam were significantly increased after bezafibrate treatment assuming an overall effect on mitochondrial biogenesis [146]. The same theory was proposed by Tina Wenz in various publications. The gene expression experiments performed during this thesis could not confirm these findings. The transcription levels of Tfam remained unchanged. PGC1-α, NRF1 were not significantly changed overall cell lines. Nevertheless, some cell lines showed an augmentation of PGC1-α and NRF1 while others remained unchanged. If an overall increase in mitochondrial mass due to increased mitochondrial biogenesis is not responsible for the increase in complex I activity another mode of action must be answerable. The unquestionable increase in fatty acid metabolism is leading to an increase of acetyl-CoA which can be used in the citrate cycle to produce NADH and $FADH_2$. These compounds are further used by complex I and complex II. But the reason why some cell lines responded to the treatment and others do not is still not clear. Has it something to do with the assembly of the complexes? Or does bezafibrate has other effects which are unknown so far? To get answers to these questions mitoGELs were used to look on the assembly and amount of the respiratory chain complexes and DIGE experiments were used to search for further changes on the proteome level. The analysis of these mitoGELs showed that the treatment with bezafibrate led to an increase of assembled supercomplexes in nine out of ten complex I deficient cell lines. Most other complexes were within the normal range and remained unchanged. The only cell line which did not respond to the treatment was the cell lines with a homozygote NDUFB9 mutation leading to a complete loss of assembled supercomplexes. This finding suggests that a certain amount of assembled complex I seems to be necessary to profit from the treatment. The cell lines with mutations *NDUFA1*, *NDUFS1* and *NDUFS2* showed a big increase in the amount of supercomplexes (+100, +80 and +16%) which was consistent to the OCR measurement. The two cell lines with the mtDNA mutations (*ND1* and *ND6*), which seemed to be unresponsive to the bezafibrate treatment in the OCR measurement, showed now in the mitoGEL analysis an increase in supercomplexes by 30-40%. The reason for these different results is not clear. It can be speculated, that the supercomplex assembly is increased, but the mutation in the complex I core subunits still prevent a proper functioning complex I. The biggest response to the treatment was again seen by the cell lines with the mutation in the *ACAD9* gene. In the cell line 35834 the bezafibrate treatment led to a significant increase of assembled supercomplexes from 60% to normal levels. The analysis of the four more cell lines with ACAD9 mutation (FibroID 62006, 62347, 68541 and 69842) showed an increase of assembled supercomplexes in two of them. This observation was also consistent with the OCR measurement. The cell lines with mutations in 68541 (p.Leu98Ser) and 68942 (p.Arg518His), which had already an almost normal assembled supercomplex, showed no improvement whereas the cell lines 62006 (splice mutation, p.Arg433Gln), 62347 (p.Glu413Lys, p.Arg518Cys) presented an increase in assembled supercomplexes. The supercomplexes were undetectable in cell line 62347 before the treatment and increased after bezafibrate treatment up to 30% of the normal level. This was the next hint that bezafibrate has a positive influence on the stability of the supercomplexes in some cell lines. The next point which was addressed was the overall influence of the bezafibrate treatment on

the proteasome. Therefore, four different cell lines with ACAD9 mutation and the highest increase in complex I activity after bezafibrate treatment (FibroID 35834, 52674, 52933 and 52935) and one control cell line were used to perform DIGE experiments. More than 200 protein spots were detected to be significantly different between patient and control and/or untreated versus bezafibrate treated samples. 58 proteins were identified to be downregulated in the patient, whereas 13 proteins were upregulated compared to the control. The amount of the proteins AIFM1, IMMT, LRPPRC, NDUAA (NDUFA10), PDPR, PHGDH and SDHA were 1,2 to 3,6-fold lower than in the control. All proteins have an important role in mitochondria and a reduced amount of these proteins might lead to impaired mitochondrial function. Mutations in *NDUFA10* cause a complex I-defect with Leigh disease [87]. Unfortunately, no reduction in the ACAD9 protein was found in the DIGE experiment. The clear reduction in the amount of ACAD9 protein was later shown in Western Blot experiments. The comparison between the proteasome of controls and ACAD9 patients could show that mutations in the gene *ACAD9* have a big influence on a numerous number of mitochondrial proteins. It seems that different pathways are influenced. That can be also seen on the proteins which are upregulated between the patients and the control. ALDOA, ENO2 and MDHM for example were 1,6-2,8-fold higher expressed in the patient than in the control. Far more interesting was the analysis of the differences in the mitochondrial proteasome with and without bezafibrate treatment. 12 proteins were identified which were significantly downregulated and 55 proteins upregulated between untreated and treated. One of the hot-spots of the upregulated proteins was again ACADVL with an significant increase of 1,6-fold. Comparable to the gene expression experiment, the most increased proteins are involved in the fatty acid metabolism (ACAA2, ALDH1L2, CAT, ECH1, HADHA, HADHB). Some proteins are involved in the electron transport (ETFA, ETFDH) [255] and some proteins are known to have a functions in the energy metabolism or interact with respiratory chain complexes (IDH2, LONP1, OPA1, AIFM1, TIMM24, ALDH1L2, CHCHD3) [169, 231, 256-258]. Consistent to the gene expression experiment no upregulation of Tfam, PGC1-α or NRF1 protein was found. To really exclude an overall increase in mitochondrial mass whole cell lysates from fibroblasts of seven selected ACAD9 patients and one control were examined on Western Blot experiments. Neither the amount of the complex II subunit SDHA nor the complex I subunits NDUFS1 and NDUFA9 was increased after the treatment. This experiment could confirm the clear increase the amount of ACADVL protein after bezafibrate treatment in all patient cell lines ranging from 22 to 209% compared to the untreated whereas another acetyl-coA hydrogenase family member ACADM was unchanged. The first time an increase of ACAD9 protein itself was observed. In 6/7 cases the amount of ACAD9 protein was increased between 18-83%. The only cell line observed which did not respond to the treatment was from a patient with a homozygous mutation causing a change from Arginine to Histidine at position 518. In fibroblasts this specific mutation did not reduce the amount of ACAD9 protein and but the supercomplex assembly was disturbed. This may lead to the assumption that this mutation averts a proper function of the ACAD9 protein and therefore causes a respiratory chain deficiency and especially complex I.

In summary the in vitro experiments could show that bezafibrate treatment has the potential to be helpful in various patients with mitochondrial disorders. The increased β-oxidation pathway provokes an

alternative source of energy and might be especially helpful for patients who respond to a ketogenic diet. All three cell lines from patients with PDHA1 mutation responded positive and underlines the hopefully effective therapy in this group of patients. The bezafibrate treatment in all other patients with complex I defect and different nuclear and mitochondrial DNA mutations (exempt *ACAD9*) led to an increase in about 50% of the cases. The result depends on the kind of mutation, complex I rest activity and needs further analysis. The most promising results have been seen in the big group of patients with ACAD9 mutation. In 76% of all cases the bezafibrate lead to an increase in OCR. The amount of ACAD9 and ACADVL protein levels were significantly upregulated and explain the positive effect on the stability of the supercomplexes. But an overall increase in mitochondrial biogenesis activity (upregulation of Tfam, NRF1 or PGC-1-α) and a consequently increase in mitochondrial mass was not observed. This finding is contrary to previous studies [146]. These first positive results in vitro encourage the initiation of a clinical trial in patients with complex I deficiency and mutations in *ACAD9*. The first and so far only known clinical trial with patients with mitochondrial disorder and administration of bezafibrate started in 2015. Six adults with myopathy and confirmed mt.3243A>G mutation were enrolled. The first results showed that bezafibrate was well tolerated with no episodes of rhabdomyolysis but final efficacy results are awaited [259, 260]. Given the estimated high frequency of 59 new ACAD9 patients born every year in Europe, and 689 worldwide this specific subgroup seems to be especially suitable for initiation of a clinical trial.

The results from the riboflavin treatment in vitro were also promising in the big group of ACAD9 patients. 60% of the treated fibroblasts cell lines responded with a significant increase of OCR. In contrast to the bezafibrate treatment no increase of ACAD9 protein itself was observed. The positive effect could be rather explained by an increase of the activity or stability of the remaining ACAD9 protein. One family with three patients with homozygous p.Arg532Trp mutation were already described as riboflavin-responsive complex I defect before the discovery of the cause of the defect ACAD9 [165, 167]. The positive effect was confirmed in one cell line of this family and another one with the same homozygous mutation. Two cell lines with the mutation heterozygous and an additional heterozygote mutation responded as well. One cell line with the mutation p.Arg518His, which did not respond to the bezafibrate treatment, showed an increase of OCR and supercomplex assembly (+76%) after riboflavin treatment. Overall the riboflavin treatment led to the improvement of complex I activity in nine out of 15 patient cell lines. This beneficial effect was also reported in 68% of the treated patients and mirrored in the survival rate. Patient with an onset of disease <1 year of age have a significantly higher survival rate when treated with oral riboflavin in contrast to untreated patients. One limitation of this observation could be that most of the deaths in this patient subgroup occurred at the end of the first year of life. This might indicate that our observation is susceptible to survivor treatment selection bias. These promising results suggest further studies and needs to be verified in a bigger cohort of cell lines and more functional studies concerning the mode of action might be also useful. However, a riboflavin and/or bezafibrate administration could be considered for phenotypically-consistent patients whilst their genetic investigations are underway. It is furthermore important to initiate next generation sequencing techniques promptly, accompanied by studies in affected tissue (if available).

For these patients, early molecular diagnosis and start of the correct therapy could be the difference between life and death.

4.3. Outlook

The implementation of NGS into the diagnostic of patients with suspected mitochondrial disorders revolutionized the field and led to the identification of numerous new disease-causing genes. The rapid development of new technologies and sequencing approaches reduced the costs and the time for the analysis of one whole exome or genome tremendously. Today it is already possible to analyse one whole genome within 50 hrs [136, 261]. The majority of genetic laboratories offer now exome or even genome sequencing as routine diagnostic. The sample preparation, the sequencing and generation of the data seems to be no challenge anymore. The analysis of this big amount of data and the extraction of biological and clinical meaningful information are still the greatest challenge. Good bioinformatic tools are mandatory. Nevertheless whole-exome sequencing or target-exome sequencing could only solve between 20-50% of the cases depending on the selection criteria [91, 119]. The reasons for unsolved cases are multilayered: a poor coverage of exons, structural variants (translocations and inversions) that move or flip DNA, not captured copy number, intronic or promotor variants, ethnical differences, unknown gene-gene interactions or even epigenetic changes and environmental factors can influence gene expression and will not be seen with whole-exome sequencing. Whole Genome Sequencing could help to detect intronic and promoter variants. Transcriptome Sequencing could help to discover new disease causes due to differences in gene expression levels. The analysis and comparison of whole-exome, transcriptome and even metabolome data from one patient can be also very helpful to find the right gene. Nevertheless, functional assays are very important to confirm the pathogenicity of the variant assumed to be responsible for the disease. One possible method will be still the transduction of primary fibroblasts from patients with the wild-type form of the mutated gene with the help of a lenti-viral system [196]. More recently Marcus et al. could show, that a cell- and organelle-directed protein/enzyme replacement therapy with the transactivator of transcription (TAT) peptide as the moiety delivery system, restored the complex I activity in patient cell lines with defects in complex I assembly factor *C6orf66* (*NDUFAF4*) [262]. This could be also a quite easy and fast method. Numerous mouse models with different mitochondrial disorders were created in order to verify the mutation, perform functional analysis or test different treatment options. The production of targeted-mutants is mostly a laborious and long-term procedure and could not be used to screen the various new mutations discovered by NGS.

Although the awareness for mitochondrial disorders increased during the last years it is still a rare disorder. Since more than ten years the BMBF founded project mitoNET establishes a network for mitochondrial disorders. Clinicians from various places in Germany and Austria record their patients in the mitoREGISTER (phenotype, diseases course, medication or laboratory information) and collect

biosamples. Currently around 2500 patients (adults and children with different mitochondrial disorders) are registered and more than 3000 biosamples were collected. With the increase of entries, it will help the clinicians to compare their patients with other patients with a similar phenotype, predict the clinical course or find the right medication. Most patients with unclear genetics, which were selected for Exome Sequencing, are included into the mitoNET. The biosample collection is a valuable source for the verification of the candidate genes. Moreover, transcriptome and metabolome analysis will be more and more important in the future. The mitoREGISTER will be also an essential source for the selection of patients for possible clinical trials. Even though the results of the in vitro studies of bezafibrate treatment in different patients with complex I defect are very promising, it cannot be transferred completely to humans. Bezafibrate is used for a long time in the treatment of hyperlipidaemia without severe side effects. The positive response of bezafibrate treatment of a small group of patients in the framework of individual curative trials will be evaluated in a bigger clinical trial with children from different centres in Austria and Germany starting in the end of 2013. The collection of biosamples (blood, serum, or even muscle or fibroblasts) at the beginning, in the course and at the end of the clinical trial could be a valuable source to follow the possible effect of the treatment.

NGS discovered a multiplicity of new genes responsible for mitochondrial disorders. Beside the complex I subunits and assembly factors more genes are discovered which have to do with the mtDNA transcription and translation, mtDNA maintenance, fission and fusion, protein import and mitochondrial co-factors resulting. Every new gene which will be identified to cause a mitochondrial disorder has the potential to result in new therapy possibilities. The heterogeneity of possible disease-causing genes requests a deep understanding of its function. Cell culture from affected individuals or mouse models will still be used to study the phenotype and find potential new therapy options. The establishment of the relatively new and cheap methods TALEN and CRISPR/Cas9 led to the generation of numerous mitochondrial disease models (e.g. NDUFS4 k.o. mice [263], SURF k.o. pig [264]). One side project during my PhD Thesis was also to generate an ACAD9 mouse model. Homozygous knock out mouse was found to be embryonically lethal (Schiff, Vockley, personal communication). Therefor CRISPR/Cas9 was used to model five different ACAD9 point mutations, leading to a variety of clinical phenotypes (absence or presence of cardiomyopathy, encephalopathy) and biochemical markers (complex I activity, amount of ACAD9 protein, FAO capacity, response to riboflavin and bezafibrate treatment). The idea was to study the pathogenesis of the disease and verify the positive effect of bezafibrate and riboflavin treatment seen in fibroblasts and test new treatment options. Unfortunately, it was not possible to get offspring with the desired mutation and establish a mouse line. It seems that the establishment of a mouse line, representing the right phenotype is still challenging, but definitely worth it and might be a project for a new PhD Thesis. The mouse models might be a good tool to test different substances, which might improve the phenotype and could be later used in a clinical trial. Nevertheless, most therapies are still focusing on the improvement of the symptoms and are not able to be curative. The idea of gene-therapy is not new and already used in the treatment of several genetic disorders like retinal disease Leber's congenital amaurosis [265], adrenoleukodystrophy [266], metachromatic leukodystrophy [267] or Parkinson's disease [268]. Some

studies could report positive results whereas others had to stop the treatment due to severe side-effects like leukemia. All clinical trials started during the last 10 years and long-term follow-ups are completely missing. In the field of mitochondrial disorders, no clinical trials on humans but a lot of mouse models are currently under investigation. The group of Chadderton et al. [269] could recently show that the intravitreal delivery of adeno-associated virus (AAV)-NDI1 into the contralateral eyes of in a mouse model of LHON disease preserves retinal function. The phenotype of another mouse model with a nuclear defect in *NDUFS4* leading to Leigh Syndrome could be also improved by the AAV2 stereotactic injection into the mediolateral vestibular nucleus [270, 271]. Another promising approach, which was already successfully used in humans, is mitochondrial replacement therapy. The first and so far only country in the world, which officially allows this technique, is the UK, but the first so-called three-parents-baby was born 2016 in Mexico and it is quite clear that many more will follow. Many other countries, like Germany and the USA, have forbidden this technique. Another possibility for families with nuclear mutation leading to mitochondrial disorder will be PIGD. This method is especially useful in families having already one or more affected children and known genetic background. After *in vitro* fertilisation only healthy embryos would be transferred. PIGD could be also used for families carrying heteroplasmic mtDNA mutations, but the grade of heteroplasmy can range between 0% and 100% in any cell or tissue. That makes it very difficult to estimate the risk of recurrence in future children. In most heteroplasmic disorders the patients have only symptoms after exceeding a certain mutation load (proportion of mutated mtDNA). Good guidelines will be needed to detect the right mutation level which may be acceptable to minimize the risk of having a sick child [272, 273]. Just recently the world was “shocked” or maybe also fascinated by the announcement of the world’s first genetically-edited babies using the gene-editing technique CRISPR to make them resistant to HIV [274]. The use of the powerful gene-editing tool CRISPR was widely thought to not yet be ready for use in human embryos for safety reasons. The technology is still experimental and DNA changes can pass to future generations, potentially with unforeseen side-effects [275]. But one thing is certain: it is possible. It’s no longer a question of whether genetically-engineered children can be bred, but with what risk - and when a CRISPR intervention in the human genome could be justified. Is it justified to use the technique that future children may be resistant to some strains of HIV or to help parents whose only wish is to have healthy children or to cure their sick child?

All together NGS will be in the near future or is already state of the art in diagnostics and can be renamed to Now-Generation Sequencing. The technology improvement during the last ten years was responsible for the identification of more than 320 new genes in the area of mitochondrial disorders. In this work, NGS was successfully used to identify known and new disease-causing variants in six patients. Within the cohort of patients with mutations in *ACAD9*, the supplementation with riboflavin revealed a beneficial effect in vitro as well as in vivo and is mirrored in a prolonged survival of the patients. An early application of NGS, coupled with cellular studies, resulting in a confirmed diagnosis, could ideally lead to a therapeutic intervention and prolonged lifetime.

5. References

1. Ernster, L. and G. Schatz, *Mitochondria: a historical review.* J Cell Biol, 1981. **91**(3 Pt 2): p. 227s-255s.
2. Hogeboom, G.H., A. Claude, and R.D. Hotch-Kiss, *The distribution of cytochrome oxidase and succinoxidase in the cytoplasm of the mammalian liver cell.* J Biol Chem, 1946. **165**(2): p. 615-29.
3. Robin, E.D. and R. Wong, *Mitochondrial DNA molecules and virtual number of mitochondria per cell in mammalian cells.* J Cell Physiol, 1988. **136**(3): p. 507-13.
4. Dyall, S.D., et al., *Non-mitochondrial complex I proteins in a hydrogenosomal oxidoreductase complex.* Nature, 2004. **431**(7012): p. 1103-7.
5. Wallace, D.C., *Mitochondrial DNA sequence variation in human evolution and disease.* Proc Natl Acad Sci U S A, 1994. **91**(19): p. 8739-46.
6. Gray, M.W., G. Burger, and B.F. Lang, *Mitochondrial evolution.* Science, 1999. **283**(5407): p. 1476-81.
7. Neupert, W., *Protein import into mitochondria.* Annu Rev Biochem, 1997. **66**: p. 863-917.
8. Frey, T.G. and C.A. Mannella, *The internal structure of mitochondria.* Trends Biochem Sci, 2000. **25**(7): p. 319-24.
9. Benard, G. and R. Rossignol, *Ultrastructure of the mitochondrion and its bearing on function and bioenergetics.* Antioxid Redox Signal, 2008. **10**(8): p. 1313-42.
10. Anderson, S., et al., *Sequence and organization of the human mitochondrial genome.* Nature, 1981. **290**(5806): p. 457-65.
11. Vafai, S.B. and V.K. Mootha, *Mitochondrial disorders as windows into an ancient organelle.* Nature, 2012. **491**(7424): p. 374-83.
12. Wallace, D.C., *Mitochondrial diseases in man and mouse.* Science, 1999. **283**(5407): p. 1482-8.
13. Bereiter-Hahn, J. and M. Voth, *Dynamics of mitochondria in living cells: shape changes, dislocations, fusion, and fission of mitochondria.* Microsc Res Tech, 1994. **27**(3): p. 198-219.
14. Chan, D.C., *Dissecting mitochondrial fusion.* Dev Cell, 2006. **11**(5): p. 592-4.
15. Neupert, W. and J.M. Herrmann, *Translocation of proteins into mitochondria.* Annu Rev Biochem, 2007. **76**: p. 723-49.
16. Lill, R., et al., *The role of mitochondria in cellular iron-sulfur protein biogenesis and iron metabolism.* Biochim Biophys Acta, 2012. **1823**(9): p. 1491-508.
17. Kozlov, A.V., K. Staniek, and H. Nohl, *Nitrite reductase activity is a novel function of mammalian mitochondria.* FEBS Lett, 1999. **454**(1-2): p. 127-30.
18. Koopman, W.J., et al., *OXPHOS mutations and neurodegeneration.* EMBO J, 2012.
19. Mimaki, M., et al., *Understanding mitochondrial complex I assembly in health and disease.* Biochim Biophys Acta, 2012. **1817**(6): p. 851-62.
20. Stroud, D.A., et al., *Accessory subunits are integral for assembly and function of human mitochondrial complex I.* Nature, 2016. **538**(7623): p. 123-126.
21. Pagniez-Mammeri, H., et al., *Mitochondrial complex I deficiency of nuclear origin I. Structural genes.* Mol Genet Metab, 2012. **105**(2): p. 163-72.
22. Formosa, L.E., et al., *Building a complex complex: Assembly of mitochondrial respiratory chain complex I.* Semin Cell Dev Biol, 2018. **76**: p. 154-162.
23. Fiedorczuk, K. and L.A. Sazanov, *Mammalian Mitochondrial Complex I Structure and Disease-Causing Mutations.* Trends Cell Biol, 2018. **28**(10): p. 835-867.
24. Ghezzi, D. and M. Zeviani, *Human diseases associated with defects in assembly of OXPHOS complexes.* Essays Biochem, 2018. **62**(3): p. 271-286.
25. Guerrero-Castillo, S., et al., *The Assembly Pathway of Mitochondrial Respiratory Chain Complex I.* Cell Metab, 2017. **25**(1): p. 128-139.
26. Sanchez-Caballero, L., S. Guerrero-Castillo, and L. Nijtmans, *Unraveling the complexity of mitochondrial complex I assembly: A dynamic process.* Biochim Biophys Acta, 2016.

27. Efremov, R.G., R. Baradaran, and L.A. Sazanov, *The architecture of respiratory complex I.* Nature, 2010. **465**(7297): p. 441-5.
28. Hunte, C., V. Zickermann, and U. Brandt, *Functional modules and structural basis of conformational coupling in mitochondrial complex I.* Science, 2010. **329**(5990): p. 448-51.
29. Janssen, R.J., et al., *Mitochondrial complex I: structure, function and pathology.* J Inherit Metab Dis, 2006. **29**(4): p. 499-515.
30. Lazarou, M., et al., *Assembly of mitochondrial complex I and defects in disease.* Biochim Biophys Acta, 2009. **1793**(1): p. 78-88.
31. Signes, A. and E. Fernandez-Vizarra, *Assembly of mammalian oxidative phosphorylation complexes I-V and supercomplexes.* Essays Biochem, 2018. **62**(3): p. 255-270.
32. Andrews, B., et al., *Assembly factors for the membrane arm of human complex I.* Proc Natl Acad Sci U S A, 2013.
33. Baertling, F., et al., *NDUFA9 point mutations cause a variable mitochondrial complex I assembly defect.* Clin Genet, 2018. **93**(1): p. 111-118.
34. Sheftel, A.D., et al., *Human ind1, an iron-sulfur cluster assembly factor for respiratory complex I.* Mol Cell Biol, 2009. **29**(22): p. 6059-73.
35. Guarani, V., et al., *TIMMDC1/C3orf1 functions as a membrane-embedded mitochondrial Complex I assembly factor through association with the MCIA complex.* Mol Cell Biol, 2013.
36. Heide, H., et al., *Complexome Profiling Identifies TMEM126B as a Component of the Mitochondrial Complex I Assembly Complex.* Cell Metab, 2012.
37. Cizkova, A., et al., *TMEM70 mutations cause isolated ATP synthase deficiency and neonatal mitochondrial encephalocardiomyopathy.* Nat Genet, 2008. **40**(11): p. 1288-90.
38. Kahlhofer, F., et al., *Accessory subunit NUYM (NDUFS4) is required for stability of the electron input module and activity of mitochondrial complex I.* Biochim Biophys Acta Bioenerg, 2017. **1858**(2): p. 175-181.
39. Luft, R., et al., *A case of severe hypermetabolism of nonthyroid origin with a defect in the maintenance of mitochondrial respiratory control: a correlated clinical, biochemical, and morphological study.* J Clin Invest, 1962. **41**: p. 1776-804.
40. Lowell, B.B. and G.I. Shulman, *Mitochondrial dysfunction and type 2 diabetes.* Science, 2005. **307**(5708): p. 384-7.
41. Modica-Napolitano, J.S., M. Kulawiec, and K.K. Singh, *Mitochondria and human cancer.* Curr Mol Med, 2007. **7**(1): p. 121-31.
42. Yu, M., *Somatic mitochondrial DNA mutations in human cancers.* Adv Clin Chem, 2012. **57**: p. 99-138.
43. Schlame, M., et al., *Deficiency of tetralinoleoyl-cardiolipin in Barth syndrome.* Ann Neurol, 2002. **51**(5): p. 634-7.
44. Patel, K.P., et al., *The spectrum of pyruvate dehydrogenase complex deficiency: clinical, biochemical and genetic features in 371 patients.* Mol Genet Metab, 2012. **106**(3): p. 385-94.
45. Gorman, G.S., et al., *Prevalence of nuclear and mitochondrial DNA mutations related to adult mitochondrial disease.* Ann Neurol, 2015. **77**(5): p. 753-9.
46. Skladal, D., J. Halliday, and D.R. Thorburn, *Minimum birth prevalence of mitochondrial respiratory chain disorders in children.* Brain, 2003. **126**(Pt 8): p. 1905-12.
47. Johns, D.R., *Seminars in medicine of the Beth Israel Hospital, Boston. Mitochondrial DNA and disease.* N Engl J Med, 1995. **333**(10): p. 638-44.
48. Di Donato, S., *Multisystem manifestations of mitochondrial disorders.* J Neurol, 2009. **256**(5): p. 693-710.
49. DiMauro, S. and E.A. Schon, *Mitochondrial respiratory-chain diseases.* N Engl J Med, 2003. **348**(26): p. 2656-68.
50. DiMauro, S., *Mitochondrial diseases.* Biochim Biophys Acta, 2004. **1658**(1-2): p. 80-8.
51. Schapira, A.H., *Mitochondrial disease.* Lancet, 2006. **368**(9529): p. 70-82.
52. Folbergrova, J. and W.S. Kunz, *Mitochondrial dysfunction in epilepsy.* Mitochondrion, 2012. **12**(1): p. 35-40.
53. Canafoglia, L., et al., *Epileptic phenotypes associated with mitochondrial disorders.* Neurology, 2001. **56**(10): p. 1340-6.
54. Taivassalo, T., et al., *The spectrum of exercise tolerance in mitochondrial myopathies: a study of 40 patients.* Brain, 2003. **126**(Pt 2): p. 413-23.

55. Calvo, S.E. and V.K. Mootha, *The mitochondrial proteome and human disease.* Annu Rev Genomics Hum Genet, 2010. **11**: p. 25-44.
56. Alberio, T., et al., *Toward the Standardization of Mitochondrial Proteomics: The Italian Mitochondrial Human Proteome Project Initiative.* J Proteome Res, 2017. **16**(12): p. 4319-4329.
57. Elstner, M., et al., *The mitochondrial proteome database: MitoP2.* Methods Enzymol, 2009. **457**: p. 3-20.
58. Craigen, W.J., *Mitochondrial DNA mutations: an overview of clinical and molecular aspects.* Methods Mol Biol, 2012. **837**: p. 3-15.
59. Chinnery, P.F., et al., *Epigenetics, epidemiology and mitochondrial DNA diseases.* Int J Epidemiol, 2012. **41**(1): p. 177-87.
60. Graham, B.H., *Diagnostic challenges of mitochondrial disorders: complexities of two genomes.* Methods Mol Biol, 2012. **837**: p. 35-46.
61. Kirby, D.M., et al., *Respiratory chain complex I deficiency: an underdiagnosed energy generation disorder.* Neurology, 1999. **52**(6): p. 1255-64.
62. Finsterer, J., et al., *EFNS guidelines on the molecular diagnosis of mitochondrial disorders.* Eur J Neurol, 2009. **16**(12): p. 1255-64.
63. Fassone, E. and S. Rahman, *Complex I deficiency: clinical features, biochemistry and molecular genetics.* J Med Genet, 2012. **49**(9): p. 578-90.
64. Koene, S., et al., *Natural disease course and genotype-phenotype correlations in Complex I deficiency caused by nuclear gene defects: what we learned from 130 cases.* J Inherit Metab Dis, 2012. **35**(5): p. 737-47.
65. Distelmaier, F., et al., *Mitochondrial complex I deficiency: from organelle dysfunction to clinical disease.* Brain, 2009. **132**(Pt 4): p. 833-42.
66. Ng, Y.S. and D.M. Turnbull, *Mitochondrial disease: genetics and management.* J Neurol, 2016. **263**(1): p. 179-91.
67. Valsecchi, F., et al., *Complex I disorders: causes, mechanisms, and development of treatment strategies at the cellular level.* Dev Disabil Res Rev, 2010. **16**(2): p. 175-82.
68. Nouws, J., et al., *Assembly factors as a new class of disease genes for mitochondrial complex I deficiency: cause, pathology and treatment options.* Brain, 2012. **135**(Pt 1): p. 12-22.
69. Leigh, D., *Subacute necrotizing encephalomyelopathy in an infant.* J Neurol Neurosurg Psychiatry, 1951. **14**(3): p. 216-21.
70. Finsterer, J., *Leigh and Leigh-like syndrome in children and adults.* Pediatr Neurol, 2008. **39**(4): p. 223-35.
71. Loeffen, J., et al., *The first nuclear-encoded complex I mutation in a patient with Leigh syndrome.* Am J Hum Genet, 1998. **63**(6): p. 1598-608.
72. Ostergaard, E., et al., *Mitochondrial encephalomyopathy with elevated methylmalonic acid is caused by SUCLA2 mutations.* Brain, 2007. **130**(Pt 3): p. 853-61.
73. Benit, P., et al., *Mutant NDUFS3 subunit of mitochondrial complex I causes Leigh syndrome.* J Med Genet, 2004. **41**(1): p. 14-7.
74. Huoponen, K., et al., *A new mtDNA mutation associated with Leber hereditary optic neuroretinopathy.* Am J Hum Genet, 1991. **48**(6): p. 1147-53.
75. Valentino, M.L., et al., *The ND1 gene of complex I is a mutational hot spot for Leber's hereditary optic neuropathy.* Ann Neurol, 2004. **56**(5): p. 631-41.
76. Ugalde, C., et al., *Mutated ND2 impairs mitochondrial complex I assembly and leads to Leigh syndrome.* Mol Genet Metab, 2007. **90**(1): p. 10-4.
77. Taylor, R.W., et al., *Progressive mitochondrial disease resulting from a novel missense mutation in the mitochondrial DNA ND3 gene.* Ann Neurol, 2001. **50**(1): p. 104-7.
78. McFarland, R., et al., *De novo mutations in the mitochondrial ND3 gene as a cause of infantile mitochondrial encephalopathy and complex I deficiency.* Ann Neurol, 2004. **55**(1): p. 58-64.
79. Komaki, H., et al., *A novel mtDNA C11777A mutation in Leigh syndrome.* Mitochondrion, 2003. **2**(4): p. 293-304.
80. Brown, M.D., et al., *The role of mtDNA background in disease expression: a new primary LHON mutation associated with Western Eurasian haplogroup J.* Hum Genet, 2002. **110**(2): p. 130-8.
81. Taylor, R.W., et al., *Leigh disease associated with a novel mitochondrial DNA ND5 mutation.* Eur J Hum Genet, 2002. **10**(2): p. 141-4.

82. Johns, D.R., M.J. Neufeld, and R.D. Park, *An ND-6 mitochondrial DNA mutation associated with Leber hereditary optic neuropathy.* Biochem Biophys Res Commun, 1992. **187**(3): p. 1551-7.
83. Fernandez-Moreira, D., et al., *X-linked NDUFA1 gene mutations associated with mitochondrial encephalomyopathy.* Ann Neurol, 2007. **61**(1): p. 73-83.
84. Hoefs, S.J., et al., *NDUFA2 complex I mutation leads to Leigh disease.* Am J Hum Genet, 2008. **82**(6): p. 1306-15.
85. Alston, C.L., et al., *Bi-allelic Mutations in NDUFA6 Establish Its Role in Early-Onset Isolated Mitochondrial Complex I Deficiency.* Am J Hum Genet, 2018. **103**(4): p. 592-601.
86. van den Bosch, B.J., et al., *Defective NDUFA9 as a novel cause of neonatally fatal complex I disease.* J Med Genet, 2012. **49**(1): p. 10-5.
87. Hoefs, S.J., et al., *NDUFA10 mutations cause complex I deficiency in a patient with Leigh disease.* Eur J Hum Genet, 2011. **19**(3): p. 270-4.
88. Berger, I., et al., *Mitochondrial complex I deficiency caused by a deleterious NDUFA11 mutation.* Ann Neurol, 2008. **63**(3): p. 405-8.
89. Ostergaard, E., et al., *Respiratory chain complex I deficiency due to NDUFA12 mutations as a new cause of Leigh syndrome.* J Med Genet, 2011. **48**(11): p. 737-40.
90. Angebault, C., et al., *Mutation in NDUFA13/GRIM19 leads to early onset hypotonia, dyskinesia and sensorial deficiencies, and mitochondrial complex I instability.* Hum Mol Genet, 2015. **24**(14): p. 3948-55.
91. Haack, T.B., et al., *Molecular diagnosis in mitochondrial complex I deficiency using exome sequencing.* J Med Genet, 2012. **49**(4): p. 277-83.
92. Pronicka, E., et al., *New perspective in diagnostics of mitochondrial disorders: two years' experience with whole-exome sequencing at a national paediatric centre.* J Transl Med, 2016. **14**(1): p. 174.
93. Haack, T.B., et al., *Mutation screening of 75 candidate genes in 152 complex I deficiency cases identifies pathogenic variants in 16 genes including NDUFB9.* J Med Genet, 2012. **49**(2): p. 83-9.
94. Friederich, M.W., et al., *Mutations in the accessory subunit NDUFB10 result in isolated complex I deficiency and illustrate the critical role of intermembrane space import for complex I holoenzyme assembly.* Hum Mol Genet, 2017. **26**(4): p. 702-716.
95. Reinson, K., et al., *Diverse phenotype in patients with complex I deficiency due to mutations in NDUFB11.* Eur J Med Genet, 2018.
96. Benit, P., et al., *Large-scale deletion and point mutations of the nuclear NDUFV1 and NDUFS1 genes in mitochondrial complex I deficiency.* Am J Hum Genet, 2001. **68**(6): p. 1344-52.
97. Loeffen, J., et al., *Mutations in the complex I NDUFS2 gene of patients with cardiomyopathy and encephalomyopathy.* Ann Neurol, 2001. **49**(2): p. 195-201.
98. Petruzzella, V., et al., *A nonsense mutation in the NDUFS4 gene encoding the 18 kDa (AQDQ) subunit of complex I abolishes assembly and activity of the complex in a patient with Leigh-like syndrome.* Hum Mol Genet, 2001. **10**(5): p. 529-35.
99. Kirby, D.M., et al., *NDUFS6 mutations are a novel cause of lethal neonatal mitochondrial complex I deficiency.* J Clin Invest, 2004. **114**(6): p. 837-45.
100. Triepels, R.H., et al., *Leigh syndrome associated with a mutation in the NDUFS7 (PSST) nuclear encoded subunit of complex I.* Ann Neurol, 1999. **45**(6): p. 787-90.
101. Procaccio, V. and D.C. Wallace, *Late-onset Leigh syndrome in a patient with mitochondrial complex I NDUFS8 mutations.* Neurology, 2004. **62**(10): p. 1899-901.
102. Benit, P., et al., *Mutant NDUFV2 subunit of mitochondrial complex I causes early onset hypertrophic cardiomyopathy and encephalopathy.* Hum Mutat, 2003. **21**(6): p. 582-6.
103. McKenzie, M. and M.T. Ryan, *Assembly factors of human mitochondrial complex I and their defects in disease.* IUBMB Life, 2010. **62**(7): p. 497-502.
104. Dunning, C.J., et al., *Human CIA30 is involved in the early assembly of mitochondrial complex I and mutations in its gene cause disease.* EMBO J, 2007. **26**(13): p. 3227-37.
105. Fassone, E., et al., *Mutations in the mitochondrial complex I assembly factor NDUFAF1 cause fatal infantile hypertrophic cardiomyopathy.* J Med Genet, 2011. **48**(10): p. 691-7.
106. Hoefs, S.J., et al., *Baculovirus complementation restores a novel NDUFAF2 mutation causing complex I deficiency.* Hum Mutat, 2009. **30**(7): p. E728-36.

107. Saada, A., et al., *Mutations in NDUFAF3 (C3ORF60), encoding an NDUFAF4 (C6ORF66)-interacting complex I assembly protein, cause fatal neonatal mitochondrial disease.* Am J Hum Genet, 2009. **84**(6): p. 718-27.
108. Saada, A., et al., *C6ORF66 is an assembly factor of mitochondrial complex I.* Am J Hum Genet, 2008. **82**(1): p. 32-8.
109. Sugiana, C., et al., *Mutation of C20orf7 disrupts complex I assembly and causes lethal neonatal mitochondrial disease.* Am J Hum Genet, 2008. **83**(4): p. 468-78.
110. Pagliarini, D.J., et al., *A mitochondrial protein compendium elucidates complex I disease biology.* Cell, 2008. **134**(1): p. 112-23.
111. Floyd, B.J., et al., *Mitochondrial Protein Interaction Mapping Identifies Regulators of Respiratory Chain Function.* Mol Cell, 2016. **63**(4): p. 621-632.
112. Fassone, E., et al., *FOXRED1, encoding an FAD-dependent oxidoreductase complex-I-specific molecular chaperone, is mutated in infantile-onset mitochondrial encephalopathy.* Hum Mol Genet, 2010. **19**(24): p. 4837-47.
113. Haack, T.B., et al., *Exome sequencing identifies ACAD9 mutations as a cause of complex I deficiency.* Nat Genet, 2010. **42**(12): p. 1131-4.
114. Nouws, J., et al., *Acyl-CoA dehydrogenase 9 is required for the biogenesis of oxidative phosphorylation complex I.* Cell Metab, 2010. **12**(3): p. 283-94.
115. Mayr, J.A., et al., *Spectrum of combined respiratory chain defects.* J Inherit Metab Dis, 2015. **38**(4): p. 629-40.
116. Wortmann, S.B., et al., *A Guideline for the Diagnosis of Pediatric Mitochondrial Disease: The Value of Muscle and Skin Biopsies in the Genetics Era.* Neuropediatrics, 2017. **48**(4): p. 309-314.
117. Dimauro, S. and G. Davidzon, *Mitochondrial DNA and disease.* Ann Med, 2005. **37**(3): p. 222-32.
118. Bugiani, M., et al., *Clinical and molecular findings in children with complex I deficiency.* Biochim Biophys Acta, 2004. **1659**(2-3): p. 136-47.
119. Calvo, S.E., et al., *Molecular diagnosis of infantile mitochondrial disease with targeted next-generation sequencing.* Sci Transl Med, 2012. **4**(118): p. 118ra10.
120. Sanger, F. and A.R. Coulson, *A rapid method for determining sequences in DNA by primed synthesis with DNA polymerase.* J Mol Biol, 1975. **94**(3): p. 441-8.
121. Sanger, F., S. Nicklen, and A.R. Coulson, *DNA sequencing with chain-terminating inhibitors.* Proc Natl Acad Sci U S A, 1977. **74**(12): p. 5463-7.
122. Smith, L.M., et al., *Fluorescence detection in automated DNA sequence analysis.* Nature, 1986. **321**(6071): p. 674-9.
123. Zhang, W., H. Cui, and L.J. Wong, *Application of Next Generation Sequencing to Molecular Diagnosis of Inherited Diseases.* Top Curr Chem, 2012.
124. Shendure, J. and H. Ji, *Next-generation DNA sequencing.* Nat Biotechnol, 2008. **26**(10): p. 1135-45.
125. Lander, E.S., et al., *Initial sequencing and analysis of the human genome.* Nature, 2001. **409**(6822): p. 860-921.
126. Venter, J.C., et al., *The sequence of the human genome.* Science, 2001. **291**(5507): p. 1304-51.
127. Institute, N.G.R. *DNA Sequencing costs*. 2018 10.12.2018]; Available from: https://www.genome.gov/images/content/costpergenome_2017.jpg.
128. Bentley, D.R., et al., *Accurate whole human genome sequencing using reversible terminator chemistry.* Nature, 2008. **456**(7218): p. 53-9.
129. Schnekenberg, R.P. and A.H. Nemeth, *Next-generation sequencing in childhood disorders.* Arch Dis Child, 2013.
130. Metzker, M.L., *Sequencing technologies - the next generation.* Nat Rev Genet, 2010. **11**(1): p. 31-46.
131. Ley, T.J., et al., *DNA sequencing of a cytogenetically normal acute myeloid leukaemia genome.* Nature, 2008. **456**(7218): p. 66-72.
132. Ng, S.B., et al., *Exome sequencing identifies the cause of a mendelian disorder.* Nat Genet, 2010. **42**(1): p. 30-5.
133. Hoischen, A., et al., *De novo mutations of SETBP1 cause Schinzel-Giedion syndrome.* Nat Genet, 2010. **42**(6): p. 483-5.

134. Ng, S.B., et al., *Exome sequencing identifies MLL2 mutations as a cause of Kabuki syndrome.* Nat Genet, 2010. **42**(9): p. 790-3.
135. Haack, T.B., et al., *Impaired riboflavin transport due to missense mutations in SLC52A2 causes Brown-Vialetto-Van Laere syndrome.* J Inherit Metab Dis, 2012. **35**(6): p. 943-8.
136. Saunders, C.J., et al., *Rapid whole-genome sequencing for genetic disease diagnosis in neonatal intensive care units.* Sci Transl Med, 2012. **4**(154): p. 154ra135.
137. Plagnol, V., et al., *A robust model for read count data in exome sequencing experiments and implications for copy number variant calling.* Bioinformatics, 2012. **28**(21): p. 2747-54.
138. Fromer, M., et al., *Discovery and statistical genotyping of copy-number variation from whole-exome sequencing depth.* Am J Hum Genet, 2012. **91**(4): p. 597-607.
139. Ku, C.S., et al., *Exome sequencing: dual role as a discovery and diagnostic tool.* Ann Neurol, 2012. **71**(1): p. 5-14.
140. Lyon, G.J., et al., *Exome sequencing and unrelated findings in the context of complex disease research: ethical and clinical implications.* Discov Med, 2011. **12**(62): p. 41-55.
141. Bell, C.J., et al., *Carrier testing for severe childhood recessive diseases by next-generation sequencing.* Sci Transl Med, 2011. **3**(65): p. 65ra4.
142. Wenz, T., et al., *Emerging therapeutic approaches to mitochondrial diseases.* Dev Disabil Res Rev, 2010. **16**(2): p. 219-29.
143. Tremblay-Mercier, J., et al., *Bezafibrate mildly stimulates ketogenesis and fatty acid metabolism in hypertriglyceridemic subjects.* J Pharmacol Exp Ther, 2010. **334**(1): p. 341-6.
144. Koh, K.K., et al., *Vascular and metabolic effects of treatment of combined hyperlipidemia: focus on statins and fibrates.* Int J Cardiol, 2008. **124**(2): p. 149-59.
145. Abourbih, S., et al., *Effect of fibrates on lipid profiles and cardiovascular outcomes: a systematic review.* Am J Med, 2009. **122**(10): p. 962 e1-8.
146. Bastin, J., et al., *Activation of peroxisome proliferator-activated receptor pathway stimulates the mitochondrial respiratory chain and can correct deficiencies in patients' cells lacking its components.* J Clin Endocrinol Metab, 2008. **93**(4): p. 1433-41.
147. Wenz, T., et al., *A metabolic shift induced by a PPAR panagonist markedly reduces the effects of pathogenic mitochondrial tRNA mutations.* J Cell Mol Med, 2011. **15**(11): p. 2317-25.
148. Golubitzky, A., et al., *Screening for active small molecules in mitochondrial complex I deficient patient's fibroblasts, reveals AICAR as the most beneficial compound.* PLoS One, 2011. **6**(10): p. e26883.
149. Casarin, A., et al., *Copper and bezafibrate cooperate to rescue cytochrome c oxidase deficiency in cells of patients with SCO2 mutations.* Orphanet J Rare Dis, 2012. **7**: p. 21.
150. Wenz, T., *PGC-1alpha activation as a therapeutic approach in mitochondrial disease.* IUBMB Life, 2009. **61**(11): p. 1051-62.
151. Salviati, L., et al., *Copper supplementation restores cytochrome c oxidase activity in cultured cells from patients with SCO2 mutations.* Biochem J, 2002. **363**(Pt 2): p. 321-7.
152. Freisinger, P., et al., *Reversion of hypertrophic cardiomyopathy in a patient with deficiency of the mitochondrial copper binding protein Sco2: is there a potential effect of copper?* J Inherit Metab Dis, 2004. **27**(1): p. 67-79.
153. Wenz, T., et al., *Activation of the PPAR/PGC-1alpha pathway prevents a bioenergetic deficit and effectively improves a mitochondrial myopathy phenotype.* Cell Metab, 2008. **8**(3): p. 249-56.
154. Yatsuga, S. and A. Suomalainen, *Effect of bezafibrate treatment on late-onset mitochondrial myopathy in mice.* Hum Mol Genet, 2012. **21**(3): p. 526-35.
155. Viscomi, C., et al., *In vivo correction of COX deficiency by activation of the AMPK/PGC-1alpha axis.* Cell Metab, 2011. **14**(1): p. 80-90.
156. Dillon, L.M., et al., *Long-Term Bezafibrate Treatment Improves Skin and Spleen Phenotypes of the mtDNA Mutator Mouse.* PLoS One, 2012. **7**(9): p. e44335.
157. Noe, N., et al., *Bezafibrate improves mitochondrial function in the CNS of a mouse model of mitochondrial encephalopathy.* Mitochondrion, 2012.
158. Djouadi, F., et al., *Correction of fatty acid oxidation in carnitine palmitoyl transferase 2-deficient cultured skin fibroblasts by bezafibrate.* Pediatr Res, 2003. **54**(4): p. 446-51.
159. Djouadi, F., et al., *Bezafibrate increases very-long-chain acyl-CoA dehydrogenase protein and mRNA expression in deficient fibroblasts and is a potential therapy for fatty acid oxidation disorders.* Hum Mol Genet, 2005. **14**(18): p. 2695-703.

160. Bonnefont, J.P., et al., *Long-term follow-up of bezafibrate treatment in patients with the myopathic form of carnitine palmitoyltransferase 2 deficiency.* Clin Pharmacol Ther, 2010. **88**(1): p. 101-8.
161. Orngreen, M.C., et al., *Bezafibrate in skeletal muscle fatty acid oxidation disorders: A randomized clinical trial.* Neurology, 2014.
162. Horvath, R., *Update on clinical aspects and treatment of selected vitamin-responsive disorders II (riboflavin and CoQ 10).* J Inherit Metab Dis, 2012. **35**(4): p. 679-87.
163. Bosch, A.M., et al., *Brown-Vialetto-Van Laere and Fazio Londe syndrome is associated with a riboflavin transporter defect mimicking mild MADD: a new inborn error of metabolism with potential treatment.* J Inherit Metab Dis, 2011. **34**(1): p. 159-64.
164. Ho, G., et al., *Maternal riboflavin deficiency, resulting in transient neonatal-onset glutaric aciduria Type 2, is caused by a microdeletion in the riboflavin transporter gene GPR172B.* Hum Mutat, 2011. **32**(1): p. E1976-84.
165. Gerards, M., et al., *Riboflavin-responsive oxidative phosphorylation complex I deficiency caused by defective ACAD9: new function for an old gene.* Brain, 2011. **134**(Pt 1): p. 210-9.
166. Saijo, T. and K. Tanaka, *Isoalloxazine ring of FAD is required for the formation of the core in the Hsp60-assisted folding of medium chain acyl-CoA dehydrogenase subunit into the assembly competent conformation in mitochondria.* J Biol Chem, 1995. **270**(4): p. 1899-907.
167. Scholte, H.R., et al., *Riboflavin-responsive complex I deficiency.* Biochim Biophys Acta, 1995. **1271**(1): p. 75-83.
168. Gempel, K., et al., *The myopathic form of coenzyme Q10 deficiency is caused by mutations in the electron-transferring-flavoprotein dehydrogenase (ETFDH) gene.* Brain, 2007. **130**(Pt 8): p. 2037-44.
169. Ghezzi, D., et al., *Severe X-linked mitochondrial encephalomyopathy associated with a mutation in apoptosis-inducing factor.* Am J Hum Genet, 2010. **86**(4): p. 639-49.
170. Nouws, J., et al., *A Patient with Complex I Deficiency Caused by a Novel ACAD9 Mutation Not Responding to Riboflavin Treatment.* JIMD Rep, 2013.
171. Panetta, J., L.J. Smith, and A. Boneh, *Effect of high-dose vitamins, coenzyme Q and high-fat diet in paediatric patients with mitochondrial diseases.* J Inherit Metab Dis, 2004. **27**(4): p. 487-98.
172. Lopes Costa, A., et al., *Beneficial effects of resveratrol on respiratory chain defects in patients' fibroblasts involve estrogen receptor and estrogen-related receptor alpha signaling.* Hum Mol Genet, 2013.
173. Lagouge, M., et al., *Resveratrol improves mitochondrial function and protects against metabolic disease by activating SIRT1 and PGC-1alpha.* Cell, 2006. **127**(6): p. 1109-22.
174. Dong, W., D. Gao, and X. Zhang, *Mitochondria biogenesis induced by resveratrol against brain ischemic stroke.* Med Hypotheses, 2007. **69**(3): p. 700-1.
175. Erb, M., et al., *Features of idebenone and related short-chain quinones that rescue ATP levels under conditions of impaired mitochondrial complex I.* PLoS One, 2012. **7**(4): p. e36153.
176. Haginoya, K., et al., *Efficacy of idebenone for respiratory failure in a patient with Leigh syndrome: a long-term follow-up study.* J Neurol Sci, 2009. **278**(1-2): p. 112-4.
177. Ikejiri, Y., et al., *Idebenone improves cerebral mitochondrial oxidative metabolism in a patient with MELAS.* Neurology, 1996. **47**(2): p. 583-5.
178. Napolitano, A., et al., *Long-term treatment with idebenone and riboflavin in a patient with MELAS.* Neurol Sci, 2000. **21**(5 Suppl): p. S981-2.
179. Lekoubou, A., et al., *Effect of long-term oral treatment with L-arginine and idebenone on the prevention of stroke-like episodes in an adult MELAS patient.* Rev Neurol (Paris), 2011. **167**(11): p. 852-5.
180. Klopstock, T., et al., *A randomized placebo-controlled trial of idebenone in Leber's hereditary optic neuropathy.* Brain, 2011. **134**(Pt 9): p. 2677-86.
181. Giorgio, V., et al., *The effects of idebenone on mitochondrial bioenergetics.* Biochim Biophys Acta, 2012. **1817**(2): p. 363-9.
182. Shrader, W.D., et al., *alpha-Tocotrienol quinone modulates oxidative stress response and the biochemistry of aging.* Bioorg Med Chem Lett, 2011. **21**(12): p. 3693-8.
183. Enns, G.M., et al., *Initial experience in the treatment of inherited mitochondrial disease with EPI-743.* Mol Genet Metab, 2012. **105**(1): p. 91-102.
184. Martinelli, D., et al., *EPI-743 reverses the progression of the pediatric mitochondrial disease--genetically defined Leigh Syndrome.* Mol Genet Metab, 2012. **107**(3): p. 383-8.

185. Sadun, A.A., et al., *Effect of EPI-743 on the clinical course of the mitochondrial disease Leber hereditary optic neuropathy.* Arch Neurol, 2012. **69**(3): p. 331-8.
186. Leipnitz, G., et al., *Evaluation of mitochondrial bioenergetics, dynamics, endoplasmic reticulum-mitochondria crosstalk, and reactive oxygen species in fibroblasts from patients with complex I deficiency.* Sci Rep, 2018. **8**(1): p. 1165.
187. Fogleman, S., et al., *CRISPR/Cas9 and mitochondrial gene replacement therapy: promising techniques and ethical considerations.* Am J Stem Cells, 2016. **5**(2): p. 39-52.
188. Tachibana, M., et al., *Mitochondrial gene replacement in primate offspring and embryonic stem cells.* Nature, 2009. **461**(7262): p. 367-72.
189. Craven, L., et al., *Pronuclear transfer in human embryos to prevent transmission of mitochondrial DNA disease.* Nature, 2010. **465**(7294): p. 82-85.
190. Tavare, A., *Scientists are to investigate "three parent IVF" for preventing mitochondrial diseases.* BMJ, 2012. **344**: p. e540.
191. Liu, H.S. and P.L. Chu, *Three-parent embryo: The therapeutic future for inherited mitochondrial diseases.* J Formos Med Assoc, 2015. **114**(11): p. 1027-8.
192. Dahiya, N. and S. Garg, *Three-parent baby: Is it ethical?* Indian J Med Ethics, 2018. **3**(2): p. 169.
193. Dimond, R. and N. Stephens, *Three persons, three genetic contributors, three parents: Mitochondrial donation, genetic parenting and the immutable grammar of the 'three x x'.* Health (London), 2018. **22**(3): p. 240-258.
194. Gomez-Tatay, L., J.M. Hernandez-Andreu, and J. Aznar, *Mitochondrial Modification Techniques and Ethical Issues.* J Clin Med, 2017. **6**(3).
195. Saxena, N., et al., *Mitochondrial Donation: A Boon or Curse for the Treatment of Incurable Mitochondrial Diseases.* J Hum Reprod Sci, 2018. **11**(1): p. 3-9.
196. Danhauser, K., et al., *Cellular rescue-assay aids verification of causative DNA-variants in mitochondrial complex I deficiency.* Mol Genet Metab, 2011. **103**(2): p. 161-6.
197. Bakker, H.D., et al., *Vitamin-responsive complex I deficiency in a myopathic patient with increased activity of the terminal respiratory chain and lactic acidosis.* J Inherit Metab Dis, 1994. **17**(2): p. 196-204.
198. Garrido-Maraver, J., et al., *Screening of effective pharmacological treatments for MELAS syndrome using yeasts, fibroblasts and cybrid models of the disease.* Br J Pharmacol, 2012. **167**(6): p. 1311-28.
199. Cornelius, N., et al., *Molecular mechanisms of riboflavin responsiveness in patients with ETF-QO variations and multiple acyl-CoA dehydrogenation deficiency.* Hum Mol Genet, 2012. **21**(15): p. 3435-48.
200. Kornblum, C., et al., *Loss-of-function mutations in MGME1 impair mtDNA replication and cause multisystemic mitochondrial disease.* Nat Genet, 2013. **45**(2): p. 214-9.
201. De Paepe, B., et al., *Effect of Resveratrol on Cultured Skin Fibroblasts from Patients with Oxidative Phosphorylation Defects.* Phytother Res, 2013.
202. Kuznetsov, A.V., et al., *Analysis of mitochondrial function in situ in permeabilized muscle fibers, tissues and cells.* Nat Protoc, 2008. **3**(6): p. 965-76.
203. Wittig, I., H.P. Braun, and H. Schagger, *Blue native PAGE.* Nat Protoc, 2006. **1**(1): p. 418-28.
204. Schagger, H., *Tricine-SDS-PAGE.* Nat Protoc, 2006. **1**(1): p. 16-22.
205. Wittig, I., et al., *Mass estimation of native proteins by blue native electrophoresis: principles and practical hints.* Mol Cell Proteomics, 2010. **9**(10): p. 2149-61.
206. Rais, I., M. Karas, and H. Schagger, *Two-dimensional electrophoresis for the isolation of integral membrane proteins and mass spectrometric identification.* Proteomics, 2004. **4**(9): p. 2567-71.
207. Unlu, M., M.E. Morgan, and J.S. Minden, *Difference gel electrophoresis: a single gel method for detecting changes in protein extracts.* Electrophoresis, 1997. **18**(11): p. 2071-7.
208. Chimi, M.A., et al., *Age-related changes in the mitochondrial proteome of the fungus Podospora anserina analyzed by 2D-DIGE and LC-MS/MS.* J Proteomics, 2013.
209. Lasonder, E., et al., *Analysis of the Plasmodium falciparum proteome by high-accuracy mass spectrometry.* Nature, 2002. **419**(6906): p. 537-42.
210. Scheving, R., et al., *Protein S-nitrosylation and denitrosylation in the mouse spinal cord upon injury of the sciatic nerve.* J Proteomics, 2012. **75**(13): p. 3987-4004.
211. Collins, M.O., L. Yu, and J.S. Choudhary, *Analysis protein complexes by 1D-SDS-PAGE and tandem mass spectrometry*. 2008.

212. Danhauser, K., *Funktionelle Analyse von seltenen DNA-Varianten in Genen, die mit einem Defekt des Atmungskettenkomplexes I assoziiert sind* 2013, Technichal University Munich.
213. Dewulf, J.P., et al., *Evidence of a wide spectrum of cardiac involvement due to ACAD9 mutations: Report on nine patients.* Mol Genet Metab, 2016. **118**(3): p. 185-9.
214. Collet, M., et al., *High incidence and variable clinical outcome of cardiac hypertrophy due to ACAD9 mutations in childhood.* Eur J Hum Genet, 2015.
215. Garone, C., et al., *Mitochondrial Encephalomyopathy Due to a Novel Mutation in ACAD9.* JAMA Neurol, 2013: p. 1-3.
216. Kohda, M., et al., *A Comprehensive Genomic Analysis Reveals the Genetic Landscape of Mitochondrial Respiratory Chain Complex Deficiencies.* PLoS Genet, 2016. **12**(1): p. e1005679.
217. Leslie, N., et al., *Neonatal multiorgan failure due to ACAD9 mutation and complex I deficiency with mitochondrial hyperplasia in liver, cardiac myocytes, skeletal muscle, and renal tubules.* Hum Pathol, 2016. **49**: p. 27-32.
218. Lagoutte-Renosi, J., et al., *Lethal Neonatal Progression of Fetal Cardiomegaly Associated to ACAD9 Deficiency.* JIMD Rep, 2015.
219. Fragaki, K., et al., *Severe defect in mitochondrial complex I assembly with mitochondrial DNA deletions in ACAD9-deficient mild myopathy.* Muscle Nerve, 2017. **55**(6): p. 919-922.
220. Repp, B.M., et al., *Clinical, biochemical and genetic spectrum of 70 patients with ACAD9 deficiency: is riboflavin supplementation effective?* Orphanet J Rare Dis, 2018. **13**(1): p. 120.
221. SurveyMonkey, I. *SurveyMonkey*. 2017 14.01.2018 [cited 2018; Available from: www.surveymonkey.com.
222. Mastantuono, E., *Whole exome sequencing (WES) to elucidate the molecular basis of cardiac disease*. 2018.
223. Schiff, M., et al., *Complex I assembly function and fatty acid oxidation enzyme activity of ACAD9 both contribute to disease severity in ACAD9 deficiency.* Hum Mol Genet, 2015.
224. Haack, T.B., et al., *Homozygous missense mutation in BOLA3 causes multiple mitochondrial dysfunctions syndrome in two siblings.* J Inherit Metab Dis, 2012.
225. Cameron, J.M., et al., *Mutations in iron-sulfur cluster scaffold genes NFU1 and BOLA3 cause a fatal deficiency of multiple respiratory chain and 2-oxoacid dehydrogenase enzymes.* Am J Hum Genet, 2011. **89**(4): p. 486-95.
226. Haack, T.B., et al., *Phenotypic spectrum of eleven patients and five novel MTFMT mutations identified by exome sequencing and candidate gene screening.* Mol Genet Metab, 2013.
227. Schwarz, J.M., et al., *MutationTaster evaluates disease-causing potential of sequence alterations.* Nat Methods, 2010. **7**(8): p. 575-6.
228. Mayr, J.A., et al., *Heterozygous mutation in the X chromosomal NDUFA1 gene in a girl with complex I deficiency.* Mol Genet Metab, 2011. **103**(4): p. 358-61.
229. Polster, B.M., *AIF, reactive oxygen species, and neurodegeneration: A "complex" problem.* Neurochem Int, 2012.
230. Benit, P., et al., *The variability of the harlequin mouse phenotype resembles that of human mitochondrial-complex I-deficiency syndromes.* PLoS One, 2008. **3**(9): p. e3208.
231. Berger, I., et al., *Early prenatal ventriculomegaly due to an AIFM1 mutation identified by linkage analysis and whole exome sequencing.* Mol Genet Metab, 2011. **104**(4): p. 517-20.
232. Tucker, E.J., et al., *Mutations in MTFMT underlie a human disorder of formylation causing impaired mitochondrial translation.* Cell Metab, 2011. **14**(3): p. 428-34.
233. Haack, T.B., et al., *Mutation screening of 75 candidate genes in 152 complex I deficiency cases identifies pathogenic variants in 16 genes including NDUFB9.* J Med Genet, 2012.
234. Djouadi, F. and J. Bastin, *Species differences in the effects of bezafibrate as a potential treatment of mitochondrial disorders.* Cell Metab, 2011. **14**(6): p. 715-6; author reply 717.
235. Wang, Y., et al., *Evidence for physical association of mitochondrial fatty acid oxidation and oxidative phosphorylation complexes.* J Biol Chem, 2010. **285**(39): p. 29834-41.
236. Lim, S.C., et al., *Loss of the Mitochondrial Fatty Acid beta-Oxidation Protein Medium-Chain Acyl-Coenzyme A Dehydrogenase Disrupts Oxidative Phosphorylation Protein Complex Stability and Function.* Sci Rep, 2018. **8**(1): p. 153.
237. Nsiah-Sefaa, A. and M. McKenzie, *Combined defects in oxidative phosphorylation and fatty acid beta-oxidation in mitochondrial disease.* Biosci Rep, 2016. **36**(2).

238. Aintablian, H.K., et al., *An atypical presentation of ACAD9 deficiency: Diagnosis by whole exome sequencing broadens the phenotypic spectrum and alters treatment approach.* Mol Genet Metab Rep, 2017. **10**: p. 38-44.
239. Nagao, M. and K. Tanaka, *FAD-dependent regulation of transcription, translation, post-translational processing, and post-processing stability of various mitochondrial acyl-CoA dehydrogenases and of electron transfer flavoprotein and the site of holoenzyme formation.* J Biol Chem, 1992. **267**(25): p. 17925-32.
240. Olsen, R.K., et al., *ETFDH mutations as a major cause of riboflavin-responsive multiple acyl-CoA dehydrogenation deficiency.* Brain, 2007. **130**(Pt 8): p. 2045-54.
241. Grad, L.I. and B.D. Lemire, *Riboflavin enhances the assembly of mitochondrial cytochrome c oxidase in C. elegans NADH-ubiquinone oxidoreductase mutants.* Biochim Biophys Acta, 2006. **1757**(2): p. 115-22.
242. Distelmaier, F., et al., *Treatable mitochondrial diseases: cofactor metabolism and beyond.* Brain, 2017. **140**(2): p. e11.
243. He, M., et al., *A new genetic disorder in mitochondrial fatty acid beta-oxidation: ACAD9 deficiency.* Am J Hum Genet, 2007. **81**(1): p. 87-103.
244. Heide, H., et al., *Complexome Profiling Identifies TMEM126B as a Component of the Mitochondrial Complex I Assembly Complex.* Cell Metab, 2012. **16**(4): p. 538-49.
245. Hirst, J., et al., *The nuclear encoded subunits of complex I from bovine heart mitochondria.* Biochim Biophys Acta, 2003. **1604**(3): p. 135-50.
246. Calvo, S.E., et al., *High-throughput, pooled sequencing identifies mutations in NUBPL and FOXRED1 in human complex I deficiency.* Nat Genet, 2010. **42**(10): p. 851-8.
247. Li, H., et al., *Histidine 103 in Fra2 is an iron-sulfur cluster ligand in the [2Fe-2S] Fra2-Grx3 complex and is required for in vivo iron signaling in yeast.* J Biol Chem, 2011. **286**(1): p. 867-76.
248. Mayr, J.A., et al., *Lipoic acid synthetase deficiency causes neonatal-onset epilepsy, defective mitochondrial energy metabolism, and glycine elevation.* Am J Hum Genet, 2011. **89**(6): p. 792-7.
249. Mayr, J.A., et al., *Thiamine pyrophosphokinase deficiency in encephalopathic children with defects in the pyruvate oxidation pathway.* Am J Hum Genet, 2011. **89**(6): p. 806-12.
250. Koyata, H. and K. Hiraga, *The glycine cleavage system: structure of a cDNA encoding human H-protein, and partial characterization of its gene in patients with hyperglycinemias.* Am J Hum Genet, 1991. **48**(2): p. 351-61.
251. Seyda, A., et al., *A novel syndrome affecting multiple mitochondrial functions, located by microcell-mediated transfer to chromosome 2p14-2p13.* Am J Hum Genet, 2001. **68**(2): p. 386-96.
252. Theunissen, T.E.J., et al., *Whole Exome Sequencing Is the Preferred Strategy to Identify the Genetic Defect in Patients With a Probable or Possible Mitochondrial Cause.* Front Genet, 2018. **9**: p. 400.
253. Kremer, L.S., et al., *Genetic diagnosis of Mendelian disorders via RNA sequencing.* Nat Commun, 2017. **8**: p. 15824.
254. Bonnefont, J.P., et al., *Bezafibrate for an inborn mitochondrial beta-oxidation defect.* N Engl J Med, 2009. **360**(8): p. 838-40.
255. Wen, B., et al., *Increased muscle coenzyme Q10 in riboflavin responsive MADD with ETFDH gene mutations due to secondary mitochondrial proliferation.* Mol Genet Metab, 2013. **109**(2): p. 154-60.
256. Ranieri, M., et al., *Mitochondrial fusion proteins and human diseases.* Neurol Res Int, 2013. **2013**: p. 293893.
257. Faou, P. and N.J. Hoogenraad, *Tom34: a cytosolic cochaperone of the Hsp90/Hsp70 protein complex involved in mitochondrial protein import.* Biochim Biophys Acta, 2012. **1823**(2): p. 348-57.
258. Zeviani, M., *OPA1 mutations and mitochondrial DNA damage: keeping the magic circle in shape.* Brain, 2008. **131**(Pt 2): p. 314-7.
259. Steele, H.E., et al., *M04 - A feasibility study of bezafibrate in mitochondrial myopathy.* Neuromuscular Disorders, 2017. **27**: p. S18.
260. Chinnery, P.F. *A Study of Bezafibrate in Mitochondrial Myopathy*. 2015 [cited 2019 14.01.2019]; Available from: https://clinicaltrials.gov/ct2/show/study/NCT02398201.

261. Dinwiddie, D.L., et al., *Diagnosis of mitochondrial disorders by concomitant next-generation sequencing of the exome and mitochondrial genome.* Genomics, 2013. **102**(3): p. 148-156.
262. Marcus, D., et al., *Replacement of the C6ORF66 Assembly Factor (NDUFAF4) Restores Complex I Activity in Patient Cells.* Mol Med, 2013. **19**(1): p. 124-34.
263. Wang, M., et al., *Mitochondrial complex I deficiency leads to the retardation of early embryonic development in Ndufs4 knockout mice.* PeerJ, 2017. **5**: p. e3339.
264. Quadalti, C., et al., *SURF1 knockout cloned pigs: Early onset of a severe lethal phenotype.* Biochim Biophys Acta Mol Basis Dis, 2018. **1864**(6 Pt A): p. 2131-2142.
265. Simonelli, F., et al., *Gene therapy for Leber's congenital amaurosis is safe and effective through 1.5 years after vector administration.* Mol Ther, 2010. **18**(3): p. 643-50.
266. Cartier, N., et al., *Lentiviral hematopoietic cell gene therapy for X-linked adrenoleukodystrophy.* Methods Enzymol, 2012. **507**: p. 187-98.
267. Biffi, A., et al., *Lentiviral hematopoietic stem cell gene therapy benefits metachromatic leukodystrophy.* Science, 2013. **341**(6148): p. 1233158.
268. LeWitt, P.A., et al., *AAV2-GAD gene therapy for advanced Parkinson's disease: a double-blind, sham-surgery controlled, randomised trial.* Lancet Neurol, 2011. **10**(4): p. 309-19.
269. Chadderton, N., et al., *Intravitreal delivery of AAV-NDI1 provides functional benefit in a murine model of Leber hereditary optic neuropathy.* Eur J Hum Genet, 2013. **21**(1): p. 62-8.
270. Quintana, A., et al., *Fatal breathing dysfunction in a mouse model of Leigh syndrome.* J Clin Invest, 2012. **122**(7): p. 2359-68.
271. Farrar, G.J., et al., *Mitochondrial disorders: aetiologies, models systems, and candidate therapies.* Trends Genet, 2013. **29**(8): p. 488-97.
272. Poulton, J. and A.L. Bredenoord, *174th ENMC international workshop: Applying pre-implantation genetic diagnosis to mtDNA diseases: implications of scientific advances 19-21 March 2010, Naarden, The Netherlands.* Neuromuscul Disord, 2010. **20**(8): p. 559-63.
273. Poulton, J., et al., *Preventing transmission of maternally inherited mitochondrial DNA diseases.* BMJ, 2009. **338**.
274. Zinkant, K., *Chinesischer Forscher will erste genetisch veränderte Babys erschaffen haben*, in *Sueddeutsche Zeitung*. 2018: online.
275. Hasson, K.D., M., *Gene-edited babies: no one has the moral warrant to go it alone*, in *The Guardian*. 2018.

6. Appendix

6.1. Supplements

6.1.1 Overview of all primers

The conformation of the mutations was performed by our great technical assistants Anne Löschner, Rosi Hellinger, Caterina Terrile, or Michael Färberböck. They used genomic primers designed with the Institute's program “ExonPrimer” and can be found in the primer database. Only primers I used by myself or primers which were important for further experiments will be listed below.

Primer	Nr.	Name	Sequence	Temp	Product length
HIV-Primer	15188	HIV F	5´ - ATAATCCACCTATCCCAGTAGGAGAAAT - 3`	60 °C	115bp
	15188	HIV R	5´ - TTTGGTCCTTGTCTTATGTCCAGAATGC - 3´		
HBV-Primer	15189	HBV F	5´ - CCGTCTGTGCCTTCTCATCTG - 3`	60 °C	104bp
	15189	HBV R	5´ - AGTCCAAGAGTYCTCTTATGYAAGACCTT - 3`		
HCV-Primer	15190	HCV_Outer F	5´ - ACTGTCTTCACGCAGAAAGCGTCTAGCCAT - 3´	55 °C	271bp
	15190	HCV_Outer R	5´ - CGAGACCTCCCGGGGCACTCGCAAGCACCC - 3´		
ACAD9+pLenti	15849	ACAD9+pLentiF	5' - AGGCATGAGCGGCTGCGGGCTC - 3'	60°C	
	15849	ACAD9+pLentiR	5' - TCAGCATGTCCTGTCCAGAGGGTGGG - 3'		
cDNA ACAD9-1	15936	ACAD9_cDNA_1F	5' - ATCAGACGTGTGTGTGTCCC - 3'	60°C	585bp
	15936	ACAD9_cDNA_1R	5' - ATCAGACGTGTGTGTGTCCC - 3'		
cDNA ACAD9-2	15937	ACAD9_cDNA_2F	5' - GTCCATCACTGTGACCCTGG - 3'	61°C	575bp
	15937	ACAD9_cDNA_2R	5' - GCAGGCGTACTCAGCAGTC - 3'		
cDNA ACAD9-3	15938	ACAD9_cDNA_3F	5' - TCGGAGATGGGTTTAAGGTG - 3'	60°C	586bp
	15938	ACAD9_cDNA_3R	5' - GTCAGCCCCAGGTCCAC - 3'		
cDNA ACAD9-4	15939	ACAD9_cDNA_4F	5' - TGACTACCAGGATCCATGAGC - 3'	60°C	589bp
	15939	ACAD9_cDNA_4R	5' - TAACAGTCATCCAGCAACGG - 3'		
cDNA BOLA3	16367	BOLA3_cDNA_f	5' - GGCATGGCTGCATGGAG - 3'	62°C	349bp
	16367	BOLA3_cDNA_r	5' - ATCTATGCAGCCAGGGCG - 3'		
cDNA AIFM1	16197	AIFM1cDNAges_F	5' - AGGCATGTTCCGGTGTGGAGGC - 3'	59°C	1960bp
	16197	AIFM1cDNAges_R	5' - TCAGTCTTCATGAATGTTGAATAGTT - 3'		
AIFM1	16162	AIFM1_seq_vect_F1	5' - GGCCAGGGTACTGATTGTATC - 3'	59°C	850bp
	16162	AIFM1_seq_vect_R2	5' - AGCATCTCCTGCCACCC - 3'		
cDNA PDHA1-inner	16194	PDHA1_cDNA_innen_F	5' - GTGCTTCATGAGGAAGATGC - 3'	59°C	1308bp
	16194	PDHA1_cDNA_innen_R	5' - TCCTTCTCCTCCCCTTAACTG - 3'		
	16195	PDHA1_cDNA_außen_F	5' - CTCCTGGGTTGTGAGGAGTC - 3'	60°C	1383bp

cDNA PDHA1-outer	16195	PDHA1_cDNA_außen_R	5' - GAACACTGTCTGGTAGCCCC - 3'		
cDNA MTFMT	16378	MTFMT_CDNA_1_F	5' - CACCATGAGGGTGTTGGTG - 3'	61°C	1174bp
	16378	MTFMT_CDNA_1_R	5' - CTACTCAATGCATTGTTGCATAGC - 3'		
cDNA PDHA1-1	16360	PDHA1_cDNA_1_F	5' - CGAGACATGGTCTTGCTACG - 3'	60°C	681bp
	16360	PDHA1_cDNA_1_R	5' - AAGCTTCGAATATCTGGCCC - 3'		
cDNA PDHA1-2	16361	PDHA1_cDNA_2_F	5' - GCTGGGATTGCTCTAGCC - 3'	59°C	581bp
	16361	PDHA1_cDNA_2_R	5' - ATGTGGTAGCCCAGCTCTTC - 3'		
cDNA PDHA1-3	16637	PDHA1_cDNA_4_F	5' - GCAGAGTGCTGGTAGCA - 3'	55°C	517bp
	16637	PDHA1_cDNA_8_R	5' - AAAGTCAGGCAGACCTCA - 3'		
cDNA NDUFB3	16231	NDUFB3_cDNA_F	5' - TCAGATTGCTGTCAGACATGG - 3'	59°C	334bp
	16231	NDUFB3_cDNA_R	5' - GATGCTTCCAGGTATTATCTTCAG - 3'		
cDNA NDUFS1-1	15230	NDUFS1_1_1_F67	5' - GGGTCGTCGTGGTCCAG - 3'	50°C	551bp
	15230	NDUFS1_1_1_R617	5' - TTCTTGTCTTCCACAGCACG - 3'		
cDNA NDUFS1-2	15231	NDUFS1_1_2_F511	5' - CCTATTTGTGACCAGGGAGG - 3'	50°C	537bp
	15231	NDUFS1_1_2_R1047	5' - GACCATTGGCTCGGTAAGTC - 3'		
cDNA NDUFS1-3	15232	NDUFS1_1_3_F948	5' - GCCACGTATGCATGAGGAC - 3'	50 °C	555bp
	15232	NDUFS1_1_3_R1502	5' - CTTCCCGAAGCAATGTCTTG - 3'		
cDNA NDUFS1-4	15233	NDUFS1_1_4_F1385	5' - AGAGCTGGCTGCATAATGAC - 3'	50°C	555bp
	15233	NDUFS1_1_4_R1939	5' - GCTGAGCTCTACCCTCAGTG - 3'		
cDNA NDUFS1-5	15234	NDUFS1_1_5_F1789	5' - ATCACACGACAGGATTTGCC - 3'	50°C	595bp
	15234	NDUFS1_1_5_R2383	5' - AACCTGTAAAGGATCACTGCACTAC - 3'		
cDNA NDUFS8	16151	NDUFS8_cDNA_F	5' - GGCAAGGCAAGTAGCGG - 3'	61°C	703bp
	16151	NDUFS8_cDNA_R	5' - GTGGTTTTATTGGGCAGCAG - 3'		
cDNA NDUFB9-1	15235	NDUFB9_1_1_F53	5' - GTGCAGTTTCCCGGCTC - 3'	50°C	364bp
	15235	NDUFB9_1_1_R416	5' - TCATCTAAGCACCATTCTGGG - 3'		
cDNA NDUFB9-2	15236	NDUFB9_1_2_F320	5' - GTCAGCATCCACAGCCATAC - 3'	50°C	385bp
	15236	NDUFB9_1_2_R704	5' - TAGGGCAAGTGCATGTTCTG - 3'		

Table S1: Overview of all used primers and conditions

6.1.2 ACAD9 patients – additional information

Table S2 shows all compound heterozygous and homozygous ACAD9 variants identified in 70 patients, including Minor allele frequency (MAF) reported in gnomAD. The MAF was used to estimate the incidence of ACAD9 deficiency in the European population. Table S3 gives an overview of the clinical characteristics. Table S4 gives detailed information on the clinical features of the ACAD9 cohort.

ID, family, sex	Country	cDNA	Protein	Variant type	MAF	cDNA	Protein	Variant type	MAF	Ref.
1, 1, F	Italy	c.130T>A	p.Phe44Ile	missense	np	c.797G>A	p.Arg266Gln	missense	1,22E-02	Haack et al. 2010
2, 1, M	Italy	c.130T>A	p.Phe44Ile	missense	np	c.797G>A	p.Arg266Gln	missense	1,22E-02	Haack et al. 2010
3, 2, F	Italy	c.797G>A	p.Arg266Gln	missense	1,22E-02	c.1249C>T	p.Arg417Cys	missense	np	Haack et al. 2010
4, 3, F	UK	c.976G>C	p.Ala326Pro	missense	5,28E-02	c.1594C>T	p.Arg532Trp	missense	4,09E-03	Haack et al. 2010
5, 4, F	Netherlands	c.1594C>T	p.Arg532Trp	missense	4,09E-03	c.1594C>T	p.Arg532Trp	missense	4,09E-03	Gerards et al. 2010, Scholte et. al. 1995
6, 4, F	Netherlands	c.1594C>T	p.Arg532Trp	missense	4,09E-03	c.1594C>T	p.Arg532Trp	missense	4,09E-03	Gerards et al. 2010, Scholte et. al. 1996
7, 4, M	Netherlands	c.1594C>T	p.Arg532Trp	missense	4,09E-03	c.1594C>T	p.Arg532Trp	missense	4,09E-03	Gerards et al. 2010, Scholte et. al. 1997
8, 5, F	Netherlands	c.380G>A	p.Arg127Gln	missense	np	c.1405C>T	p.Arg469Trp	missense	0.0003754	Gerards et al. 2010, Scholte et. al. 1998
9, 6, F	Canada	c.1553G>A	p.Arg518His	missense	8.66e-5	c.1553G>A	p.Arg518His	missense	8.66e-5	Nouws et al. 2010
10, 7, F	Thailand/ Germany	c.187G>T	p.Glu63X	nonsense	np	c.1237G>A	p.Glu413Lys	missense	1,63E-02	Nouws et al. 2010
11, 7, F	Thailand/ Germany	c.187G>T	p.Glu63X	nonsense	np	c.1237G>A	p.Glu413Lys	missense	1,63E-02	Nouws et al. 2010
12, 8, M	Turkey	c.1594C>T	p.Arg532Trp	missense	4,09E-03	c.1594C>T	p.Arg532Trp	missense	4,09E-03	Haack et al. 2012
13, 8, F	Turkey	c.1594C>T	p.Arg532Trp	missense	4,09E-03	c.1594C>T	p.Arg532Trp	missense	4,09E-03	Haack et al. 2012
14, 8, F	Turkey	c.1594C>T	p.Arg532Trp	missense	4,09E-03	c.1594C>T	p.Arg532Trp	missense	4,09E-03	Haack et al. 2012
15, 9, M	Not available	c.260T>A	p.Ile87Asn	missense	np	c.976G>A	p.Ala326Pro	missense	np	Calvo et al. 2012
16, 10, M	Italy	c.1240C>T	p.Arg414Cys	missense	1,22E-02	c.1240C>T	p.Arg414Cys	missense	1,22E-02	Garone et al. 2013
17, 11, F	Turkey	c.659C>T	p.Ala220Val	missense	np	c.659C>T	p.Ala220Val	missense	np	Nouws et al. 2014
18, 12, M	France	c.1030-1G>T	acceptor splice	splice	np	c.1249C>T	p.Arg417Cys	missense	np	Lagoutte-Renosi et al. 2015
19, 13, F	West Africa	c.976G>A	p.Ala326Pro	missense	5,28E-02	c.1595G>A	p.Arg532Gln	missense	8,17E-03	Collet et al. 2015
20, 14, F	Portugal	c.358delT	p.Phe120fs	frameshift	0.000109	c.1594C>T	p.Arg532Trp	missense	4,09E-03	Collet et al. 2015
21, 15, F	France	c.976G>C	p.Ala326Pro	missense	5,28E-02	c.1595G>A	p.Arg532Gln	missense	8,17E-03	Collet et al. 2015
22, 16, F	France	c.151-2A>G	acceptor splice	splice site	np	c.1298G>A	p.Arg433Gln	missense	4,06E-03	Collet et al. 2015
23, 17, M	French Caribbean	c.1237G>A	p.Glu413Lys	missense	1,63E-02	c.1552C>T	p.Arg518Cys	missense	8.66e-5	Collet et al. 2015
24, 18, F	French Caribbean	c.1552C>T	p.Arg518Cys	missense	8.66e-5	c.1564-6_1569del	splice site	splice	np	Collet et al. 2015
25, 19, F	French Caribbean	c.1A>G	p.Met1?	start lost	1,23E-02	c.796C>T	P.Arg266Trp	missense	8,12E-03	Collet et al. 2015
26, 20, F	Japan	c.1150G>A	p.Val384Met	missense	4,07E-03	c.1817T>A	p.Leu606His	missense	np	Kohda et al. 2016
27, 21, F	Japan	c.811T>G	p.Cys271Gly	missense	np	c.1766-2A>G	splice site	splice site	np	Kohda et al. 2016
28, 22, M	not available	c.187G>T	p.Glu63X	nonsense	np	c.941T>C	p.Leu314Pro	missense	np	Leslie et al. 2016, Valencia et al. 2016
29, 23, F	Poland	c.514G>A	p.Gly172Arg	missense	1,80E-02	c.803C>T	p.Ser268Phe	missense	8,12E-03	Pronicka et al. 2016
30, 24, M	Poland	c.1552C>T	p.Arg518Cys	missense	8.66e-5	c.1553G>A	p.Arg518His	missense		Pronicka et al. 2016
31, 25, M	Poland	c.728C>G	p.Thr243Arg	missense	8,12E-03	c.1552C>T	p.Arg518Cys	missense	8.66e-5	Pronicka et al. 2016
32, 26, F	Morocco	c.1636G>C	p.Val546Leu	missense	np	c.1636G>C	p.Val546Leu	missense	np	Dewulf et al. 2016
33, 26, F	Morocco	c.1636G>C	p.Val546Leu	missense	np	c.1636G>C	p.Val546Leu	missense	np	Dewulf et al. 2016
34, 26, M	Morocco	c.1636G>C	p.Val546Leu	missense	np	c.1636G>C	p.Val546Leu	missense	np	Dewulf et al. 2016
35, 26, F	Morocco	c.1636G>C	p.Val546Leu	missense	np	c.1636G>C	p.Val546Leu	missense	np	Dewulf et al. 2016

ID, family, sex	Country	cDNA	Protein	Variant type	MAF	cDNA	Protein	Variant type	MAF	Ref.
36, 27, M	Belgium	c.509C>T	p.Ala170Val	missense	1,22E-02	c.1687C>G	p.His563Asp	missense	np	Dewulf et al. 2016
37, 27, F	Belgium	c.509C>T	p.Ala170Val	missense	1,22E-02	c.1687C>G	p.His563Asp	missense	np	Dewulf et al. 2016
38, 28, F	Congo	c.1240C>A	p.Arg414Ser	missense	4,06E-03	c.1650_1672dup	p.Leu558fs	frameshift	np	Dewulf et al. 2016
39, 28, F	Congo	c.1240C>A	p.Arg414Ser	missense	4,06E-03	c.1650_1672dup	p.Leu558fs	frameshift	np	Dewulf et al. 2016
40, 28, F	Congo	c.1240C>A	p.Arg414Ser	missense	4,06E-03	c.1650_1672dup	p.Leu558fs	frameshift	np	Dewulf et al. 2016
41, 29, F	Tunisia	c.1240C>T	p.Arg414Cys	missense	1,22E-02	c.1240C>T	p.Arg414Cys	missense	1,22E-02	Fragaki et al. 2016
42, 30, M	Austria	c.1690G>A	p.Glu564Lys	missense	4,07E-03	c.1832A>G	p.Tyr611Cys	missense	8,12E-03	This study
43, 31, M	Pakistan	c.1553G>A	p.Arg518His	missense	1,08E-02	c.1553G>A	p.Arg518His	missense	1,08E-02	This study
44, 32, F	Asia	c.293T>C	p.Leu98Ser	missense	np	c.293T>C	p.Leu98Ser	missense	np	This study
45, 33, F	Sri Lanka	c.1253A>G	p.Asp418Gly	missense	np	c.1253A>G	p.Asp418Gly	missense	np	This study
46, 33, M	Sri Lanka	c.1253A>G	p.Asp418Gly	missense	np	c.1253A>G	p.Asp418Gly	missense	np	This study
47, 33, M	Sri Lanka	c.1253A>G	p.Asp418Gly	missense	np	c.1253A>G	p.Asp418Gly	missense	np	This study
48, 34, F	Italy	c.857T>C	p.Leu286Pro	missense	np	c.1240C>T	p.Arg414Cys	missense	1,22E-02	This study
49, 35, F	France	c.976G>C	p.Ala326Pro	missense	5,28E-02	c.1651A>G	p.Ser551Gly	missense	np	This study
50, 36, M	Bahrain	c.1684G>A	p.Asp562Asn	missense	4.34e-5	c.1684G>A	p.Asp562Asn	missense	4.34e-5	This study
51, 37, F	not available	c.1805C>T	p.Ser602Phe	missense	np	c.1805C>T	p.Ser602Phe	missense	np	This study
52, 37, M	not available	c.1805C>T	p.Ser602Phe	missense	np	c.1805C>T	p.Ser602Phe	missense	np	This study
53, 38, M	Nigeria	c.868G>A	p.Gly290Arg	missense	3,23E-02	c.1237G>A	p.Glu413Lys	missense	1,63E-02	This study
54, 38, M	Nigeria	c.868G>A	p.Gly290Arg	missense	3,23E-02	c.1237G>A	p.Glu413Lys	missense	1,63E-02	This study
55, 38, M	Nigeria	c.868G>A	p.Gly290Arg	missense	3,23E-02	c.1237G>A	p.Glu413Lys	missense	1,63E-02	This study
56, 39, F	UK	c.976G>C	p.Ala326Pro	missense	5,28E-02	c.1594C>T	p.Arg532Trp	missense	4,09E-03	This study
57, 40, M	UK	c.665T>A	p.Ile222Asn	missense	np	c.1249C>T	p.Arg417Cys	missense	np	This study
58, 40, M	UK	c.665T>A	p.Ile222Asn	missense	np	c.1249C>T	p.Arg417Cys	missense	np	This study
59, 41, M	UK	c.1150G>A	p.Val384Met	missense	4,07E-03	c.1168G>A	p.Ala390Thr	missense	1,44E-02	This study
60, 41, M	UK	c.1150G>A	p.Val384Met	missense	4,07E-03	c.1168G>A	p.Ala390Thr	missense	1,44E-02	This study
61, 42, F	UK	c.1552C>T	p.Arg518Cys	missense	8.66e-5	c.1715G>A	p.Cys572Tyr	missense	np	This study
62, 43, F	Belgium	c.976G>C	p.Ala326Pro	missense	5,28E-02	c.1552C>T	p.Arg518Cys	missense	8.66e-5	This study
63, 44, M	Italy	c.1240C>T	p.Arg414Cys	missense	1,22E-02	c.1646G>A	p.Arg549Gln	missense	8.18e-6	This study
64, 45, F	Germany/ Poland	c.569C>T	p.Ala190Val	missense	4,07E-03	c.1405C>T	p.Arg469Trp	missense	0.0003754	This study
65, 46, M	Italy	c.1240C>T	p.Arg414Cys	missense	1,22E-02	c.1240C>T	p.Arg414Cys	missense	1,22E-02	This study
66, 46, M	Italy	c.1240C>T	p.Arg414Cys	missense	1,22E-02	c.1240C>T	p.Arg414Cys	missense	1,22E-02	This study
67, 47, M	Italy	c.555-2A>G	splice site	splice site	np	c.1168G>A	p.Ala390Thr	missense	1,44E-02	This study
68, 48, M	China	c.797G>A	p.Arg266Gln	missense	1,22E-02	c.1359-1G>A	splice site	splice site	np	This study
69, 49, F	China	c.1737T>G	p.Asn579Lys	missense	np	c.1240C>T	p.Arg414Cys	missense	1,22E-02	This study
70, 50, F	China	c.988A>C	p.Lys330Gln	missense	0.002096	c.988A>C	p.Lys330Gln	missense	0.002096*	This study

Table S2: ACAD9 variants and MAF = Minor allele frequency reported in gnomAD, np = not present,* uncertain diagnosis due to high allele frequency

ID, Family, Sex	Age of onset	Current age in day (* if dead)	Prenatal findings	Cardiomyopathy	Arrhythmias, any kind	Cardiological features	Neurological features	Effect of Riboflavin (rated by physician)	Effect of Riboflavin (cells)
1, 1, F	neonatal	49*		PS	NA	HCM	NA	untreated	beneficial effect
2, 1, M	neonatal	3600		PS	NA	HCM	no	beneficial effect	beneficial effect
3, 2, F	early infancy	4320*		PS	NA	HCM	no	beneficial effect	beneficial effect
4, 3, F	1 w	750*		DS	no	DCM	mild ID	beneficial effect	beneficial effect
5, 4, F	4 y	15480		no	no	No	no	beneficial effect	NA
6, 4, F	4 y	12240		no	no	No	mild ID	beneficial effect	beneficial effect
7, 4, M	4 y	14760		no	no	No	no	beneficial effect	NA
8, 5, F	early childhood	10800		DS	no	HCM	mild DD	beneficial effect	NA
9, 6, F	8 m	6480		PS	NA	HCM	no	beneficial effect	beneficial effect
10, 7, F	4 m	180*		PS	NA	HCM	NA	NA	NA
11, 7, F	6 m	240*		PS	NA	HCM	NA	NA	NA
12, 8, M	6 m	5370*	Oligohydramnios	DS	no	HCM, DCM	mild DD	beneficial effect	beneficial effect
13, 8, F	4.5 m	2160	Oligohydramnios	DS	no	HCM	mild DD	beneficial effect	NA
14, 8, F	4 m	3240	Oligohydramnios	DS	no	HCM, DCM	mild DD	beneficial effect	NA
15, 9, M	neonatal	28*		PS	NA	NA	NA	NA	NA
16, 10, M	1 y	6840		no	NA	No	mild ID, mild DD	beneficial effect	NA
17, 11,F	neonatal	180*		DS	no	HCM	NA	no effect	NA
18, 12,M	prenatal	1*		PS	PS	HCM	NA	untreated	Beneficial effect
19, 13, F	neonatal	70*	IGR, fetal rhythm abnormalities	PS	PS	HCM	no	untreated	NA
20, 14, F	1 y	2160*		PS	PS	HCM, DCM	NA	untreated	beneficial effect
21, 15, F	18 m	5400		PS	no	HCM	no	untreated	no effect
22, 16, F	9 y	12600		PS	no	HCM	no	NA	no effect
23, 17,M	4 m	7920		PS	no	HCM	no	untreated	no effect
24, 18, F	15 m	630*		PS	NA	HCM	no	untreated	NA
25, 19, F	1 y	540*		DS	no	HCM	no	untreated	NA
26, 20, F	2 w	14	IGR	PS	NA	HCM	NA	NA	NA
27, 21, F	14 y	5040		PS	NA	HCM	NA	NA	NA
28, 22,M	neonatal	1*	IGR, fetal rhythm abnormalities	PS	PS	HCM, DCM	NA	NA	NA
29, 23, F	2 d	3180		PS	DS	HCM	mild DD	no effect	NA
30, 24,M	1 m	90*	32 Hbd: preterm uterus contractions	PS	DS	HCM, DCM	mild DD	untreated	NA
31, 25,M	2 y	3240		no	no	no	no	NA	NA
32, 26, F	neonatal	150*	prematurely 26.7w due to pre-eclampsia	NA	NA	NA	NA	NA	NA
33, 26, F	2 m	315*		DS	DS	HCM	severe DD	no effect	NA
34, 26,M	15 d	270*		PS	NA	HCM	mild ID, severe DD	untreated	NA
35, 26, F	15 m	3240		NA	NA	NA	mild ID, mild DD	beneficial effect	NA

ID, Family, Sex	Age of onset	Current age in day (* if dead)	Prenatal findings	Cardiomyopathy	Arrhythmias, any kind	Cardiological features	Neurological features	Effect of Riboflavin (rated by physician)	Effect of Riboflavin (cells)
36, 27,M	12 y	10440		PS	NA	HCM	mild DD	NA	NA
37, 27, F	8 y	9360		PS	NA	HCM	mild ID, mild DD	untreated	NA
38, 28, F	2 d	9*	born after preclampsia of the mother, 29w	NA	NA	NA	NA	untreated	NA
39, 28, F	neonatal	2*		PS	NA	HCM	NA	untreated	NA
40, 28, F	neonatal	180*		PS	NA	HCM, DCM	mild ID	no effect	NA
41, 29, F	6 y	12240		no	NA	No	no	NA	NA
42, 30,M	prenatal	2*	lissencephalopathy agenesis of the corpus callosum, IGR	PS	NA	DCM	NA	untreated	no effect
43, 31,M	3 m	120*		PS	no	HCM	NA	untreated	NA
44, 32, F	7 y	5040		no	NA	No	no	no effect	no effect
45, 33, F	4 m	540*		PS	NA	DCM	mild ID, severe DD	untreated	NA
46, 33,M	9 m	3960		DS	no		no	beneficial effect	NA
47, 33,M	7m	720		DS	no	HCM	mild ID, mild DD	beneficial effect	NA
48, 34, F	neonatal	2880		DS	no	HCM, DCM	mild ID, mild DD	no effect	Beneficial effect
49, 35, F	1 y	3960*		PS	no	HCM	mild ID, mild DD	NA	NA
50, 36,M	neonatal	1080	hydronephrosis left, IGR	no	no	no	mild DD	NA	NA
51, 37, F	2 m	180*		PS	NA	HCM, DCM	NA	untreated	NA
52, 37,M	10 y	4680		PS	no	HCM	mild ID, mild DD	beneficial effect	NA
53, 38,M	9 m	270*		PS	no	HCM	no	untreated	NA
54, 38,M	9 m	3210		PS	PS	HCM	severe ID, mild DD	beneficial effect	NA
55, 38,M	prenatal	280		PS	PS	HCM	mild ID, mild DD	beneficial effect	NA
56, 39, F	neonatal	1*	oligoidramnios, IGR, decreased child movements	PS	NA	HCM	NA	untreated	NA
57, 40,M	neonatal	28*		no	no	no	NA	no effect	NA
58, 40,M	6 m	210*		NA	NA	NA	no	untreated	NA
59, 41,M	2 y	13680		PS	no	HCM	mild DD	no effect	NA
60, 41,M	9 y	15840		DS	NA	NA	no	no effect	NA
61, 42, F	2 m	NA		PS	NA	HCM	no	NA	NA
62, 43, F	2 y	1080		PS	NA	HCM	no	untreated	NA
63, 44,M	neonatal	3240		PS	no	HCM	mild DD	beneficial effect	NA
64, 45, F	1 y	6000		PS	no	HCM	mild DD	beneficial effect	NA
65, 46,M	infancy	15840*		PS	NA	HCM, DCM	no	NA	NA
66, 46,M	neonatal	5760		PS	no	HCM	no	no effect	NA
67, 47,M	neonatal	60*		PS	NA	HCM	severe DD	no effect	NA
68, 48,M	2 y	1260		PS	no	HCM, DCM	mild DD	beneficial effect	NA
69, 49, F	10 m	1350		PS	no	HCM, DCM	mild DD	beneficial effect	NA
70, 50, F	4 m	2340		no	no	no	mild ID, mild DD	beneficial effect	NA

Table S3: Clinical characteristics of 70 patients with mutations in *ACAD9*, DCM = Dilated Cardiomyopathy, DD = developmental delay, DS = developing symptom, HCM = Hypertrophic cardiomyopathy, ID = intellectual disability; PS = presenting symptom; NA = not available

	Number	n available	Percent
Prenatal findings			
Cardiomegaly	1	60	2
Rhythm abnormalities	2	60	3
Decreased child movements	1	60	2
Oligohydramnios	4	60	7
Intrauterine growth failure	6	60	10
Neonatal course			
Lactic acidosis	21	63	33
Cardiomyopathy	15	63	24
Rhythm abnormalities	4	54	7
Respiratory failure necessitating artificial ventilation	6	54	11
Severe liver dysfunction/failure	2	54	4
Severe renal dysfuntion/failure	2	54	4
Most frequent clinical findings			
Cardiomyopathy at presentation/ during course	44/56	66/66	67/85
Muscular weakness at presentation/ during course	21/37	48/49	44/75
Exercise intolerance at presentation/ during course	21/34	49/47	43/72
Neurological findings			
Severe intellectual disability (clinical impression)	1	51	2
Mild intellectual disability (clinical impression)	14	48	29
Severe developmental delay (clinical impression)	4	52	8
Mild developmental delay (clinical impression)	23	51	45
Optic atrophy, retinits pigmentosa	0	70	0
Neuroradiological findings			
MRI: basal ganglia alterations	4	24	17
MRI: leukoencephalopathy	5	21	24
MRI: global brain atrophy	2	20	10
MRI: isolated cerebellar atrophy	1	20	5
MRS: lactate peak (any location)	2	16	13
Activities of daily living			
Age adequate behaviour	27	39	69
Attending/finished regular school	26	41	63
Able to sit independently	34	42	81
Able to walk independently	33	41	80
Able to eat and drink independently	33	41	80
Able to perform personal hygiene independently	30	41	73
Able to communicate with words/ sentences	34/31	43/42	79/74

Table S4: Clinical features of the ACAD9 cohort (taken from [220])

6.1.3 MTFMT patients – additional information

Supp. Table 3 Genetic and phenotypic findings in MTMFT - mutant individuals

Patient ID	Sex	AO	Age	Variations: Nucleotide	Variations: Amino Acid	OXPHOS activities in muscle: RCC	OXPHOS activities in muscle: % of lower control range	MRI	Clinical features
#33009[a]	M	17 y	17 y[b]	c.146_153del c.626C>T	p.Arg49Leufs*58 p.Arg181Serfs*5	I IV	65% Normal	T_2-hyperintensities in midbrain and crus cerebri	Slight developmental delay in childhood, episode of fatigue and disturbed vision at age 17 y, ventricular septum defect, lactic acidosis in CSF, deceased at age 17 y after cardiosurgery.
#33467[a]	M	15 y	22 y	c.146_153del c.626C>T	p.Arg49Leufs*58 p.Arg181Serfs*5	I IV	76%, 50%[b] 100%, 81%[b]	T_2-hyperintensity in midbrain and patchy signal changes in white matter	Developmental delay in childhood, short stature and growth hormone deficiency, at age 15 y acquired strabism of the right eye, unstable gait and muscular hypotonia. Increased serum and CSF lactate levels. No COX-negative fibres in histochemistry. Clinically stable condition at age 22 y.
#49728	F	1 m	14 m[b]	c.626C>T c.878G>A	p.Arg181Serfs*5 p.Ser293Asn	I IV	21% 49%	Symmetric T_2-hyperintensities in putamen, globus pallidus and brainstem	Microcephaly, "metabolic stroke", convulsions, episode with severe lactic acidosis; deceased at age 14 m. Histochemistry mild lipid accumulation in type I fibers.
#52181	F	2 m	19 m[b]	c.219_222del c.626C>T	p.Glu74Lysfs*3 p.Arg181Serfs*5	I IV	21% Normal	Symmetric T_2-hyperintensities of the nucleus caudatus, globus pallidus and mesencephalon, extensive damage of the white matter with cystic lesions	Microcephaly, severe muscular hypotonia and developmental delay; deceased at age 19 m due to respiratory failure during pneumonia. No COX-negative fibres in histochemistry.
#54502	M	3 m	6 y	c.626C>T c.994C>T	p.Arg181fs*5 p.Arg332*	I IV	65%, 21%[c] 45%, Normal[c]	T_2-hyperintensities in subcortical frontal and parietal white matter, splenium callosum	Developmental delay, muscular hypotonia, intermittent strabism. Lactic acidosis. No COX-negative fibres in histochemistry.
#56713	M	8 m	6 y	c.73C>T c.626C>T	p.Gln25* p.Arg181Serfs*5	I IV	64% 100%	Symmetric T_2-signal intensive lesions of the putamen and globus pallidus Pinealis cyst	Microcephaly, truncal hypotonia, ataxia. At 4 y cognitive and speech development retarded by about 1.5 y..
#56902	M	20 m	5 y	c.452C>T c.994C>T	p.Pro151Leu p.Arg332*	I IV	89% 80%	Periventricular T_2-signal intense lesions, confluent in the centrum semiovale, lesion in the splenium callosum	Loss of gait during infection, severe muscular hypotonia. Microcephaly, growth retardation. Serum and CSF lactic acidosis. Non-compaction cardiomyopathy. Merosin-deficient but no SDH or COX-negative fibres in histochemistry.
#73922	M	birth	15 n	c.452C>T c.626C>T	p.Pro151Leu p.Arg181Serfs*5	I IV	7% 92%	Mild cortical atrophy and myelination delay at age 7 m	Muscular hypotonia, lactic acidosis. Mild hypertrophic cardiomyopathy. Body height, length and head circumference 1^{st}-10^{th} percentile.
#8432723	M	birth	12 y	c.626C>T c.766C>T	p.Arg181Serfs*5 p.Gln256*	I IV	43% normal	Periductal T_2-signal intense grey matter lesions and white matter involvement at the centrum semiovale	Severe developmental delay, abnormal breathing pattern; short stature and microcephaly; lactic acidosis; relative COX-deficiency in muscle histochemistry.
#44409 (Haack et al)	M	3 y	24 y	c.626C>T c.994C>T	p.Arg181Serfs*5 p.Arg332*	I IV PDHc	38% Normal 75%	T_2-signal intensive lesions of caudate nucleus, putamen, medulla oblongata and periventricular white matter	External ophthalmoplegia, partial optic atrophy, mental retardation, tetraspasticity (lower>upper limbs), neurosensoral bladder dysfunction, stable condition.
#61606 (Haack et al)	F	16 m	6.5 y	c.626C>T c.626C>T	p.Arg181Serfs*5 p.Arg181Serfs*5	I IV	12% Normal	T_2-signal intensive bilateral lesions of the putamen and in the fronto-parietal white matter	Microcephaly, ataxia, muscular hypotonia. Retardation of gross a fine motor development and social skills.
P1 (Tucker et al)	F	9 y	21 y	c.382C>T c.626C>T	p.Arg128* p.Arg181Serfs*5	I (III) IV	Decreased Low normal Decreased	T_2-hyperintensities in the Nn lentiformis, caudatus, and ruber, midbrain tectum, corpus callosum, and subcortical white matter	Acquired strabism (internuclear ophthalmoplegia), pale optic discs, developmental / mental retardation, elevated lactic acid and pyruvate levels, Wolff-Parkinson-White syndrome.
P1 cousin	M	9 y	18 y	c.382C>T c.626C>T	p.Arg128* p.Arg181Serfs*5	I IV	Decreased Decreased	"signal abnormality" affecting periaqueductal grey matter of midbrain and upper pons	Developmental delay, optic atrophy, mild bilateral pyramidal tract signs, impaired visual acuity, mildly dysmorphic facies, elevated CSF lactic acid levels, Wolff-Parkinson-White syndrome, episode of acute deterioration with weakness and ataxia, good recovery.
P2 (Tucker et al)	F	5 y	5 y[b]	c.374C>T c.626C>T	p.Ser125Leu p.Arg181Serfs*5	I III IV	Decreased Decreased Decreased	Hyperintensities in putamen, globus pallidus and brainstem	Cushing disease due to pituitary adenoma, elevated lactic acid levels in CSF, seizures following anesthesia, neurologic deterioration.
P1 (Neeve et al.)	F	3 y	16 y	c.452C>T c.994C>T	p.Pro151Leu p.Arg332*	I IV IV (Fib)	59% 78% Normal	T_2-hyperintensities in nucleus caudatus, putamen. Abnormalities in dorsal periventricular white matter.	Developmental delay, muscular hypotonia, atxic gait, dysarthria. Subsacrolemmal accumulation of mitochondria, no COX-negative or ragged red fibres.
P2 (sister P1) (Neeve et al.)	F	5 y	6 y	c.425C>T c.994C>T	p.Pro151Leu p.Arg332*	N.d.		Normal at 4 y of age	Developmental delay, muscular hypotonia, tremor.

M, male; F, female; m, months; N.d., not determined; y, years; RCC, mitochondrial respiratory chain complex; PDHc, Pyruvate dehydrogenase complex; AO, Age at onset; CSF, cerebrospinal fluid; MRI, magnetic resonance imaging; [a] these individuals are siblings; [b] patient deceased.
Reduced activity values of respiratory chain complexes(RCC) I, II, III, IV are given in relation to citrate synthase (CS) activity in mUnit / mUnit CS in percent of the lower control range.

Table S5: Mutations and clinical feature of patients with mutations in *MTFMT*

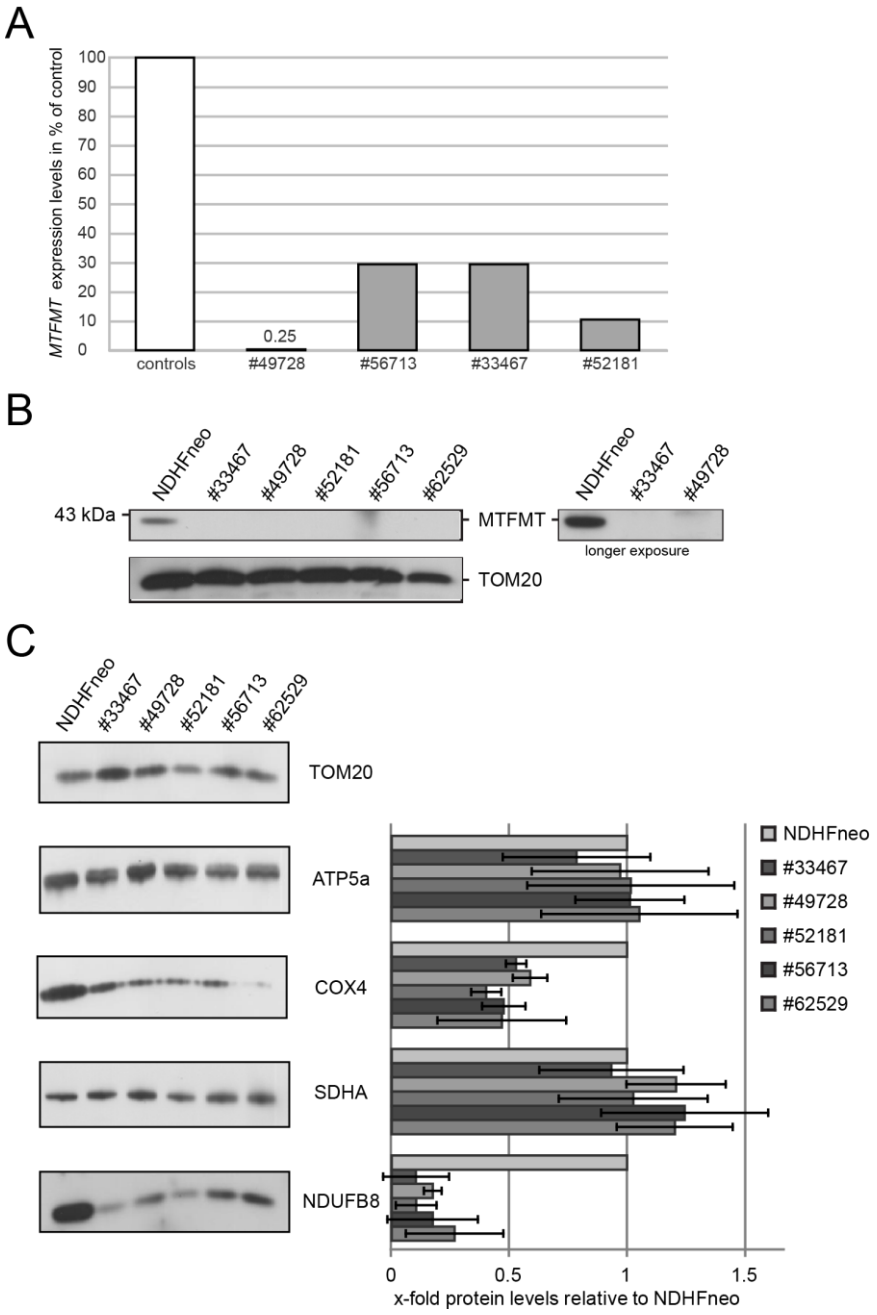

Figure S1: Quantification of MTFMT expression by qPCR (A) and immunoblot investigation of steady state levels of MTFMT (B) and respiratory chain complexes (C). qPCR values are mean of two measurements and are given relative to the mean of three controls. Values of quantified OXPHOS subunits have been corrected for loading of mitochondrial proteins (TOM20) and represent the mean of three experiments relative to a control. Error bars indicate +/- 1 standard deviation (taken from [226].)

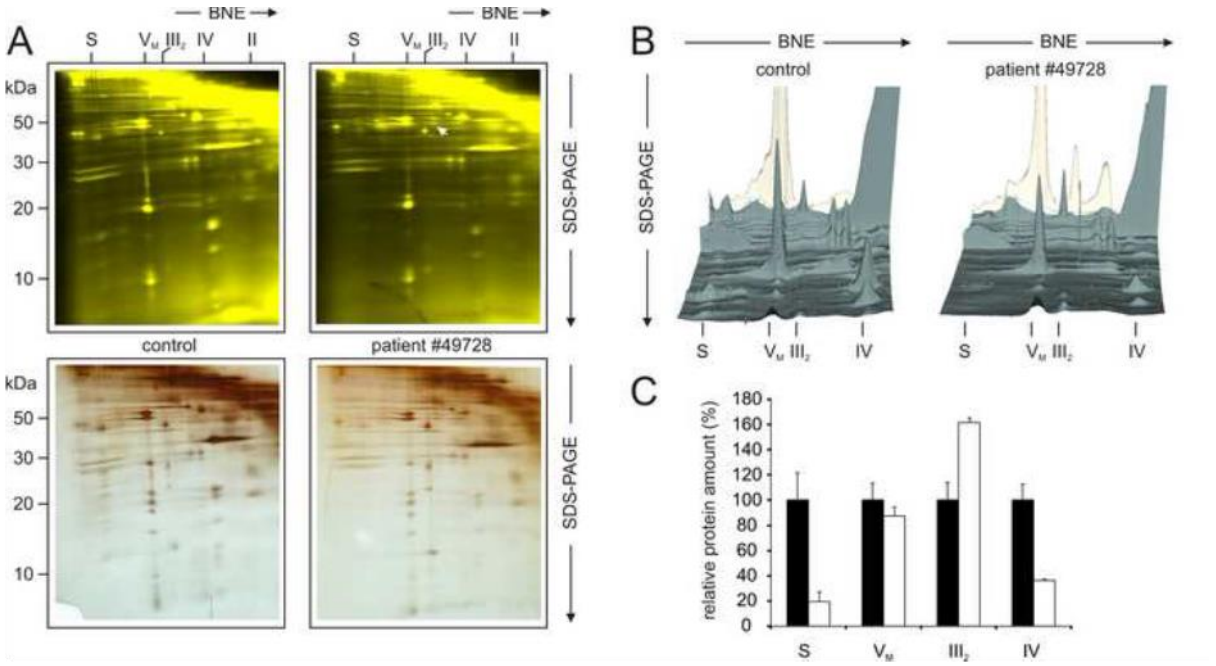

Figure S2: 2D-BN-SDS Gel showed the decreased supercomplex assembly in patient 49728 (C = healthy control, P = Patient 49728)

6.1.4 Gene expression experiment – additional data

The following list gives an overview of patient cell lines included into the gene expression experiment

FibroID	Mutation	Response to bezafibrate treatment (CI activity)
NHDF-neo	control	+ 12,9
47041	control	+9,8
45863	control	+14,5
33545	NDUFA1	+ 15,5
33255	NDUFS1	+ 68,8
33023	XPNPEP3	n.d.
18699	tRNA	+ 5,9
33460	NDUFS1	+ 88,6
47103	NDUFB9	+ 12,0
33027	NDUFS8	+ 12,4
33464	ND3	+ 12,6
45157	ND1	+ 2,4
33461	unclear	n.d.
33281	unclear	+ 34,9
33008	unclear	+9,8

Table S6. Selection of patient cell lines used in the gene expression experiment

Genes	function	Fold-change	p-value
CDA	Cytidine deaminase	- 1,84	6,2E-05
RGS12	guanosine triphosphatase (GTPase)-activating protein, transcriptional repressor	- 1,36	2,933E-05
RCE1	maintenance and processing of CAAX-type prenylated proteins	- 1,36	4,838E-05
RUVBL1	Possesses single-stranded DNA-stimulated ATPase and ATP-dependent DNA helicase (3' to 5') activity	- 1,32	4,616E-05
UCK2	Uridine-cytidine kinase 2	- 1,23	7,992E-05
SKAP2	adaptor protein, essential role in the src signalling pathway, inhibition of PTK2B/RAFTK activity and regulation of alpha-synuclein phosphorylation, involvement in B-cell and macrophage adhesion processes	+ 1,55	3,805E-06
MARK4	encodes a member of the microtubule affinity-regulating kinase family, it kinases phosphorylate microtubule-associated proteins and regulates the transition between stable and dynamic microtubules	+ 1,57	4,229E-05
CART1	Unclear in humans, in rodents, necessary for survival of the forebrain mesenchyme and may also be involved in development of the cervix	+ 1,58	4,317E-05
FZD6	Encodes 7-transmembrane domain proteins that are receptors for WNT signalling proteins	+ 1,59	3,894E-06
PJA2	Responsible for ubiquitination of cAMP-dependent protein kinase type I and type II-alpha/beta regulatory subunits and for targeting them for proteasomal degradation	+ 1,64	4,329E-05

Table S7: List of genes with the highest fold-change after 3-day bezafibrate treatment

List of all 45 genes which were significantly downregulated between control and complex I patients. Yellow highlighted genes are especially interesting and genes marked in green were detected in the gene expression and the DIGE experiment.

Gene	Illumina ID	p-value	fold-change
ADAMTSL4	ILMN_1777683	7,6599E-05	-1,22
C10ORF37	ILMN_1747741	4,0925E-05	-1,28
C11ORF31	ILMN_1786872	9,7788E-06	-1,26
C12ORF48	ILMN_1654429	1,9707E-05	-1,31
CDA	ILMN_1714592	6,2176E-05	-1,84
CHST10	ILMN_1736828	2,3874E-05	-1,22
CXORF15	ILMN_2134176	8,9823E-06	-1,30
DDX23	ILMN_1784218	2,7678E-05	-1,21

DKFZP686O24166	ILMN_1669972	9,7744E-05	-1,29
FAF1	ILMN_1667016	2,5006E-05	-1,19
FAM57A	ILMN_1673899	6,4104E-08	-1,36
HBB	ILMN_2100437	4,6896E-05	-1,20
HS.136697	ILMN_1849435	1,5924E-06	-1,20
HS.201113	ILMN_1867174	4,261E-05	-1,18
HS.353697	ILMN_1853257	1,4666E-06	-1,15
HS.536981	ILMN_1860238	2,6884E-05	-1,11
HS.538971	ILMN_1869196	4,575E-05	-1,09
HS.545467	ILMN_1855310	6,6695E-06	-1,20
HS.559999	ILMN_1907847	1,489E-05	-1,22
HS.561241	ILMN_1916341	8,665E-06	-1,16
HS.571887	ILMN_1823809	8,3949E-05	-1,15
HS.572030	ILMN_1879326	6,6145E-05	-1,30
HS.576103	ILMN_1908210	2,1409E-06	-1,16
IQCE	ILMN_1689220	3,9566E-06	-1,15
LEO1	ILMN_1801553	9,8063E-06	-1,16
LOC642732	ILMN_1651507	4,0359E-05	-1,33
LOC642780	ILMN_1752798	3,0181E-05	-1,66
LOC644707	ILMN_1659023	7,7356E-05	-1,12
LOC646976	ILMN_1658905	4,1904E-05	-1,18
LOC649443	ILMN_1666798	4,2424E-06	-1,15
LOC730684	ILMN_1909473	6,1463E-08	-1,15
MRPL46	ILMN_1722838	1,6413E-05	-1,18
NXT1	ILMN_1760280	3,1121E-05	-1,30
PLAG1	ILMN_1674280	9,2382E-05	-1,11
PSD4	ILMN_2154115	3,9892E-05	-1,22
PVRL1	ILMN_1695549	6,2035E-05	-1,26
RCE1	ILMN_2337492	4,838E-05	-1,36
RGS12	ILMN_1791314	2,9326E-05	-1,36
RUVBL1	ILMN_1693108	4,616E-05	-1,32
SFRS12IP1	ILMN_1728001	1,2981E-05	-1,21
SIP1	ILMN_2344002	4,5281E-05	-1,29
TOR3A	ILMN_1768181	5,9822E-05	-1,32
UCK2	ILMN_1768662	7,9921E-05	-1,23
ZNF585B	ILMN_1773835	8,3778E-05	-1,15
ZNF597	ILMN_2162358	5,5311E-05	-1,25

Table S8: List of all significantly changed downregulated between control and 13 complex I patients

List of all 52 genes which were significantly upregulated between control and complex I patients. Yellow highlighted genes are especially interesting and genes marked in green were detected in the gene expression and the DIGE experiment.

Gene	Illumina ID	p-value	fold-change
C10ORF113	ILMN_1770130	4,6679E-07	1,29
C7ORF28A	ILMN_1784166	6,0962E-05	1,20
CACNA1C	ILMN_1898404	6,5983E-06	1,26
CAMK2B	ILMN_2279796	4,1293E-05	1,36
CAPZB	ILMN_2053921	9,6652E-05	1,18
CART1	ILMN_1724540	4,3173E-05	1,58
CST5	ILMN_1688022	6,1694E-05	1,21
DHH	ILMN_1799996	9,501E-05	1,34
DNAH8	ILMN_1763775	2,7985E-05	1,23
DOC2A	ILMN_1812477	3,9858E-05	1,11
DUOX2	ILMN_1786335	1,3738E-06	1,16
FABP6	ILMN_1721559	9,2441E-05	1,18
FZD6	ILMN_1659297	3,8939E-06	1,59
HS.23246	ILMN_1823083	8,7579E-05	1,13
HS.382131	ILMN_1840957	4,6737E-05	1,14
HS.540965	ILMN_1850677	4,4704E-06	1,17
HS.543313	ILMN_1875874	6,2211E-05	1,16
HS.554319	ILMN_1863308	6,2164E-05	1,14
HS.560586	ILMN_1843728	5,6714E-05	1,14
HS.572657	ILMN_1895025	2,1628E-05	1,23
HS.582861	ILMN_1902433	9,83E-06	1,49
KRT82	ILMN_1676086	2,7064E-06	1,23
LCE1E	ILMN_1689849	9,3679E-05	1,29
LOC345222	ILMN_2367290	2,1473E-05	1,31
LOC651100	ILMN_1683920	3,3328E-06	1,16
LOC651974	ILMN_1775525	3,7246E-05	1,22
MARK4	ILMN_1651604	4,2293E-05	1,57
MED23	ILMN_1690999	6,8485E-05	1,19
MYO1B	ILMN_2093027	6,5282E-05	1,35
OAS1	ILMN_1672606	1,4802E-05	1,19
OR2T8	ILMN_1771209	6,9349E-05	1,26
PCBP3	ILMN_1687216	1,3152E-06	1,35
PIGA	ILMN_1802390	7,4198E-05	1,33
PIGN	ILMN_2352724	5,8252E-05	1,22
PJA2	ILMN_1688702	4,3289E-05	1,64
PPP1R1B	ILMN_1690096	7,1286E-05	1,28
PRUNE2	ILMN_2075526	3,2652E-05	1,33
PSD3	ILMN_1717477	1,9039E-06	1,43
RB1CC1	ILMN_1736796	3,3606E-05	1,23
RC3H2	ILMN_1710738	9,1549E-05	1,25
RNF141	ILMN_1815010	1,0618E-05	1,35
SKAP2	ILMN_2125010	3,8047E-06	1,55
SLC9A2	ILMN_1738849	7,051E-05	1,30

STX12	ILMN_1773901	8,4206E-05	1,21
SULT1A1	ILMN_1778756	8,2198E-06	1,26
TMPRSS3	ILMN_1675677	7,0672E-05	1,16
TTRAP	ILMN_2183216	5,0399E-05	1,41
UQCRH	ILMN_1792138	5,592E-06	1,30
USP8	ILMN_2094587	8,671E-05	1,28
WDR78	ILMN_2251225	4,0288E-05	1,31
WRB	ILMN_2085922	8,5279E-07	1,19
ZCCHC10	ILMN_2213680	8,3311E-05	1,19

Table S9: List of all significantly changed upregulated between control and 13 complex I patients

List of all 30 genes which were significantly downregulated after 72hrs bezafibrate treatment in controls and complex I patients.

Gene	Illumina ID	p-value	fold-change
AFAP1	ILMN_1660424	2,7688E-05	-1,21
APITD1	ILMN_1660424	4,0782E-05	-1,22
CDKN2D	ILMN_1748883	8,5985E-05	-1,18
CXCL6	ILMN_2161577	3,1443E-05	-1,56
ESM1	ILMN_1773262	1,9719E-06	-1,45
FCRLB	ILMN_1782015	8,1838E-08	-1,29
FJX1	ILMN_1746465	1,9766E-08	-1,25
FLJ37228	ILMN_1809167	2,5806E-05	-1,22
FST	ILMN_1712896	2,8878E-05	-1,23
HS.388347	ILMN_1898518	5,5733E-05	-1,23
HS.539368	ILMN_1865340	4,9184E-05	-1,11
HSPA5	ILMN_1773865	1,1553E-05	-1,20
IL8	ILMN_2184373	9,4691E-06	-1,46
INPP4B	ILMN_2198878	7,2051E-05	-1,21
KIAA1524	ILMN_1728225	7,4287E-05	-1,32
KRT19	ILMN_1730777	9,3079E-05	-1,70
LOC653492	ILMN_1771123	7,7614E-05	-1,20
LOC728285	ILMN_1660067	8,9291E-05	-1,39
LOC728758	ILMN_2134855	1,1302E-05	-1,25
LOC728946	ILMN_1669119	5,657E-05	-1,48
MCCC1	ILMN_1760174	8,7613E-05	-1,14
MMP12	ILMN_1768035	3,1199E-05	-1,36
SDF2L1	ILMN_1749213	1,2829E-05	-1,22
SEMA3A	ILMN_1765641	9,0615E-05	-1,14
SLC7A14	ILMN_1676602	6,7668E-06	-1,49
SNX7	ILMN_2290686	1,7158E-05	-1,20
STAMBPL1	ILMN_1682799	9,4598E-05	-1,22
THAP10	ILMN_1767542	4,1093E-05	-1,22

TRIM6	ILMN_1656910	1,4172E-05	-1,14
WEE1	ILMN_1778561	2,0492E-05	-1,24

Table S10: List of all downregulated genes after bezafibrate treatment in patients and controls

List of all 62 genes which were significantly upregulated after 72hrs bezafibrate treatment in controls and complex I patients. Yellow highlighted genes are especially interesting and genes marked in green were detected in the gene expression and the DIGE experiment

Gene	Illumina ID	p-value	fold-change
ABCA1	ILMN_1766054	1,6802E-07	1,81
ABCC3	ILMN_1677814	1,5746E-10	1,90
ACAA2	ILMN_1660199	3,5475E-08	1,69
ACADVL	ILMN_2352009	1,9393E-09	2,05
ADFP	ILMN_1801077	2,4491E-10	3,54
AFF3	ILMN_1775235	7,9553E-05	1,23
AKR1C2	ILMN_2412336	7,9729E-06	1,35
ALDH1A3	ILMN_2139970	3,1799E-06	1,61
ALDH1A3	ILMN_1807439	2,0519E-05	1,74
ANGPT1	ILMN_1677723	5,7553E-06	1,24
ANGPTL4	ILMN_1707727	4,1544E-12	11,41
ASPA	ILMN_1692824	1,2475E-05	1,51
ASS1	ILMN_1708778	4,5609E-06	1,94
C5ORF33	ILMN_1698770	4,6739E-05	1,24
C7orf67	ILMN_1790315	2,5437E-05	1,31
CAT	ILMN_1651705	1,6593E-07	1,62
CD36	ILMN_1796094	4,1532E-05	1,28
CFD	ILMN_1777190	2,1113E-05	1,51
CHSY3	ILMN_1740407	4,8763E-05	1,19
CLDND2	ILMN_2077680	2,7283E-06	1,57
CLIC3	ILMN_1796423	1,8027E-05	1,24
CPT1A	ILMN_1696316	1,6796E-09	2,00
CPT1B	ILMN_1791754	1,5741E-07	1,55
CRYAB	ILMN_1729216	4,147E-05	1,36
DBC1	ILMN_1741603	2,7728E-06	1,27
DNHL1	ILMN_2052495	3,8181E-05	1,12
ECH1	ILMN_1653115	1,5497E-06	1,80
ETFA	ILMN_1718924	5,9415E-06	1,29
ETFB	ILMN_2300970	6,6989E-05	1,24
ETFDH	ILMN_1758034	4,0445E-05	1,36
FAM113B	ILMN_1712431	7,8476E-05	1,26
GPC4	ILMN_1789502	4,4617E-08	1,56
HADHB	ILMN_2197846	4,5791E-05	1,31
HS.374023	ILMN_1861270	5,9989E-05	1,55

IGFBP4	ILMN_1665865	1,3089E-05	1,48
IL7R	ILMN_1691341	4,5308E-06	1,33
IMPA2	ILMN_2094061	4,1575E-09	2,16
IMPDH2	ILMN_1705737	2,8632E-06	1,14
INSC	ILMN_2340643	4,4392E-05	1,26
ITGA3	ILMN_1685397	9,82E-05	1,28
JAG1	ILMN_1691376	5,2353E-05	1,22
KLF11	ILMN_1751656	1,4678E-11	2,18
KRT7	ILMN_2163723	1,4884E-05	1,54
LOC642506	ILMN_1663935	9,7738E-05	1,16
MBOAT5	ILMN_1805225	3,1431E-05	1,20
MMD	ILMN_1733937	8,519E-06	1,34
MPPE1	ILMN_1776515	1,625E-05	1,18
OR11H1	ILMN_2072401	2,9108E-05	1,27
PDK4	ILMN_1684982	2,3623E-10	8,73
PHGDH	ILMN_1704537	7,3553E-06	1,23
RCAN1	ILMN_2367239	6,8482E-05	1,24
SEMA7A	ILMN_1756312	3,5811E-05	1,28
SLC16A5	ILMN_1755649	1,7504E-05	1,30
SLC1A1	ILMN_1658917	9,8168E-08	1,38
SLC25A20	ILMN_1741392	7,1229E-07	1,58
SLC38A4	ILMN_1794890	2,391E-05	1,44
STEAP2	ILMN_1809101	9,3008E-06	1,25
TMED5	ILMN_1803279	7,7211E-06	1,27
TMEM135	ILMN_1700202	2,5081E-08	1,35
TNFRSF21	ILMN_1699695	1,0074E-06	1,60
WFS1	ILMN_1759023	3,643E-08	1,41
ZBED5	ILMN_1664424	2,1321E-06	1,13

Table S11: List of all upregulated genes after bezafibrate treatment in patients and controls

6.1.5 DIGE experiment – additional data

The following list gives an overview of patient cell lines included into the DIGE experiment

FibroID	Mutation	Complex I activity	Response to bezafibrate treatment
NHDF-neo	WT	100	+ 12,0
35834	ACAD9	35,7	+ 89,5
52674	ACAD9	48,0	+ 42,5
52933	ACAD9	36,6	+ 141,0

52935	ACAD9	43,1	+ 53,4

Table S12: Selection of patient cell lines used in the DIGE experiment

List of all 53 significantly down regulated proteins between controls and ACAD9 patients identified with ESI/Maldi/MS in the 2D-DIGE Gel experiment. The yellow highlighted proteins are the most interesting ones.

Spot No	Protein	AC Nr	Localisation	Mass	PI	p-value	Fold-change
1287	ACO1	P21399	Cytoplasma	98399	6,23	4,50E-05	-1,95
1506	ACSL4	O60488	Mitochondrion outer membrane	79188	8,66	0,021	-1,36
1683	AIFM1	O95831	Mitochondrion intermembrane space and inner membrane	55812	6,86	0,036	-1,56
1445	ALDH18A1	P54886	Mitochondrion inner membrane	87302	6,66	0,041	-1,17
2197	ALDH1B1	P30837	Mitochondrion matrix	55280	5,96	0,0024	-1,71
1290	ALDH1L2	Q3SY69	Mitochondrion	101746	6,13	6,00E-05	-2,1
2166	ALDH7A1	P49419	Mitochondrion, Nucleus	55584	6,47	0,00061	-1,56
2247	ALDH9A1	P49189	Cytoplasma	53670	5,69	0,0011	-1,42
2714	ALDOC	P09972	Nucleus, Cytoplasm	39324	6,46	0,0095	-1,58
1698	ANXA6	P08133	Cytoplasm	75742	5,41	9,30E-05	-3,53
2205	ATP5A1	P25705	Mitochondrion inner membrane	55209	8,29	0,011	-1,53
3284	ATP5C1	P36542	Mitochondrion, Mitochondrion inner membrane	30165	9,02	0,057	-1,21
1703	ATP6V1A	P38606	Ubiquitous	68304	5,34	0,0056	-1,61
2161	ATP6V1B2	P21281	Endomembrane system, Peripheral membrane protein, Melanosome	56500	5,57	0,003	-1,57
2406	BCKDHA	P12694	Mitochondrion matrix	45513	6,32	0,033	-1,15
3689	CHCHD3	Q9NX63	Mitochondrion inner membrane	26021	8,5	0,034	-1,36
3658	CLPP	Q16740	Mitochondrion matrix	24165	5,56	0,0046	-1,64
1938	CPNE3	O75131	Ubiquitous	59999	5,6	0,0011	-1,46
3284	DECR1	Q16698	Mitochondrion	32149	8,79	0,057	-1,21
2021	DLD	P09622	Mitochondrion matrix	55024	6,5	0,0017	-1,49
2247	DLST	P36957	Mitochondrion	41389	5,9	0,0011	-1,42
3708	ECHS1	P30084	Mitochondrion matrix	28342	5,88	0,0002	-1,31
3351	ETFA	P13804	Mitochondrion matrix	34450	7,2	0,0015	-1,6
3708	ETHE1	O95571	Mitochondrion matrix	26491	6,05	0,0002	-1,31
1589	FKBP9	O95302	Endoplasmic reticulum	60371	4,84	0,029	-1,37
1965	GLB1	P16278	Lysosome, Cytoplasm, perinuclear region	73035	5,89	8,90E-07	-2,21
2157	GLS	O94925	Mitochondrion	71560	7,01	0,0032	-1,65
1614	HADHA	P40939	Mitochondrion	79009	8,98	0,025	-1,34
2460	HADHB	P55084	Mitochondrion	47484	9,24	0,00092	-1,44

3852	HSD17B10	Q99714	Mitochondrion	26791	7,87	0,019	-1,94
1698	HSPA8	P11142	Cytoplasm, Melanosome	70766	5,37	9,30E-05	-3,53
1657	HSPA9	P38646	Mitochondrion	68759	5,44	0,0046	-1,5
1400	IMMT	Q16891	Mitochondrion inner membrane	83678	6,08	1,10E-05	-2,06
1431	KIAA1279	Q96EK5	Mitochondrion	71814	5,34	0,019	-1,18
1631	LMNA	P02545	Nucleus. Nucleus envelope	73808	6,57	1,60E-05	-2,28
1180	LONP1	P36776	Mitochondrion matrix	99358	5,64	0,009	-1,56
883	LRPPRC	P42704	Mitochondrion	151839	5,53	0,0004	-1,27
3284	MTCH2	Q9Y6C9	Mitochondrion inner membrane	33199	8,28	0,057	-1,21
2817	NDUFA10	O95299	Mitochondrion matrix	37147	6,87	0,00038	-1,82
1445	OPA1	O60313	Mitochondrion inner membrane	111631	6,04	0,041	-1,17
3008	PDHB	P11177	Mitochondrion	35904	5,38	1,30E-05	-1,49
2022	PDIA3	P30101	Endoplasmic reticulum lumen	54265	5,61	0,0041	-1,49
1400	PDPR	Q8NCN5	Mitochondrion matrix	99364	5,73	1,10E-05	-2,06
2062	PHGDH	O43175	Plasma membrane, cytoplasma	56519	6,31	0,0021	-3,62
2197	PMPCA	Q10713	Mitochondrion matrix	54646	5,88	0,0024	-1,71
3967	PRDX3	P30048	Mitochondrion	21468	5,77	0,0069	-1,37
3343	PYCR1	P32322	Mitochondrion	33229	7,16	0,047	-1,44
1700	SDHA	P31040	Mitochondrion inner membrane	68012	6,25	0,024	-1,41
3561	SIRT3	Q9NTG7	Mitochondrion matrix	28534	5,65	1,50E-05	-2,05
3907	SSR2	P43308	Endoplasmic reticulum membrane, Single-pass type I membrane protein.	18273	7,03	0,069	-1,45
1631	TRAP1	Q12931	Mitochondrion	73546	6,13	1,60E-05	-2,28
3852	VDAC1	P21796	Mitochondrion outer membrane	30641	8,63	0,019	-1,94
3142	VDAC2	P45880	Mitochondrion outer membrane	31435	7,66	0,059	-1,05

Table S12: List of all significantly down regulated proteins between controls and ACAD9 patients identified with ESI/Maldi/MS

List of all 12 significantly upregulated proteins between controls and ACAD9 patients identified with ESI/Maldi/MS in the 2D-DIGE Gel experiment. The yellow highlighted proteins are the most interesting ones.

Spot No	**Protein**	**AC Number**	**Localisation**	**Mass**	**PI**	**p-value**	**Fold-change**
1781	ACADVL	P49748	Mitochondrion	66175	7,74	0,024	1,27
2145	ADSL	P30566	Ubiquitously	54758	6,73	0,0058	1,33
2772	ALDOA	P04075	Cytoplasm	39288	8,39	7,80E-06	2,81
2871	C12orf10	Q9HB07	Mitochondrion	37112	5,5	0,0048	7,51
2335	ENO1	P06733	Cytoplasm, Cell membrane	47037	6,99	0,097	2,77
1872	FUS	P35637	Nucleus	53426	9,4	0,017	1,52
1737	GAPDH	P04406	Cytoplasm	35922	8,58	0,00021	1,86
1596	GPD2	P43304	Mitochondrion	76361	6,3	0,00035	2,1
1566	HADHA	P40939	Mitochondrion	79009	8,98	0,0012	1,49

3166	HSD17B4	P51659	Peroxisome	33451	6,6	0,033	1,5
3157	MDH2	P40926	Mitochondrion matrix	33000	8,54	0,0095	1,61
2359	PGD	P52209	Cytoplasm	53008	6,88	0,061	2,08

Table S13: List of all significantly up- regulated proteins between controls and ACAD9 patients identified with ESI/Maldi/MS

List of all 12 significantly downregulated after bezafibrate treatment in controls and ACAD9 patients identified with ESI/Maldi/MS in the 2D-DIGE Gel experiment.

Spot No	Protein	AC Number	Localisation	Mass	PI	p-value	Fold-change
2346	ACOT9	Q9Y305	Mitochondrion	47694	7,79	0,014	-1,29
2376	ACTR3	P61158	Cytoplasm	47239	5,61	0,034	-1,09
2800	ALDOA	P04075	Cytoplasm	39288	8,39	0,014	-1,59
1822	CORO1B	Q9BR76	Cytoplasma, Cytoskeleton	54234	5,6	0,0046	-1,28
2335	ENO1	P06733	Cytoplasm, Cell membrane	47037	6,99	0,023	-1,26
2336	FH	P07954	Mitochondrion	50081	6,99	0,0064	-1,22
2998	GAPDH	P04406	Cytoplasm, cytosol, Nucleus	35922	8,58	0,0018	-1,16
3068	MTHFD2	P13995	Mitochondrion	34137	7,34	0,00021	-1,28
4300	MYL12B	O14950	Nucleus	19647	4,69	0,012	-1,22
2359	PGD	P52209	Cytoplasm	53008	6,88	0,036	-1,35
2789	TSTA3	Q13630	Vesicles, Cytoplasm	35892	6,12	0,0018	-1,11
2128	WARS2	Q9UGM6	Mitochondrion matrix	53034	5,83	0,038	-1,17

Table S14: List of all significantly down- regulated proteins after bezafibrate treatment in controls and ACAD9 patients identified with ESI/Maldi/MS

List of all 55 significantly upregulated proteins after bezafibrate treatment in controls and ACAD9 patients identified with ESI/Maldi/MS in the 2D-DIGE Gel experiment. The yellow highlighted proteins are especially interesting and proteins marked in green were detected in the gene expression and the DIGE experiment.

Spot No	Protein	AC Nr.	Localisation	Mass	PI	p-value	Fold-change
2637	ACAA2	P42765	Mitochondrion	41924	8,32	0,000065	1,73
1799	ACADVL	P49748	Mitochondrion	66175	7,74	0,00024	2,38
1485	ACSL4	O60488	Mitochondrion outer membrane	79188	8,66	0,011	1,54
1683	AIFM1	O95831	Mitochondrion intermembrane space and inner membrane	55812	6,86	0,026	1,13
1445	ALDH18A1	P54886	Mitochondrion inner membrane	87302	6,66	0,071	1,13
1302	ALDH1L2	Q3SY69	Mitochondrion	101746	6,13	0,048	1,17
1936	ALDH4A1	P30038	Mitochondrion	59034	6,96	0,000053	1,56
2247	ALDH9A1	P49189	Cytoplasma	53670	5,69	0,015	1,16

3284	ATP5C1	P36542	Mitochondrion, Mitochondrion inner membrane	30165	9,02	0,026	1,18
1703	ATP6V1A	P38606	Ubiquitous	68304	5,34	0,017	1,12
1930	CAT	P04040	Peroxisome	59624	6,95	0,016	1,22
3689	CHCHD3	Q9NX63	Mitochondrion inner membrane	26021	8,5	0,00019	1,34
3658	CLPP	Q16740	Mitochondrion matrix	24165	5,56	0,077	1,16
1938	CPNE3	O75131	Ubiquitous	59999	5,6	0,044	1,29
1720	DDX17	Q92841	Nucleus	80272	8,53	0,013	1,49
3284	DECR1	Q16698	Mitochondrion	32149	8,79	0,026	1,18
2247	DLST	P36957	Mitochondrion	41389	5,9	0,015	1,16
3383	ECH1	Q13011	Mitochondrion	32205	5,99	0,0005	1,71
2485	EIF4A2	Q14240	Cytoplasm, Cytoskeleton	46402	5,33	0,0062	1,22
3351	ETFA	P13804	Mitochondrion matrix	34450	7,2	0,0049	1,25
1829	ETFDH	Q16134	Mitochondrion inner membrane	64675	6,52	0,011	1,33
1872	FUS	P35637	Nucleus	53426	9,4	0,0088	1,50
2027	GLS	O94925	Mitochondrion	71560	7,01	0,048	1,24
547	GPD2	P43304	Mitochondrion	76361	6,3	0,015	1,41
3261	HADH	Q16836	Mitochondrion matrix	32838	8,38	0,015	1,17
1720	HADHA	P40939	Mitochondrion	79009	8,98	0,013	1,49
2497	HADHB	P55084	Mitochondrion	47484	9,24	0,0048	1,25
1720	HNRNPM	P52272	Nucleus	77384	8,85	0,013	1,49
3166	HSD17B4	P51659	Mitochondrion	33451	6,6	0,0091	1,16
2494	HSDL2	Q6YN16	Peroxisome	45394	8,07	0,0083	1,38
1917	HSPD1	P10809	Mitochondrion	61187	5,24	0,022	1,27
2575	IDH2	P48735	Mitochondrion	46614	8,32	0,0075	1,58
2940	IDH3A	P50213	Mitochondrion	36640	5,71	0,04	1,22
1431	KIAA1279	Q96EK5	Mitochondrion	71814	5,34	0,0082	1,15
3150	LDHA	P00338	Cytoplasm	36557	8,46	0,021	1,28
1807	LMNA	P02545	Nucleus, Nucleus envelope	73808	6,57	0,0056	1,95
1180	LONP1	P36776	Mitochondrion matrix	99358	5,64	0,079	1,18
883	LRPPRC	P42704	Mitochondrion	151839	5,53	0,046	1,20
3157	MDH2	P40926	Mitochondrion matrix	33000	8,54	0,014	1,19
1777	ME2	P23368	Mitochondrion matrix	63414	6,58	0,071	1,4
4390	MRPL18	Q9H0U6	Mitochondrion	20577	9,99	0,014	1,14
3284	MTCH2	Q9Y6C9	Mitochondrion inner membrane	33199	8,28	0,026	1,18
1361	MUT	P22033	Mitochondrion matrix	79340	5,98	0,036	1,17
1445	OPA1	O60313	Mitochondrion inner membrane	111631	6,04	0,071	1,13
3008	PDHB	P11177	Mitochondrion	35904	5,38	0,039	1,04
2068	PDIA3	P30101	Endoplasmic reticulum lumen	54265	5,61	0,021	1,21
3971	PRDX3	P30048	Mitochondrion	21468	5,77	0,024	1,18
3343	PYCR1	P32322	Mitochondrion	33229	7,16	0,081	1,10
1720	SLC25A13	Q9UJS0	Mitochondrion inner membrane	74175	8,79	0,013	1,49
3907	SSR2	P43308	Endoplasmic reticulum membrane, Single-pass type I membrane protein	18273	7,03	0,056	1,24

1436	TARS2	Q9BW92	Mitochondrion matrix	81036	7,31	0,03	1,22
3205	TOMM34	Q15785	Mitochondrion outer membrane	34559	9,12	0,0063	1,77
1631	TRAP1	Q12931	Mitochondrion	73546	6,13	0,045	1,24
962	UBA1	P22314	Nucleus, Cytoplasm	117849	5,49	0,0097	1,27

Table S15: List of all significantly up- regulated proteins after bezafibrate treatment in controls and ACAD9 patients identified with ESI/Maldi/MS

6.1.5 Lentiviral transduction- additional information

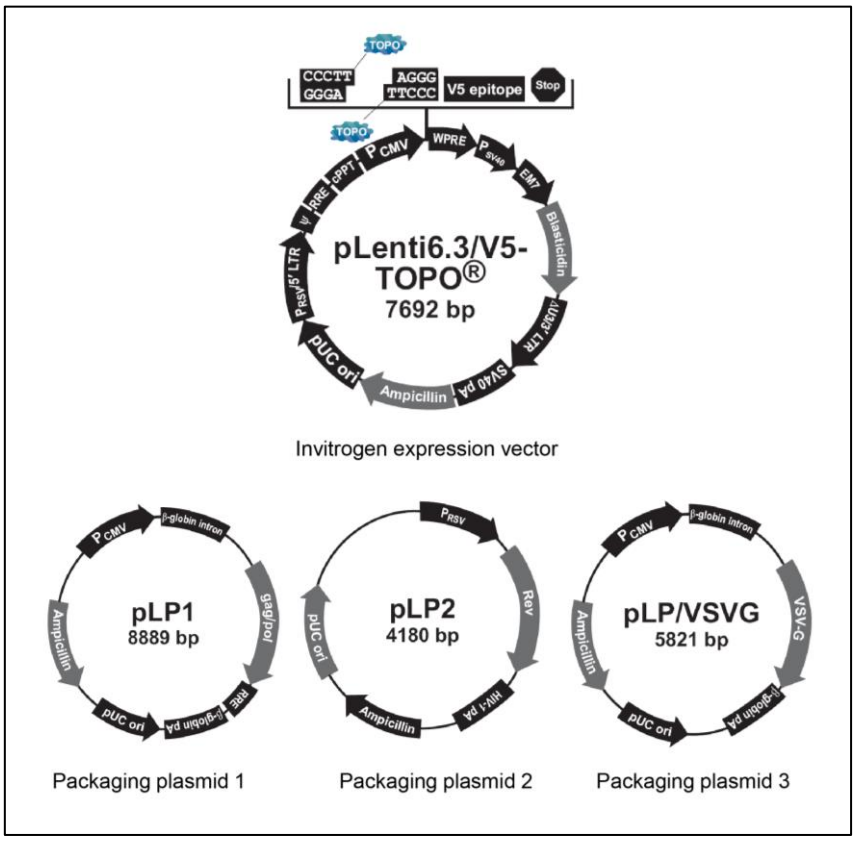

Figure S3: Vector card of the used p.Lenti6.3/V5 TOPO cloning vector and packaging plasmids (Invitrogen)

6.1.6 List of figures

6.1.7 List of tables

6.2 Acknowledgement

At this point I would like to thank all the people who are involved in many steps during my PhD time. Firstly; I would like to thank the Institute of Human Genetics for giving me the opportunity to work in this group. I especially want to thank Dr. Holger Prokisch for his guidance and critical but always useful comments on my work. I want to thank Prof. Dr. med. Thomas Meitinger for his financial support and giving me the opportunity to travel to numerous stimulating conferences.

My special thanks go to my doctoral thesis supervisor Prof. Dr. Jerzy Adamski for his support, help and straightforwardness and all the efforts he took to finish this project. I would like to thank Prof. Dr. Heiko Witt and Prof. Angelika Schnieke for their participation in my thesis committee.

A large part of this work has several cooperation partners whom I would also like to thank. Thanks a lot to Dr. Ilka Wittig and Valentina Strecker from the Goethe University Frankfurt for their multiple friendly receptions in their laboratories, the possibility of carrying out the various proteomic experiments and the many fruitful discussions. I would also like to thank Dr. Hans Mayr, Franz Zimmermann and Prof. Wolfgang Sperl from Salzburg for the implementation of enzymatic measurements and immunohistochemical experiments and for their valuable assistance.

Furthermore, I want to thank all past and present colleagues at the Institute of Human Genetics. Special thanks to: Arcangela, Robert, Marieta, Katharina, Caroline, Laura, Eliska, Michael, Caterina, Susanne, Thomas, Riccardo and Thomas. They were always supporting me with experience, help, advice and motivation and created an incredible friendly working environment.

All this would have never been possible without the love and support of my family. Thanks to my parents who constantly supported me my entire life and always keeping faith in me. I would like to thank my husband who was mentally supporting me every moment and being able to stand me during this time.
Saving the best for last, I would like to dedicate this thesis to my wonderful little daughters Theresa and Veronika.

7. Publications

Repp B, Mastantuono E, Alston C, Schiff M, Haack TB, Rötig A, Ardissone A, Lombès A, Catarino CB, Diodato D, Schottmann G, Poulton J, Burlina A, Jonckheere A, Munnich A, Rolinski B, Ghezzi D, Rokicki D, Wellesley D, Martinelli D, Wenhong D, Lamantea E, Ostergaard E, Pronicka E, Pierre G, Smeets HJM, Wittig I, Scurr I, de Coo IFM, Moroni I, Smet J, Mayr JA, Dai L, de Meirleir L, Schuelke M, Zeviani M, Morscher RJ, McFarland R, Seneca S, Klopstock T, Meitinger T, Wieland T, Strom TM, Herberg U, Ahting U, Sperl W, Nassogne MC, Ling H, Fang F, Freisinger P, Van Coster R, Strecker V, Taylor RW, Häberle J, Vockley J, Prokisch H, Wortmann S. , Clinical, biochemical and genetic spectrum of 70 patients with ACAD9 deficiency: is riboflavin supplementation effective? Orphanet J Rare Dis. 2018 Jul 19

Kremer LS, Bader DM, Mertes C, Kopajtich R, Pichler G, Iuso A, Haack TB, Graf E, Schwarzmayr T, Terrile C, Koňaříková E, **Repp B**, Kastenmüller G, Adamski J, Lichtner P, Leonhardt C, Funalot B, Donati A, Tiranti V, Lombes A, Jardel C, Gläser D, Taylor RW, Ghezzi D, Mayr JA, Rötig A, Freisinger P, Distelmaier F, Strom TM, Meitinger T, Gagneur J, Prokisch H, Genetic diagnosis of Mendelian disorders via RNA sequencing, Nat Commun. 2017 Jun,12;8:15824

Iuso A, **Repp B**, Biagosch C, Terrile C, Prokisch H, Assessing Mitochondrial Bioenergetics in Isolated Mitochondria from Various Mouse Tissues Using Seahorse XF96 Analyzer, Methods Mol Biol. 2017

Catarino CB, Ahting U, Gusic M, Iuso A, **Repp B**, Peters K, Biskup S, von Livonius B, Prokisch H, Klopstock T, Characterization of a Leber's hereditary optic neuropathy (LHON) family harboring two primary LHON mutations m.11778G>A and m.14484T>C of the mitochondrial DNA, Mitochondrion. 2017 Sep, ;36:15-20

Franko A, Huypens P, Neschen S, Irmler M, Rozman J, Rathkolb B, Neff F, Prehn C, Dubois G, Baumann M, Massinger R, Gradinger D, Przemeck GK, **Repp B**, Aichler M, Feuchtinger A, Schommers P, Stöhr O, Sanchez-Lasheras C, Adamski J, Peter A, Prokisch H, Beckers J, Walch AK, Fuchs H, Wolf E, Schubert M, Wiesner RJ, Hrabě de Angelis M, Bezafibrate improves insulin sensitivity and metabolic flexibility in STZ-treated diabetic mice, Diabetes. 2016 Jun 9. pii: db151670. [Epub ahead of print]

Collet M, Assouline Z, Bonnet D, Rio M, Iserin F, Sidi D, Goldenberg A, Lardennois C, Metodiev MD, **Haberberger B**, Haack T, Munnich A, Prokisch H, Rötig A. High incidence and variable clinical outcome of cardiac hypertrophy due to ACAD9 mutations in childhood, Eur J Hum Genet. 2015 Dec 16. doi: 10.1038/ejhg.2015.264

Schiff M, **Haberberger B,** Xia C, Mohsen AW, Goetzman ES, Wang Y, Uppala R, Zhang Y, Karunanidhi A, Prabhu D, Alharbi H, Prochownik EV, Haack T, Häberle J, Munnich A, Rötig A, Taylor RW, Nicholls RD, Kim JJ, Prokisch H, Vockley J. Complex I assembly function and fatty acid oxidation enzyme activity of ACAD9 both contribute to disease severity in ACAD9 deficiency Hum Mol Genet. 2015 Jun 1;24(11):3238-47. doi: 10.1093/hmg/ddv074. Epub 2015 Feb 26.

Haack TB, Gorza M, Danhauser K, Mayr JA, **Haberberger B**, Wieland T, Kremer L, Strecker V, Graf E, Memari Y, Ahting U, Kopajtich R, Wortmann SB, Rodenburg RJ, Kotzaeridou U, Hoffmann GF, Sperl W, Wittig I, Wilichowski E, Schottmann G, Schuelke M, Plecko B, Stephani U, Strom TM, Meitinger T, Prokisch H, Freisinger P. Phenotypic spectrum of eleven patients and five novel MTFMT mutations identified by exome sequencing and candidate gene screening. Mol Genet Metab. 2014 Mar;111(3):342-52. doi: 10.1016/j.ymgme.2013.12.010. Epub 2013 Dec 25

Jackson CB, Nuoffer J, Hahn D, Prokisch H, **Haberberger B**, Gautschi M, Gallati S, Schaller A, Mutations in SDHD lead to autosomal recessive encephalomyopathy and isolated mitochondrial complex II deficiency, *J Med Genet* J Med Genet. 2013 Dec 23. doi: 10.1136/jmedgenet-2013-101932. [Epub ahead of print]

Ashraf H, Gee H, Woerner S, Xie L, Vega-Warner V, Lovric S, Fang H, Song X, Cattran D, Avila-Casado C, Paterson A, Nitschké P, Bole-Feysot C, Cochat P, Esteve-Rudd J, **Haberberger B**, Allen S, Zhou W, Airik R, Otto E, Barua M, Al-Hamed M, Kari J, Böckenhauer D, Kleta R, El Desoky S, Hacihamdioglu D, Gok F, Washburn J, Wiggins R, Choi M, Lifton R, Levy S, Han Z, Salviati L, Prokisch H, Williams D, Pollak M, Clarke C, Pei Y, Antignac C, Hildebrandt F Exome resequencing reveals ADCK4 mutations as novel causes of steroidresistant nephrotic syndrome *J Clin Invest.* 2013 Aug 15

Haack TB, Rolinski B, **Haberberger B**, Zimmermann F, Schum J, Strecker V, Graf E, Athing U, Hoppen T, Wittig I, Sperl W, Freisinger P, Mayr JA, Strom TM, Meitinger T, Prokisch H, Homozygous missense mutation in BOLA3 causes multiple mitochondrial dysfunctions syndrome in two siblings., *J Inherit Metab Dis*. 2012 May 5

Haack TB, **Haberberger B**, Frisch EM, Wieland T, Iuso A, Gorza M, Strecker V, Graf E, Mayr JA, Herberg U, Hennermann JB, Klopstock T, Kuhn KA, Ahting U, Sperl W, Wilichowski E, Hoffmann GF, Tesarova M, Hansikova H, Zeman J, Plecko B, Zeviani M, Wittig I, Strom TM, Schuelke M, Freisinger P, Meitinger T, Prokisch H., Molecular diagnosis in mitochondrial complex I deficiency using exome sequencing. *J Med Genet*. 2012 Apr;49(4):277-83.

Mayr JA, Haack TB, Graf E, Zimmermann FA, Wieland T, **Haberberger B**, Superti-Furga A, Kirschner J, Steinmann B, Baumgartner MR, Moroni I, Lamantea E, Zeviani M, Rodenburg RJ, Smeitink J, Strom TM, Meitinger T, Sperl W, Prokisch H. Lack of the mitochondrial protein acylglycerol kinase causes Sengers syndrome. *Am J Hum Genet*. 2012 Feb 10;90(2):314-20

Haack TB, Madignier F, Herzer M, Lamantea E, Danhauser K, Invernizzi F, Koch J, Freitag M, Drost R, Hillier I, **Haberberger B**, Mayr JA, Ahting U, Tiranti V, Rötig A, Iuso A, Horvath R, Tesarova M, Baric I, Uziel G, Rolinski B, Sperl W, Meitinger T, Zeviani M, Freisinger P, Prokisch H. Mutation screening of 75 candidate genes in 152 complex I deficiency cases identifies pathogenic variants in 16 genes including NDUFB9., *J Med Genet*. 2012 Feb;49(2):83-9

Haack TB, Danhauser K, **Haberberger B**, Hoser J, Strecker V, Boehm D, Uziel G, Lamantea E, Invernizzi F, Poulton J, Rolinski B, Iuso A, Biskup S, Schmidt T, Mewes HW, Wittig I, Meitinger T, Zeviani M, Prokisch H. Exome sequencing identifies ACAD9 mutations as a cause of complex I deficiency. **Nat Genet**. 2010 Dec;42(12):1131-4